

An Introduction to Thermal Field Theory and Some of its Application

Munshi G. Mustafa

Theory Division, Saha Institute of Nuclear Physics, Homi Bhabha National Institute, Kolkata - 700064, India

E-mail: munshigolam.mustafa@saha.ac.in

ABSTRACT: In this article an introduction to the thermal field theory within imaginary time vis-a-vis Matsubara formalism has been discussed in details. The imaginary time formalism has been introduced through both the operatorial and the functional integration method. The prescription to perform frequency sum for boson and fermion has been discussed in details. Green's function both in Minkowski time as well as in Euclidean time has been derived. The tadpole diagram in $\lambda\phi^4$ theory and the self-energy in ϕ^3 theory have been computed and their consequences have also been discussed. The basic features of general two point functions, such as self-energy and propagator, for both fermions and bosons in presence of a heat bath have been discussed. The imaginary time has also been introduced from the relation between the functional integral and the partition function. Then the free partition functions and thermodynamic quantities for scalar, fermion and gauge field, and interacting scalar field have been obtained from first principle calculation. The quantum electrodynamics (QED) and gauge fixing have been discussed in details. The one-loop self-energy for electron and photon in QED have been obtained in hard thermal loop (HTL) approximation. The dispersion properties and collective excitations of both electron and photon in a material medium in presence of a heat bath have been presented. The spectral representation of fermion and gauge boson propagators have been obtained. In HTL approximation, the generalisation of QED results of two point functions to quantum chromodynamics (QCD) have been outlined that mostly involve group theoretical factors. Therefore, one learns about the collective excitations in a QCD plasma from the acquired knowledge of QED plasma excitations. Then, some subtleties of finite temperature field theory have been outlined. As an effective field theory approach the HTL resummation and the HTL perturbation theory (HTLpt) have been introduced. The leading order(LO), next-to-leading order (NLO) and next-to-next-leading order (NNLO) free energy and pressure for deconfined QCD medium created in heavy-ion collisions have been computed within HTLpt. The general features of the deconfined QCD medium have also been outlined with non-perturbative effects like gluon condensate and Gribov-Zwanziger action. The dilepton production rates from quark-gluon plasma with these non-perturbative effects have been computed and discussed in details.

Contents

1	Introduction	2
1.1	Need for Thermal Field Theory	4
1.2	Notations and Convention	4
2	A Brief Review of Some Facts	6
2.1	Review of Equilibrium Statistical Thermodynamics	6
2.1.1	Partition function for one bosonic degree of freedom	7
2.1.2	Partition function for one fermionic degree of freedom	8
2.1.3	Partition function for non-interacting gases of fermions and bosons	9
2.2	Brief Review of Quantum Mechanics	10
2.2.1	Schrödinger picture (SP)	11
2.2.2	Heisenberg picture (HP)	11
2.2.3	Dirac or Interaction picture (IP)	12
2.3	Functional Integration	13
2.4	Grassmann Variables	16
3	Imaginary Time Formalism	17
3.1	Connection to Imaginary Time and Matsubara Formalism	17
3.2	Matsubara Formalism (Operatorial Method)	19
3.3	Evolution Operator and \mathcal{S} -Matrix	20
3.4	Two-Point Correlation Function: Green's Function	21
3.4.1	Green's function at $T = 0$ in Minkowski time (real time)	21
3.4.2	Green's function at $T \neq 0$ Minkowski time (real time)	22
3.4.3	Green's function at $T \neq 0$ in Euclidean time (imaginary time)	24
3.5	Periodicity (Anti-periodicity) of the Green's Function	25
3.6	Discrete Frequency (Matsubara Frequency)	25
3.7	Dictionary: $T = 0$ to $T \neq 0$ Field Theory (Imaginary Time)	29
3.8	Feynman Rules	30
4	Frequency Sum	30
4.1	Bosonic Frequency Sum	31
4.1.1	Separation of vacuum and matter part	32
4.1.2	Choice of contour:	33
4.2	Fermionic Frequency Sum for Zero Chemical Potential ($\mu = 0$)	34
4.2.1	Separation of vacuum and matter part	35
4.2.2	Choice of contour	36
4.3	Examples of Frequency Sum for Bosonic Case	36

5	Scalar Theory	41
5.1	Tadpole Diagram in $\lambda\phi^4$ Theory	41
5.2	One-Loop Self-Energy in ϕ^3 -Theory	43
6	Partition Function	50
6.1	Relation of Functional Integration and the Partition Function	52
6.2	Scalar Field Partition Function	53
6.2.1	Partition function for free real scalar field	53
6.2.2	Partition function for interacting scalar field	57
6.2.3	Pressure	60
6.3	Fermion Field	60
6.3.1	Fermionic Lagrangian and conserved charge	60
6.3.2	Partition function and pressure for free fermions	62
6.3.3	A reverse way: first number density and then pressure and entropy density for fermions	65
7	General Structure of Fermionic Two-point Functions at $T \neq 0$	67
7.1	Fermion Self-Energy	67
7.2	Fermion Propagator	68
8	General structure of Gauge Boson Two-point Functions at $T \neq 0$	70
8.1	Covariant Description	70
8.2	Tensor Decomposition	71
8.3	General Structure of Self-energy of a Vector Particle in a Thermal Medium	73
8.4	Massless Vector Gauge Boson Propagator in Covariant Gauge	74
8.5	Massive Vector Boson Propagator	76
9	Quantum Electrodynamics (QED)	78
9.1	Dirac Field	78
9.2	Pure Gauge Field	79
9.3	Electromagnetic Lagrangian	80
9.4	Gauge Fixing	80
9.5	Free Photon Partition Function	84
9.6	One-loop Fermion Self-energy Σ and Structure Functions \mathcal{A} and \mathcal{B} in HTL approximation	88
9.7	Dispersion of Fermionic Quasiparticles and Collective Excitations in HTL Approximation	92
9.8	Spectral Representation of Fermion Propagator	94
9.9	Calculation of Π_L and Π_T from One-loop Photon Self-energy in HTL Approximation	95
9.10	Dispersion Relation and Collective Excitations of Photon in HTL Approximation	98
9.11	Spectral Representation of Gauge Boson Propagator	100

10 Quantum Chromodynamics (QCD)	101
10.1 QCD Lagrangian	102
10.2 One-loop Gluon Self-energy in HTL Approximation	103
10.3 One-loop Quark Self-energy in HTL Approximation	105
11 Subtleties in Finite Temperature Field Theory	106
12 Hard Thermal Loop (HTL) Resummation and HTL Perturbation Theory	107
12.1 HTL Resummation	107
12.2 HTL perturbation Theory (HTLpt)	109
12.3 One-loop Quark Free Energy in HTLpt	110
12.4 One-loop Gluon Free Energy in HTLpt	114
12.5 Leading Order (LO) Thermodynamics of QGP in HTLpt	118
12.6 Next-to-leading Order (NLO) Thermodynamics of QGP in HTLpt	119
12.7 Next-to-next-leading Order (NNLO) Thermodynamics of QGP in HTLpt	119
13 Thermal Medium with Non-perturbative Effects	121
13.1 Quark Propagation in QGP with Gluon Condensate	123
13.1.1 Quark self-energy	123
13.1.2 Quark propagator and dispersion	125
13.1.3 Spectral representation of the quark propagator	127
13.2 Quark Propagation in QGP with Gribov-Zwanziger Action	127
13.2.1 Gribov-Zwanziger action and its consequences	127
13.2.2 Quark self-energy	129
13.2.3 Quark propagator and dispersion	129
13.2.4 Spectral representation of the quark propagator	131
13.2.5 Quark-Photon vertex	132
13.3 Dilepton Production Rate from QGP	133
13.3.1 Dilepton rate in presence of thermal medium	133
13.3.2 Dilepton production rate from QGP with gluon condensate	134
13.3.3 Dilepton production rate from QGP with Gribov-Zwanziger action	141
14 Conclusion	146
A Appendix	146
A.1 One-loop Fermionic Sum Integrals	146
A.2 One-loop Bosonic Sum Integrals	148
A.3 Braaten-Pisarski-Yuan (BPY) Prescription	148

1 Introduction

The conventional quantum field theory is formalized at zero temperature. This is a framework to describe a wide class of phenomena in particle physics in the energy range covered by all experiments, i.e., a tool to deal with complicated many body problems or interacting system. The theoretical predictions under this framework, for example the cross sections of particle collisions in an accelerator, are extremely good to describe experimental data. With some modifications, it also plays a crucial role in atomic, nuclear and condensed matter physics. However, our real world is certainly of non-zero temperature. It is natural to wonder when and to what extent effects arising due to non-zero temperature are relevant, and what new phenomena could arise due to a thermal background. To understand these, one needs a prescription of quantum field theory in thermal background and the general context of thermal field theory can be illustrated as below:

In Fig. 1, the simple two body process is displayed at zero temperature and it can be characterized by an observable as

$$\mathcal{O} = \langle q_1 q_2 | p_1 p_2 \rangle. \quad (1.1)$$

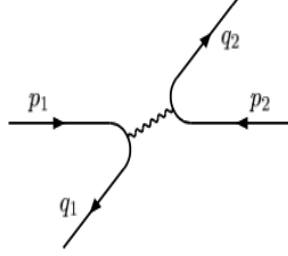


Figure 1: Simple $2 \rightarrow 2$ process at zero temperature.

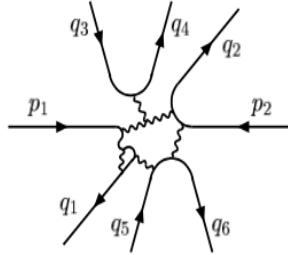


Figure 2: Complicated many body process at zero temperature.

In Fig. 2, the complicated many body process is displayed at zero temperature and it can

be characterized by

$$\mathcal{O} = \langle q_1 q_2 \cdots q_6 | p_1 p_2 \rangle. \quad (1.2)$$

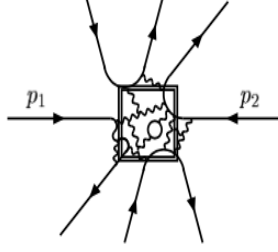


Figure 3: Complicated many body process at non-zero temperature.

Now, in Fig. 3, the complicated many body process is displayed at non-zero temperature. However, the \square in Fig. 3 is simple because the ergodic system may thermalize and their average properties can then be characterized just by thermal fluctuations in presence of temperature T and chemical potential μ as

$$\langle \mathcal{O} \rangle_T = \mathcal{Z}^{-1} \text{Tr} \left[e^{-\beta(H - \mu N)} \mathcal{O} \right], \quad (1.3)$$

where $\beta = 1/T$ and \mathcal{Z} is the partition function, H is the Hamiltonian and N is the conserved number in the system. Angular braces $\langle \cdots \rangle_T$ indicate thermal average. The (1.3) means that though a many body scattering process is complicated but can be addressed only through the thermal averaged properties observed over a long period of time. This indicates that the dynamics has to be ergodic that allows a thermodynamic treatment. So, this brings the well-established realm of statistical mechanics and the problem becomes manageable such that each observable can be expressed in terms of T and μ . Thus, the thermal field theory [1–14] is a combination of quantum field theory and statistical mechanics that provides a tool to deal with complicated many body problems with interactions among its components at finite T and μ . Studies of physical systems at finite temperature have led, in the past, to many interesting properties such as phase transitions, blackbody radiation etc. However, the study of complicated quantum mechanical systems at finite temperature has had a systematic development only in the past few decades. There are now well developed and well understood formalisms to describe finite temperature field theories. There are now three well defined formalisms:

1. Imaginary time (Matsubara) formalism [1].
2. Real time (Schwinger-Keldysh) formalism [2, 3].
3. Thermo field dynamics (Umezawa) formalism [4].

In this article, we will review the imaginary time formalism in thermal field theory and its applications.

1.1 Need for Thermal Field Theory

The goal of thermal field theory is to describe a large ensemble of multiple interacting particles (including gauge interactions) in thermal environment. It also describes creation and annihilation of new processes which were not present in vacuum field theory. It has been used to study questions such as phase transitions involving symmetry restoration in theories with spontaneously broken symmetry [8, 9, 15]. One can also study the evolution of the universe at early times and cosmology [16–21] which clearly is a system at high temperature. The finite temperature field theory has widely been applied to thermal neutrino production [22–27], neutrino oscillations [28], leptogenesis [29–32], $\mathcal{N} = 4$ superasymmetric Yang-Mills theory [33–37], string theory and Anti de-sitter space/Conformal Field Theory (Ads/CFT) correspondence [38–41], blackhole physics [42], thermal axion production [43–45], thermal graviton production [46, 47] and in gravitational waves [48]. It has also been applied to condensed matter physics [5–7, 49–52].

It has also been used to high energy nuclear and particle physics to describe the many body system. One of such current field of interest is Quark-Gluon Plasma (QGP), which is a complicated many body system [53–56] produced in high energy heavy-ion collisions at Relativistic Heavy-Ion Collider (RHIC) at Brookhaven National Laboratory (BNL) and Large Hadron Collider (LHC) at the European Organization for Nuclear Research (CERN) and likely to be produced at future Facility for Antiproton and Ion Research (FAIR) experiment in GSI and Nuclotron-based Ion Collider fAcility (NICA) experiment in DUBNA containing quarks (fermions) and gluons (gauge particles) that involve high temperature and/or density. QGP is a thermalized state of matter in which (quasi)free quarks and gluons are deconfined from hadrons, so that the color degrees of freedom become manifest over a large volume, than merely in a hadronic volume. QGP expands, cools, hadronizes and hadrons reach to the detector and one needs to have unambiguous signatures to discover QGP. But, unfortunately most of signals are circumstantial. Thus, in order to understand the properties of a QGP and to make unambiguous predictions about signature of QGP formation, one needs a profound description of QGP. For this purpose we have to use Quantum Chromodynamics (QCD) at finite temperature and chemical potential [10, 13, 14, 57–65].

1.2 Notations and Convention

In this article, the following notations and conventions will be followed:

- The metric in Minkowski space-time $g_{\mu\nu} = \text{diag}(1, -1, -1, -1)$.
- Will be using $\hbar = c = k_B = 1$ unless mentioned otherwise therein. So, temperature has dimension of mass $[M]$ whereas that for length and time is $[M^{-1}]$.
- I_m represents $m \times m$ unit matrix.

- Greek indices are used for four-vectors in space-time.
- Einstein summation convention: repeated indices are summed over unless stated otherwise; $A^\mu B_\mu = A_0 B_0 - \mathbf{A} \cdot \mathbf{B}$; $A^\mu A_\mu = A_0^2 - \mathbf{A}^2$.
- ∂_μ : derivative wrt μ coordinate.
- A four vector $P \equiv (p_0, \vec{p})$ and $p = |\vec{p}|$.
- Fermionic field $\bar{\psi} = \psi^\dagger \gamma_0$.

This review article has been organized as follows: in section 2 we review some known facts which will be needed for our purpose. These are the equilibrium statistical thermodynamics in subsec 2.1, the three pictures in quantum mechanics in subsec 2.2, the functional integration in subsec 2.3 and the Grassmann variables in subsec 2.4. In section 3 we introduce the imaginary time formalism: we present the connection to imaginary time and Matsubara formalism in subsec 3.1, the operatorial method of Matsubara formalism in subsec 3.2, the evolution operator and the \mathcal{S} -Matrix in subsec 3.3, the Green's function at $T \neq 0$ in subsec 3.4, the periodicity and antiperiodicity of Green's function in subsec 3.5, Matsubara frequency in subsec 3.6, a short summary of imaginary time formalism in tabular form in subsec 3.7 and Feynman rules in subsec 3.8. In section 4 we discuss discrete frequency sum: we present bosonic frequency sum in subsec 4.1, fermionic frequency sum in subsec 4.2 and some examples of bosonic sum in subsec 4.3. We discuss scalar theory at $T \neq 0$ in section 5: first the tadpole diagram in $\lambda\phi^4$ -theory in subsec 5.1 and then one-loop self-energy in ϕ^3 -theory in section 5.2. We discuss partition function in section 6: first the relation of the functional integration and the partition function and then connection with the imaginary time in subsec 6.1, the partition function for free and interacting scalar fields in subsec. 6.2 and then the partition function for free fermionic field in subsec 6.3. In section 7 we present the general structure of fermion two-point functions at $T \neq 0$ while in section 8 the general structure of vector boson two-point functions at $T \neq 0$ is presented. In section 9 we discuss quantum electrodynamics (QED) at $T \neq 0$: gauge fixing, free photon partition function, one-loop electron self-energy, effective electron propagator and its spectral representation, collective excitations of electrons, photon self-energy, effective photon propagator and its spectral representation and collective excitations of photons. In section 10 we present quantum chromodynamics (QCD) at $T \neq 0$ by generalising the QED results of two point functions in HTL approximation to QCD that mostly involve group theoretical factors and learn about the collective excitations in QCD. Some subtleties at finite temperature have been discussed in section 11. In section 12 the HTL resummation and HTL perturbation theory have been outlined along with application to QCD thermodynamics in leading order (LO), next-to-leading order (NLO) and next-to-next-leading order (NNLO). In section 13 the two-point functions and the collective excitations of quarks considering non-perturbative effects like gluon-condensates and Gribov-Zwanziger action have been discussed in details. As an application of those non-perturbative effects, the dilepton production rates from QGP created in relativistic heavy-ion collisions have been

calculated. Finally, we conclude this review article in section 14 and an appendix is presented in section A.

2 A Brief Review of Some Facts

2.1 Review of Equilibrium Statistical Thermodynamics

In this subsection, we define some of the basic relations in equilibrium statistical mechanics [66]. In thermal equilibrium, the statistical behaviour of a quantum system is usually investigated through an appropriate ensemble. In general the density matrix for a system is defined as

$$\rho(\beta) = e^{-\beta\mathcal{H}} , \quad (2.1)$$

where $\beta = 1/T$ (the Boltzmann constant $k_B \equiv 1$ is assumed) and \mathcal{H} is the Hamiltonian of the system for a given choice of ensemble. For canonical ensemble, $\mathcal{H} = H$. For grand canonical ensemble, $\mathcal{H} = H - \mu N$ with H is the dynamical Hamiltonian and N is the number operator representing difference of particles and antiparticles. N commutes with H and also it is hermitian. It has simultaneous eigenstate. It is also extensive variable (scales with volume V) in the thermodynamic limit. At finite temperature the qualitative behaviours of a system are almost independent on the nature of the ensemble, so the choice of the ensemble is kept arbitrary for general discussions.

With the given density matrix, the finite temperature property of any theory is described by the partition function

$$\mathcal{Z} = \text{Tr} \rho = \text{Tr} \left(e^{-\beta\mathcal{H}} \right) = \sum_n \left\langle n \left| e^{-\beta\mathcal{H}} \right| n \right\rangle , \quad (2.2)$$

where $|n\rangle$ is a many-particle state in the full Hilbert space. Trace stands for sum over a complete many-particles states in Hilbert space.

In the infinite volume limit:

$$\text{Thermodynamic potential:} \quad \Omega(\beta) = -T \ln \mathcal{Z}. \quad (2.3a)$$

$$\text{Pressure:} \quad P = -\frac{\partial}{\partial V} \Omega(\beta) = -\frac{\Omega(\beta)}{V}. \quad (2.3b)$$

$$\text{Number:} \quad N_i = \frac{\partial}{\partial \mu_i} (T \ln \mathcal{Z}). \quad (2.3c)$$

$$\text{Entropy:} \quad S = \frac{\partial}{\partial T} (T \ln \mathcal{Z}). \quad (2.3d)$$

$$\text{Energy:} \quad E = -PV + TS + \mu_i N_i. \quad (2.3e)$$

The thermal expectation value of any physical observable can be defined as

$$\langle \mathcal{A} \rangle_\beta = \mathcal{Z}^{-1}(\beta) \text{Tr} [\rho(\beta) \mathcal{A}] = \mathcal{Z}^{-1}(\beta) \text{Tr} \left[e^{-\beta\mathcal{H}} \mathcal{A} \right] . \quad (2.4)$$

The correlation function of any two observables is given as

$$\langle \mathcal{AB} \rangle_\beta = \mathcal{Z}^{-1}(\beta) \text{Tr} [\rho(\beta) \mathcal{AB}] = \mathcal{Z}^{-1}(\beta) \text{Tr} \left[e^{-\beta\mathcal{H}} \mathcal{AB} \right] . \quad (2.5)$$

2.1.1 Partition function for one bosonic degree of freedom

Consider a time-dependent single-particle quantum mechanical mode is occupied by bosons. Each boson in that mode has the same energy ω . There may be 0, 1, 2, or any number of bosons occupying that state without any interaction. So, it could be thought as a set of non-interacting quantized simple harmonic oscillators [13] and a Hamiltonian for each oscillator is given as

$$\mathcal{H} = \frac{1}{2}\omega \left(aa^\dagger + a^\dagger a \right), \quad (2.6)$$

where a^\dagger and a are, respectively, the boson creation and annihilation operators and their action on a number eigenstate are

$$a^\dagger |n\rangle = \sqrt{n+1} |n+1\rangle, \quad (2.7a)$$

$$a |n\rangle = \sqrt{n} |n-1\rangle, \quad (2.7b)$$

with $a|0\rangle = 0$ and the n -th excited state is built as

$$|n\rangle = \frac{1}{\sqrt{n!}} \left(a^\dagger \right)^n |0\rangle. \quad (2.8)$$

The coefficients in (2.7a) and (2.7b) follow from the requirements that a^\dagger and a be the hermitian conjugates and that $a^\dagger a$ be the number operator \hat{N} with

$$\hat{N}|n\rangle = a^\dagger a |n\rangle = n |n\rangle, \quad (2.9)$$

where a and a^\dagger satisfy the commutation relation

$$[a, a^\dagger] = aa^\dagger - a^\dagger a = 1. \quad (2.10)$$

Combining (2.6) and (2.10) the Hamiltonian becomes

$$\mathcal{H} = \omega \left(a^\dagger a + \frac{1}{2} \right) = \omega \left(\hat{N} + \frac{1}{2} \right). \quad (2.11)$$

Now the partition function for one bosonic degree of freedom can be written from (2.2) as

$$\mathcal{Z}_B = \sum_{n=0}^{\infty} \langle n | e^{-\beta\omega(\hat{N}+\frac{1}{2})} | n \rangle = e^{-\frac{\beta\omega}{2}} \sum_{n=0}^{\infty} e^{-\beta\omega n} = \frac{e^{-\frac{\beta\omega}{2}}}{1 - e^{-\beta\omega}}. \quad (2.12)$$

According to (2.3a) the logarithm of the partition function is of interest. From (2.12) one obtains

$$\ln \mathcal{Z}_B = -\frac{\beta\omega}{2} - \ln(1 - e^{-\beta\omega}), \quad (2.13)$$

where the first term originates from the zero-point energy, $\frac{1}{2}\omega$ in the Hamiltonian in (2.11).

2.1.2 Partition function for one fermionic degree of freedom

Like previous subsection, we consider a time-dependent single-particle quantum mechanical mode is occupied by fermions with each fermion in that mode has the same energy ω . We note that the Pauli exclusion principle restricts the occupation of a single-particle mode by more than one fermion. Therefore, there are only two states of the system as

$$|0\rangle \quad \text{and} \quad |1\rangle. \quad (2.14)$$

Now the Hamiltonian for each fermion [13] is given as

$$H = \frac{1}{2}\omega \left(\alpha^\dagger \alpha - \alpha \alpha^\dagger \right), \quad (2.15)$$

where α^\dagger and α are, respectively, the fermion creation and annihilation operators. They operate on the two states in (2.14) as

$$\alpha^\dagger |0\rangle = |1\rangle, \quad (2.16a)$$

$$\alpha |1\rangle = |0\rangle, \quad (2.16b)$$

$$\alpha^\dagger |1\rangle = 0, \quad (2.16c)$$

$$\alpha |0\rangle = 0. \quad (2.16d)$$

So, these operators have the properties that the operation of α^2 and $(\alpha^\dagger)^2$ on any of the states in (2.14) is zero. The coefficients in (2.16a) to (2.16d) follow from the requirements that α^\dagger and α be the hermitian conjugates and that $\alpha^\dagger \alpha$ be the number operator \hat{N} with

$$\hat{N}|n\rangle = \alpha^\dagger \alpha |n\rangle = n|n\rangle, \quad (2.17)$$

where α and α^\dagger satisfy the anticommutation relation

$$\{\alpha, \alpha^\dagger\} = \alpha \alpha^\dagger + \alpha^\dagger \alpha = 1. \quad (2.18)$$

Combining (2.15) and (2.18) the Hamiltonian becomes

$$H = \omega \left(\alpha^\dagger \alpha - \frac{1}{2} \right) = \omega \left(\hat{N} - \frac{1}{2} \right). \quad (2.19)$$

For grand canonical ensemble $\mathcal{H} = H - \mu \hat{N}$ and the partition function for one fermionic degree of freedom can be written from (2.2) as

$$\begin{aligned} \mathcal{Z}_{\mathcal{F}} &= \sum_{n=0}^1 \langle n | e^{-\beta(H - \mu \hat{N})} | n \rangle = e^{\frac{\beta\omega}{2}} \sum_{n=0}^1 e^{-\beta(\omega - \mu)n} \\ &= e^{\frac{\beta\omega}{2}} \left(1 + e^{-\beta(\omega - \mu)} \right). \end{aligned} \quad (2.20)$$

The logarithm of the partition function for a fermion

$$\ln \mathcal{Z}_{\mathcal{F}} = \frac{\beta\omega}{2} + \ln \left(1 + e^{-\beta(\omega - \mu)} \right), \quad (2.21)$$

where the first term originates from the zero-point energy, $\frac{1}{2}\omega$ in the Hamiltonian in (2.19).

Similarly, one can obtain the partition function for an antifermion by replacing $\mu \rightarrow -\mu$ in (2.20) as

$$\mathcal{Z}_{\bar{F}} = e^{\frac{\beta\omega}{2}} \left(1 + e^{-\beta(\omega+\mu)}\right), \quad (2.22)$$

and logarithm reads as

$$\ln \mathcal{Z}_{\bar{F}} = \frac{\beta\omega}{2} + \ln \left(1 + e^{-\beta(\omega+\mu)}\right). \quad (2.23)$$

2.1.3 Partition function for non-interacting gases of fermions and bosons

Now we consider a gas consisting non-interacting fermions and bosons. In principle they can interact among themselves to come to thermal equilibrium. Once it achieves thermal equilibrium then one can slowly switch off the interactions. Such a non-interacting system may well describe [13] the atmosphere around us, electrons in metal or white dwarf star, blackbody radiation in a heated cavity or the cosmic microwave background radiation etc.

The partition function for a non-interacting gas consisting fermions, antifermions and bosons as

$$\mathcal{Z} = \prod_{\alpha} \mathcal{Z}_F^{\alpha} \times \mathcal{Z}_{\bar{F}}^{\alpha} \times \mathcal{Z}_B^{\alpha}, \quad (2.24)$$

where α represents the single particle states of each mode corresponding to fermions, antifermions and bosons. Now using (2.12), (2.20) and (2.22)

$$\mathcal{Z} = \prod_{\alpha} e^{\frac{\beta\omega_{\alpha}}{2}} \left(1 + e^{-\beta(\omega_{\alpha}-\mu)}\right) e^{\frac{\beta\omega_{\alpha}}{2}} \left(1 + e^{-\beta(\omega_{\alpha}+\mu)}\right) e^{-\frac{\beta\omega_{\alpha}}{2}} \left(1 - e^{-\beta\omega_{\alpha}}\right)^{-1} \quad (2.25)$$

$$\begin{aligned} \ln \mathcal{Z} = & \sum_{\alpha} \frac{\beta\omega_{\alpha}}{2} + \sum_{\alpha} \ln \left(1 + e^{-\beta(\omega_{\alpha}-\mu)}\right) + \sum_{\alpha} \frac{\beta\omega_{\alpha}}{2} + \sum_{\alpha} \ln \left(1 + e^{-\beta(\omega_{\alpha}+\mu)}\right) \\ & - \sum_{\alpha} \frac{\beta\omega_{\alpha}}{2} - \sum_{\alpha} \ln \left(1 - e^{-\beta\omega_{\alpha}}\right). \end{aligned} \quad (2.26)$$

The \sum_{α} is over single particles states. In infinite volume limit $\sum_{\alpha} \rightarrow \frac{V}{(2\pi)^3} \int d^3p$.

The logarithm of the partition function becomes

$$\begin{aligned} \ln \mathcal{Z} = & \frac{V}{(2\pi)^3} \int d^3p \left[\frac{\beta\omega}{2} + \ln \left(1 + e^{-\beta(\omega-\mu)}\right) + \ln \left(1 + e^{-\beta(\omega+\mu)}\right) \right. \\ & \left. - \ln \left(1 - e^{-\beta\omega}\right) \right], \end{aligned} \quad (2.27)$$

we note that for massless species $\omega = p$. We will also obtain this results using thermal field theory in later subsections 6.2, 6.3.2 and 9.5.

The thermodynamic potential in (2.3a) can be written as

$$\Omega(\beta) = -T \ln \mathcal{Z} = -\frac{VT}{(2\pi)^3} \int d^3p \left[\frac{\beta\omega}{2} + \ln \left(1 + e^{-\beta(\omega-\mu)} \right) + \ln \left(1 + e^{-\beta(\omega+\mu)} \right) - \ln \left(1 - e^{-\beta\omega} \right) \right]. \quad (2.28)$$

Therefore, various thermodynamic quantities in (2.3b) to (2.3e) can easily be computed for non-interacting gas of fermions and bosons.

Now, if there are interactions, it becomes difficult to compute partition function for interacting system. The partition function reads from (2.2) as

$$\mathcal{Z} = \text{Tr} \rho = \text{Tr} \left(e^{-\beta\mathcal{H}} \right) = \sum_n \langle n | e^{-\beta\mathcal{H}} | n \rangle, \quad (2.29)$$

where $|n\rangle$ is a many-particle state in the full Hilbert space. Trace stands for sum over expectation values of all possible states in Hilbert space. There are infinite number of such states in quantum field theory (QFT). If the particles or fields are non-interacting, then it is easier to compute $\mathcal{Z}(\beta)$ as we have seen above. For an interacting system the partition function cannot be computed exactly if one expands even in perturbation series in interaction strength in a given theory. Matsubara (Imaginary time) formalism[1] represents a diagrammatic way of calculating the partition function and other physical observables perturbatively in order by order of the coupling strength of a given theory, analogous to $T = 0$ (vacuum) field theory.

2.2 Brief Review of Quantum Mechanics

In studying a quantum mechanical system or a system described by a quantum field theory, one is basically interested in determining the time evolution operator. In the standard framework of quantum mechanics, one solves the Schrödinger equation to determine the energy eigenvalues and eigenstates simply because the time evolution operator is related to the Hamiltonian.

Quantum systems are regarded as wave functions that satisfies the Schrödinger differential equation as

$$i \frac{d}{dt} |\psi(t)\rangle = \mathcal{H} |\psi(t)\rangle, \quad (2.30)$$

which governs the dynamics of the system in time.

Observables are represented by hermitian operators which act on the wave function. Thus the Hamiltonian of the system, \mathcal{H} , is the operator which describes the total energy of the quantum system as

$$\mathcal{H} |\psi(t)\rangle = E |\psi(t)\rangle. \quad (2.31)$$

There are three pictures in quantum mechanics due to Schrödinger, Heisenberg and Dirac. Below we briefly outline the three pictures in quantum mechanics [67].

2.2.1 Schrödinger picture (SP)

In the Schrödinger picture, the operators stay fixed while the Schrödinger equation changes the basis with time.

Since, all physical operators \mathcal{O}_S are time independent, one can write

$$\dot{\mathcal{O}}_S = 0. \quad (2.32)$$

The basis vector changes with time via the Schrödinger equation as

$$\frac{d}{dt}|\psi(t)\rangle_S = -i\mathcal{H}|\psi(t)\rangle_S \quad (2.33)$$

The differential equation leads to an expression for the wave function as

$$|\psi(t)\rangle_S = e^{-i\mathcal{H}t}|\psi(0)\rangle_S. \quad (2.34)$$

indicates that all physical state vectors are time dependent. A quantum operator as the argument of the exponential function is defined in terms of its power series expansion as

$$\begin{aligned} e^{-i\mathcal{H}t} &= \sum_{n=0}^{\infty} \frac{1}{n!} (-i\mathcal{H}t)^n \\ &= 1 - i\mathcal{H}t - \frac{1}{2}(\mathcal{H}t)^2 + \dots \end{aligned} \quad (2.35)$$

This is how the states pick up their time-dependence.

2.2.2 Heisenberg picture (HP)

In the Heisenberg picture, it is the operators which change in time while the basis of the space remains fixed.

Since the basis does not change with time which is accomplished by adding a term to the Schrödinger states to eliminate the time-dependence as

$$|\psi(0)\rangle_H = e^{i\mathcal{H}t}|\psi(t)\rangle_S = |\psi(0)\rangle_S, \quad (2.36a)$$

$$\frac{\partial}{\partial t}|\psi(0)\rangle_H = 0. \quad (2.36b)$$

We may define operators in the Heisenberg picture via expectation values of a Schrödinger operator as

$$\begin{aligned} \langle \mathcal{O}_S \rangle &= {}_S\langle \psi(t) | \mathcal{O}_S | \psi(t) \rangle_S \\ &= {}_S\langle \psi(0) | e^{i\mathcal{H}t} \mathcal{O}_S e^{-i\mathcal{H}t} | \psi(0) \rangle_S \\ &= {}_H\langle \psi(0) | (e^{i\mathcal{H}t} \mathcal{O}_S e^{-i\mathcal{H}t}) | \psi(0) \rangle_H. \end{aligned} \quad (2.37)$$

The operators in the Heisenberg picture, therefore, pick up time-dependence through unitary transformations as

$$\mathcal{O}_H(t) = e^{i\mathcal{H}t} \mathcal{O}_S e^{-i\mathcal{H}t} = U^\dagger(t) \mathcal{O}_S U(t), \quad (2.38)$$

where the Heisenberg Picture is related to the Schrödinger Picture through unitary transformation $U(t) = e^{-i\mathcal{H}t}$, where \mathcal{H} is the full Hamiltonian of the system as

$$\mathcal{H} = \mathcal{H}_0 + \mathcal{H}', \quad (2.39)$$

where \mathcal{H}_0 is the free part and \mathcal{H}' is the interacting part.

We may ascertain the Heisenberg operators' time-dependence through differentiation as

$$\begin{aligned} \frac{d\mathcal{O}_H(t)}{dt} &= i\mathcal{H}e^{i\mathcal{H}t}\mathcal{O}_S e^{-i\mathcal{H}t} - ie^{i\mathcal{H}t}\mathcal{O}_S \mathcal{H}e^{-i\mathcal{H}t} + \frac{\partial\mathcal{O}_H}{\partial t} \\ &= i \underbrace{(\mathcal{H}\mathcal{O}_H - \mathcal{O}_H\mathcal{H})}_{\text{Commutator}} + \frac{\partial\mathcal{O}_H}{\partial t} \\ &= i[\mathcal{H}, \mathcal{O}_H] + \frac{\partial\mathcal{O}_H}{\partial t}. \end{aligned} \quad (2.40)$$

The operators are thus governed by a differential equation known as Heisenberg's equation.

2.2.3 Dirac or Interaction picture (IP)

The Dirac (Interaction) picture is a sort of intermediary between the Schrödinger picture and the Heisenberg picture as both the quantum states and the operators carry time dependence. It is especially useful for problems including explicitly time-dependent interaction terms in the Hamiltonian.

In the interaction picture, the state vectors are again defined as transformations of the Schrödinger states by the free part of the Hamiltonian as

$$|\psi(t)\rangle_I = e^{i\mathcal{H}_0 t} |\psi(t)\rangle_S. \quad (2.41)$$

The Dirac operators are transformed similarly to the Heisenberg operators as

$$\mathcal{O}_I(t) = e^{i\mathcal{H}_0 t} \mathcal{O}_S e^{-i\mathcal{H}_0 t}. \quad (2.42)$$

The relation between interaction picture and Schrödinger picture is similar to Heisenberg picture except that the unitary transformation involves free Hamiltonian \mathcal{H}_0 instead of full one \mathcal{H} as $U(t) = e^{-i\mathcal{H}t}$. The purpose of it is to describe the interaction in terms of free fields.

The states in the interaction picture in (2.41) evolve in time similar to Heisenberg states as

$$\begin{aligned} \frac{d}{dt} |\psi(t)\rangle_I &= i\mathcal{H}_0 |\psi(t)\rangle_I + e^{i\mathcal{H}_0 t} \frac{d}{dt} |\psi(t)\rangle_S \\ &= i\mathcal{H}_0 |\psi(t)\rangle_I + e^{i\mathcal{H}_0 t} (-i\mathcal{H}) |\psi(t)\rangle_S \\ &= i\mathcal{H}_0 |\psi(t)\rangle_I + e^{i\mathcal{H}_0 t} (-i(\mathcal{H}_0 + \mathcal{H}')) e^{-i\mathcal{H}_0 t} |\psi(t)\rangle_I \\ &= i\mathcal{H}_0 |\psi(t)\rangle_I - i\mathcal{H}_0 |\psi(t)\rangle_I - ie^{i\mathcal{H}_0 t} \mathcal{H}' e^{-i\mathcal{H}_0 t} |\psi(t)\rangle_I \\ &= -ie^{i\mathcal{H}_0 t} \mathcal{H}' e^{-i\mathcal{H}_0 t} |\psi(t)\rangle_I \\ &= -i\mathcal{H}'(t) |\psi(t)\rangle_I, \end{aligned} \quad (2.43)$$

where the interacting term of the Hamiltonian is defined similarly as

$$\mathcal{H}'(t) = e^{i\mathcal{H}_0 t} \mathcal{H}' e^{-i\mathcal{H}_0 t}. \quad (2.44)$$

Therefore, the state vectors in the interaction picture evolve in time according to the interaction term only.

It can be easily shown through differentiation of (2.42) that operators in the interaction picture evolve in time according only to the free Hamiltonian as

$$\begin{aligned} \frac{d\mathcal{O}_I(t)}{dt} &= i\mathcal{H}_0 e^{i\mathcal{H}_0 t} \mathcal{O}_S e^{-i\mathcal{H}_0 t} - i e^{i\mathcal{H}_0 t} \mathcal{O}_S \mathcal{H}_0 e^{-i\mathcal{H}_0 t} + \frac{\partial \mathcal{O}_I}{\partial t} \\ &= i \underbrace{\left(\mathcal{H}_0 \mathcal{O}_I(t) - \mathcal{O}_I(t) \mathcal{H}_0 \right)}_{\text{Commutator}} + \frac{\partial \mathcal{O}_I}{\partial t} \\ &= i \left[\mathcal{H}_0, \mathcal{O}_I(t) \right] + \frac{\partial \mathcal{O}_I}{\partial t}. \end{aligned} \quad (2.45)$$

The interaction picture admits that the operators act on the state vector at different times and form the basis for quantum field theory and many other newer methods.

2.3 Functional Integration

We know that the partition function of statistical mechanics completely describes a system in equilibrium. Likewise, a system in quantum field theory is fully described by an integral over all space-time paths allowed, which is also known as path integral [68, 69]. In this subsection we will derive the path integral formalism.

If a particle is observed in the state $|\phi_a\rangle$ at a time t_0 , then the wave function after some time t will evolve as

$$|\phi_b\rangle = e^{-i \int_0^t \mathcal{H} dt} |\phi_a\rangle. \quad (2.46)$$

We assume that the Hamiltonian is time-independent then the transition amplitude for going from a state $|\phi_a\rangle$ to another state $|\phi_b\rangle$ after a time t can simply be written as

$$\langle \phi_b | e^{-i\mathcal{H}t} | \phi_a \rangle. \quad (2.47)$$

In statistical mechanics the most interesting cases are the ones where the system returns to its initial state after a time t , then transition amplitude in (2.47) can be written as

$$\langle \phi_a | e^{-i\mathcal{H}t} | \phi_a \rangle. \quad (2.48)$$

Let $\hat{\phi}(\vec{x}, 0)$ be Schödinger picture field operator at time $t = 0$ and let $\hat{\pi}(\vec{x}, 0)$ be its conjugate momentum operator. The eigenstates of the field operator are denoted by $|\phi\rangle$ and those for momentum operator are $|\pi\rangle$. They satisfy the eigenvalue equations as

$$\hat{\phi}(\vec{x}, 0) |\phi\rangle = \phi(\vec{x}) |\phi\rangle, \quad (2.49a)$$

$$\hat{\pi}(\vec{x}, 0) |\pi\rangle = \pi(\vec{x}) |\pi\rangle, \quad (2.49b)$$

where $\phi(\vec{x})$ and $\pi(\vec{x})$ are corresponding eigenvalues. Now we define the completeness and orthogonality relations for field ϕ

$$\begin{aligned} \int d\phi(x) |\phi\rangle \langle \phi| &= 1 \\ \langle \phi_a | \phi_b \rangle &= \prod_x \delta(\phi_a(\vec{x}) - \phi_b(\vec{x})), \end{aligned} \quad (2.50)$$

and for momentum density π as

$$\begin{aligned} \int \frac{1}{2\pi} d\pi(x) |\pi\rangle \langle \pi| &= 1 \\ \langle \pi_a | \pi_b \rangle &= \prod_x \delta(\pi_a(\vec{x}) - \pi_b(\vec{x})), \end{aligned} \quad (2.51)$$

and their overlap is defined as

$$\langle \phi | \pi \rangle = \exp \left(i \int d^3x \pi(\vec{x}) \phi(\vec{x}) \right). \quad (2.52)$$

The probability amplitude is described by the time evolution from the initial state to final state through all intermediate states at the time intervals Δt . Now, splitting the time interval $(0, t)$ into N equal steps of size $\Delta t = t/N$. With this the probability amplitude in (2.48) can be written as

$$\langle \phi_a | e^{-i\mathcal{H}t} | \phi_a \rangle = \langle \phi_a | \underbrace{e^{-i\mathcal{H}\Delta t} \times \dots \times e^{-i\mathcal{H}\Delta t}}_{N \text{ times}} | \phi_a \rangle. \quad (2.53)$$

Now a complete set of states is inserted after each time interval in (2.53), alternating between the one in (2.50) and (2.51) as

$$\begin{aligned} \langle \phi_a | e^{-i\mathcal{H}t} | \phi_a \rangle &= \lim_{N \rightarrow \infty} \int \left(\prod_{i=1}^N \frac{1}{2\pi} d\pi_i d\phi_i \right) \langle \phi_a | \pi_N \rangle \langle \pi_N | e^{-i\mathcal{H}\Delta t} | \phi_N \rangle \\ &\quad \times \langle \phi_N | \pi_{N-1} \rangle \langle \pi_{N-1} | e^{-i\mathcal{H}\Delta t} | \phi_{N-1} \rangle \dots \dots \dots \\ &\quad \times \langle \phi_2 | \pi_1 \rangle \langle \pi_1 | e^{-i\mathcal{H}\Delta t} | \phi_1 \rangle \langle \phi_1 | \phi_a \rangle, \end{aligned} \quad (2.54)$$

where every second term can be rewritten using the overlap in (2.52) which always appear on the form

$$\langle \phi_{i+1} | \pi_i \rangle = \exp \left(i \int d^3x \pi_i(\vec{x}) \phi_{i+1}(\vec{x}) \right), \quad (2.55)$$

and just following (2.48) the last term becomes

$$\langle \phi_1 | \phi_a \rangle = \delta(\phi_1 - \phi_a). \quad (2.56)$$

Now the exponential in (2.54) can be expanded for small time interval Δt as

$$\langle \pi_i | e^{-i\mathcal{H}_i \Delta t} | \phi_i \rangle \approx \langle \pi_i | (1 - i\mathcal{H}_i \Delta t + \dots) | \phi_i \rangle. \quad (2.57)$$

In (2.54), the Hamiltonian \mathcal{H}_i always appears between two states with same index i which indicates that the Hamiltonian is always evaluated at the same point in time. Now one can write (2.57) as

$$\begin{aligned}\langle \pi_i | (1 - i\mathcal{H}_i \Delta t) | \phi_i \rangle &= \langle \pi_i | \phi_i \rangle (1 - i\mathcal{H}_i \Delta t) \\ &= (1 - i\mathcal{H}_i \Delta t) \exp \left(-i \int d^3x \pi_i(\vec{x}) \phi_i(\vec{x}) \right).\end{aligned}\quad (2.58)$$

Now, the expansion in first order in (2.58) can be changed back to exponential as

$$\langle \pi_i | e^{-i\mathcal{H}_i \Delta t} | \phi_i \rangle \approx e^{-i\mathcal{H}_i \Delta t} \exp \left(-i \int d^3x \pi_i(\vec{x}) \phi_i(\vec{x}) \right). \quad (2.59)$$

The Hamiltonian \mathcal{H} is the integral of Hamiltonian density \mathcal{H}_d as

$$\mathcal{H}_i = \int d^3x \mathcal{H}_d(\pi_i(\vec{x}) \phi_i(\vec{x})). \quad (2.60)$$

Now, the transition amplitude in (2.54) can be written as

$$\begin{aligned}\langle \phi_a | e^{-i\mathcal{H}t} | \phi_a \rangle &= \frac{1}{2\pi} \lim_{N \rightarrow \infty} \int \prod_{i=1}^N d\pi_i d\phi_i \delta(\phi_1 - \phi_a) \\ &\times \exp \left(-i\Delta t \sum_{j=1}^N \int d^3x \left[\mathcal{H}_d(\pi_j, \phi_j) - \frac{\pi_j(\phi_{j+1} - \phi_j)}{\Delta t} \right] \right).\end{aligned}\quad (2.61)$$

where $\phi_{N+1} = \phi_a = \phi_1$. In the continuum limit in time, one can write

$$\begin{aligned}\lim_{N \rightarrow \infty} i\Delta t \sum_{j=1}^N \left[\pi_j \frac{(\phi_{j+1} - \phi_j)}{\Delta t} - \mathcal{H}_d(\pi_j, \phi_j) \right] \\ \rightarrow i \int_0^{t_f} dt \left(\pi(\vec{x}, t) \frac{\partial \phi(\vec{x}, t)}{\partial t} - \mathcal{H}_d(\pi(\vec{x}, t), \phi(\vec{x}, t)) \right).\end{aligned}\quad (2.62)$$

The transition amplitude can now be written as

$$\begin{aligned}\langle \phi_a | e^{-i\mathcal{H}t} | \phi_a \rangle &= \int \mathcal{D}\pi \int_{\phi(\vec{x}, 0) = \phi_a(\vec{x})}^{\phi(\vec{x}, t) = \phi_a(\vec{x})} \mathcal{D}\phi \\ &\times \exp \left[i \int_0^{t_f} dt \int d^3x \left(\pi(\vec{x}, t) \frac{\partial \phi(\vec{x}, t)}{\partial t} - \mathcal{H}_d(\pi(\vec{x}, t), \phi(\vec{x}, t)) \right) \right],\end{aligned}\quad (2.63)$$

where the functional integration is denoted by \mathcal{D} . The integration runs over all possible momenta $\pi(\vec{x}, t)$ whereas $\phi(\vec{x}, t)$ is restricted by the boundary conditions, starts at $\phi_a(\vec{x})$ at initial time $t = 0$ and ends at $\phi_a(\vec{x})$ final time $t = t_f$.

The Hamiltonian density of a system is given as

$$\mathcal{H}_d = \pi(\vec{x}, t) \frac{\partial \phi(\vec{x}, t)}{\partial t} - \mathcal{L}(\phi(\vec{x}, t), \dot{\phi}(\vec{x}, t)), \quad (2.64)$$

where $\mathcal{L}(\phi(\vec{x}, t), \dot{\phi}(\vec{x}, t))$ is the Lagrangian density of a system. Now combining (2.63) and (2.64), the transition amplitude can be written as

$$\langle \phi_a | e^{-i\mathcal{H}t} | \phi_a \rangle = \int_{\phi(\vec{x}, 0) = \phi_a(\vec{x})}^{\phi(\vec{x}, t) = \phi_a(\vec{x})} \mathcal{D}\phi e^{i \int_0^t dt \int d^3x \mathcal{L}(\phi(\vec{x}, t), \dot{\phi}(\vec{x}, t))} = \int_{\phi(\vec{x}, 0) = \phi_a(\vec{x})}^{\phi(\vec{x}, t) = \phi_a(\vec{x})} \mathcal{D}\phi e^{iS[\phi]}, \quad (2.65)$$

where $S[\phi]$ is the action of a system. This is the so-called path integral, and here the transition amplitude for a system is simply the sum over all possible paths it may take in going from its initial to its final state.

2.4 Grassmann Variables

The basic feature of Grassmann variables [70, 71] is that they anticommute, so integrals over Grassmann variables are very convenient for dealing with fermionic fields, being described by anticommutation relations. In this subsec, the Grassmann algebra is defined and some integrals which will be needed later on are calculated.

A single Grassmann variable ξ is defined by anticommutation relation as

$$\{\xi, \xi\} = 0. \quad (2.66)$$

It can be generalized to a set of N variables ξ_i and a paired set ξ_i^\dagger . The algebra is defined by

$$\{\xi_i, \xi_j\} = \{\xi_i, \xi_j^\dagger\} = \{\xi_i^\dagger, \xi_j^\dagger\} = 0. \quad (2.67)$$

In particular, from (2.66) the square of any Grassmann number is zero:

$$\xi^2 = 0. \quad (2.68)$$

Because of this the most general function of ξ is defined by using a Taylor series expansion as

$$\xi = a + b\xi, \quad (2.69)$$

where a and b are c -numbers. Using anticommutation rules one can obtain the ordering as

$$\xi_1 \eta_1 \cdots \xi_N \eta_N = (-1)^{\frac{1}{2}N(N-1)} \xi_1 \cdots \xi_N \eta_1 \cdots \eta_N, \quad (2.70)$$

for two Grassmann variables ξ and η . The integration is defined as

$$\int d\xi = 0, \quad (2.71a)$$

$$\int d\xi \xi = 1, \quad (2.71b)$$

and when performing an integral over multiple Grassmann variables, the following sign convention will be used

$$\int d\xi_1 \int d\xi_2 \xi_2 \xi_1 = +1, \quad (2.72)$$

that is, doing the inner integral first. The Gaussian integral over a complex Grassmann variable is defined as

$$\int d\xi^\dagger d\xi e^{-\xi^\dagger b \xi} = \int d\xi^\dagger d\xi (1 - \xi^\dagger b \xi), \quad (2.73)$$

through Taylor expansion and all higher orders vanish. Using anticommutation of ξ and ξ^\dagger one gets

$$\int d\xi^\dagger d\xi e^{-\xi^\dagger b \xi} = \int d\xi^\dagger d\xi (1 + \xi \xi^\dagger b) = b, \quad (2.74)$$

It can be generalized to N Grassmann variables that results in a Gaussian integral involving $N \times N$ matrix d as

$$\int d\xi_1^\dagger d\xi_1 \cdots d\xi_N^\dagger d\xi_N e^{-\xi^\dagger d \xi}. \quad (2.75)$$

This can be calculated by considering N Grassmann variables and components D_{ij} of the matrix which make the exponent hermitian: $(\xi^* D_{ij} \xi)^* = \xi D_{ij} \xi^*$, and expanding the integral, keeping in mind that due to (2.68) only one term will be non-zero

$$\int \prod d\xi_i^* d\xi_i e^{-\xi_i^* D_{ij} \xi_j} = \int d\xi_1^* d\xi_1 \cdots d\xi_N^* d\xi_N \frac{1}{N!} (-\xi_{i_1}^* D_{i_1 j_1} \xi_{j_1}) \cdots (-\xi_{i_N}^* D_{i_N j_N} \xi_{j_N}). \quad (2.76)$$

Now ordering ξ and $d\xi$ following (2.70) one can write

$$\begin{aligned} \int \prod d\xi_i^* d\xi_i e^{-\xi_i^* D_{ij} \xi_j} &= \frac{1}{N!} \int d\xi_1^* \cdots d\xi_N^* \xi_{i_1}^* \cdots \xi_{i_N}^* \int d\xi_1 \cdots d\xi_N \xi_{j_1} \cdots \xi_{j_N} D_{i_1 j_1} \cdots D_{i_N j_N} \\ &= \frac{1}{N!} \varepsilon_{i_1 \cdots i_N} \varepsilon_{j_1 \cdots j_N} D_{i_1 j_1} \cdots D_{i_N j_N} \\ &= \det D, \end{aligned} \quad (2.77)$$

where ε appears from permuting $\xi_{i_1}^* \cdots \xi_{i_N}^*$ to $\xi_1^* \cdots \xi_N^*$, then $\xi_{j_1} \cdots \xi_{j_N}$. Now using the ordering in (2.70) twice for the integrals, one obtains

$$\int d\xi_1^\dagger d\xi_1 \cdots d\xi_N^\dagger d\xi_N e^{-\xi^\dagger d \xi} = \det D. \quad (2.78)$$

which we will be needed for computing the partition function in functional integration approach for fermion and ghost fields later.

3 Imaginary Time Formalism

3.1 Connection to Imaginary Time and Matsubara Formalism

For a given Schrödinger operator, \mathcal{A}_S , the Heisenberg operator, $\mathcal{A}_H(t)$ can be written from (2.38) as

$$\mathcal{A}_H(t) = e^{i\mathcal{H}t} \mathcal{A}_S e^{-i\mathcal{H}t}. \quad (3.1)$$

The thermal correlation function of two operators can also be written from (2.5) as

$$\begin{aligned}
\langle \mathcal{A}_H(t) \mathcal{B}_H(t') \rangle_\beta &= \mathcal{Z}^{-1}(\beta) \text{Tr} \left[e^{-\beta \mathcal{H}} \mathcal{A}_H(t) \mathcal{B}_H(t') \right] \\
&= \mathcal{Z}^{-1}(\beta) \text{Tr} \left[e^{-\beta \mathcal{H}} e^{i\mathcal{H}t} \mathcal{A}_S e^{-i\mathcal{H}t} e^{i\mathcal{H}t'} \mathcal{B}_S e^{i\mathcal{H}t'} \right] \\
&= \mathcal{Z}^{-1}(\beta) \text{Tr} \left[e^{i\mathcal{H}(t+i\beta)} \mathcal{A}_S e^{-i\mathcal{H}t} e^{\beta \mathcal{H}} e^{-\beta \mathcal{H}} e^{i\mathcal{H}t'} \mathcal{B}_S e^{i\mathcal{H}t'} \right] \\
&= \mathcal{Z}^{-1}(\beta) \text{Tr} \left[e^{i\mathcal{H}(t+i\beta)} \mathcal{A}_S e^{-i\mathcal{H}(t+i\beta)} e^{-\beta \mathcal{H}} e^{i\mathcal{H}t'} \mathcal{B}_S e^{i\mathcal{H}t'} \right] \\
&= \mathcal{Z}^{-1}(\beta) \text{Tr} \left[e^{-\beta \mathcal{H}} e^{i\mathcal{H}t'} \mathcal{B}_S e^{i\mathcal{H}t'} e^{i\mathcal{H}(t+i\beta)} \mathcal{A}_S e^{-i\mathcal{H}(t+i\beta)} \right] \\
&= \mathcal{Z}^{-1}(\beta) \text{Tr} \left[e^{-\beta \mathcal{H}} \mathcal{B}_H(t') \mathcal{A}_H(t+i\beta) \right] \\
&= \langle \mathcal{B}_H(t') \mathcal{A}_H(t+i\beta) \rangle_\beta,
\end{aligned} \tag{3.2}$$

This is called Kubo-Martin-Schwinger (KMS) relation. This relation holds irrespective of Grassmann parities of the operators, *viz.*, for bosonic as well as fermionic operator. In the following we have number of points to emphasize:

1. This KMS relation will lead to periodicity for boson and anti-periodicity for fermions because of commutation and anti-commutation relations, respectively.
2. The imaginary temperature $i\beta = i/T$ is connected to the time t , which means that the temperature is related to the imaginary time as $\beta = it$ as shown in Fig. 4. This is called *Wick rotation*.

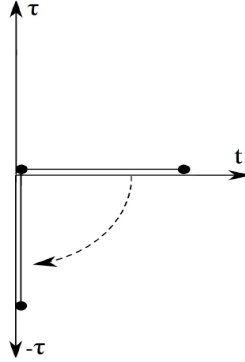


Figure 4: The Wick rotation in the imaginary time axis: $t = -i\tau$

3. It is important to note that the Boltzmann factor $e^{-\beta \mathcal{H}}$ acquires the form of a time evaluation operator ($e^{-i\mathcal{H}t}$) for imaginary time ($\beta = it$) through analytic continuation. It may be a mere coincidence but there may be some deeper connection which is not known yet!
4. $\beta = 1/T = it \Rightarrow \beta$ becomes finite.

5. Using the time evolution operator, one can obtain \mathcal{S} -Matrix, and thus Feynman rules and diagrams.
6. The Matsubara (imaginary time) formalism [1] yields a way of evaluating partition function and other quantities through a diagrammatic method which is similar to that in zero temperature field theory.

We note that there are two prescriptions for Matsubara formalism : i) Operatorial Method ii) Path Integral Method. In the next subsec 3.2, we will discuss operatorial formalism while the path integral or functional integral formalism will be illustrated when we discuss partition function of a system later in subsec 6.1 .

3.2 Matsubara Formalism (Operatorial Method)

The Hamiltonian of a system can be decomposed as

$$\mathcal{H} = \mathcal{H}_0 + \mathcal{H}' , \quad (3.3)$$

where \mathcal{H}_0 and \mathcal{H}' are the free and interaction parts, respectively. The purpose of doing so is to describe the interaction in terms of free field (free theory). However, $\mathcal{H}_0 = H_0 - \mu N$ for grand canonical ensemble but we do it in general.

Now one can write the density matrix from (2.1) as

$$\begin{aligned} \rho(\beta) &= e^{-\beta\mathcal{H}} = e^{-\beta\mathcal{H}_0} e^{-\beta\mathcal{H}'} = \rho_0(\beta) \mathcal{S}(\beta) \\ \text{with } \rho_0(\beta) &\equiv e^{-\beta\mathcal{H}_0}, \text{ and } \mathcal{S}(\beta) = e^{\beta\mathcal{H}_0} e^{-\beta\mathcal{H}} = \rho_0^{-1}(\beta) \rho(\beta). \end{aligned} \quad (3.4)$$

The density matrix can have evolution equation [12] with $0 \leq \tau \leq \beta$:

$$\begin{aligned} \frac{\partial \rho_0(\tau)}{\partial \tau} &= \frac{\partial}{\partial \tau} (e^{-\tau\mathcal{H}_0}) = -\mathcal{H}_0 \rho_0(\tau) \\ \frac{\partial \rho(\tau)}{\partial \tau} &= \frac{\partial}{\partial \tau} (e^{-\tau\mathcal{H}}) = -\mathcal{H} \rho(\tau) = -(\mathcal{H}_0 + \mathcal{H}') \rho(\tau). \end{aligned} \quad (3.5)$$

Now $\mathcal{S}(\tau)$ satisfies the evolution equation with $0 \leq \tau \leq \beta$, following (3.4) and (3.5), as

$$\begin{aligned} \frac{\partial \mathcal{S}(\tau)}{\partial \tau} &= \frac{\partial}{\partial \tau} [\rho_0^{-1}(\tau) \rho(\tau)] = \frac{\partial \rho_0^{-1}(\tau)}{\partial \tau} \rho(\tau) + \rho_0^{-1}(\tau) \frac{\partial \rho(\tau)}{\partial \tau} \\ &= \frac{\partial}{\partial \tau} (e^{\tau\mathcal{H}_0}) \rho(\tau) + \rho_0^{-1}(\tau) [-(\mathcal{H}_0 + \mathcal{H}')] \rho(\tau) \\ &= \rho_0^{-1}(\tau) \mathcal{H}_0 \rho(\tau) - \rho_0^{-1}(\tau) \mathcal{H}_0 \rho(\tau) - \rho_0^{-1}(\tau) \mathcal{H}' \rho(\tau) \\ &= -\rho_0^{-1}(\tau) \mathcal{H}' \rho(\tau) = -\rho_0^{-1}(\tau) \mathcal{H}' \rho_0(\tau) \mathcal{S}(\tau) \\ &= -e^{\tau\mathcal{H}_0} \mathcal{H}' e^{-\tau\mathcal{H}_0} \mathcal{S}(\tau) \\ &= -\mathcal{H}'_1(\tau) \mathcal{S}(\tau) , \end{aligned} \quad (3.6)$$

with modified interaction Hamiltonian is related to Schrödinger picture as $\mathcal{H}'_1(\tau) = e^{\tau\mathcal{H}_0} \mathcal{H}' e^{-\tau\mathcal{H}_0}$ in quantum field theory. We note following points in general:

Operator in interaction picture in quantum field theory: $\mathcal{A}(t) = e^{i\mathcal{H}_0 t} \mathcal{A} e^{-i\mathcal{H}_0 t}$; Adjoint operator: $\mathcal{A}^\dagger(t) = e^{i\mathcal{H}_0 t} \mathcal{A}^\dagger e^{-i\mathcal{H}_0 t}$; Transformed adjoint operator: $\mathcal{A}^T(t) = e^{i\mathcal{H}_0 t} \mathcal{A}^\dagger e^{-i\mathcal{H}_0 t}$. This implies that $\mathcal{A}^\dagger(t) = \mathcal{A}^T(t)$.

On the other hand, the operator in τ space: $\mathcal{A}(\tau) = e^{\tau\mathcal{H}_0} \mathcal{A} e^{-\tau\mathcal{H}_0}$; Adjoint operator: $\mathcal{A}^\dagger(\tau) = e^{-\tau\mathcal{H}_0} \mathcal{A}^\dagger e^{\tau\mathcal{H}_0}$; Transformed adjoint operator: $\mathcal{A}^T(\tau) = e^{\tau\mathcal{H}_0} \mathcal{A}^\dagger e^{-\tau\mathcal{H}_0}$. This indicates that $\mathcal{A}^\dagger(\tau) \neq \mathcal{A}^T(\tau)$. Thus, the transformation in τ is not unitary, $\mathcal{A}^\dagger(\tau) \neq \mathcal{A}(\tau)$, for real τ because the adjoint of an operator does not coincide with the transformed adjoint operator. This can be avoided if τ is imaginary, $\tau = it$. Under such rotation a hermitian field remains hermitian with the *appropriate definition of hermiticity for complex coordinates*, $\phi^\dagger(\tau = it) = \phi(\tau^*)$, because the argument becomes complex. This makes Matsubara formalism an *imaginary time* formalism as shown pictorially in Fig. 4. The Matsubara formalism becomes almost equivalent to zero temperature field theory with exception that τ becomes finite $0 \leq \tau \leq \beta$.

3.3 Evolution Operator and S-Matrix

The evaluation operator in (3.6) in a finite interval $0 \leq \tau \leq \beta$ reads (dropped superscript 'I') as [12]

$$\frac{\partial \mathcal{S}(\tau)}{\partial \tau} = -\mathcal{H}'(\tau) \mathcal{S}(\tau) , \quad (3.7)$$

With boundary condition $\mathcal{S}(0) = 1$, $\mathcal{H}' \rightarrow 0$. At $\tau = 0$ all fields are free. This implies that interaction builds on with the evolution and leads to $\mathcal{S}(\tau)$. Other way, when the interaction is turned on, the free particles move in, interact and then move away in the finite interval $0 \leq \tau \leq \beta$.

Integrating (3.7) in the interval $0 \leq \tau \leq \beta$, one can get

$$\mathcal{S}(\beta) - \mathcal{S}(0) = - \int_0^\beta d\tau \mathcal{H}'(\tau) \mathcal{S}(\tau) \quad (3.8)$$

This is an exact equation obeyed by $\mathcal{S}(\tau)$ but cannot be solved. Using the same iterative method as zero temperature case [12]:

$$\mathcal{S}(\beta) = \mathcal{T} \left[\exp \left(- \int_0^\beta \mathcal{H}' d\tau \right) \right] , \quad (3.9)$$

where \mathcal{T} is the time ordered product in imaginary time $\tau = it$. This (3.9) is same as zero temperature field theory with the exception that the imaginary time integration is in finite interval $0 \leq \tau \leq \beta$. For a given interaction \mathcal{H}' , one can expand the exponential and each term in the expansion will lead to Feynman diagram of various orders in interaction strength (coupling of the theory). We can now make following comments on Feynman rules:

1. The interaction vertex is same as those of zero temperature.

2. The symmetry factor for a given loop diagram is same as those of zero temperature.
3. What should be the structure of finite temperature propagator in imaginary time is not clear yet!.
4. What should be the form of finite temperature loop integral in imaginary time is not clear yet.

3.4 Two-Point Correlation Function: Green's Function

3.4.1 Green's function at $T = 0$ in Minkowski time (real time)

The Greens function for $T = 0$ in Minkowski time is defined [72] as

$$G(X, X') = \langle 0 | \mathcal{T}_t [\Phi(X) \Phi(X')] | 0 \rangle, \quad (3.10)$$

where $X \equiv (x_0, \vec{x})$ and the time ordered (\mathcal{T}_t) product of two fields in real time:

$$\mathcal{T}_t [\Phi(X) \Phi(X')] = \Theta(t - t') \Phi(X) \Phi(X') + \Theta(t' - t) \Phi(X') \Phi(X), \quad (3.11)$$

where the scalar field can be expressed as

$$\Phi(X) = \int \frac{d^3 k}{(2\pi)^{3/2}} \frac{1}{(2\omega_k)^{1/2}} \left[a(k) e^{-iK \cdot X} + a^\dagger(k) e^{iK \cdot X} \right], \quad (3.12)$$

with $K \equiv (k_0, \vec{k})$, $\omega_k = \sqrt{k^2 + m^2}$, $a(k)$ is the annihilation operator and $a^\dagger(k)$ is the creation operator.

The vacuum is defined as $a(k)|0\rangle = 0$.

The multiparticle states can be written from (2.8) as

$$|n\rangle = |n_1(k_1), n_2(k_2), n_3(k_3) \dots \rangle = \prod_i \frac{[a^\dagger(k_i)]^{n_i(k_i)}}{\sqrt{n_i(k_i)!}} |0\rangle, \quad (3.13a)$$

$$a(k_i) |n_i(k_i)\rangle = \sqrt{n(k_i)} |n_i(k_i) - 1\rangle, \quad (3.13b)$$

$$a^\dagger(k_i) |n_i(k_i)\rangle = \sqrt{n(k_i) + 1} |n_i(k_i) + 1\rangle. \quad (3.13c)$$

Using (3.10), (3.12), (3.13a), (3.13b) and (3.13c), the Green's function¹ can be written as

$$G(X - X') = \int \frac{d^4 K}{(2\pi)^4} \frac{e^{-iK \cdot (X - X')}}{K^2 - m^2} = \int \frac{d^4 K}{(2\pi)^4} e^{-iK \cdot (X - X')} G(K), \quad (3.14)$$

where the momentum space Green's function is given as

$$G(K) = \frac{1}{K^2 - m^2} = \frac{1}{k_0^2 - \omega_k^2}. \quad (3.15)$$

¹One can also get it as a solution of Klein Gordon equation with a unit source term.

We note that though Green's function is a two-point function, it depends on the differences of the two endpoints because of translational invariance. Now, this $G(X - X')$ describes the free propagation of scalar particle from X' to X for $x_0 = t > x'_0 = t'$ implying creation at X' and destruction at X .

Now $G(K)$ has poles at $k_0 = \pm\omega_k$ on the real axis. With Feynman prescription one can write $G(K)$ in (3.15) by shifting its poles in complex plane as

$$\begin{aligned}\Delta_F(K) &= \frac{1}{K^2 - m^2 + i\epsilon'} = \frac{1}{k_0^2 - (\omega_k - i\epsilon)^2} \\ &= \frac{1}{2\omega_k} \left[\frac{1}{k_0 - \omega_k + i\epsilon} - \frac{1}{k_0 + \omega_k - i\epsilon} \right],\end{aligned}\quad (3.16)$$

where $\Delta_F(K)$ is complex and ϵ and ϵ' are small number and related by $\epsilon' = 2\epsilon\omega_k$. However, we do not distinguish them as $\epsilon \rightarrow 0$ at the end of the calculation. Now (3.14) can be written with Feynman prescription as

$$\Delta_F(X - X') = \int \frac{d^4 K}{(2\pi)^4} \frac{e^{-iK \cdot (X - X')}}{K^2 - m^2 + i\epsilon'} = \int \frac{d^4 K}{(2\pi)^4} e^{-iK \cdot (X - X')} \Delta_F(K), \quad (3.17)$$

Integrating over k_0 in complex k_0 plane [72], one finds

$$\begin{aligned}\Delta_F(X - X') &= -i \int \frac{d^3 k}{(2\pi)^3} \frac{1}{2\omega_k} \left[e^{-iK \cdot (X - X')} \Theta(t - t') + e^{iK \cdot (X - X')} \Theta(t' - t) \right] \Big|_{k_0 = \omega_k} \\ i\Delta_F(X - X') &= \int \frac{d^3 k}{(2\pi)^3} \frac{1}{2\omega_k} \left[e^{-iK \cdot (X - X')} \Theta(t - t') + e^{iK \cdot (X - X')} \Theta(t' - t) \right] \Big|_{k_0 = \omega_k} \\ &= \langle 0 | \mathcal{T}_t [\Phi(X) \Phi(X')] | 0 \rangle,\end{aligned}\quad (3.18)$$

which is the Feynman propagator. Now comparing (3.18) and (3.10), the Green's function becomes

$$G(X - X') = \int \frac{d^3 k}{(2\pi)^3} \frac{1}{2\omega_k} \left[e^{-iK \cdot (X - X')} \Theta(t - t') + e^{iK \cdot (X - X')} \Theta(t' - t) \right] \Big|_{k_0 = \omega_k}, \quad (3.19)$$

where the first part in right side is for retarded time ($t > t'$) whereas the second part is for advanced time ($t' > t$).

3.4.2 Green's function at $T \neq 0$ Minkowski time (real time)

Greens function in thermal environment in Minkowski time can be written as

$$\begin{aligned}G_\beta(X, X') &= i\Delta_F(X - X') = \langle |\mathcal{T}_t [\Phi(X) \Phi(X')] | \rangle_\beta \\ &= \frac{1}{\mathcal{Z}(\beta)} \text{Tr} \left(e^{-\beta \mathcal{H}} \mathcal{T}_t [\Phi(X) \Phi(X')] \right) \\ &= \frac{1}{\mathcal{Z}(\beta)} \sum_n \langle n | \mathcal{T}_t [\Phi(X) \Phi(X')] | n \rangle e^{-\beta E_n},\end{aligned}\quad (3.20)$$

where $\langle \rangle_\beta$ is the thermal expectation value and $\mathcal{Z}(\beta)$ is the partition function. Trace stands for sum over a complete many-particles states in Hilbert space, which is replaced by a sum that runs over a complete many-particle states $|n\rangle$ weighted by the Boltzmann factor $e^{-\beta E_n}$ in thermal environment², a little different than $T = 0$ case.

We would now like to compute the Green's function [61, 62] for $t > t'$ using (3.11) and (3.12) as

$$\begin{aligned}
G_\beta^>(X, X') &= \frac{1}{\mathcal{Z}(\beta)} \int \frac{d^3k}{(2\pi)^{3/2}} \frac{d^3k'}{(2\pi)^{3/2}} \frac{1}{(2\omega_k)^{1/2}} \frac{1}{(2\omega_{k'})^{1/2}} \sum_n e^{-\beta E_n} \\
&\quad \times \left\langle n \left| \left\{ a(k)e^{-iK \cdot X} + a^\dagger(k)e^{iK \cdot X} \right\} \left\{ a(k')e^{-iK' \cdot X'} + a^\dagger(k')e^{iK' \cdot X'} \right\} \right| n \right\rangle \\
&= \frac{1}{\mathcal{Z}(\beta)} \int \frac{d^3k}{(2\pi)^{3/2}} \frac{d^3k'}{(2\pi)^{3/2}} \frac{1}{(2\omega_k)^{1/2}} \frac{1}{(2\omega_{k'})^{1/2}} \sum_n e^{-\beta E_n} \\
&\quad \left\langle n \left| a(k)a(k')e^{-iK \cdot X}e^{-iK' \cdot X'} + a^\dagger(k)a(k')e^{iK \cdot X}e^{-iK' \cdot X'} \right. \right. \\
&\quad \left. \left. + a(k)a^\dagger(k')e^{-iK \cdot X}e^{iK' \cdot X'} + a^\dagger(k)a^\dagger(k')e^{iK \cdot X}e^{iK' \cdot X'} \right| n \right\rangle. \tag{3.21}
\end{aligned}$$

On using (3.13b), (3.13c) and the orthonormal conditions, the second and third terms in (3.21) would survive as

$$\begin{aligned}
G_\beta^>(X - X') &= \frac{1}{\mathcal{Z}(\beta)} \int \frac{d^3k}{(2\pi)^{3/2}} \frac{d^3k'}{(2\pi)^{3/2}} \frac{1}{(2\omega_k)^{1/2}} \frac{1}{(2\omega_{k'})^{1/2}} \sum_n e^{-\beta E_n} \\
&\quad \times \left[\sqrt{n(k)n(k')} \delta^3(\vec{k} - \vec{k}') e^{i(K \cdot X - K' \cdot X')} \right. \\
&\quad \left. + \sqrt{[n(k) + 1][n(k') + 1]} \delta^3(\vec{k} - \vec{k}') e^{-i(K \cdot X + K' \cdot X')} \right] \\
&= \frac{1}{\mathcal{Z}(\beta)} \int \frac{d^3k}{(2\pi)^3} \frac{1}{2\omega_k} \sum_n e^{-\beta E_n} \left[(n(k) + 1) e^{-iK \cdot (X - X')} \right. \\
&\quad \left. + n(k) e^{iK \cdot (X - X')} \right]. \tag{3.22}
\end{aligned}$$

Now we use

$$\begin{aligned}
\frac{1}{\mathcal{Z}(\beta)} \sum_n n(k) e^{-\beta E_n} &= \frac{1}{\mathcal{Z}(\beta)} \sum_n n(k) e^{-\beta \omega_k n(k)} = \frac{1}{\mathcal{Z}(\beta)} \sum_n n \left[e^{-\beta \omega_k} \right]^n \\
&= \frac{1}{e^{\beta \omega_k} - 1} \equiv n_B(\omega(k)), \tag{3.23}
\end{aligned}$$

$$\frac{1}{\mathcal{Z}(\beta)} \sum_n e^{-\beta E_n} = 1, \tag{3.24}$$

where $n_B(\omega_k)$ is the Bose-Einstein distribution.

²We note that the Lorentz invariance is broken at $T \neq 0$ which we will discuss later in details. However, E can be written in the rest frame of the medium (heat bath) as $E = u_\mu K^\mu = u \cdot K$, where u is four velocity of the medium (heat bath) in its rest frame with $u_\mu = (1, 0, 0, 0)$.

Combining (3.23) and (3.24) with (3.22), we can have

$$G_{\beta}^{>}(X - X') = \int \frac{d^3k}{(2\pi)^3} \frac{1}{2\omega_k} \left[(1 + n_B) e^{-iK \cdot (X - X')} + n_B e^{iK \cdot (X - X')} \right], \quad (3.25)$$

which is the Green's function for $t > t'$. At $T = 0$, $n_B(\omega_k) = 0$ and (3.25) reduces to

$$G_{\beta}^{>}(X - X') = \int \frac{d^3k}{(2\pi)^3} \frac{1}{2\omega_k} e^{-iK \cdot (X - X')}, \quad (3.26)$$

which agrees with the first term in (3.19).

Now the physical interpretations of Eq.(3.25) are given below:

- At finite T , like zero temperature ($T = 0$), a scalar field which is created at X' , i.e., t' propagates to X at t and then annihilated.
- Besides spontaneous creation at X' , there will also be induced creation (first term in (3.25) involving n_B) at X' and absorption (second term involving n_B) at X due to the presence of heat bath.

Similarly, the Green's function for $t' > t$ can be obtained from the symmetry property ($K \rightarrow -K$) as

$$G_{\beta}^{<}(X - X') = \int \frac{d^3k}{(2\pi)^3} \frac{1}{2\omega_k} \left[n_B e^{-iK \cdot (X - X')} + (1 + n_B) e^{iK \cdot (X - X')} \right], \quad (3.27)$$

which reduces to the second term in (3.19) at $T = 0$ as

$$G_{\beta}^{<}(X - X') = \int \frac{d^3k}{(2\pi)^3} \frac{1}{2\omega_k} e^{iK \cdot (X - X')}. \quad (3.28)$$

3.4.3 Green's function at $T \neq 0$ in Euclidean time (imaginary time)

Following (3.2), the thermal Green's function can be written as

$$\begin{aligned} G_{\beta}(\tau, \tau') &= \langle \mathcal{T} [\Phi_H(\tau) \Phi_H(\tau')] \rangle_{\beta} \\ &= \mathcal{Z}^{-1}(\beta) \text{Tr} \left(e^{-\beta \mathcal{H}} \mathcal{T} [\Phi_H(\tau) \Phi_H(\tau')] \right) \end{aligned} \quad (3.29)$$

with $\Phi_H(\tau) = e^{\tau \mathcal{H}} \Phi e^{-\tau \mathcal{H}}$. The time variables τ, τ' lie between $0 \leq \tau \leq \beta$ and $0 \leq \tau' \leq \beta$. \mathcal{T} is imaginary time ordering. We have suppressed spatial dependence as it could be included any time. The field Φ can represent bosonic/fermionic field. The spinor indices are also suppressed here but can be taken care wherever needed. Imaginary time ordering \mathcal{T} is same as zero temperature field theory. Then

$$\mathcal{T} [\Phi_H(\tau) \Phi_H(\tau')] = \Theta(\tau - \tau') \Phi_H(\tau) \Phi_H(\tau') \pm \Theta(\tau' - \tau) \Phi_H(\tau') \Phi_H(\tau), \quad (3.30)$$

where \pm refer to boson/fermion, respectively.

Though Green's function is a two-point function, it depends on the differences of the two endpoints because of translational invariance as $G_{\beta}(\vec{x} - \vec{x}'; \tau - \tau')$. The time variables τ, τ' lie between $0 \leq \tau \leq \beta$ and $0 \leq \tau' \leq \beta$. This implies that two-point function has $-\beta \leq \tau - \tau' \leq \beta$.

3.5 Periodicity (Anti-periodicity) of the Green's Function

The thermal Green's function [12] from (3.29) for $\tau > \tau'$:

$$\begin{aligned}
G_\beta(\vec{x}, \vec{x}'; \tau, \tau') &= \mathcal{Z}^{-1}(\beta) \text{Tr} \left(e^{-\beta \mathcal{H}} \mathcal{T} [\Phi_H(\vec{x}, \tau) \Phi_H(\vec{x}', \tau')] \right) \\
&\stackrel{=}{=} \mathcal{Z}^{-1}(\beta) \text{Tr} \left[e^{-\beta \mathcal{H}} \Phi_H(\vec{x}, \tau) \Phi_H(\vec{x}', \tau') \Theta(\tau - \tau') \right] \\
&\stackrel{=}{=} \mathcal{Z}^{-1}(\beta) \text{Tr} \left[\Theta(\tau - \tau') \Phi_H(\vec{x}', \tau') e^{-\beta \mathcal{H}} \Phi_H(\vec{x}, \tau) \right] \\
&\stackrel{=}{=} \mathcal{Z}^{-1}(\beta) \text{Tr} \left[\Theta(\tau - \tau') e^{-\beta \mathcal{H}} e^{\beta \mathcal{H}} \Phi_H(\vec{x}', \tau') e^{-\beta \mathcal{H}} \Phi_H(\vec{x}, \tau) \right] \\
&\stackrel{=}{=} \mathcal{Z}^{-1}(\beta) \text{Tr} \left[\Theta(\tau - \tau') e^{-\beta \mathcal{H}} \Phi_H(\vec{x}', \tau' + \beta) \Phi_H(\vec{x}, \tau) \right] \\
&\stackrel{=}{=} \pm \mathcal{Z}^{-1}(\beta) \text{Tr} \left[e^{-\beta \mathcal{H}} \Theta(\tau - \tau') \Phi_H(\vec{x}, \tau) \Phi_H(\vec{x}', \tau' + \beta) \right] \\
&= \pm G_\beta(\vec{x}, \vec{x}'; \tau, \tau' + \beta).
\end{aligned} \tag{3.31}$$

We have used the cyclic properties of the trace, inserted the unit operator $1 = e^{-\beta \mathcal{H}} e^{\beta \mathcal{H}}$, and used the time evolution of the state: $\Phi_H(\vec{x}', \tau' + \beta) = e^{\beta \mathcal{H}} \Phi_H(\vec{x}', \tau') e^{-\beta \mathcal{H}}$.

Since the Green's function alters sign for Dirac field after one period of β , this means that the Dirac fields must be antiperiodic in imaginary time as $\Phi(\vec{x}, \tau) = -\Phi(\vec{x}, \tau + \beta)$, whereas bosonic fields are periodic as they do not change sign as $\Phi(\vec{x}, \tau) = \Phi(\vec{x}, \tau + \beta)$. Since we didn't touch upon space direction, it remains unaffected as: $-\infty \leq x \leq \infty \Rightarrow \text{open}$.

In $T = 0$ (Minkowski space-time) both space and time remain open: $-\infty \leq x \leq \infty$ and $-\infty \leq t \leq \infty$. Topology: Structure of space-time at $R^4 = R^3 \times R^1$ where both space and time are open and in equal footing. In $T \neq 0$ (Euclidean space; imaginary time): space remains open $-\infty \leq x \leq \infty \Rightarrow R^3$. Time remains closed: $0 \leq \tau \leq \beta \Rightarrow R^1 \rightarrow S^1$ (circle). Topology: Structure of space-time at $T \neq 0$ is transformed as $R^4 = R^3 \times R^1 \Rightarrow R^3 \times S^1$. This changes the temporal components leaving the spatial components unaffected. *It amounts to decoupling of space and time and the theory is no longer Lorentz invariant.*

Further, the chemical potential can also be inducted by transforming the temporal component of the gauge field, through a substitution $\partial_0 - i\mu$ in the Lagrangian. Such substitution changes the temporal component while leaving the spatial components of the gauge field unaltered. It also decouples space and time and the theory is no more Lorentz invariant. *In addition to explicitly breaking the Lorentz invariance, the presence of a chemical potential may additionally break other internal symmetries.*

At T and $\mu \neq 0$ field theory is equivalent to quantising a quantum system in finite box, i.e., one dimensional box in τ direction ($0 \leq \tau \leq \beta$) but space remains open, i.e., $R^3 \times S^1$ in which Lorentz invariance is broken.

3.6 Discrete Frequency (Matsubara Frequency)

The Fourier decomposition of Green's function [12] in real time (Minkowski space-time)

$$\begin{aligned}
G(\vec{x}, \vec{x}'; t, t') &= \int \frac{d^4 K}{(2\pi)^4} e^{-iK \cdot (X - X')} G(K) \\
&= \int \frac{d^3 k}{(2\pi)^3} e^{i\vec{k} \cdot (\vec{x} - \vec{x}')} \int \frac{dk_0}{2\pi} e^{-ik_0(x_0 - x'_0)} G(k_0, \vec{k}),
\end{aligned} \tag{3.32}$$

where a four vector is defined as $Q \equiv (q_0, \mathbf{q})$ and $G(K)$ is momentum space Green's function.

For convenience we assume $X' = 0 \Rightarrow x' = 0, x'_0 = t' = 0$:

$$G(\mathbf{x}, 0; t, 0) = \int \frac{d^3 k}{(2\pi)^3} e^{i\vec{k} \cdot \vec{x}} \int \frac{dk_0}{2\pi} e^{-ik_0 t} G(k_0, \vec{k}). \tag{3.33}$$

Now switching over from Minkowski space (real time) to Euclidean space (imaginary time): $t \rightarrow -i\tau; \quad k_0 \rightarrow ik_4, \quad \vec{x} \rightarrow \vec{x}$ and $\vec{k} \rightarrow \vec{k}$. With this (3.33) reads as

$$G_\beta(\vec{x}, \tau) = \int \frac{d^3 k}{(2\pi)^3} e^{i\vec{k} \cdot \vec{x}} \int \frac{d(ik_4)}{2\pi} e^{-i(ik_4)(-i\tau)} G(k_0 = ik_4, \vec{k}). \tag{3.34}$$

Since τ is finite ($0 \leq \tau \leq \beta$), the corresponding Fourier transform reads as

$$\int \frac{d(ik_4)}{2\pi} f(ik_4, \vec{k}) \rightarrow \frac{1}{\beta} \sum_{n=-\infty}^{n=+\infty} f(k_0 = ik_4 = i\omega_n, \vec{k}). \tag{3.35}$$

The finiteness of Euclidean time τ will result in discrete frequency with a \sum over it.

Now (3.34) reads as

$$G_\beta(\vec{x}, \tau) = \frac{1}{\beta} \sum_{n=-\infty}^{n=+\infty} \int \frac{d^3 k}{(2\pi)^3} e^{i\vec{k} \cdot \vec{x}} e^{-i\omega_n \tau} G_\beta(k_0 = i\omega_n, \vec{k}). \tag{3.36}$$

This indicates that going from Minkowski to Euclidean time, one needs to replace

$$\int \frac{d^4 K}{(2\pi)^4} \rightarrow \frac{1}{\beta} \sum_{n=-\infty}^{n=+\infty} \int \frac{d^3 k}{(2\pi)^3}. \tag{3.37}$$

We can now drop the space dependent part in (3.36) as it is irrelevant for the time being but can be put back when required:

$$G_\beta(\tau) = \frac{1}{\beta} \sum_{m=-\infty}^{m=+\infty} e^{-i\omega_m \tau} G_\beta(i\omega_m), \tag{3.38}$$

where the inverse transformation is given as

$$G_\beta(i\omega_m) = \frac{1}{2} \int_{-\beta}^{+\beta} d\tau e^{i\omega_m \tau} G_\beta(\tau), \tag{3.39}$$

with $\omega_m = m\pi/\beta$; $m = 0, \pm 1, \pm 2, \pm 3, \dots$ as all integer modes are allowed in Fourier transformation. However, the value of m will be restricted according to (3.31) because the two points function for bosonic fields satisfies periodicity condition as , $G_\beta(\tau) = G_\beta(\tau + \beta)$, whereas the two points function for fermionic fields satisfies anti-periodicity condition as $G_\beta(\tau) = -G_\beta(\tau + \beta)$.

We now split (3.39) as

$$\begin{aligned} G_\beta(i\omega_m) &= \frac{1}{2} \int_{-\beta}^0 d\tau e^{i\omega_m \tau} G_\beta(\tau) + \frac{1}{2} \int_0^\beta d\tau e^{i\omega_m \tau} G_\beta(\tau) \\ &= \pm \frac{1}{2} \int_{-\beta}^0 d\tau e^{i\omega_m \tau} G_\beta(\tau + \beta) + \frac{1}{2} \int_0^\beta d\tau e^{i\omega_m \tau} G_\beta(\tau) \end{aligned} \quad (3.40)$$

where in the first term ‘+’ refers to boson whereas ‘-’ refers to fermion. Now we make changes $\tau \rightarrow -\tau$ in the first term as

$$G_\beta(i\omega_m) = \pm \frac{1}{2} \int_0^\beta d\tau e^{-i\omega_m \tau} G_\beta(-\tau + \beta) + \frac{1}{2} \int_0^\beta d\tau e^{i\omega_m \tau} G_\beta(\tau). \quad (3.41)$$

Again in the first term of (3.41) we change a variable as $-\tau + \beta = \tau \Rightarrow$ upper limit: 0 and lower limit: β , then

$$\begin{aligned} G_\beta(i\omega_m) &= \pm \frac{1}{2} \int_0^\beta d\tau e^{i\omega_m(\tau-\beta)} G_\beta(\tau) + \frac{1}{2} \int_0^\beta d\tau e^{i\omega_m \tau} G_\beta(\tau) \\ &= \frac{1}{2} \left(1 \pm e^{-i\omega_m \beta} \right) \int_0^\beta d\tau e^{i\omega_m \tau} G_\beta(\tau) = \frac{1}{2} \left(1 \pm e^{-i \frac{m\pi}{\beta} \beta} \right) \int_0^\beta d\tau e^{i\omega_m \tau} G_\beta(\tau) \\ &= \frac{1}{2} \left(1 \pm (-1)^m \right) \int_0^\beta d\tau e^{i\omega_m \tau} G_\beta(\tau). \end{aligned} \quad (3.42)$$

We note that ‘+’ is for boson. This implies that m has to be even $\Rightarrow \omega_n = \frac{2\pi n}{\beta}$ with $n \in \mathbb{Z}$. Now, ‘-’ is for fermion which implies that m has to be odd $\Rightarrow \omega_n = \frac{(2n+1)\pi}{\beta}$ with $n \in \mathbb{Z}$. Thus,

$$\begin{aligned} G_\beta(\tau) &= \frac{1}{\beta} \sum_{n=-\infty}^{n=+\infty} e^{-i\omega_n \tau} G_\beta(i\omega_n) \\ G_\beta(i\omega_n) &= \int_0^\beta d\tau e^{i\omega_n \tau} G_\beta(\tau), \end{aligned} \quad (3.43)$$

with the discrete Matsubara frequency ω_n as the characteristics of the imaginary time and represented by

$$k_0 = ik_4 = i\omega_n = \begin{cases} \frac{2n\pi i}{\beta} & \text{for boson ,} \\ \frac{(2n+1)\pi i}{\beta} & \text{for fermion.} \end{cases}$$

Now, the complete Green's function:

$$G_\beta(\vec{x}, \tau) = \frac{1}{\beta} \sum_{n=-\infty}^{+\infty} \int \frac{d^3k}{(2\pi)^3} e^{-i(\omega_n\tau - \vec{k}\cdot\vec{x})} G_\beta(i\omega_n, \vec{k}), \quad (3.44)$$

$$G_\beta(i\omega_n, \vec{k}) = \int_0^\beta d\tau \int d^3x e^{i(\omega_n\tau - \vec{k}\cdot\vec{x})} G_\beta(\vec{x}, \tau). \quad (3.45)$$

3.7 Dictionary: $T = 0$ to $T \neq 0$ Field Theory (Imaginary Time)

$T = 0; -\infty \leq t \leq \infty$	$T \neq 0; 0 \leq \tau(=it) \leq \beta$
Topology: $R^4 = R^3 \times R^1$ $-\infty \leq x, t \leq \infty$ (open)	Topology: $R^4 = R^3 \times S$ $-\infty \leq x, \leq \infty$ (open); $0 \leq \tau \leq \beta$ (closed)
Operator in Interaction Picture $\mathcal{A}_I(t) = e^{i\mathcal{H}_0 t} \mathcal{A}_S e^{-i\mathcal{H}_0 t}$ $\mathcal{A}_I^T(t) = e^{i\mathcal{H}_0 t} \mathcal{A}_S^\dagger e^{-i\mathcal{H}_0 t} \Rightarrow \mathcal{A}_I^\dagger(t) = \mathcal{A}_I^T(t)$ Transformation is Unitary	Operator in Interaction Picture $\mathcal{A}_I(\tau) = e^{\tau\mathcal{H}_0} \mathcal{A}_S e^{-\tau\mathcal{H}_0}$ $\mathcal{A}_I^T(\tau) = e^{\tau\mathcal{H}_0} \mathcal{A}_S^\dagger e^{-\tau\mathcal{H}_0} \Rightarrow \mathcal{A}_I^\dagger(\tau) \neq \mathcal{A}_I^T(\tau)$ It's not Unitary
Interaction Hamiltonian in IP $\mathcal{H}'_I(t) = e^{i\mathcal{H}_0 t} \mathcal{H}'_S e^{-i\mathcal{H}_0 t}$	Interaction Hamiltonian in IP $\mathcal{H}'_I(\tau) = e^{\tau\mathcal{H}_0} \mathcal{H}'_S e^{-\tau\mathcal{H}_0}$
Time evolution $i \frac{\partial \Phi(t)}{\partial t} = \mathcal{H}'_I(t) \Phi(t)$ $\Phi(t)$ is built up from $\Phi(0)$	Time evolution $\frac{\partial \mathcal{S}(\tau)}{\partial \tau} = -\mathcal{H}'_I(\tau) \mathcal{S}(\tau)$ $\mathcal{S}(\tau)$ is built up from $\mathcal{S}(0)$
\mathcal{S} -Matrix $\mathcal{S} = \mathcal{T} \left[\exp \left(-i \int_{-\infty}^{\infty} \mathcal{H}'_I(t) dt \right) \right]$ \mathcal{T} : Time ordering	\mathcal{S} -Matrix $\mathcal{S}(\beta) = \mathcal{T} \left[\exp \left(- \int_0^\beta \mathcal{H}'_I(\tau) d\tau \right) \right]$ \mathcal{T} : Imaginary time ordering
Wicks Theorem	Same
Vertex	Same
Symmetry factor	Same
Boundary Conditions $G(X, X')$ $-\infty < X, X' < \infty$	Boundary Conditions $G_\beta(\vec{x}, \vec{x}'; \tau, \tau') = \pm G_\beta(\vec{x}, \vec{x}'; \tau, \tau' + \beta)$ (+) for boson; (-) for fermion
Green's Function $G(X, X') = \langle 0 \mathcal{T} [\Phi(X) \Phi(X')] 0 \rangle$	Green's Function $G_\beta(\vec{x}, \vec{x}'; \tau, \tau') = \langle \mathcal{T} [\Phi_H(\vec{x}, \tau) \Phi_H^\dagger(\vec{x}', \tau')] \rangle_\beta$ $G_\beta(\vec{x}, \vec{x}'; \tau, \tau') = \frac{\langle \mathcal{T} [\Phi_I(\vec{x}, \tau) \Phi_I^\dagger(\vec{x}', \tau') \mathcal{S}(\beta)] \rangle_{\beta, 0}}{\langle \mathcal{S}(\beta) \rangle_{\beta, 0}}$ $\beta, 0$ indicates the thermal expectation with free theory [12]
Propagator (Momentum Space GF) $i\Delta_F(K) = G(K), \quad K \equiv (k_0, \vec{k}), \quad k = \vec{k} $ k_0 is continuous k is continuous	Propagator (Momentum Space GF) $i\Delta_F(k_0, \vec{k}) = G(k_0, \vec{k}), \quad k = \vec{k} $ $k_0 = ik_4 = i\omega_n = \begin{cases} \frac{2n\pi i}{\beta} & \text{for boson,} \\ \frac{(2n+1)\pi i}{\beta} & \text{for fermion.} \end{cases}$ k is continuous
Loop integral $\int \frac{d^4 K}{(2\pi)^4};$ k_0 is continuous k is continuous	Loop integral $\frac{1}{\beta} \sum_{k_0} \frac{d^3 k}{(2\pi)^3};$ $k_0 = ik_4 = i\omega_n = \begin{cases} \frac{2n\pi i}{\beta} & \text{for boson,} \\ \frac{(2n+1)\pi i}{\beta} & \text{for fermion.} \end{cases}$ k is continuous

3.8 Feynman Rules

Now following the table we can write the Feynman rules for $T \neq 0$ as

- The propagator is same as $T = 0$ but with the fourth component of Minkowski momentum is now discrete

$$k_0 = ik_4 = i\omega_n = \begin{cases} \frac{2n\pi i}{\beta} & \text{for boson ,} \\ \frac{(2n+1)\pi i}{\beta} & \text{for fermion.} \end{cases}$$

- The loop integral at $T = 0$ should be replaced as

$$\int \frac{d^4 K}{(2\pi)^4} \rightarrow \frac{1}{\beta} \sum_{k_0} \frac{d^3 k}{(2\pi)^3}, \quad (3.46)$$

where the fourth component of Minkowski momentum is replace by discrete frequency

$$k_0 = ik_4 = i\omega_n = \begin{cases} \frac{2n\pi i}{\beta} & \text{for boson ,} \\ \frac{(2n+1)\pi i}{\beta} & \text{for fermion.} \end{cases}$$

- Vertex is same as the $T = 0$ field theory.
- Symmetry factor for a given diagram is same as the $T = 0$ field theory.

Once the Feynman amplitudes are written using these Feynman rules, one needs now to compute the discrete frequency sum. Below we discuss the techniques to evaluate the frequency sum at finite T .

4 Frequency Sum

The Euclidean time Green's function in coordinate space:

$$G_\beta(\vec{x}, \tau) \stackrel{\tau > 0}{=} -\frac{1}{\beta} \sum_{n=-\infty}^{n=+\infty} \int \frac{d^3 k}{(2\pi)^3} e^{i\vec{k} \cdot \vec{x}} \frac{e^{-i\omega_n \tau}}{\omega_n^2 + \omega_k^2} \quad (4.1)$$

with $\omega_n = 2\pi nT$ and $\omega_k = \sqrt{k^2 + m^2}$.

We need to perform the discrete frequency sum:

$$T \sum_{n=-\infty}^{n=+\infty} \frac{e^{-i\omega_n \tau}}{\omega_n^2 + \omega_k^2} \quad (4.2)$$

Also in order to calculate matrix element corresponding to a given Feynman diagram in theory, we need to perform frequency sums. There are two types of frequency sums: bosonic and fermionic.

4.1 Bosonic Frequency Sum

In general the form of the bosonic frequency sum can be written as

$$\frac{1}{\beta} \sum_{n=-\infty}^{n=+\infty} f(k_0 = i\omega_n = 2\pi inT) \quad (4.3)$$

where k_0 is the fourth (temporal) component of momentum in Minkowski space-time and f is a meromorphic function ³.

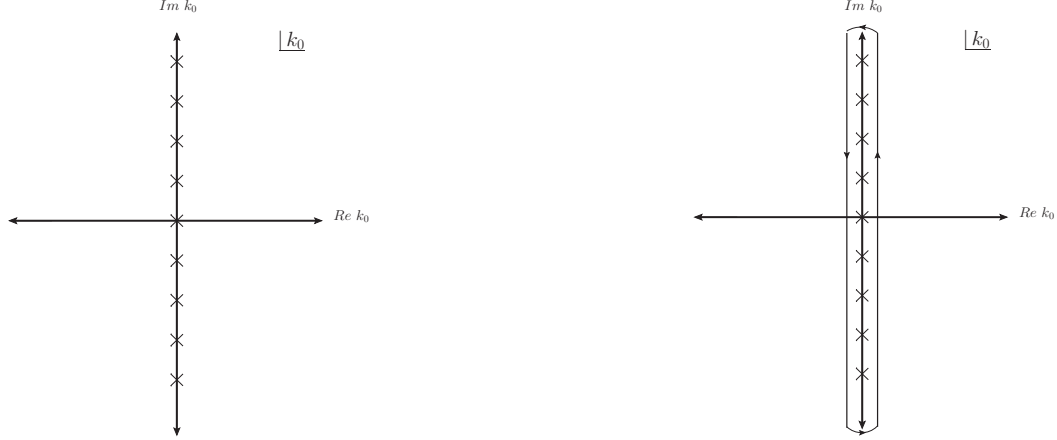


Figure 5: Poles of $\coth(\beta k_0/2)$ at $k_0 = 2\pi inT; n = 0, 1, 2 \dots$, in complex k_0 plane

We know hyperbolic cotangent has poles at $\coth(n\pi i)$ with residue unity. Therefore, one can insert hyperbolic cotangent with suitable argument as [13, 14]

$$\frac{1}{\beta} \sum_{n=-\infty}^{n=+\infty} f(k_0 = i\omega_n = 2\pi inT) \text{Res} \left[\frac{\beta}{2} \coth \left(\frac{\beta k_0}{2} \right) \right], \quad (4.4)$$

where hyperbolic cotangent corresponds to poles (see Fig. 5) at

$$\coth \left(\frac{\beta k_0}{2} \right) = \coth(n\pi i) \Rightarrow k_0 = \frac{2\pi in}{\beta} = i\omega_n \quad (4.5)$$

with residues $2/\beta$, and $\text{Res} \left[\frac{\beta}{2} \coth \left(\frac{\beta k_0}{2} \right) \right]$ will lead to unity.

Then one can write (4.4) without any loss of generality as

$$\begin{aligned} & \frac{1}{\beta} \sum_{n=-\infty}^{n=+\infty} f(k_0) \text{Res} \left[\frac{\beta}{2} \coth \left(\frac{\beta k_0}{2} \right) \right] \\ &= \frac{1}{\beta} \sum_{n=-\infty}^{n=+\infty} \frac{\beta}{2} \text{Res} \left[f(k_0) \coth \left(\frac{\beta k_0}{2} \right); \Rightarrow \text{poles : } k_0 = i\omega_n = \frac{2\pi in}{\beta} \right]. \end{aligned} \quad (4.6)$$

³A meromorphic function is a ratio of two well-behaved (holomorphic) functions in complex plane as $f(z) = g(z)/h(z)$ with $h(z) \neq 0$. However such a function will still be well-behaved if it has finite order, isolated poles and zeros and no essential singularities or branch cuts in its domain.

Employing the residue theorem in reverse the sum over residues can now be expressed as an integral over a contour C in $\angle k_0$ enclosing the poles of the meromorphic function $f(k_0)$ but excluding the poles of the hyperbolic cotangent ($k_0 = i\omega_n = 2\pi iT$) as

$$\begin{aligned} \frac{1}{\beta} \sum_{n=-\infty}^{n=+\infty} \text{Res} \left[f(k_0) \frac{\beta}{2} \coth \left(\frac{\beta k_0}{2} \right) \right] &= \frac{T}{2\pi i} \oint_{C_1 \cup C_2} dk_0 f(k_0) \frac{\beta}{2} \coth \left(\frac{\beta k_0}{2} \right) \\ &= \frac{1}{2\pi i} \oint_{C_1 \cup C_2} dk_0 f(k_0) \frac{1}{2} \coth \left(\frac{\beta k_0}{2} \right), \end{aligned} \quad (4.7)$$

where i the numerator of RHS of (4.7) is absorbed as $i dk_0 = d(ik_0) = dk_0$.

Now, some important points to note on Eq.(4.7):

- $[\exp(\beta k_0) - 1]^{-1}$ vis-a-vis $\coth(\beta k_0/2)$ has series of poles at $k_0 = i\omega_n = 2\pi iT$ and is bounded and analytic everywhere except at poles.
- $f(k_0 = i\omega_n)$ is a meromorphic function which has simple poles but no essential singularities or branch cuts.
- The simple poles of $f(k_0 = i\omega_n)$ should not coincide the series of poles of $[\exp(\beta k_0) - 1]^{-1} \Rightarrow f(k_0 = i\omega_n)$ should not have singularity along the imaginary k_0 axis.
- The contour C can be divided into two half circles in complex k_0 plane C_1 and C_2 [13] without enclosing the poles of the $[\exp(\beta k_0) - 1]^{-1}$ vis-a-vis $\coth(\beta k_0/2)$ but the contours C_1 and C_2 should enclose poles of $f(k_0)$ as shown in Fig. 5, provided the meromorphic function $f(k_0)$ should decrease fast to achieve convergence.
- If all these properties are satisfied then $T \sum_{n=-\infty}^{n=+\infty} f(k_0 = i\omega_n)$ can be replaced by contour integration and this is equivalent to switching (analytically continuing) from Euclidean time (discrete frequency in Euclidean space) to real time (continuous frequency in Minkowski space-time).

4.1.1 Separation of vacuum and matter part

We know [13]

$$\begin{aligned} \frac{1}{2} \coth \left(\frac{\beta k_0}{2} \right) &= \frac{1}{2} \frac{\exp(\beta k_0/2) + \exp(-\beta k_0/2)}{\exp(\beta k_0/2) - \exp(-\beta k_0/2)} = \frac{1}{2} \frac{\exp(\beta k_0) + 1}{\exp(\beta k_0) - 1} \\ &= \frac{1}{2} \left[1 + \frac{2}{\exp(\beta k_0) - 1} \right]. \end{aligned} \quad (4.8)$$

Using (4.8) and (4.7) in (4.3) the bosonic sum integral can be written as

$$\frac{1}{\beta} \sum_{n=-\infty}^{n=+\infty} f(k_0 = i\omega_n) = \frac{1}{2\pi i} \oint_{C_1 \cup C_2} dk_0 f(k_0 = i\omega_n) \left[\frac{1}{2} + \frac{1}{\exp(\beta k_0) - 1} \right] \quad (4.9)$$

which separates $T = 0$ (vacuum) and $T \neq 0$ (medium) part.

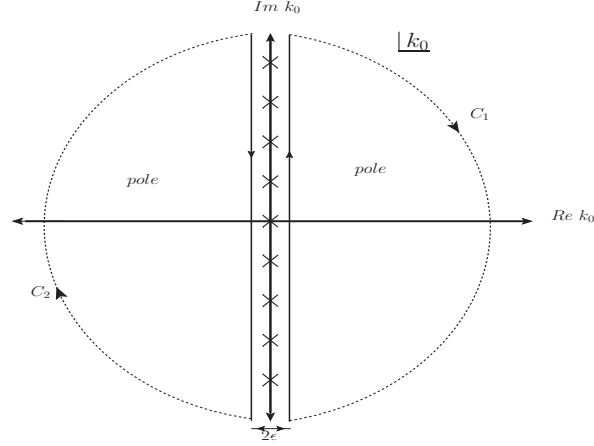


Figure 6: Contours C_1 and C_2 that include the poles of the meromorphic function $f(k_0)$ in complex k_0 plane. The contours are also shifted by an amount $\pm\epsilon$ from the $\text{Im}k_0$ line to exclude the poles of $\coth(\beta k_0/2)$ at $k_0 = 2\pi i n T$.

4.1.2 Choice of contour:

As discussed above, the contour C can be divided into two half circles C_1 and C_2 in complex k_0 plane that excludes the poles of the $[\exp(\beta k_0) - 1]^{-1}$ vis-a-vis $\coth(\beta k_0/2)$ but includes the poles of the meromorphic function $f(k_0)$ as shown in Fig. 6, the integrand converges. Lets choose the contour C_1 which goes from $\epsilon - i\infty$ to $\epsilon + i\infty$ whereas the contour C_2 goes from $-\epsilon + i\infty$ to $-\epsilon - i\infty$.

Now (4.9) can be decomposed as

$$\begin{aligned} \frac{1}{\beta} \sum_{n=-\infty}^{n=+\infty} f(k_0 = i\omega_n) &= \frac{1}{2\pi i} \int_{\epsilon-i\infty}^{\epsilon+i\infty} dk_0 f(k_0 = i\omega_n) \left[\frac{1}{2} + \frac{1}{e^{\beta k_0} - 1} \right] \Rightarrow \text{along } C_1 \\ &+ \frac{1}{2\pi i} \int_{-\epsilon+i\infty}^{-\epsilon-i\infty} dk_0 f(k_0 = i\omega_n) \left[-\frac{1}{2} - \frac{1}{e^{-\beta k_0} - 1} \right] \Rightarrow \text{along } C_2, \end{aligned} \quad (4.10)$$

where we note the following:

- The first term contains pole for $k_0 > 0$ in the contour C_1 .
- The overall negative sign in the second term is due to pole $k_0 < 0$ in the contour C_2 .
- Also in the second term the argument of the exponential is negative because it has to converge as $k_0 \rightarrow -\infty$, since the contour C_2 is in the left half plane.

Now we make a substitution $k_0 \rightarrow -k_0$ in the second term in (4.10) can be written as

$$\begin{aligned} \frac{1}{2\pi i} \int_{\epsilon-i\infty}^{\epsilon+i\infty} d(-k_0) f(-k_0) \left[-\frac{1}{2} - \frac{1}{\exp(\beta k_0) - 1} \right] &= \frac{1}{2\pi i} \int_{-i\infty}^{+i\infty} dk_0 f(-k_0) \frac{1}{2} \\ &+ \frac{1}{2\pi i} \int_{\epsilon-i\infty}^{\epsilon+i\infty} dk_0 f(-k_0) \frac{1}{\exp(\beta k_0) - 1} \end{aligned} \quad (4.11)$$

Using (4.11) in (4.10), one gets

$$\begin{aligned} \frac{1}{\beta} \sum_{n=-\infty}^{n=+\infty} f(k_0 = i\omega_n) &= \frac{1}{2\pi i} \int_{-i\infty}^{+i\infty} dk_0 \frac{1}{2} [f(k_0) + f(-k_0)] \\ &+ \frac{1}{2\pi i} \int_{\epsilon-i\infty}^{\epsilon+i\infty} dk_0 [f(k_0) + f(-k_0)] \frac{1}{\exp(\beta k_0) - 1}. \end{aligned} \quad (4.12)$$

We note that the Contour is in right half plane. The first term in RHS is vacuum contribution whereas the second term is matter contribution. One can use either (4.7) or (4.9) or (4.12) conveniently.

4.2 Fermionic Frequency Sum for Zero Chemical Potential ($\mu = 0$)

. In general the form of the fermionic frequency sum can be written as

$$\frac{1}{\beta} \sum_{n=-\infty}^{n=+\infty} f(k_0 = i\omega_n = (2n+1)i\pi T), \quad (4.13)$$

where k_0 is the fourth (temporal) component of momentum in Minkowski space-time and the $f(k_0)$ is a meromorphic function. We know hyperbolic tangent has poles at $\tanh(\frac{\pi i}{2} + n\pi i)$ with residue unity. Therefore, one can insert hyperbolic tangent with suitable argument as [13, 14]

$$\frac{1}{\beta} \sum_{n=-\infty}^{n=+\infty} f(k_0 = i\omega_n = (2n+1)i\pi T) \text{Res} \left[\frac{\beta}{2} \tanh \left(\frac{\beta k_0}{2} \right) \right], \quad (4.14)$$

where hyperbolic tangent corresponds to poles at

$$\tanh \left(\frac{\beta k_0}{2} \right) = \tanh \left(\frac{\pi i}{2} + n\pi i \right) \Rightarrow k_0 = \frac{(2n+1)i\pi n}{\beta} = i\omega_n \quad (4.15)$$

with residues $2/\beta$. Then one can write (4.14) without any loss of generality as

$$\begin{aligned} &\frac{1}{\beta} \sum_{n=-\infty}^{n=+\infty} f(k_0) \text{Res} \left[\frac{\beta}{2} \tanh \left(\frac{\beta k_0}{2} \right) \right] \\ &= \frac{1}{\beta} \sum_{n=-\infty}^{n=+\infty} \frac{\beta}{2} \text{Res} \left[f(k_0) \tanh \left(\frac{\beta k_0}{2} \right) ; \Rightarrow \text{poles } : k_0 = i\omega_n = \frac{(2n+1)i\pi}{\beta} \right]. \end{aligned} \quad (4.16)$$

Employing the residue theorem, as before, in reverse the sum over residues can now be expressed as an integral over contours C_1 and C_2 in $\angle k_0$ enclosing the poles of the meromorphic function $f(k_0)$ but excluding the poles of hyperbolic tangent ($k_0 = i\omega_n = (2n+1)\pi iT$) as

$$\begin{aligned} \frac{1}{\beta} \sum_{n=-\infty}^{n=+\infty} f(k_0) \frac{\beta}{2} \tanh\left(\frac{\beta k_0}{2}\right) &= \frac{T}{2\pi i} \oint_{C_1 \cup C_2} dk_0 f(k_0) \frac{\beta}{2} \tanh\left(\frac{\beta k_0}{2}\right) \\ &= \frac{1}{2\pi i} \oint_{C_1 \cup C_2} dk_0 f(k_0) \frac{1}{2} \tanh\left(\frac{\beta k_0}{2}\right), \end{aligned} \quad (4.17)$$

where contours C_1 and C_2 are represented in Fig. 7

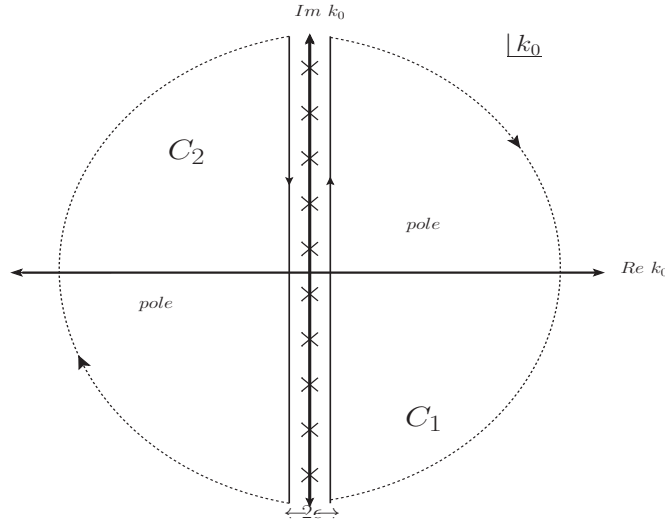


Figure 7: Contours C_1 and C_2 that include the poles of the meromorphic function $f(k_0)$ in complex k_0 plane for fermion with zero chemical potential ($\mu = 0$). The contours are also shifted by an amount $\pm\epsilon$ from the $\text{Im}k_0$ line to exclude the poles of $\tanh(\beta k_0/2)$ at $k_0 = (2n+1)i\pi T$; $n = 0, 1, 2, \dots$.

4.2.1 Separation of vacuum and matter part

We know

$$\begin{aligned} \frac{1}{2} \tanh\left(\frac{\beta k_0}{2}\right) &= \frac{1}{2} \frac{\exp(\beta k_0/2) - \exp(-\beta k_0/2)}{\exp(\beta k_0/2) + \exp(-\beta k_0/2)} = \frac{1}{2} \frac{\exp(\beta k_0) - 1}{\exp(\beta k_0) + 1} \\ &\quad + \frac{1}{2} \left[1 - \frac{2}{\exp(\beta k_0) + 1} \right]. \end{aligned} \quad (4.18)$$

Using (4.18) and (4.17) in (4.13) the fermionic sum integral can be written as

$$\frac{1}{\beta} \sum_{n=-\infty}^{n=+\infty} f(k_0 = i\omega_n) = \frac{1}{2\pi i} \oint_{C_1 \cup C_2} dk_0 f(k_0 = i\omega_n) \left[\frac{1}{2} - \frac{1}{\exp(\beta k_0) + 1} \right] \quad (4.19)$$

which separates $T = 0$ (vacuum) and $T \neq 0$ (medium) part.

4.2.2 Choice of contour

Proceeding same way as the bosonic case before, one can write

$$\begin{aligned} T \sum_{n=-\infty}^{n=+\infty} f(k_0 = i\omega_n) &= \frac{1}{2\pi i} \int_{-i\infty}^{+i\infty} d(k_0) \frac{1}{2} [f(k_0) + f(-k_0)] \\ &\quad + \frac{1}{2\pi i} \int_{\epsilon-i\infty}^{\epsilon+i\infty} d(k_0) [f(k_0) + f(-k_0)] \frac{1}{\exp(\beta k_0) + 1}. \end{aligned} \quad (4.20)$$

We note that the Contour is in right half plane. The first term in RHS is vacuum contribution whereas the second term is matter contribution. One can use either (4.17) or (4.19) or (4.20) conveniently.

4.3 Examples of Frequency Sum for Bosonic Case

The Euclidean time bosonic Green's function in coordinate space can be written as

$$G_\beta(\vec{x}, \tau) \stackrel{\tau > 0}{=} -\frac{1}{\beta} \sum_{n=-\infty}^{n=+\infty} \int \frac{d^3 k}{(2\pi)^3} e^{i\vec{k} \cdot \vec{x}} \frac{e^{-i\omega_n \tau}}{\omega_n^2 + \omega_k^2}, \quad (4.21)$$

with $\omega_n = 2\pi nT$ and $\omega_k = \sqrt{k^2 + m^2}$. Now we put back $i\omega_n = k_0$, the fourth component of Minkowski momentum to write the standard form as given in (4.3) without any loss generality:

$$\begin{aligned} G_\beta(\vec{x}, \tau) \stackrel{\tau > 0}{=} &\int \frac{d^3 k}{(2\pi)^3} e^{i\vec{k} \cdot \vec{x}} \frac{1}{\beta} \sum_{n=-\infty}^{n=+\infty} \frac{e^{-k_0 \tau}}{k_0^2 - \omega_k^2} \\ \stackrel{\tau > 0}{=} &\int \frac{d^3 k}{(2\pi)^3} e^{i\vec{k} \cdot \vec{x}} \frac{1}{\beta} \sum_{n=-\infty}^{n=+\infty} f(k_0 = i\omega_n). \end{aligned} \quad (4.22)$$

Now we perform the frequency sum. As discussed the sum integration can be performed using either (4.7) or (4.9) or (4.12) conveniently. However, we would use (4.7) for the purpose

$$\begin{aligned} \frac{1}{\beta} \sum_{n=-\infty}^{n=+\infty} f(k_0 = i\omega_n) \stackrel{\tau > 0}{=} &\frac{1}{\beta} \sum_{n=-\infty}^{n=+\infty} \frac{e^{-k_0 \tau}}{k_0^2 - \omega_k^2} \\ \stackrel{\tau > 0}{=} &\frac{1}{2\pi i} \oint_C dk_0 \frac{e^{-k_0 \tau}}{k_0^2 - \omega_k^2} \frac{1}{2} \coth\left(\frac{\beta k_0}{2}\right). \end{aligned} \quad (4.23)$$

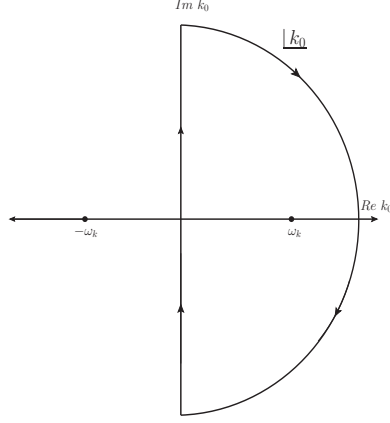


Figure 8: Contour corresponding to the Integral I_1^0 in the complex k_0 plane.

We now rewrite (4.23) here

$$\begin{aligned} \frac{1}{\beta} \sum_{n=-\infty}^{n=+\infty} f(k_0 = i\omega_n) &\stackrel{\tau > 0}{=} \frac{1}{\beta} \sum_{n=-\infty}^{n=+\infty} \frac{e^{-k_0 \tau}}{k_0^2 - \omega_k^2} \\ &\stackrel{\tau > 0}{=} \frac{1}{2\pi i} \oint_C dk_0 \frac{e^{-k_0 \tau}}{k_0^2 - \omega_k^2} \frac{1}{2} \coth\left(\frac{\beta k_0}{2}\right). \end{aligned} \quad (4.24)$$

Using (4.12), one gets (we drop $\tau > 0$ from all equations below)

$$\begin{aligned} \frac{1}{\beta} \sum_{n=-\infty}^{n=+\infty} f(k_0 = i\omega_n) &= \frac{1}{2\pi i} \int_{-i\infty}^{+i\infty} dk_0 \frac{1}{2} [f(k_0) + f(-k_0)] + \frac{1}{2\pi i} \int_{\epsilon-i\infty}^{\epsilon+i\infty} dk_0 [f(k_0) + f(-k_0)] \frac{1}{e^{\beta k_0} - 1} \\ &= \frac{1}{2\pi i} \int_{-i\infty}^{+i\infty} dk_0 \frac{1}{2} \left[\frac{e^{-k_0 \tau}}{k_0^2 - \omega_k^2} + \frac{e^{k_0 \tau}}{k_0^2 - \omega_k^2} \right] + \frac{1}{2\pi i} \int_{\epsilon-i\infty}^{\epsilon+i\infty} dk_0 \left[\frac{e^{-k_0 \tau}}{k_0^2 - \omega_k^2} + \frac{e^{k_0 \tau}}{k_0^2 - \omega_k^2} \right] \frac{1}{e^{\beta k_0} - 1} \\ &= I_1^0 + I_2^0 + I_3^\beta + I_4^\beta, \end{aligned} \quad (4.25)$$

where I_1^0 and I_2^0 are for $T = 0$ parts whereas I_3^β and I_4^β are for $T \neq 0$ parts. We now evaluate them below:

$$I_1^0 = \frac{1}{2\pi i} \int_{-i\infty}^{+i\infty} dk_0 \frac{1}{2} \frac{e^{-k_0 \tau}}{k_0^2 - \omega_k^2} \quad (4.26)$$

- Poles: $k_0 = \pm \omega_k$
- Convergence: for $\tau > 0$, $e^{-k_0 \tau}$ converges in the domain $0 \leq \tau \leq \beta$ only for $k_0 = \omega_k$. The relevant contour is given in Fig. 8.

$$I_1^0 = \frac{1}{2} \frac{1}{2\pi i} \times (2\pi i) \lim_{k_0 \rightarrow \omega_k} \frac{(k_0 - \omega_k)}{(k_0 - \omega_k)(k_0 + \omega_k)} e^{-k_0 \tau} = \frac{1}{2} \frac{e^{-\omega_k \tau}}{2\omega_k}. \quad (4.27)$$

$$I_2^0 = \frac{1}{2\pi i} \int_{-i\infty}^{+i\infty} dk_0 \frac{1}{2} \frac{e^{k_0 \tau}}{k_0^2 - \omega_k^2} \quad (4.28)$$

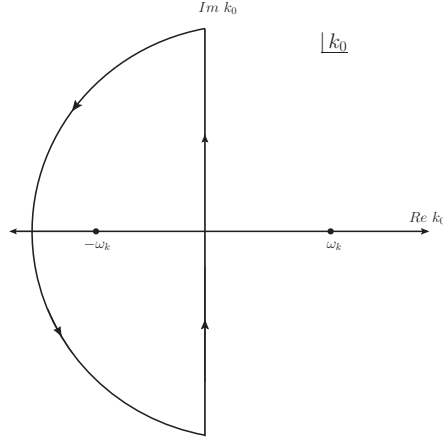


Figure 9: Contour corresponding to the Integral I_2^0 in complex k_0 plane.

- Poles: $k_0 = \pm\omega_k$
- Convergence: for $\tau > 0$, $e^{k_0 \tau}$ converges in the domain $0 \leq \tau \leq \beta$ only for $k_0 = -\omega_k$. The relevant contour is given in Fig. 9. Note that the contour is anticlockwise so it will induct a negative sign.

$$I_2^0 = \frac{1}{2} \frac{1}{2\pi i} \times (-2\pi i) \lim_{k_0 \rightarrow -\omega_k} \frac{(k_0 + \omega_k)}{(k_0 - \omega_k)(k_0 + \omega_k)} e^{k_0 \tau} = \frac{1}{2} \frac{e^{-\omega_k \tau}}{2\omega_k} = I_1^0. \quad (4.29)$$

$$I_3^\beta = \frac{1}{2\pi i} \int_{\epsilon - i\infty}^{\epsilon + i\infty} dk_0 \frac{e^{-k_0 \tau}}{k_0^2 - \omega_k^2} \frac{1}{e^{\beta k_0} - 1}. \quad (4.30)$$

- Poles: $k_0 = \pm\omega_k$
- Convergence: for $\tau > 0$, $e^{-k_0 \tau} / (e^{\beta k_0} - 1) \sim e^{-k_0 \tau} e^{-\beta k_0}$ converges in the domain $0 \leq \tau \leq \beta$ only for $k_0 = \omega_k$. The relevant contour is given in Fig. 10.

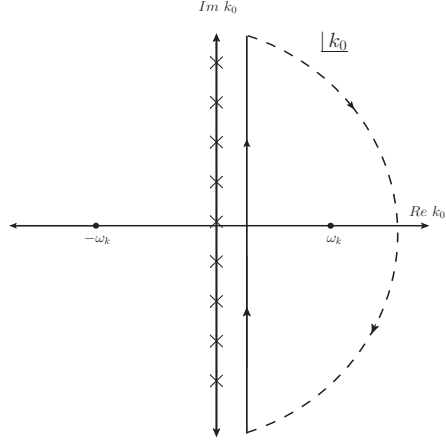


Figure 10: Contour corresponding to the Integral I_3^β in complex k_0 plane.

$$I_3^0 = \frac{1}{2\pi i} \times (2\pi i) \lim_{k_0 \rightarrow \omega_k} \frac{(k_0 + \omega_k)}{(k_0 - \omega_k)(k_0 - \omega_k)} e^{k_0 \tau} = \frac{1}{2\omega_k} \frac{e^{-\omega_k \tau}}{e^{\beta k_0} - 1} = \frac{e^{-\omega_k \tau}}{2\omega_k} n_B(\omega_k). \quad (4.31)$$

$$I_4^\beta = \frac{1}{2\pi i} \int_{\epsilon - i\infty}^{\epsilon + i\infty} dk_0 \frac{e^{k_0 \tau}}{k_0^2 - \omega_k^2} \frac{1}{e^{\beta k_0} - 1}. \quad (4.32)$$

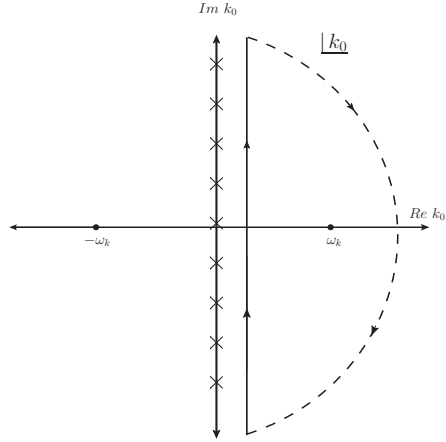


Figure 11: Contour corresponding to the Integral I_4^β in complex k_0 plane.

- Poles: $k_0 = \pm\omega_k$
- Convergence: for $\tau > 0$, $e^{k_0\tau}/(e^{\beta k_0} - 1) \sim e^{k_0\tau} e^{-\beta k_0}$ converges in the domain $0 \leq \tau \leq \beta$ only for $k_0 = \omega_k$ and $\beta > \tau$. The relevant contour is given in Fig. 11

$$I_4^0 = \frac{1}{2\pi i} \times (2\pi i) \lim_{k_0 \rightarrow \omega_k} \frac{(k_0 + \omega_k)}{(k_0 - \omega_k)(k_0 - \omega_k)} e^{k_0\tau} = \frac{1}{2\omega_k} \frac{e^{\omega_k\tau}}{e^{\beta k_0} - 1} = \frac{e^{\omega_k\tau}}{2\omega_k} n_B(\omega_k). \quad (4.33)$$

At this point it is worth noting that the contours for I_1^0 , I_3^β and I_4^β are in right half plane whereas that for I_2^0 is in the left half plane.

Now combining (4.27), (4.29), (4.31) and (4.33) with (4.25), one gets for $\tau > 0$ as

$$\begin{aligned} \frac{1}{\beta} \sum_{n=-\infty}^{n=+\infty} f(k_0 = i\omega_n) &\stackrel{\tau > 0}{=} I_1^0 + I_2^0 + I_3^\beta + I_4^\beta \\ &\stackrel{\tau > 0}{=} \frac{1}{2\pi i} \oint_C dk_0 \frac{e^{-k_0\tau}}{k_0^2 - \omega_k^2} \frac{1}{2} \coth\left(\frac{\beta k_0}{2}\right) \\ &\stackrel{\tau > 0}{=} \frac{1}{2\pi i} \times (2\pi i) \left[R_1|_{k_0=\omega_k} + R_2|_{k_0=-\omega_k} \right] \\ &\stackrel{\tau > 0}{=} \frac{e^{-\omega_k\tau}}{2\omega_k} + \frac{e^{-\omega_k\tau}}{2\omega_k} n_B(\omega_k) + \frac{e^{\omega_k\tau}}{2\omega_k} n_B(\omega_k) \\ &\stackrel{\tau > 0}{=} \frac{e^{-\omega_k\tau}}{2\omega_k} (1 + n_B(\omega_k)) + \frac{e^{\omega_k\tau}}{2\omega_k} n_B(\omega_k). \end{aligned} \quad (4.34)$$

Again putting (4.34) in (4.21) one gets Euclidean time Green's function for $\tau > 0$ as

$$G_\beta(\vec{x}, \tau) \stackrel{\tau > 0}{=} \int \frac{d^3k}{(2\pi)^3} \frac{1}{2\omega_k} \left[(1 + n_B(\omega_k)) e^{-\omega_k\tau} e^{i\vec{k}\cdot\vec{x}} + n_B(\omega_k) e^{\omega_k\tau} e^{i\vec{k}\cdot\vec{x}} \right]. \quad (4.35)$$

Now changing $\vec{k} \rightarrow -\vec{k}$ in the second term inside the square braces, leads to the Euclidean time green's function as

$$G_\beta(\vec{x}, \tau) \stackrel{\tau > 0}{=} \int \frac{d^3k}{(2\pi)^3} \frac{1}{2\omega_k} \left[(1 + n_B(\omega_k)) e^{-\omega_k\tau} e^{i\vec{k}\cdot\vec{x}} + n_B(\omega_k) e^{\omega_k\tau} e^{-i\vec{k}\cdot\vec{x}} \right]. \quad (4.36)$$

If one makes a Wick rotation $\tau \rightarrow it$ to Minkowski time, it becomes

$$\begin{aligned} G_\beta(\vec{x}, t) &\stackrel{t > 0}{=} \int \frac{d^3k}{(2\pi)^3} \frac{1}{2\omega_k} \left[(1 + n_B(\omega_k)) e^{-i\omega_k t} e^{i\vec{k}\cdot\vec{x}} + n_B(\omega_k) e^{i\omega_k t} e^{-i\vec{k}\cdot\vec{x}} \right] \\ &\stackrel{t > 0}{=} \int \frac{d^3k}{(2\pi)^3} \frac{1}{2\omega_k} \left[(1 + n_B(\omega_k)) e^{-iK \cdot X} + n_B(\omega_k) e^{iK \cdot X} \right], \end{aligned} \quad (4.37)$$

which agrees with the real time Green's function in (3.25).

5 Scalar Theory

5.1 Tadpole Diagram in $\lambda\phi^4$ Theory

The \mathcal{S} -matrix in Euclidean time as given in (3.9)

$$\mathcal{S}(\beta) = \mathcal{T} \left[\exp \left(- \int_0^\beta \mathcal{H}' d\tau \right) \right] = \sum_N \frac{[\dots]^N}{N!}, \quad (5.1)$$

where \mathcal{T} is the time ordered product in imaginary time $\tau = it$. Following the same procedure as $T = 0$ field theory the scalar Lagrangian is given as

$$\mathcal{L} = \frac{1}{2} \left[\partial_\mu \phi \partial^\mu \phi - \frac{1}{2} m^2 \phi^2 \right] - \frac{\lambda}{4!} \phi^4 = \mathcal{L}_0 + \mathcal{L}_I, \quad (5.2)$$

where ϕ is a scalar field, λ is the coupling in the theory and \mathcal{L}_0 is the free scalar field Lagrangian. The interaction Lagrangian is

$$\mathcal{L}_I = - \frac{1}{4!} \lambda \phi^4. \quad (5.3)$$

4! comes from how many ways the ϕ fields can be arranged. Vertex is $-i\lambda$ (same as vacuum). The interaction Lagrangian in (5.3) will lead to the tadpole diagram as shown in Fig 12.

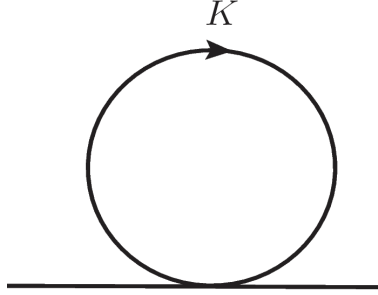


Figure 12: Tadpole diagram in $\lambda\phi^4$ theory.

Symmetry factor: After contraction how the remaining legs (fields) are connected to the interaction vertex. The topology of the tadpole diagram in ϕ^4 theory is given in Fig. 12, which results from one contraction involving two ϕ fields and remaining two ϕ fields can then be connected to the vertex in two ways. So, the symmetry factor is 1/2 (same as vacuum).

The amplitude corresponding to the tadpole diagram in Fig 12 can be written following the Feynman rules defined earlier as

$$\begin{aligned} \Pi &= \frac{1}{2} (-i\lambda) \int \frac{d^4 K}{(2\pi)^4} \frac{i}{K^2 - m^2} = \frac{1}{2} (-i\lambda) \frac{1}{\beta} \sum_{k_0} \int \frac{d^3 k}{(2\pi)^3} \frac{i}{k_0^2 - \omega_k^2} \\ &= \frac{1}{2} \lambda \int \frac{d^3 k}{(2\pi)^3} \frac{1}{\beta} \sum_{k_0} \frac{1}{k_0^2 - \omega_k^2}, \end{aligned} \quad (5.4)$$

where $\omega_k = \sqrt{k^2 + m^2}$ and Π is independent of external momentum.

Now the function under the frequency sum is same as those in (4.22) for $\tau = 0$. So one can write

$$\begin{aligned} \frac{1}{\beta} \sum_{k_0} \frac{1}{k_0^2 - \omega_k^2} &= \left[I_1^0 + I_2^0 + I_3^\beta + I_4^\beta \right] \Big|_{\tau=0} \\ &= \left[\frac{e^{-\omega_k \tau}}{2\omega_k} + \frac{e^{-\omega_k \tau}}{2\omega_k} n_B(\omega_k) + \frac{e^{\omega_k \tau}}{2\omega_k} n_B(\omega_k) \right] \Big|_{\tau=0} \\ &= \frac{1}{2\omega_k} \left[1 + 2n_B(\omega_k) \right]. \end{aligned} \quad (5.5)$$

Using (5.5) in (5.4), one can write

$$\Pi = \frac{1}{4} \lambda \int \frac{d^3 k}{(2\pi)^3} \frac{1}{\omega_k} \left[1 + 2n_B(\omega_k) \right]. \quad (5.6)$$

Now, we note that

- the first term is the vacuum ($T = 0$) contribution and it is ultraviolet divergent. This could be regulated using dimensional regularisation at $T = 0$ and it vanishes.
- the second term is finite as it involves the Bose-Einstein distribution, which falls off exponentially for large ω_k or momentum. The finite temperature does not cause any ultraviolet divergence but induces infrared divergence⁴.

The second term can be written for ($m = 0$) as

$$\begin{aligned} \Pi &= \frac{1}{4} \lambda \frac{4\pi}{(2\pi)^3} \int_0^\infty dk \, k^2 \frac{1}{k} \frac{2}{e^{\beta k} - 1} = \frac{1}{4\pi^2} \lambda \int_0^\infty dk \, k \frac{1}{e^{\beta k} - 1} \\ &= \frac{\lambda T^2}{4\pi^2} \int_0^\infty \frac{dx \, x}{e^x - 1} \quad [\text{Assumed } x = \beta k] \\ &= \frac{\lambda T^2}{4\pi^2} \zeta(2) = \frac{\lambda T^2}{24}. \end{aligned} \quad (5.7)$$

where we have used

$$\int_0^\infty \frac{dx \, x^{n-1}}{e^x - 1} = (n-1)! \zeta(n). \quad (5.8)$$

We note that $\Pi = \lambda T^2/24$ will act as a thermal mass of the scalar field at finite temperature. We will discuss this in details when the dispersion property of a particle at finite T will be discussed later.

⁴At $m = 0$ and $|k| \rightarrow 0 \Rightarrow n_B(\omega_k = 0) = 1/(1-1) \rightarrow \infty$ there is an infrared divergence due to zero bosonic mode caused by $\omega_n = 2\pi nT$ for $n = 0$. We will come back later how can this infrared divergence be regulated.

5.2 One-Loop Self-Energy in ϕ^3 -Theory

. We consider three scalar fields ϕ , ϕ_1 and ϕ_2 which differ by masses. The interaction Lagrangian density is given by

$$\mathcal{L}_I = -\lambda\phi(x)\phi_1(x)\phi_2(x), \quad (5.9)$$

where λ is the interaction strength.

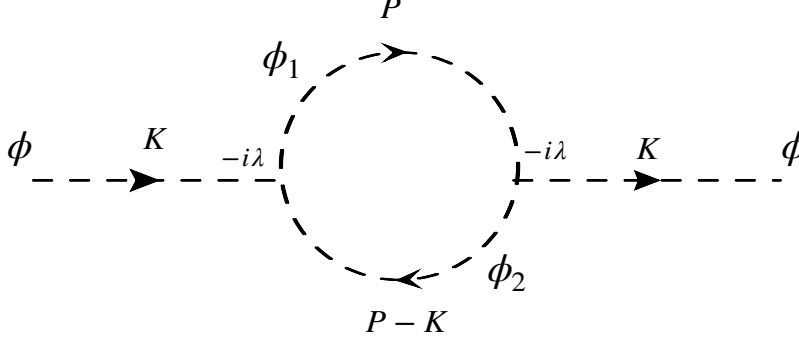


Figure 13: Scalar self-energy diagram in ϕ^3 -theory at $T \neq 0$.

Our aim is to compute the diagram in Fig. 13, which occurs typically in one-loop approximation of the self-energy of the field ϕ . The self-energy can be written from Fig. 13 as

$$\Pi_2(K) = \int \frac{d^4 P}{(2\pi)^4} (-i\lambda) \frac{i}{P^2 - m_1^2} (-i\lambda) \frac{i}{(P - K)^2 - m_2^2}, \quad (5.10)$$

where P is the momentum of the ϕ_1 field with mass m_1 , $P - K$ is the momentum of the ϕ_2 field with mass m_2 . The self-energy can be written as

$$\begin{aligned} \Pi_2(k_0, k) &= \lambda^2 \int \frac{d^3 p}{(2\pi)^3} T \sum_{p_0} \frac{1}{(p_0^2 - E_p^2)[(p_0 - k_0)^2 - E_{p-k}^2]} \\ &= \lambda^2 \int \frac{d^3 p}{(2\pi)^3} T \sum_{p_0} f(p_0 = i\omega_n, k_0 = i\omega_m), \end{aligned} \quad (5.11)$$

where $E_p^2 = p^2 + m_1^2$ and $E_{p-k}^2 = (p - k)^2 + m_2^2$. Now the frequency sum over p_0 should be replaced by the contour integral given in (4.12) as

$$\begin{aligned} T \sum_{p_0} f(p_0 = i\omega_n, k_0 = i\omega_m) &= \frac{1}{2\pi i} \int_{-i\infty}^{i\infty} dp_0 \frac{1}{2} [f(p_0) + f(-p_0)] \\ &\quad + \frac{1}{2\pi i} \int_{\epsilon-i\infty}^{\epsilon+i\infty} dp_0 \frac{f(p_0) + f(-p_0)}{e^{\beta p_0} - 1} \\ &= I_1^0 + I_2^0 + I_3^\beta + I_4^\beta. \end{aligned} \quad (5.12)$$

Calculation of I_1^0 :

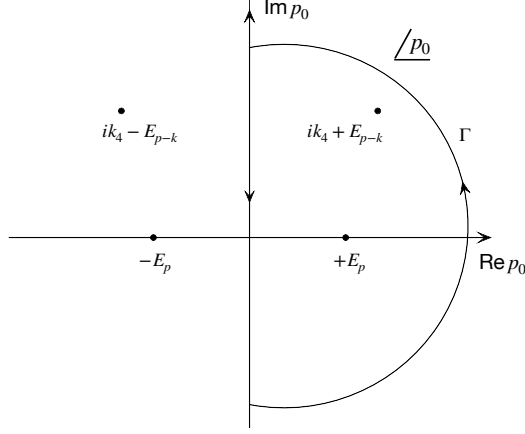


Figure 14: Contour corresponding to the integral I_1^0 in complex p_0 plane.

$$I_1^0 = \frac{1}{2\pi i} \frac{1}{2} \int_{-i\infty}^{i\infty} dp_0 f(p_0) = \frac{1}{2\pi i} \frac{1}{2} \int_{-i\infty}^{i\infty} dp_0 \frac{1}{(p_0^2 - E_p^2)[(p_0 - k_0)^2 - E_{p-k}^2]}, \quad (5.13)$$

which has four poles at $p_0 = \pm E_p$ and $k_0 \pm E_{p-k}$ with $k_0 = ik_4 = i\omega_m$. The contour is in right half plane as shown in Fig. 14 from the definition of the conversion of frequency sum to contour integral. Therefore,

$$\begin{aligned} I_1^0 &= \frac{1}{2\pi i} \frac{1}{2} \int_{-i\infty}^{i\infty} dp_0 f(p_0) = \frac{1}{2\pi i} \times \frac{1}{2} \times 2\pi i \times \text{sum of residues} \\ &= \frac{1}{2} \left[R_1^0|_{p_0=E_p} + R_2^0|_{p_0=k_0+E_{p-k}} \right] \\ &= -\frac{1}{2} \left[\frac{1}{2E_p} \frac{1}{(E_p - k_0)^2 - E_{p-k}^2} + \frac{1}{2E_{p-k}} \frac{1}{(E_{p-k} + k_0)^2 - E_p^2} \right]. \end{aligned} \quad (5.14)$$

Calculation of I_2^0 :

$$I_2^0 = \frac{1}{2\pi i} \frac{1}{2} \int_{-i\infty}^{i\infty} dp_0 f(-p_0) = \frac{1}{2\pi i} \frac{1}{2} \int_{-i\infty}^{i\infty} dp_0 \frac{1}{(p_0^2 - E_p^2)[(p_0 + k_0)^2 - E_{p-k}^2]}, \quad (5.15)$$

which has four poles at $p_0 = \pm E_p$ and $-k_0 \pm E_{p-k}$. The contour is in left half plane as shown in Fig. 15. Therefore,

$$I_2^0 = \frac{1}{2\pi i} \frac{1}{2} \int_{-i\infty}^{i\infty} dp_0 \frac{1}{2} f(-p_0) = \frac{1}{2\pi i} \times \frac{1}{2} \times (-2\pi i) \times \text{sum of residues}, \quad (5.16)$$

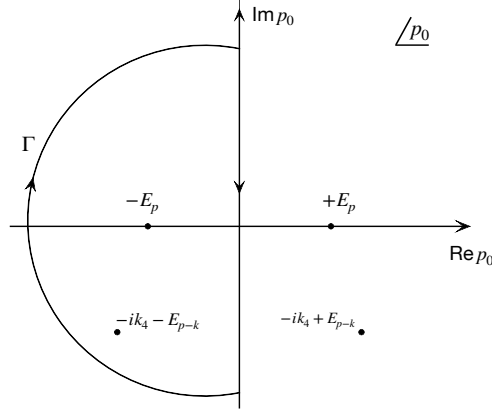


Figure 15: Contour corresponding to the integral I_2^0 in complex p_0 plane.

where negative sign in the right hand side is due to the contour in clockwise direction. We can now write

$$\begin{aligned}
 I_2^0 &= -\frac{1}{2} \left[R_1^{0'} \Big|_{p_0=-E_p} + R_2^{0'} \Big|_{p_0=-k_0-E_{p-k}} \right] \\
 &= -\frac{1}{2} \left[\frac{1}{2E_p} \frac{1}{(E_p - k_0)^2 - E_{p-k}^2} + \frac{1}{2E_{p-k}} \frac{1}{(E_{p-k} + k_0)^2 - E_p^2} \right]. \quad (5.17)
 \end{aligned}$$

Calculation of I_3^β :

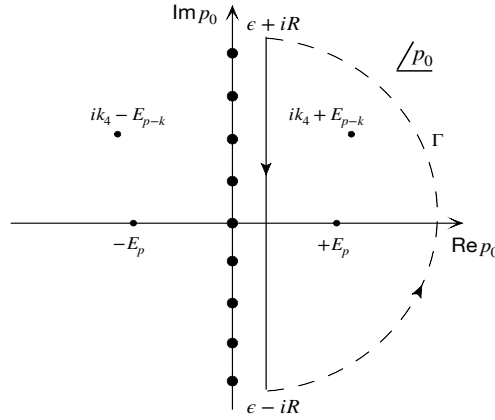


Figure 16: Contour corresponding to the integral I_3^β in complex p_0 plane.

$$I_3^\beta = \frac{1}{2\pi i} \int_{\epsilon-i\infty}^{\epsilon+i\infty} dp_0 \frac{f(p_0)}{e^{\beta p_0} - 1} = \frac{1}{2\pi i} \int_{\epsilon-i\infty}^{\epsilon+i\infty} dp_0 \frac{1}{(p_0^2 - E_p^2)[(p_0 - k_0)^2 - E_{p-k}^2]} \frac{1}{e^{\beta p_0} - 1} \quad (5.18)$$

which has four poles at $p_0 = \pm E_p$ and $k_0 \pm E_{p-k}$. The contour is in right half plane as shown Fig. 16. Therefore,

$$\begin{aligned}
I_3^\beta &= \frac{1}{2\pi i} \int_{\epsilon-i\infty}^{\epsilon+i\infty} dp_0 \frac{f(p_0)}{e^{\beta p_0} - 1} = \frac{1}{2\pi i} \times 2\pi i \times \text{sum of residues} \\
&= \left[R_3^\beta \Big|_{p_0=E_p} + R_4^\beta \Big|_{p_0=k_0+E_{p-k}} \right] \\
&= - \left[\frac{1}{2E_p} \frac{1}{(E_p - k_0)^2 - E_{p-k}^2} \frac{1}{e^{\beta E_p} - 1} + \frac{1}{2E_{p-k}} \frac{1}{(E_{p-k} + k_0)^2 - E_p^2} \frac{1}{e^{\beta(k_0+E_{p-k})} - 1} \right] (5.19)
\end{aligned}$$

Using $k_0 = ik_4 = i\omega_m = 2\pi imT$ we get

$$e^{\beta(k_0+E_{p-k})} - 1 = e^{\beta E_{p-k}} - 1, \quad (5.20)$$

as $(e^{2\pi im})^T = 1$. Now we can write

$$I_3^\beta = - \left[\frac{1}{2E_p} \frac{1}{(E_p - k_0)^2 - E_{p-k}^2} \frac{1}{e^{\beta E_p} - 1} + \frac{1}{2E_{p-k}} \frac{1}{(E_{p-k} + k_0)^2 - E_p^2} \frac{1}{e^{\beta E_{p-k}} - 1} \right] (5.21)$$

Calculation of I_4^β :

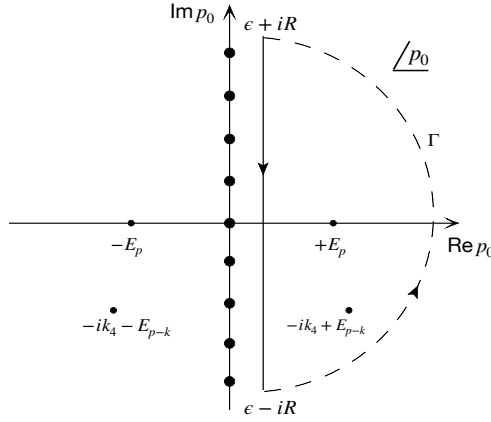


Figure 17: Contour corresponding to the integral I_4^β in complex p_0 plane.

$$I_4^\beta = \frac{1}{2\pi i} \int_{\epsilon-i\infty}^{\epsilon+i\infty} dp_0 \frac{f(-p_0)}{e^{\beta p_0} - 1} = \frac{1}{2\pi i} \int_{\epsilon-i\infty}^{\epsilon+i\infty} dp_0 \frac{1}{(p_0^2 - E_p^2)[(p_0 + k_0)^2 - E_{p-k}^2]} \frac{1}{e^{\beta p_0} - 1} (5.22)$$

which has four poles at $p_0 = \pm E_p$ and $-k_0 \pm E_{p-k}$. The contour is in right half plane as

shown in Fig. 17. Therefore,

$$\begin{aligned}
I_4^\beta &= \frac{1}{2\pi i} \int_{\epsilon-i\infty}^{\epsilon+i\infty} dp_0 \frac{f(-p_0)}{e^{\beta p_0} - 1} = \frac{1}{2\pi i} \times 2\pi i \times \text{sum of residues} \\
&= \left[R_3^{\beta'} \Big|_{p_0=E_p} + R_4^{\beta'} \Big|_{p_0=-k_0+E_{p-k}} \right] \\
&= - \left[\frac{1}{2E_p} \frac{1}{(E_p + k_0)^2 - E_{p-k}^2} \frac{1}{e^{\beta E_p} - 1} + \frac{1}{2E_{p-k}} \frac{1}{(E_{p-k} - k_0)^2 - E_p^2} \frac{1}{e^{\beta(E_{p-k}-k_0)} - 1} \right] \\
&= - \left[\frac{1}{2E_p} \frac{1}{(E_p + k_0)^2 - E_{p-k}^2} \frac{1}{e^{\beta E_p} - 1} + \frac{1}{2E_{p-k}} \frac{1}{(E_{p-k} - k_0)^2 - E_p^2} \frac{1}{e^{\beta E_{p-k}} - 1} \right] \quad (5.23)
\end{aligned}$$

Using (5.12), (5.14), (5.17), (5.21) and (5.23) in (5.11), one can have the self-energy expression as

$$\begin{aligned}
\Pi_2(k_0 = i\omega_m, k) &= -\lambda^2 \int \frac{d^3 p}{(2\pi)^3} \frac{1}{4E_p E_{p-k}} \\
&\quad \left[(1 + n_B(E_p) + n_B(E_{p-k})) \left(\frac{1}{k_0 - E_p - E_{p-k}} - \frac{1}{k_0 + E_p + E_{p-k}} \right) \right. \\
&\quad \left. - (n_B(E_p) - n_B(E_{p-k})) \left(\frac{1}{k_0 - E_p + E_{p-k}} - \frac{1}{k_0 + E_p - E_{p-k}} \right) \right] \quad (5.24)
\end{aligned}$$

where $n_B(E_i) = 1/(e^{\beta E_i} - 1)$. The terms $1/(k_0 \pm E_p \pm E_{p-k})$ and $1/(k_0 \mp E_p \pm E_{p-k})$ are the Landau damping factors. We note the following points on (5.24):

- It is to be noted that the Bose-Einstein distribution function $n_B(E_i)$ appearing in $\Pi_2(k_0, k)$ involves on-shell energies E_p and E_{p-k} of the internal lines of the self-energy but the energies of the internal lines should be off-shell. This implies that there should be cut or discontinuity in $\Pi_2(k_0, k)$.
- $\Pi_2(k_0 = i\omega_m, k)$ is defined for discrete imaginary values of $k_0 = i\omega_m = 2\pi i m T$. One could make analytic continuation in whole complex plane by putting $k_0 = i\omega_m \rightarrow \omega + i\eta$ if $\Pi_2^*(k_0 = i\omega_m, k) = \Pi_2(k_0^*, k)$.
- It is easy to see that the analytic extension has cuts along the real axis and the discontinuity along the cuts is pure imaginary:

$$\text{Disc } \Pi_2(k_0 = i\omega_m, k) = \Pi_2(k_0 = \omega + i\eta, k) - \Pi_2(k_0 = \omega - i\eta, k) = 2i \text{Im } \Pi_2(k_0 = \omega + i\eta, k). \quad (5.25)$$

- The discontinuity can easily be obtained by finding out $\text{Im } \Pi_2(k_0 = \omega + i\eta, k)$. Using the relation

$$\text{Im } f(q_0 = \omega + i\eta, q) = \text{Im} \left(\frac{1}{q_0 + q \mp \eta} \right) = \pm \pi \delta(q_0 + q) = -\text{Sgn}(\eta) \delta(q_0 + q), \quad (5.26)$$

one can find the $\text{Im } \Pi_2(k_0 = \omega + i\eta, k)$ as

$$\begin{aligned}
\text{Im } \Pi_2(\omega, k) &= \pi \lambda^2 \int \frac{d^3 p}{(2\pi)^3} \frac{1}{4E_p E_{p-k}} \\
&\times \left[\left\{ (1 + n_B(E_p))(1 + n_B(E_{p-k})) - n_B(E_p)n_B(E_{p-k}) \right\} \right. \\
&\times \left\{ \delta(\omega - E_p - E_{p-k}) - \delta(\omega + E_p + E_{p-k}) \right\} \\
&- \left\{ n_B(E_p)(1 + n_B(E_{p-k})) - n_B(E_{p-k})(1 + n_B(E_p)) \right\} \\
&\times \left. \left\{ \delta(\omega - E_p + E_{p-k}) - \delta(\omega + E_p - E_{p-k}) \right\} \right].
\end{aligned} \tag{5.27}$$

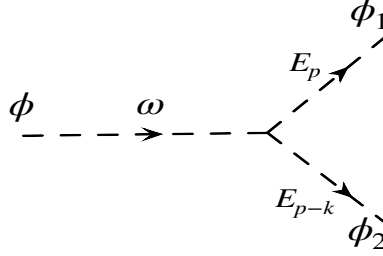


Figure 18: Feynman diagram for decay process in ϕ^3 -theory at $T = 0$.

- At $T = 0$

$$\text{Im } \Pi_2(\omega, k) = \pi \lambda^2 \int \frac{d^3 p}{(2\pi)^3} \frac{1}{4E_p E_{p-k}} \left\{ \delta(\omega - E_p - E_{p-k}) - \delta(\omega + E_p + E_{p-k}) \right\}.$$

The first term with energy conserving $\delta(\omega - E_p - E_{p-k})$ indicates a decay process $\phi \rightarrow \phi_1 + \phi_2$ as shown in Fig. 18. The energy conserving $\delta(\omega + E_p + E_{p-k})$ in the second term will never be satisfied and hence does not correspond to any physical process.

- At $T \neq 0$ the available phase space is weighted by the distribution function. There will also be additional processes compared to $T = 0$ case above. The processes are related by principle of detailed balance.

(a) Consider the first term in (5.27):

$$\left[(1 + n_B(E_p))(1 + n_B(E_{p-k})) - n_B(E_p)n_B(E_{p-k}) \right] \delta(\omega - E_p - E_{p-k}).$$

The term $(1 + n_B(E_p))(1 + n_B(E_{p-k}))\delta(\omega - E_p - E_{p-k})$ indicates a decay process $\phi \rightarrow \phi_1 + \phi_2$ in Fig. 19(a) similar to $T = 0$ case but modified by thermal weight factor. The

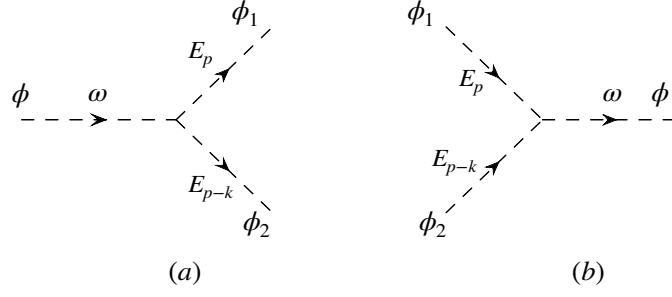


Figure 19: Feynman diagram for various processes in ϕ^3 -theory at $T \neq 0$.

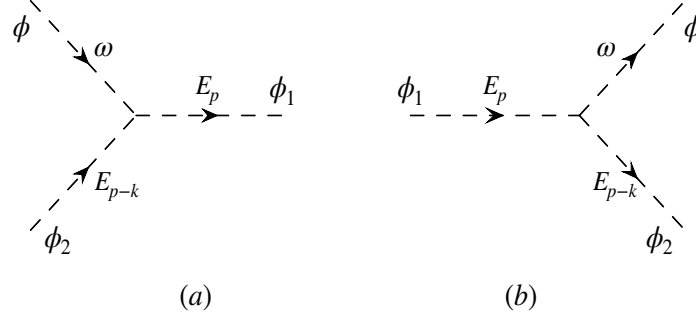


Figure 20: Feynman diagram for various processes in ϕ^3 -theory at $T \neq 0$.

term $n_B(E_p)n_B(E_{p-k})\delta(\omega - E_p - E_{p-k})$ indicates a reverse process $\phi_1 + \phi_2 \rightarrow \phi$ in Fig. 19(b) which was not there in $T = 0$ case.

(b) Consider the third term in (5.27):

$$\left[n_B(E_p)(1 + n_B(E_{p-k})) - n_B(E_{p-k})(1 + n_B(E_p)) \right] \delta(\omega - E_p + E_{p-k}).$$

The term $n_B(E_p)(1 + n_B(E_{p-k}))\delta(\omega - E_p + E_{p-k})$ indicates a absorption process $\phi + \phi_2 \rightarrow \phi_1$ in Fig. 20(a). The term $n_B(E_{p-k})(1 + n_B(E_p))\delta(\omega - E_p + E_{p-k})$ indicates an emission process $\phi_1 \rightarrow \phi + \phi_2$ in Fig. 20(b). These process were not there in $T = 0$ case.

(c) Consider the fourth term in (5.27):

$$\left[n_B(E_p)(1 + n_B(E_{p-k})) - n_B(E_{p-k})(1 + n_B(E_p)) \right] \delta(\omega + E_p - E_{p-k}).$$

The term $n_B(E_p)(1 + n_B(E_{p-k}))\delta(\omega + E_p - E_{p-k})$ indicates a absorption process $\phi + \phi_1 \rightarrow \phi_2$ as shown in Fig. 21(a) whereas the term $n_B(E_{p-k})(1 + n_B(E_p))\delta(\omega + E_p - E_{p-k})$

implies an emission process $\phi_2 \rightarrow \phi + \phi_1$ in Fig. 21(b). These processes were not there in $T = 0$ case.

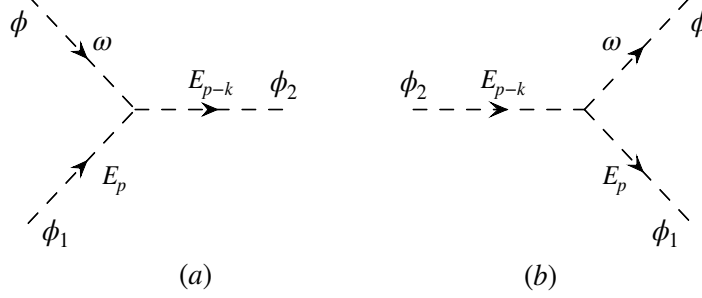


Figure 21: Feynman diagram for various processes in ϕ^3 -theory at $T \neq 0$.

6 Partition Function

Using (3.9) the density matrix of the system in (3.4) becomes

$$\begin{aligned}
 \rho(\beta) &\equiv e^{-\beta\mathcal{H}} = \rho_0(\beta)S(\beta) = e^{-\beta\mathcal{H}_0} \mathcal{T} \left(e^{-\int_0^\beta \mathcal{H}' d\tau} \right) \\
 &= e^{-\beta\mathcal{H}_0} \sum_{l=0}^{\infty} \frac{1}{l!} \mathcal{T} \left(- \int_0^\beta \mathcal{H}' d\tau \right)^l.
 \end{aligned} \tag{6.1}$$

Using this the partition function in (2.29) becomes

$$\begin{aligned}
 \mathcal{Z}(\beta) = \text{Tr} \rho(\beta) &= \text{Tr} \left[e^{-\beta\mathcal{H}_0} \sum_{l=0}^{\infty} \frac{1}{l!} \mathcal{T} \left(- \int_0^\beta \mathcal{H}' d\tau \right)^l \right] \\
 &= \text{Tr} \left[e^{-\beta\mathcal{H}_0} + e^{-\beta\mathcal{H}_0} \sum_{l=1}^{\infty} \frac{1}{l!} \mathcal{T} \left(- \int_0^\beta \mathcal{H}' d\tau \right)^l \right] \\
 &= \text{Tr} \left[e^{-\beta\mathcal{H}_0} \right] + \text{Tr} \left[e^{-\beta\mathcal{H}_0} \sum_{l=1}^{\infty} \frac{1}{l!} \mathcal{T} \left(- \int_0^\beta \mathcal{H}' d\tau \right)^l \right] \\
 &= \mathcal{Z}_0 + \mathcal{Z}_I^l,
 \end{aligned} \tag{6.2}$$

where the free (\mathcal{Z}_0) and the interaction (\mathcal{Z}_I^l) pieces are separated out by expanding around the free piece.

The logarithm of the partition function is of interest as far as thermodynamic quantities are concerned. We can write as

$$\begin{aligned}\ln \mathcal{Z}(\beta) &= \ln \left[\mathcal{Z}_0 + \mathcal{Z}_I^l \right] = \ln \left\{ \mathcal{Z}_0 \left[1 + \frac{\mathcal{Z}_I^l}{\mathcal{Z}_0} \right] \right\} = \ln \mathcal{Z}_0 + \ln \left[1 + \frac{\mathcal{Z}_I^l}{\mathcal{Z}_0} \right], \\ &= \ln \mathcal{Z}_0 + \left[\frac{\mathcal{Z}_I^l}{\mathcal{Z}_0} - \frac{1}{2} \left(\frac{\mathcal{Z}_I^l}{\mathcal{Z}_0} \right)^2 + \dots \right].\end{aligned}\quad (6.3)$$

where

$$\begin{aligned}\ln \mathcal{Z}_I &= \ln \left[1 + \frac{\mathcal{Z}_I^l}{\mathcal{Z}_0} \right] = \ln \left(1 + \frac{\text{Tr} \left[e^{-\beta \mathcal{H}_0} \sum_{l=1}^{\infty} \frac{1}{l!} \mathcal{T} \left(- \int_0^{\beta} \mathcal{H}' d\tau \right)^l \right]}{\text{Tr} [e^{-\beta \mathcal{H}_0}]} \right) \\ &= \ln \left(1 + \sum_l \frac{1}{l!} \left\langle \mathcal{T} \left(- \int_0^{\beta} \mathcal{H}' d\tau \right)^l \right\rangle_0 \right) = \ln \left[1 + \sum_l \frac{\langle \mathcal{F}_I^l \rangle_0}{l!} \right],\end{aligned}\quad (6.4)$$

where $\langle \dots \rangle_0$ is the expectation value with respect to non-interacting ensemble. We know that \mathcal{H}' contains one power of coupling in the theory. Now an expansion of $\langle \mathcal{F}_I^l \rangle_0$ up to 3rd order in l ($= 1, 2, 3$) means an expansion of $\ln \mathcal{Z}_I$ up to third order in coupling, which can then be written as

$$\ln \mathcal{Z}_I \approx \ln \left[1 + \langle \mathcal{F}_I \rangle_0 + \frac{1}{2} \langle \mathcal{F}_I^2 \rangle_0 + \frac{1}{6} \langle \mathcal{F}_I^3 \rangle_0 \right] = \ln(1 + x). \quad (6.5)$$

Again expanding $\ln(1 + x) = \sum_{j=1}^{\infty} (-1)^{j+1} x^j / j$, one can write

$$\begin{aligned}\ln \mathcal{Z}_I &\approx x - \frac{1}{2} x^2 + \frac{1}{3} x^3 + \dots \\ &\approx \langle \mathcal{F}_I \rangle_0 + \frac{1}{2} \left(\langle \mathcal{F}_I^2 \rangle_0 - \langle \mathcal{F}_I \rangle_0^2 \right) + \frac{1}{6} \left(\langle \mathcal{F}_I^3 \rangle_0 - 3 \langle \mathcal{F}_I \rangle_0 \langle \mathcal{F}_I^2 \rangle_0 + 2 \langle \mathcal{F}_I \rangle_0^3 \right) \\ &\approx (\ln \mathcal{Z}_I)_1 + (\ln \mathcal{Z}_I)_2 + (\ln \mathcal{Z}_I)_3,\end{aligned}\quad (6.6)$$

where we have assembled the terms according to the power of coupling. Using (6.6) in (6.3), the perturbative expansion of the partition function becomes

$$\ln \mathcal{Z} \approx \ln \mathcal{Z}_0 + (\ln \mathcal{Z}_I)_1 + (\ln \mathcal{Z}_I)_2 + (\ln \mathcal{Z}_I)_3, \quad (6.7)$$

where

$$(\ln \mathcal{Z}_I)_1 = \langle \mathcal{F}_I \rangle_0, \quad (6.8)$$

$$(\ln \mathcal{Z}_I)_2 = \frac{1}{2} \left(\langle \mathcal{F}_I^2 \rangle_0 - \langle \mathcal{F}_I \rangle_0^2 \right), \quad (6.9)$$

$$(\ln \mathcal{Z}_I)_3 = \frac{1}{6} \left(\langle \mathcal{F}_I^3 \rangle_0 - 3 \langle \mathcal{F}_I \rangle_0 \langle \mathcal{F}_I^2 \rangle_0 + 2 \langle \mathcal{F}_I \rangle_0^3 \right). \quad (6.10)$$

This is a perturbative expansion of the partition function around the free theory and one needs to compute it in order by order of the coupling strength of a given theory. As discussed earlier that the Trace in (6.2) stands for sum over expectation values of all possible states in Hilbert space and there are infinite number of such states in quantum field theory. So, for an interacting system the partition function will extremely be tedious to compute even if one expands in perturbation series in interaction strength in a given theory. It would be convenient to compute the partition function in functional or path integral approach.

6.1 Relation of Functional Integration and the Partition Function

Since we will be dealing with statistical thermodynamics problem when the system returns to its initial state after a time evolution from $t = 0$ to t , the corresponding transition can be written in a functional form as $\langle \phi_a | e^{-i\mathcal{H}t} | \phi_a \rangle$, assuming the Hamiltonian is time independent that simplifies the transition amplitude from one state to other.

The transition amplitude in Minkowski space-time is obtained in functional integration approach in (2.65) as

$$\langle \phi_a | e^{-i\mathcal{H}t} | \phi_a \rangle = \int_{\phi(\vec{x},0)=\phi_a(\vec{x})}^{\phi(\vec{x},t)=\phi_a(\vec{x})} \mathcal{D}\phi e^{i \int_0^t dt \int d^3x \mathcal{L}(\phi(\vec{x},t), \dot{\phi}(\vec{x},t))} = \int_{\phi(\vec{x},0)=\phi_a(\vec{x})}^{\phi(\vec{x},t)=\phi_a(\vec{x})} \mathcal{D}\phi e^{iS[\phi]}, \quad (6.11)$$

where $S[\phi]$ is the action of a system. This is the so-called path integral, and where \mathcal{D} is the functional or path integral runs over all possible paths of the field $\phi(x)$. These fields are restricted by boundary conditions while going from initial time $t = 0$ to final time $t_f = t$ as discussed in subsec 2.3. The action in Minkowski space-time is written as

$$S[\phi] = \int d^4X \mathcal{L} = \int_0^t dt \int d^3x \mathcal{L}. \quad (6.12)$$

Now, the partition function in (2.2) reads as

$$\mathcal{Z} = \text{Tr} \rho = \text{Tr} \left(e^{-\beta \mathcal{H}} \right) = \sum_n \left\langle n \left| e^{-\beta \mathcal{H}} \right| n \right\rangle, \quad (6.13)$$

where the summation over n includes all the possible energy eigenstates of the system in Hilbert space. In the continuum case the summation becomes an integral, and the eigenstates $|\phi\rangle$ form a complete set, each with energy E_ϕ . Thus, the partition function becomes

$$\mathcal{Z} = \int d\phi \left\langle \phi \left| e^{-\beta \mathcal{H}} \right| \phi \right\rangle \left(= \int d\phi e^{-\beta E_\phi} \right). \quad (6.14)$$

If one compares (6.11) and (6.14), there is a striking similarity between the path integral formulation of the transition amplitude in quantum field theory and the partition function in statistical mechanics provided that

1. the Boltzmann factor $e^{-\beta\mathcal{H}}$ acquires the form of a time evaluation operator ($e^{-i\mathcal{H}t}$) for imaginary time ($\beta = it$) through analytic continuation.
2. the time interval $[0, t]$ in the transition amplitude in (6.11) takes the role of β in the partition function with interval $[0, \beta]$ along with $\tau = it$. This is known as *Wick rotation* that rotates the integration by 90° in complex plane as displayed in Fig. 4.
3. the field ϕ obey periodic or anti-periodic boundary condition, $\phi(\vec{x}, 0) = \pm\phi(\vec{x}, \beta)$, as discussed earlier in subsec. 3.5.

With this the transition amplitude can be regarded as the partition function in path integral approach as

$$\begin{aligned}
\mathcal{Z} = \text{Tr}\rho &= \text{Tr}\left(e^{-\beta\mathcal{H}}\right) = \int d\phi \left\langle \phi \left| e^{-\beta\mathcal{H}} \right| \phi \right\rangle = \int \mathcal{D}\phi e^{i \int_0^\beta dt \int d^3x \mathcal{L}} \\
&\stackrel{t \rightarrow -i\tau}{=} \int_{\phi(\vec{x}, 0) = \pm\phi(\vec{x}, \beta)} \mathcal{D}\phi e^{\int_0^\beta d(it) \int d^3x \mathcal{L}(t \rightarrow -i\tau)} \\
&= \int_{\phi(\vec{x}, 0) = \pm\phi(\vec{x}, \beta)} \mathcal{D}\phi e^{\int_0^\beta d\tau \int d^3x \mathcal{L}(t \rightarrow -i\tau)}. \tag{6.15}
\end{aligned}$$

One can compute the partition function in Euclidean time τ and discrete frequency $i\omega_n$ directly using (6.15).

6.2 Scalar Field Partition Function

6.2.1 Partition function for free real scalar field

A real non-interacting scalar field Lagrangian is given in (5.2) by

$$\mathcal{L}_0 = \frac{1}{2} \partial_\mu \phi \partial^\mu \phi - \frac{1}{2} m^2 \phi^2 = \frac{1}{2} \left[\left(\frac{\partial \phi}{\partial t} \right)^2 - (\nabla \phi)^2 - m^2 \phi^2 \right], \tag{6.16}$$

in Minkowski space-time. This can be written only in Euclidean time [13, 63–65] as

$$\mathcal{L}_0(t \rightarrow -i\tau) \stackrel{t \rightarrow -i\tau}{=} \frac{1}{2} \left[(\partial_t \phi)^2 - (\nabla \phi)^2 - m^2 \phi^2 \right] = -\frac{1}{2} \left[(\partial_\tau \phi)^2 + (\nabla \phi)^2 + m^2 \phi^2 \right]. \tag{6.17}$$

The Fourier transform of the field $\phi(X)$ can be written as

$$\begin{aligned}
\phi(X) = \phi(x, \tau) &\stackrel{t \rightarrow -i\tau}{k_0 \rightarrow i\omega_n} \frac{1}{\sqrt{V\beta}} \sum_K e^{-iK \cdot X} \phi(K) = \frac{1}{\sqrt{V\beta}} \sum_K e^{i\vec{k} \cdot \vec{x}} e^{-i(\omega_n)(-i\tau)} \phi(\omega_n, \vec{k}) \\
&= \frac{1}{\sqrt{V\beta}} \sum_K e^{i\vec{k} \cdot \vec{x}} e^{-i\omega_n \tau} \phi(\omega_n, \vec{k}), \tag{6.18}
\end{aligned}$$

where $\sum_K = \sum_{n, \vec{k}}$ and V is the three volume.

Using (6.17) in (6.15), one can write the partition function for free scalar field as

$$\mathcal{Z}_0 = \int_{\phi(\vec{x},0)=\phi(\vec{x},\beta)} \mathcal{D}\phi e^{-\frac{1}{2} \int_0^\beta d\tau \int d^3x [(\partial_\tau \phi)^2 + (\nabla \phi)^2 + m^2 \phi^2]}, \quad (6.19)$$

where scalar field obeys periodicity condition.

Now we calculate explicitly the terms in the exponential of (6.19):

First term:

$$\begin{aligned} & \int_0^\beta d\tau \int d^3x (\partial_\tau \phi)^2 = \int d^4X \frac{1}{V\beta} \sum_K \sum_{K'} \partial_\tau \left[e^{-i\omega_n \tau} e^{i\vec{k} \cdot \vec{x}} \phi(\omega_n, \vec{k}) \right] \\ & \times \partial_\tau \left[e^{-i\omega_m \tau} e^{i\vec{k}' \cdot \vec{x}} \phi(\omega_m, \vec{k}') \right] \\ & = \int d^4X \frac{1}{V\beta} \sum_K \sum_{K'} e^{i(\vec{k} + \vec{k}') \cdot \vec{x}} e^{-i(\omega_n + \omega_m)\tau} \phi(\omega_n, \vec{k}) (-i\omega_n) (-i\omega_m) \phi(\omega_m, \vec{k}') \\ & = \frac{1}{V\beta} \sum_K \sum_{K'} \left[V \delta^3(\vec{k} + \vec{k}') \right] [\beta \delta(-\omega_n - \omega_m)] \phi(\omega_n, \vec{k}) (-i\omega_n) (-i\omega_m) \phi(\omega_m, \vec{k}') \\ & = \sum_K \phi(\omega_n, \vec{k}) \omega_n^2 \phi(-\omega_n, -\vec{k}) = \sum_K \omega_n^2 \phi(K) \phi(-K) \\ & = \sum_K \omega_n^2 \phi^*(K) \phi(K), \end{aligned} \quad (6.20)$$

where we have used $\phi(K) = \phi^*(-K)$ since $\phi(X)$ is real in (6.18). We have also used of the following relations:

$$\int_0^\beta d\tau e^{i(-\omega_n - \omega_m)\tau} = \beta \delta(-\omega_n - \omega_m), \quad (6.21)$$

$$\int d^3x e^{i(\vec{k} + \vec{k}') \cdot \vec{x}} = V \delta^3(\vec{k} + \vec{k}'), \quad (6.22)$$

$$\omega_{-n} = -\frac{2\pi n}{\beta} = -\omega_n. \quad (6.23)$$

Second term:

$$\int_0^\beta d\tau \int d^3x (\nabla \phi)^2 = \sum_K k^2 \phi^*(K) \phi(K). \quad (6.24)$$

Third term:

$$\int_0^\beta d\tau \int d^3x m^2 \phi^2 = \sum_K m^2 \phi^*(K) \phi(K). \quad (6.25)$$

Using (6.20), (6.24) and (6.25) one can write

$$\begin{aligned}
-\frac{1}{2} \int_0^\beta d\tau \int d^3x \left[(\partial_\tau \phi)^2 + (\nabla \phi)^2 + m^2 \phi^2 \right] &= -\frac{1}{2} \sum_K \phi^*(K) \left[k_0^2 + k^2 + m^2 \right] \phi(K) \\
&= -\frac{1}{2} \sum_K \phi^*(K) \left[k_0^2 + \omega_k^2 \right] \phi(K) \\
&= -\frac{1}{2} \sum_K \phi^*(K) \mathcal{G}_0^{-1}(K) \phi(K), \quad (6.26)
\end{aligned}$$

where $\mathcal{G}_0^{-1} = (\omega_n^2 + \omega_k^2)$ is the free inverse propagator in Euclidean time with energy $\omega_k = \sqrt{k^2 + m^2}$.

Using (6.26) in (6.19) one can write the free scalar field partition function as

$$\begin{aligned}
\mathcal{Z}_0 &= \int_{\phi(\vec{x},0)=\phi(\vec{x},\beta)} \mathcal{D}\phi \exp \left[-\frac{1}{2} \sum_K \phi^*(K) [\mathcal{G}_0^{-1}(K)] \phi(K) \right] \\
&= \prod_K \int_{\phi(\vec{x},0)=\phi(\vec{x},\beta)} \mathcal{D}\phi \exp \left[-\frac{1}{2} \phi^*(K) [\mathcal{G}_0^{-1}(K)] \phi(K) \right]. \quad (6.27)
\end{aligned}$$

We also note that inverse propagator is in general a diagonal matrix.

The integral can be performed using the standard identity⁵

$$\int d^D y \, e^{-\frac{1}{2} \mathbf{y} \cdot \hat{A} \mathbf{y}} = (2\pi)^{D/2} (\det \hat{A})^{-1/2}, \quad (6.28)$$

for hermitian positive definite matrix \hat{A} and D is the dimension of the system. The partition function can now be written as

$$\mathcal{Z}_0 = N [\det \mathcal{G}_0^{-1}]^{-\frac{1}{2}}, \quad (6.29)$$

where the determinant is taken over momentum space as $\mathcal{G}_0^{-1}(K)$ is diagonal. We also note that the constant factor is absorbed in N , which is irrelevant as it is temperature independent. Now the logarithm of a partition function up to a constant, becomes

$$\begin{aligned}
\ln \mathcal{Z}_0 &= \ln [\det [\mathcal{G}_0^{-1}(K)]]^{-\frac{1}{2}} \\
&= -\frac{1}{2} \ln \prod_K [\mathcal{G}_0^{-1}(K)] = -\frac{1}{2} \sum_K \ln [\mathcal{G}_0^{-1}(K)] \\
&= -\frac{1}{2} \sum_{n,k} \ln (\omega_n^2 + \omega_k^2) = -\frac{1}{2} V \int \frac{d^3 k}{(2\pi)^3} \sum_n \ln (\omega_n^2 + \omega_k^2). \quad (6.30)
\end{aligned}$$

⁵This identity is a generalisation of the one dimensional Gaussian integral $\int_{-\infty}^{\infty} dx \, \exp(-\frac{1}{2} a y^2) = \sqrt{2\pi/a}$ and can be shown by expressing the bilinear $\mathbf{y} \cdot \hat{A} \mathbf{y}$ in terms of eigenvalues of \hat{A} .

Below we perform the sum integral as

$$T \sum_n \frac{1}{T} \ln(\omega_n^2 + \omega_k^2) = T \sum_{k=0} \frac{1}{T} \ln(-k_0^2 + \omega_k^2) = T \sum_{k_0} \frac{1}{T} [\ln(\omega_k - k_0) + \ln(\omega_k + k_0)] \quad (6.31)$$

where $\omega = i\omega_n = k_0$.

Now concentrating on the first term: using (4.7) we can write

$$\begin{aligned} T \sum_{k_0} \frac{1}{T} \ln(\omega_k - k_0) &= \frac{1}{2\pi iT} \oint dk_0 \ln(\omega_k - k_0) \frac{1}{2} \coth\left(\frac{\beta k_0}{2}\right) \\ &= -\frac{1}{4\pi iT} \oint dk_0 \left(\frac{-1}{\omega_k - k_0}\right) \int dk_0 \coth\left(\frac{\beta k_0}{2}\right) \\ &= \frac{1}{4\pi iT} \oint dk_0 \left(\frac{1}{\omega_k - k_0}\right) \int dk_0 \coth\left(\frac{\beta k_0}{2}\right) \\ &= \frac{1}{4\pi iT} \oint dk_0 \left(\frac{1}{\omega_k - k_0}\right) \frac{2}{\beta} \ln\left[\sinh\left(\frac{\beta k_0}{2}\right)\right] \\ &= \frac{1}{2\pi i} \oint dk_0 \left(\frac{1}{\omega_k - k_0}\right) \ln\left[\sinh\left(\frac{\beta k_0}{2}\right)\right] \\ &= \ln\left[\sinh\left(\frac{\beta \omega_k}{2}\right)\right]. \end{aligned} \quad (6.32)$$

Similarly for the second term: choosing the opposite contour as the first one we get,

$$T \sum_{k_0} \ln(\omega_k + k_0) = \ln\left[\sinh\left(\frac{\beta \omega_k}{2}\right)\right], \quad (6.33)$$

we note here that there will be a term of $i\pi$ in (6.33), which we neglect as it would make partition function imaginary. So, the results of frequency sum in (6.31) can be written as,

$$\begin{aligned} T \sum_n \frac{1}{T} \ln(\omega_n^2 + \omega_k^2) &= 2 \ln\left[\sinh\left(\frac{\beta \omega_k}{2}\right)\right] \\ &= \beta \omega_k - 2 \ln 2 + 2 \ln(1 - e^{-\beta \omega_k}). \end{aligned} \quad (6.34)$$

We used

$$\begin{aligned} \sinh\left(\frac{\beta \omega_k}{2}\right) &= \frac{1}{2} \left(e^{\frac{\beta \omega_k}{2}} - e^{-\frac{\beta \omega_k}{2}}\right) = \frac{1}{2} e^{\frac{\beta \omega_k}{2}} (1 - e^{-\beta \omega_k}) \\ \therefore \ln\left[\sinh\left(\frac{\beta \omega_k}{2}\right)\right] &= \frac{\beta \omega_k}{2} - \ln 2 + \ln(1 - e^{-\beta \omega_k}). \end{aligned} \quad (6.35)$$

Now using (6.34) in (6.30) one gets logarithm of the partition function

$$\ln \mathcal{Z}_0 = -V \int \frac{d^3 k}{(2\pi)^3} \left[\frac{\beta \omega_k}{2} - \ln 2 + \ln(1 - e^{-\beta \omega_k}) \right], \quad (6.36)$$

where again $\ln 2$ can be neglected as it is independent of temperature. This agrees with the result obtained in (2.13).

The free energy density for free scalar field can be obtained from (2.3a) as

$$F_0 = -T \ln \mathcal{Z}_0 = VT \int \frac{d^3k}{(2\pi)^3} \left[\frac{\beta\omega_k}{2} + \ln \left(1 - e^{-\beta\omega_k} \right) \right], \quad (6.37)$$

In the infinite volume limit the pressure for free scalar field can be obtained from (2.3b) as

$$\mathcal{P}_0 = -\frac{\Omega_0}{V} = T \int \frac{d^3k}{(2\pi)^3} \left[-\frac{\beta\omega_k}{2} - \ln \left(1 - e^{-\beta\omega_k} \right) \right], \quad (6.38)$$

where the first term is the zero temperature part.

6.2.2 Partition function for interacting scalar field

The interaction Lagrangian density as given in (5.2) as

$$\mathcal{L}_I = -\frac{\lambda}{4!} \phi^4, \quad (6.39)$$

The partition function in first order λ as given in (6.8)

$$(\ln \mathcal{Z}_I)_1 = \langle \mathcal{F}_I \rangle_0 = \frac{1}{\mathcal{Z}_0} \text{Tr} \left[e^{-\beta \mathcal{H}_0} \mathcal{T} \left(- \int_0^\beta \mathcal{H}' d\tau \right) \right]. \quad (6.40)$$

Using path integral it becomes [13]

$$\begin{aligned} (\ln \mathcal{Z}_I)_1 &= \frac{\int \mathcal{D}\phi \mathcal{S}_I e^{i\mathcal{S}_0[\phi]}}{\int \mathcal{D}\phi e^{i\mathcal{S}_0[\phi]}} \\ &= \frac{\int_{\text{periodic}} \mathcal{D}\phi \left(- \int_0^\beta d\tau \int d^3x \mathcal{L}_I(t \rightarrow -i\tau) \right) e^{-\int_0^\beta d\tau \int d^3x \mathcal{L}_0(t \rightarrow -i\tau)}}{\int_{\text{periodic}} \mathcal{D}\phi e^{-\int_0^\beta d\tau \int d^3x \mathcal{L}_0(t \rightarrow -i\tau)}}, \end{aligned} \quad (6.41)$$

where free partition function is already calculated in (6.27) as

$$\mathcal{Z}_0 = \int_{\text{periodic}} \mathcal{D}\phi_{n,\vec{k}} \exp \left[-\frac{1}{2} \sum_{n,k} [\omega_n^2 + \omega_k^2] |\phi_{n,\vec{k}}|^2 \right]. \quad (6.42)$$

Now we need to compute the numerator of (6.41). Using the same method as the free case one can proceed as [13, 64]

$$(\ln \mathcal{Z}_I)_1 = \frac{1}{\mathcal{Z}_0} \int_{\text{periodic}} \mathcal{D}\phi_{n,\vec{k}} \left(\lambda \int_0^\beta d\tau \int d^3x \phi^4 \right) \exp \left[-\frac{1}{2} \sum_{n,k} [\omega_n^2 + \omega_k^2] |\phi_{n,\vec{k}}|^2 \right] \quad (6.43)$$

Using the Fourier decomposition of fields in (6.18), one can get

$$\begin{aligned}
\lambda \int_0^\beta d\tau \int d^3x \phi^4 &= \frac{\lambda}{(V\beta)^2} \sum_{m_1, \vec{q}_1} \sum_{m_2, \vec{q}_2} \sum_{m_3, \vec{q}_3} \sum_{m_4, \vec{q}_4} \phi_{m_1, \vec{q}_1} \phi_{m_2, \vec{q}_2} \phi_{m_3, \vec{q}_3} \phi_{m_4, \vec{q}_4} \\
&\times \int_0^\beta d\tau \int d^3x e^{i(\vec{q}_1 + \vec{q}_2 + \vec{q}_3 + \vec{q}_4) \cdot x} e^{-i(\omega_{m_1} + \omega_{m_2} + \omega_{m_3} + \omega_{m_4})\tau} \\
&= \frac{\lambda}{(V\beta)^2} \sum_{m_1, \vec{q}_1} \sum_{m_2, \vec{q}_2} \sum_{m_3, \vec{q}_3} \sum_{m_4, \vec{q}_4} \phi_{m_1, \vec{q}_1} \phi_{m_2, \vec{q}_2} \phi_{m_3, \vec{q}_3} \phi_{m_4, \vec{q}_4} \\
&\times \beta \delta(-\omega_{m_1} - \omega_{m_2} - \omega_{m_3} - \omega_{m_4}) V \delta^3(\vec{q}_1 + \vec{q}_2 + \vec{q}_3 + \vec{q}_4). \quad (6.44)
\end{aligned}$$

We have used two delta functions following (6.21) and (6.22) from τ and x integrations, respectively and they guarantee the energy momentum conservation in the interaction vertex. Now, the non-zero contribution comes when $\omega_{m_1} = -\omega_{m_2}$, $\omega_{m_3} = -\omega_{m_4}$ and $\vec{q}_1 = -\vec{q}_2$, $\vec{q}_3 = -\vec{q}_4$. Obviously, there are another two combination that would give non-zero contributions. This allows 3 non-zero permutations among ω_{m_i} and q_i . Then one can write

$$\lambda \int_0^\beta d\tau \int d^3x \phi^4 = 3\lambda(\beta V) \left(\frac{1}{V\beta} \right)^2 \sum_{m, \vec{q}} \sum_{l, \vec{p}} |\phi_{m, \vec{q}}|^2 |\phi_{l, \vec{p}}|^2. \quad (6.45)$$

Using (6.45) in (6.43), one gets

$$\begin{aligned}
(\ln \mathcal{Z}_I)_1 &= 3\lambda\beta V \left(\frac{1}{V\beta} \right)^2 \sum_{m, \vec{q}} \sum_{l, \vec{p}} \frac{\prod_{n, \vec{k}} \int_{\text{periodic}} \mathcal{D}\phi_{n, \vec{k}} |\phi_{m, \vec{q}}|^2 |\phi_{l, \vec{p}}|^2 \exp \left[-\frac{1}{2} (\omega_n^2 + \omega_k^2) |\phi_{n, \vec{k}}|^2 \right]}{\prod_{n, \vec{k}} \int_{\text{periodic}} \mathcal{D}\phi_{n, \vec{k}} \exp \left[-\frac{1}{2} (\omega_n^2 + \omega_k^2) |\phi_{n, \vec{k}}|^2 \right]} \\
&= 3\lambda\beta V \left(\frac{1}{V\beta} \right)^2 \left[\sum_{n, \vec{k}} \frac{\int_{\text{periodic}} \mathcal{D}\phi_{n, \vec{k}} |\phi_{n, \vec{k}}|^2 \exp \left[-\frac{1}{2} (\omega_n^2 + \omega_k^2) |\phi_{n, \vec{k}}|^2 \right]}{\int_{\text{periodic}} \mathcal{D}\phi_{n, \vec{k}} \exp \left[-\frac{1}{2} (\omega_n^2 + \omega_k^2) |\phi_{n, \vec{k}}|^2 \right]} \right]^2, \quad (6.46)
\end{aligned}$$

if $m = l = n$ and $\vec{q} = \vec{p} = \vec{k}$, the integral over $\phi_{n, \vec{k}}$ gets factorised as above. When $m \neq l \neq n$ and $\vec{q} \neq \vec{p} \neq \vec{k}$, the $\phi_{n, \vec{k}}$ integral in the numerator and denominator are identical and they cancel out, thus the integral disappears.

Using Gaussian integral $\int dy y^{2n} e^{-\alpha y^2} = \Gamma(n + 1/2)/\alpha^{n+1/2}$, one gets

$$\begin{aligned}
(\ln \mathcal{Z}_I)_1 &= 3\lambda\beta V \left(\frac{1}{V\beta} \right)^2 \left[\frac{\Gamma(1 + \frac{1}{2})}{\alpha^{3/2}} \times \frac{\alpha^{1/2}}{\Gamma(\frac{1}{2})} \right]^2 = 3\lambda\beta V \left(\frac{1}{V\beta} \right)^2 \left[\frac{1}{2\alpha} \right]^2 \\
&= 3\lambda\beta V \left(\frac{1}{V\beta} \right)^2 \left[\sum_{n, k} \frac{1}{(\omega_n^2 + \omega_k^2)} \right]^2 = 3\lambda\beta V \left[\frac{1}{V\beta} \sum_{n, k} \frac{1}{\omega_n^2 + \omega_k^2} \right]^2. \quad (6.47)
\end{aligned}$$

Taking continuum limit $\sum_k \rightarrow V \int d^3k/(2\pi)^3$, one gets

$$(\ln \mathcal{Z}_I)_1 = 3 \lambda \beta V \left[\frac{1}{\beta} \sum_n \int \frac{d^3k}{(2\pi)^3} \frac{1}{\omega_n^2 + \omega_k^2} \right]^2. \quad (6.48)$$

where the \sum_n is Euclidean. Casting this into Minkowski $\omega_n = k_4 = -ik_0$, one can write

$$(\ln \mathcal{Z}_I)_1 = - 3 \lambda \beta V \left[\frac{1}{\beta} \sum_{k_0} \int \frac{d^3k}{(2\pi)^3} \frac{1}{k_0^2 - \omega_k^2} \right]^2, \quad (6.49)$$

where one can use contour integration in (4.4) vis-a-vis (4.7) and (4.9). We also note the following points:

- The term inside the square braces are the sum-integral that comes from the loop integral $\int d^4K/(2\pi)^4$ and the scalar propagator $(1/(k_0^2 - k^2 - m^2) = 1/(k_0^2 - \omega_k^2)$ with energy $\omega_k = \sqrt{k^2 + m^2}$.
 - λ is the interaction vertex.
 - βV is the left out factor that comes from the energy-momentum conservation (e.g., (6.44)) in the vertex.
 - The square, $[\dots]^2$, indicates that two loops connected to one interaction point λ .
- \Rightarrow All these together correspond to a topologically distinct diagram $\left[\text{figure} \right]$.
- 3 is the symmetry factor that comes from 3 different permutation of contraction allowed by the energy-momentum conservation.

Now the first order correction to the scalar partition function in (6.49) can be represented in Feynman diagram as

$$(\ln \mathcal{Z}_I)_1 = - 3 \beta V \times \text{figure}. \quad (6.50)$$

The frequency sum in (6.49) is exactly similar to that of tadpole diagram as done in Subsec. 5.1 but with different symmetry factor (1/2). Excluding this 1/2 factor and λ and the zero temperature part, the result of the sum integral can be obtained from (5.7) as $T^2/12$. Thus, the first order correction to the scalar partition function in (6.49) becomes

$$(\ln \mathcal{Z}_I)_1 = - 3 \lambda \beta V \left[\frac{1}{\beta} \sum_n \int \frac{d^3k}{(2\pi)^3} \frac{1}{k_0^2 - \omega_k^2} \right]^2 = - 3 \lambda \beta V \frac{T^4}{144} = - \lambda \frac{VT^3}{48}. \quad (6.51)$$

6.2.3 Pressure

The logarithm of the scalar partition function up to first order in coupling can now be written using (6.3), (6.36) and (6.51) as

$$\begin{aligned}\ln \mathcal{Z}(\beta) &= \ln \mathcal{Z}_0 + (\ln \mathcal{Z}_I)_1 \\ &= -V \int \frac{d^3k}{(2\pi)^3} \ln \left(1 - e^{-\beta\omega_k}\right) - \lambda \frac{VT^3}{48} + \mathcal{O}(\lambda^2),\end{aligned}\quad (6.52)$$

where we have also dropped the $T = 0$ contribution in $\ln \mathcal{Z}_0$. In the infinite volume limit the pressure up to first order can be obtained as

$$\begin{aligned}\mathcal{P} = -\frac{\Omega}{V} &= -T \int \frac{d^3k}{(2\pi)^3} \ln \left(1 - e^{-\beta\omega_k}\right) - \lambda \frac{T^4}{48} + \mathcal{O}(\lambda^2) \\ &= \frac{\pi^2 T^4}{90} - \lambda \frac{T^4}{48} + \mathcal{O}(\lambda^2),\end{aligned}\quad (6.53)$$

where Ω is the thermodynamic potential. The other thermodynamic quantities can be obtained from pressure. One can also compute the higher order corrections to the partition function following (6.9) and (6.10), and thus higher order thermodynamic quantities.

6.3 Fermion Field

Until now we have discussed partition function for real scalar field and its pressure up to first order in coupling. In this section we will compute the partition function for free fermionic fields. The computation of interacting fermionic partition function is postponed until we introduce gauge theory, quantum electrodynamics (QED). Since fermions are anticommuting fields, they are Grassmann variables. We start this section by reviewing some of the properties of Fermionic fields.

6.3.1 Fermionic Lagrangian and conserved charge

The Lagrangian density that describes the non-interacting fermion is given in Minkowski space-time [72, 73] as

$$\mathcal{L} = \bar{\psi} (i\not{\partial} - m) \psi, \quad (6.54)$$

where m is the mass of the fermion and the fields ψ and $\bar{\psi}$ are to be treated independently. The γ -matrices in Dirac-Pauli representation are given as

$$\gamma^0 = \begin{pmatrix} I & 0 \\ 0 & -I \end{pmatrix} \quad \text{and} \quad \gamma^i = \begin{pmatrix} 0 & \sigma^i \\ -\sigma^i & 0 \end{pmatrix}, \quad (6.55)$$

where I is a 2×2 unit matrix and the Pauli matrices σ^i 's are

$$\sigma^1 = \begin{pmatrix} 0 & 1 \\ 1 & 0 \end{pmatrix} \quad \sigma^2 = \begin{pmatrix} 0 & -i \\ i & 0 \end{pmatrix} \quad \text{and} \quad \sigma^3 = \begin{pmatrix} 1 & 0 \\ 0 & -1 \end{pmatrix}. \quad (6.56)$$

Using the Euler-Lagrange equation for $\bar{\psi}$ field

$$\frac{\partial \mathcal{L}}{\partial \bar{\psi}} = \partial_\mu \left(\frac{\partial \mathcal{L}}{\partial (\partial^\mu \bar{\psi})} \right) \Rightarrow (i\gamma^\mu \partial_\mu - m) \psi = \partial_\mu [0] = 0, \quad (6.57)$$

one gets the Dirac equation for ψ field. The Hamiltonian density is given as

$$\mathcal{H}_d = \pi \partial_0 \psi + \partial_0 \bar{\psi} \bar{\pi} - \mathcal{L}. \quad (6.58)$$

The conjugate momenta can be obtained as

$$\pi = \frac{\partial \mathcal{L}}{\partial (\partial_0 \psi)} = i\psi^\dagger, \quad (6.59)$$

$$\bar{\pi} = \frac{\partial \mathcal{L}}{\partial (\partial_0 \bar{\psi})} = 0. \quad (6.60)$$

Using (6.59) and (6.60) in (6.58), the Hamiltonian density becomes

$$\begin{aligned} \mathcal{H}_d &= i\psi^\dagger \partial_0 \psi - \bar{\psi} (i\partial - m) \psi = i\bar{\psi} \gamma^0 \partial_0 \psi - i\bar{\psi} \gamma^0 \partial_0 \psi + i\bar{\psi} \gamma^i \partial_i \psi + \bar{\psi} m \psi \\ &= i\bar{\psi} (\gamma^i \partial_i + m) \psi. \end{aligned} \quad (6.61)$$

This is the Hamiltonian density for canonical ensemble. However, allowing a local transformation, *i.e.*, α depends on X , one gets

$$\begin{aligned} \mathcal{L} \rightarrow \mathcal{L}' &= \bar{\psi} e^{i\alpha(X)} (i\partial - m) \psi e^{-i\alpha(X)} = \bar{\psi} (i\partial - m) \psi + \bar{\psi} \partial \alpha(X) \psi \\ &= \mathcal{L} + \bar{\psi} \partial \alpha(X) \psi. \end{aligned} \quad (6.62)$$

As seen if $\alpha(X) = \alpha$, is a constant, then $\mathcal{L}' = \mathcal{L}$, the Lagrangian density is invariant under global symmetry. This symmetry will lead to a conserved current according to Noether's theorem. By solving the equation of motion for α , one gets

$$\begin{aligned} \partial_\mu \left(\frac{\partial \mathcal{L}'}{\partial (\partial^\mu \alpha)} \right) &= \frac{\partial \mathcal{L}'}{\partial \alpha} \\ \partial_\mu [\bar{\psi} \gamma^\mu \psi] &= \partial_\mu j^\mu = 0, \end{aligned} \quad (6.63)$$

where the conserved current is found as

$$j^\mu = \bar{\psi} \gamma^\mu \psi. \quad (6.64)$$

Now the temporal component $j^0 = \bar{\psi} \gamma^0 \psi = \bar{\psi}^\dagger \psi = \rho$ is associated with conserved number density. The conserved number can be obtained as

$$N = \int d^3x j^0 = \int d^3x \bar{\psi}^\dagger \psi = \int d^3x \rho. \quad (6.65)$$

Now, the new Hamiltonian density in presence of chemical potential associated with a conserved number becomes

$$\mathcal{H}_d - \mu \rho = i\bar{\psi} (\gamma^i \partial_i + m) \psi - \mu \rho = \bar{\psi} (i\gamma^i \partial_i + m - \mu \gamma^0) \psi. \quad (6.66)$$

The corresponding new Lagrangian density becomes

$$\mathcal{L} = \bar{\psi} (i\gamma^\mu \partial_\mu - m + \mu\gamma^0) \psi, \quad (6.67)$$

which indicates that the presence of the chemical potential is like changing the zeroth component of the gauge field (external field), through the substitution $\partial_0 \rightarrow \partial_0 - i\mu$ in the Lagrangian.

6.3.2 Partition function and pressure for free fermions

The partition function for free fermionic field reads from (6.15) as

$$\mathcal{Z}_0 = \int_{\psi(\vec{x},0)=-\psi(\vec{x},\beta)} \mathcal{D}[\bar{\psi}] \mathcal{D}[\psi] e^{\int_0^\beta d\tau \int d^3x \mathcal{L}(t \rightarrow -i\tau)}. \quad (6.68)$$

As before, the Fourier transform of the fermionic fields $\psi(X)$ and $\bar{\psi}(X)$ can be written as

$$\begin{aligned} \psi(X) &= \psi(\vec{x}, \tau) \stackrel{t \rightarrow -i\tau}{k_0 \rightarrow i\omega_n} \frac{1}{\sqrt{V\beta}} \sum_K e^{-iK \cdot X} \psi(K) = \frac{1}{\sqrt{V\beta}} \sum_{n, \vec{k}} e^{i\vec{k} \cdot \vec{x}} e^{-i\omega_n \tau} \psi(\omega_n, \vec{k}), \\ \bar{\psi}(X) &= \bar{\psi}(\vec{x}, \tau) \stackrel{t \rightarrow -i\tau}{k_0 \rightarrow i\omega_n} \frac{1}{\sqrt{V\beta}} \sum_K e^{iK \cdot X} \bar{\psi}(K) = \frac{1}{\sqrt{V\beta}} \sum_{n, \vec{k}} e^{-i\vec{k} \cdot \vec{x}} e^{i\omega_n \tau} \bar{\psi}(\omega_n, \vec{k}). \end{aligned} \quad (6.69)$$

where V is the three volume. The Lagrangian density in (6.67) can now be written in Euclidean time as

$$\begin{aligned} \mathcal{L}(t \rightarrow -i\tau) &\stackrel{t \rightarrow -i\tau}{=} \bar{\psi} (i\gamma^\mu \partial_\mu - m + \mu\gamma^0) \psi \stackrel{t \rightarrow -i\tau}{=} \bar{\psi} (i\gamma^0 \partial_0 - i\gamma^i \partial_i - m + \mu\gamma^0) \psi \\ &= -\bar{\psi} (\gamma^0 \partial_\tau + i\gamma^i \partial_i + m - \mu\gamma^0) \psi. \end{aligned} \quad (6.70)$$

Using the Fourier transformed of fermionic fields in (6.69) we compute

$$\begin{aligned} \int_0^\beta d\tau \int d^3x \mathcal{L}(t \rightarrow -i\tau) &= -\frac{1}{V\beta} \int_0^\beta d\tau \int d^3x \sum_{n, \vec{k}} \sum_{m, \vec{k}'} e^{-i\vec{k} \cdot \vec{x}} e^{i\omega_n \tau} \bar{\psi}(\omega_n, \vec{k}) \\ &\quad [\gamma^0 \partial_\tau + i\gamma^i \partial_i + m - \mu\gamma^0] e^{i\vec{k}' \cdot \vec{x}} e^{-i\omega_m \tau} \psi(\omega_m, \vec{k}') \\ &= -\frac{1}{V\beta} \int_0^\beta d\tau \int d^3x \sum_{n, \vec{k}} \sum_{m, \vec{k}'} e^{-i\vec{k} \cdot \vec{x}} e^{i\omega_n \tau} \bar{\psi}(\omega_n, \vec{k}) \\ &\quad [\gamma^0(-i\omega_m) + i\gamma^i(ik'_i) + m - \mu\gamma^0] e^{i\vec{k}' \cdot \vec{x}} e^{-i\omega_m \tau} \psi(\omega_m, \vec{k}') \\ &= -\frac{1}{V\beta} \sum_{n, \vec{k}} \sum_{m, \vec{k}'} \bar{\psi}(\omega_n, \vec{k}) [\gamma^0(-i\omega_m) + i\gamma^i(ik'_i) + m - \mu\gamma^0] \psi(\omega_m, \vec{k}') \\ &\quad \times \beta \delta(\omega_n - \omega_m) V \delta^3(\vec{k}' - \vec{k}) \\ &= -\sum_{n, \vec{k}} \bar{\psi}(\omega_n, \vec{k}) [-\gamma^0(i\omega_n + \mu) - \gamma^i k_i + m] \psi(\omega_n, \vec{k}) \\ &= -\sum_{n, \vec{k}} \bar{\psi}(\omega_n, \vec{k}) \left[S_0^{-1}((i\omega_n + \mu), \vec{k}) \right] \psi(\omega_n, \vec{k}), \end{aligned} \quad (6.71)$$

where $S_0^{-1}(i\omega_n + \mu, \vec{k})$ is the inverse of free fermionic propagator in presence of chemical potential μ . The partition function in (6.68) becomes

$$\begin{aligned}\mathcal{Z}_0 &= \prod_{n, \vec{k} \text{ antiperiodic}} \int \mathcal{D}[\bar{\psi}] \mathcal{D}[\psi] e^{-\bar{\psi}(\omega_n, \vec{k}) [S_0^{-1}((i\omega_n + \mu), \vec{k})] \psi(\omega_n, \vec{k})} \\ &= \prod_{n, k} \det \left[S_0^{-1}((i\omega_n + \mu), \vec{k}) \right],\end{aligned}\quad (6.72)$$

where we have used the result of the functional integral in (2.78) involving Grassman variables. The logarithm of \mathcal{Z}_0 becomes

$$\begin{aligned}\ln \mathcal{Z}_0 &= \sum_{n, k} \ln \det \left[S_0^{-1}((i\omega_n + \mu), \vec{k}) \right] \\ &= \sum_{n, k} \ln \det \left[-\gamma^0(i\omega_n + \mu) - \gamma^i k_i + m \right] = \sum_{n, k} \ln \det[Y].\end{aligned}\quad (6.73)$$

Now one can write

$$\begin{aligned}\det[Y] &= \det \left\{ \begin{pmatrix} -(i\omega_n + \mu) & 0 \\ 0 & (i\omega_n + \mu) \end{pmatrix} + \begin{pmatrix} 0 & -\vec{\sigma} \cdot \vec{k} \\ \vec{\sigma} \cdot \vec{k} & 0 \end{pmatrix} + \begin{pmatrix} m & 0 \\ 0 & m \end{pmatrix} \right\} \\ &= \det \left\{ \begin{pmatrix} -(i\omega_n + \mu) + m & -\vec{\sigma} \cdot \vec{k} \\ \vec{\sigma} \cdot \vec{k} & (i\omega_n + \mu) + m \end{pmatrix} \right\},\end{aligned}\quad (6.74)$$

where each element is a 2×2 matrix. Using the identity $(\vec{\sigma} \cdot \vec{k})^2 = k^2$, one can compute the determinant as

$$\det[Y] = [k^2 + m^2 - (i\omega_n + \mu)^2]^2. \quad (6.75)$$

Combining (6.75) and (6.73), one can write

$$\begin{aligned}\ln \mathcal{Z}_0 &= 2 \sum_{n, k} \ln [k^2 + m^2 - (i\omega_n + \mu)^2] \\ &= 2V \sum_n \int \frac{d^3 k}{(2\pi)^3} [\ln((\omega_k - \mu) - i\omega_n) + \ln((\omega_k + \mu) + i\omega_n)],\end{aligned}\quad (6.76)$$

where $\omega_k = \sqrt{k^2 + m^2}$ and \sum_k is replaced by $V \int \frac{d^3 k}{(2\pi)^3}$.

Now we will perform the frequency sum in (6.76):

First term: using (4.17), one can write

$$\begin{aligned}\sum_n \ln[(\omega_k - \mu) - i\omega_n] &= T \sum_n \frac{1}{T} \ln[(\omega_k - \mu) - k_0] \\ &= \frac{1}{2\pi iT} \oint dk_0 \ln[(\omega_k - \mu) - k_0] \frac{1}{2} \tanh\left(\frac{\beta k_0}{2}\right) \\ &= -\frac{1}{4\pi iT} \oint dk_0 \left(\frac{-1}{(\omega_k - \mu) - k_0} \right) \int dk_0 \tanh\left(\frac{\beta k_0}{2}\right) \\ &= \frac{1}{4\pi iT} \oint dk_0 \left(\frac{1}{(\omega_k - \mu) - k_0} \right) \int dk_0 \tanh\left(\frac{\beta k_0}{2}\right)\end{aligned}$$

$$\begin{aligned}
&= \frac{1}{4\pi iT} \oint dk_0 \left(\frac{1}{(\omega_k - \mu) - k_0} \right) \frac{2}{\beta} \ln \left[\cosh \left(\frac{\beta k_0}{2} \right) \right] \\
&= \frac{1}{2\pi i} \oint dk_0 \left(\frac{1}{(\omega_k - \mu) - k_0} \right) \ln \left[\cosh \left(\frac{\beta k_0}{2} \right) \right] \\
&= \ln \left[\cosh \left(\frac{\beta(\omega_k - \mu)}{2} \right) \right] \\
&= \ln \left[\frac{1}{2} \left(e^{\beta(\omega_k - \mu)/2} + e^{-\beta(\omega_k - \mu)/2} \right) \right] \\
&= \ln \left[\frac{1}{2} e^{\beta(\omega_k - \mu)/2} \left(1 + e^{-\beta(\omega_k - \mu)} \right) \right] \\
&= \left[\frac{\beta(\omega_k - \mu)}{2} - \ln 2 + \ln \left(1 + e^{-\beta(\omega_k - \mu)} \right) \right] \\
&= \left[\frac{\beta(\omega_k - \mu)}{2} + \ln \left(1 + e^{-\beta(\omega_k - \mu)} \right) \right], \tag{6.77}
\end{aligned}$$

where again $\ln 2$ is neglected as it is independent of temperature.

Second term:

$$\begin{aligned}
\sum_n \ln[(\omega_k + \mu) + i\omega_n] &= T \sum_n \frac{1}{T} \ln[(\omega_k - \mu) - k_0] = \ln \left[\cosh \left(\frac{\beta(\omega_k + \mu)}{2} \right) \right] \\
&= \left[\frac{\beta(\omega_k + \mu)}{2} - \ln 2 + \ln \left(1 + e^{-\beta(\omega_k + \mu)} \right) \right] \\
&= \left[\frac{\beta(\omega_k + \mu)}{2} + \ln \left(1 + e^{-\beta(\omega_k + \mu)} \right) \right]. \tag{6.78}
\end{aligned}$$

Now using (6.77) and (6.78) in (6.76), one gets logarithm of the partition function

$$\ln \mathcal{Z}_0 = 2V \int \frac{d^3 k}{(2\pi)^3} \left[\beta\omega_k + \ln \left(1 + e^{-\beta(\omega_k - \mu)} \right) + \ln \left(1 + e^{+\beta(\omega_k + \mu)} \right) \right], \tag{6.79}$$

which agrees with that obtained in quantum statistical mechanics in (2.21) and (2.23).

The free energy density for free fermionic field can be obtained as

$$F_0 = -\frac{T \ln \mathcal{Z}_0}{V} = -2T \int \frac{d^3 k}{(2\pi)^3} \left[\beta\omega_k + \ln \left(1 + e^{-\beta(\omega_k - \mu)} \right) + \ln \left(1 + e^{+\beta(\omega_k + \mu)} \right) \right] \tag{6.80}$$

In the infinite volume limit the pressure for fermionic field can be obtained as

$$\mathcal{P}_0 = -F_0 = 2T \int \frac{d^3 k}{(2\pi)^3} \left[\beta\omega_k + \ln \left(1 + e^{-\beta(\omega_k - \mu)} \right) + \ln \left(1 + e^{+\beta(\omega_k + \mu)} \right) \right], \tag{6.81}$$

where the first term is the zero temperature part which should be dropped as it only shifts the vacuum energy. After performing the integration of temperature dependent part, one obtains pressure for free massless fermion

$$\mathcal{P}_0 = \frac{7\pi^2 T^4}{180} + \frac{\mu^2 T^2}{6} + \frac{\mu^4}{12\pi^2}. \tag{6.82}$$

6.3.3 A reverse way: first number density and then pressure and entropy density for fermions

The partition function in Minkowski space time can be written

$$\mathcal{Z}(\beta, [\mu]) = \int \mathcal{D}[\bar{\psi}] \mathcal{D}[\psi] e^{i \int d^4 X \mathcal{L}(\psi, \bar{\psi}; [\mu])}. \quad (6.83)$$

The pressure can be written as

$$\mathcal{P}(\beta; [\mu]) = \frac{1}{\mathcal{V}} \ln \mathcal{Z}(T; [\mu]) = \frac{T}{V} \ln \mathcal{Z}(T; [\mu]), \quad (6.84)$$

where the four-volume, $\mathcal{V} = \beta V$ with V is the three-volume.

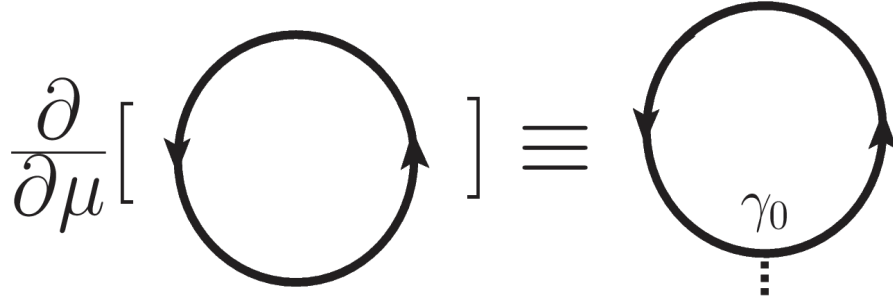


Figure 22: The Feynman diagram for number density originating from μ derivative of the pressure diagram that brings a γ_0 .

Now the number density ρ can be obtained [74, 75] as

$$\rho \equiv \frac{\partial \mathcal{P}(\beta; [\mu])}{\partial \mu} = \frac{i}{\mathcal{V} \mathcal{Z}[\beta; j]} \int \mathcal{D}[\bar{\psi}] \mathcal{D}[\psi] \int d^4 x \bar{\psi}(x) \gamma_0 [\mu] \psi(x) e^{(i \int d^4 x \mathcal{L}(\psi, \bar{\psi}; [\mu]))}. \quad (6.85)$$

The full fermionic propagator in presence of uniform μ can be written as

$$i\mathcal{S}_{\alpha\sigma}[\mu](x, x') = \frac{\int \mathcal{D}[\bar{\psi}] \mathcal{D}[\psi] \psi_\alpha(x) \bar{\psi}_\sigma(x') \exp(i \int d^4 x \mathcal{L}(\psi, \bar{\psi}; [\mu]))}{\int \mathcal{D}[\bar{\psi}] \mathcal{D}[\psi] \exp(i \int d^4 x \mathcal{L}(\psi, \bar{\psi}; [\mu]))}. \quad (6.86)$$

Now using (6.86) and performing the traces over Dirac and coordinate indices in (6.85) one can write

$$\begin{aligned} \rho &= \int \frac{d^4 K}{(2\pi)^4} \text{tr} [iS[\mu](K) (-i)\gamma_0[\mu](K, -K; 0)] \\ &= \int \frac{d^4 K}{(2\pi)^4} \text{tr} [S[\mu](K) \gamma_0[\mu](K, -K; 0)], \end{aligned} \quad (6.87)$$

where 'tr' indicates the trace over the Dirac indices.

Now if we consider free fermions, then the full propagator $S[\mu]$ can be replaced by the free fermion propagator $S_0[\mu]$ and the number density in (6.87) can be written as

$$\rho_0 = \int \frac{d^4 K}{(2\pi)^4} \text{tr} [S_0[\mu](K) \gamma_0[\mu](K, -K; 0)], \quad (6.88)$$

The expression for number density in (6.88) corresponds to Feynman diagram in Fig. 22. The free fermionic propagator for momentum K in helicity representation is given in (7.23) as

$$S_0(K) = \frac{\gamma_0 - \vec{\gamma} \cdot \hat{k}}{2d_+(k_0, k)} + \frac{\gamma_0 + \vec{\gamma} \cdot \hat{k}}{2d_-(k_0, k)}, \quad (6.89)$$

$$\text{with } d_{\pm} = k_0 \mp k. \quad (6.90)$$

Using (6.89) in (6.88) and performing the trace over Dirac matrices, we get

$$\rho_0(T, \mu) = 2 \int \frac{d^3 k}{(2\pi)^3} \frac{1}{\beta} \sum_{k_0=(2n+1)\pi i T + \mu} \left[\frac{1}{k_0 - k} + \frac{1}{k_0 + k} \right]. \quad (6.91)$$

We note here that the chemical potential is not considered in the propagator but considered in the discrete frequency as $k_0 = i\omega_n + \mu$. This shifts the pole of \tanh by an amount μ in (4.17). This will lead to same result as will see below.

For computing the frequency sum in (6.91), we use the standard technique of contour integration as given in (4.19) in presence of μ as

$$\frac{1}{2\pi i} \oint_C \left[\frac{1}{k_0 - k} + \frac{1}{k_0 + k} \right] \frac{\beta}{2} \tanh \left(\frac{\beta(k_0 - \mu)}{2} \right) dk_0 = \frac{\beta}{2} \frac{1}{2\pi i} \times (-2\pi i) \sum \text{Residues}. \quad (6.92)$$

It is noted that the first term of (6.92) has a simple pole at $k_0 = k$. On the other hand the second term also has a simple pole at $k_0 = -k$. After calculating the residues, one obtains the number density [74, 75]

$$\begin{aligned} \rho_0(T, \mu) &= - \int \frac{d^3 k}{(2\pi)^3} \left[\tanh \frac{\beta(k - \mu)}{2} - \tanh \frac{\beta(k + \mu)}{2} \right] \\ &= 2 \int \frac{d^3 k}{(2\pi)^3} [n(k - \mu) - n(k + \mu)], \end{aligned} \quad (6.93)$$

where $n(x) = 1/(e^{\beta x} + 1)$, is the Fermi-Dirac distribution function.

Now, by integrating the first line of (6.93) w.r.t. μ , one obtains the pressure for non-interacting fermion gas as

$$\mathcal{P}_0(T, \mu) = 2T \int \frac{d^3 k}{(2\pi)^3} \left[\beta k + \ln \left(1 + e^{-\beta(k - \mu)} \right) + \ln \left(1 + e^{-\beta(k + \mu)} \right) \right], \quad (6.94)$$

where the first term is the zero-point energy that produces usual vacuum divergence. It also agrees with that obtained in (6.81). The entropy density for non-interacting can be obtained

from pressure as

$$\begin{aligned} \mathcal{S}_0(T, \mu) = \frac{\partial \mathcal{P}_0}{\partial T} = 2 \int \frac{d^3 k}{(2\pi)^3} & \left[\ln \left(1 + e^{-\beta(k-\mu)} \right) + \ln \left(1 + e^{-\beta(k+\mu)} \right) \right. \\ & \left. + \frac{\beta(k-\mu)}{e^{\beta(k-\mu)} + 1} + \frac{\beta(k+\mu)}{e^{\beta(k+\mu)} + 1} \right]. \end{aligned} \quad (6.95)$$

7 General Structure of Fermionic Two-point Functions at $T \neq 0$

7.1 Fermion Self-Energy

A theory possessing only fermions and gauge bosons with no bare masses for fermions is chirally invariant for all orders. It is to be noted that the theory is also parity invariant. At $T = 0$, chiral invariance has two implications: i) there are no $\bar{\psi}\psi$ coupling in any finite order of perturbation theory, ii) the general form of the fermion self-energy can be written as [76]

$$\Sigma(P) = -\mathcal{A}\not{P}, \quad (7.1)$$

for particle momentum $P \equiv (p_0 = \omega, \vec{p})$, $p = |\vec{p}|$ and \mathcal{A} is Lorentz invariant structure function which is function of P^2 .

The effective fermion propagator can be written from (7.12) as

$$S^*(P) = \frac{1}{\not{P} - \Sigma(P)} = \frac{\not{P}}{(1 + \mathcal{A})P^2}. \quad (7.2)$$

The poles, $P^2 = 0$ are on the light cone, $\omega = p$ and $(1 + \mathcal{A})$ modifies the residues.

At $T \neq 0$, the above item i) still holds whereas item ii) does not. At $T \neq 0$, the system will not be in a vacuum because at such high temperature there will be antiparticles present in equal numbers as the particles. This constitutes a heat bath which introduces a special Lorentz frame. So, the heat bath has four velocity $u^\mu = (1, 0, 0, 0)$ with $u^\mu u_\mu = 1$. The presence of four velocity means that the most general ansatz for fermion self-energy [76] will be of the form

$$\Sigma(P) = -\mathcal{A}\not{P} - \mathcal{B}\not{u}, \quad (7.3)$$

where \mathcal{B} is another Lorentz invariant structure function in addition to \mathcal{A} . Since $P^2 = \omega^2 - p^2$, one can interpret $\omega = p_0 = P^\mu u_\mu$ and $p = (P^\mu u_\mu - P^2)^{1/2}$ as Lorentz invariant energy and momentum, respectively. The Lorentz invariant structure functions are obtained as follows:

We now write from (7.3) as

$$\Sigma\not{P} = -\mathcal{A}P^2 - \mathcal{B}\not{P}\not{u}, \quad (7.4a)$$

$$\Sigma\not{u} = -\mathcal{A}\not{P}\not{u} - \mathcal{B}. \quad (7.4b)$$

Taking trace of (7.4a) and (7.4b), we get

$$\text{Tr}[\Sigma\not{P}] = -4\mathcal{A}P^2 - 4\mathcal{B}(P \cdot u), \quad (7.5a)$$

$$(P \cdot u) \text{Tr}[\Sigma\not{u}] = -4\mathcal{A}(P \cdot u)^2 - 4\mathcal{B}(P \cdot u). \quad (7.5b)$$

Solving (7.5a) and (7.5b), one obtains

$$\mathcal{A}(\omega, p) = \frac{1}{4} \frac{\text{Tr} [\Sigma \not{P}] - (P \cdot u) \text{Tr} [\Sigma \not{u}]}{(P \cdot u)^2 - P^2}. \quad (7.6)$$

Further one can write

$$P^2 \text{Tr} [\Sigma \not{u}] = -4\mathcal{A}P^2 (P \cdot u) - 4\mathcal{B}P^2, \quad (7.7a)$$

$$(P \cdot u) \text{Tr} [\Sigma \not{P}] = -4\mathcal{A}P^2 (P \cdot u) - 4\mathcal{B} (P \cdot u)^2. \quad (7.7b)$$

Solving (7.7a) and (7.7b), one obtains

$$\mathcal{B}(\omega, p) = \frac{1}{4} \frac{P^2 \text{Tr} [\Sigma \not{u}] - (P \cdot u) \text{Tr} [\Sigma \not{P}]}{(P \cdot u)^2 - P^2}. \quad (7.8)$$

Now in the rest frame of the heat bath, $u^\mu = (1, 0, 0, 0)$, the most general ansatz for fermionic self-energy reads [76] as

$$\Sigma(P) = -\mathcal{A}(\omega, p) \not{P} - \mathcal{B}(\omega, p) \gamma_0, \quad (7.9)$$

with structure functions

$$\mathcal{A}(\omega, p) = \frac{1}{4p^2} (\text{Tr} [\Sigma \not{P}] - \omega \text{Tr} [\Sigma \gamma_0]), \quad (7.10a)$$

$$\mathcal{B}(\omega, p) = \frac{1}{4p^2} (P^2 \text{Tr} [\Sigma \gamma_0] - \omega \text{Tr} [\Sigma \not{P}]). \quad (7.10b)$$

7.2 Fermion Propagator



Figure 23: Pictorial representation of Dyson-Schwinger equation for effective fermion propagator.

In Fig.23 we represent the full propagator by $S^*(P)$ and the bare propagator by $S_0(P)$ and self-energy as $\Sigma(P)$, then the full propagator is written as,

$$\begin{aligned} S^*(P) &= S_0(P) + S_0(P) \Sigma(P) S^*(P) \\ S^*(P) S^{*-1}(P) &= S_0(P) S^{*-1}(P) + S_0(P) \Sigma(P) S^*(P) S^{*-1}(P) \\ 1 &= S_0(P) S^{*-1}(P) + S_0(P) \Sigma(P) \\ S_0^{-1}(P) &= S_0^{-1}(P) S_0(P) S^{*-1}(P) + S_0^{-1}(P) S_0(P) \Sigma(P) \\ S^{*-1}(P) &= S_0^{-1}(P) - \Sigma(P) \\ S^{*-1}(P) &= \not{P} - \Sigma(P), \end{aligned} \quad (7.11)$$

which is known as fermionic Dyson-Schwinger equation. The effective fermion propagator can be obtained as

$$S^*(P) = \frac{1}{\not{P} - \Sigma(P)}. \quad (7.12)$$

Using (7.3) one can write the effective propagator as

$$S^*(P) = \frac{1}{(1 + \mathcal{A})\not{P} + \mathcal{B}\not{u}} = \frac{(1 + \mathcal{A})\not{P} + \mathcal{B}\not{u}}{[(1 + \mathcal{A})\not{P} + \mathcal{B}\not{u}]^2} = \frac{\not{P} - \Sigma(P)}{\mathcal{D}} = \frac{S^{*-1}(P)}{\mathcal{D}}, \quad (7.13)$$

where the Lorentz invariant quantity \mathcal{D} is given as

$$\mathcal{D}(p, u) = [(1 + \mathcal{A})\not{P} + \mathcal{B}\not{u}]^2 = (1 + \mathcal{A})^2 \not{P}^2 + 2(1 + \mathcal{A})\mathcal{B}P \cdot u + \mathcal{B}^2. \quad (7.14)$$

In the rest frame of heat bath, Eq.(7.14) reads as

$$\begin{aligned} \mathcal{D}(p, \omega) &= (1 + \mathcal{A})^2(\omega^2 - p^2) + 2(1 + \mathcal{A})\mathcal{B}\omega + \mathcal{B}^2 = [(1 + \mathcal{A})\omega + \mathcal{B}]^2 - (1 + \mathcal{A})^2 p^2 \\ &= [(1 + \mathcal{A})(\omega - p) + \mathcal{B}][(1 + \mathcal{A})(\omega + p) + \mathcal{B}] = \mathcal{D}_+ \mathcal{D}_-, \end{aligned} \quad (7.15)$$

where

$$\mathcal{D}_\pm(p, \omega) = (1 + \mathcal{A})(\omega \mp p) + \mathcal{B}. \quad (7.16)$$

In free case $\mathcal{A} = \mathcal{B} = 0$ and Eq.(7.16) becomes

$$d_\pm(p, \omega) = \omega \mp p. \quad (7.17)$$

Combining (7.15) and (7.13), one can write the effective propagator as

$$S^*(P) = \frac{S^{*-1}(P)}{\mathcal{D}_+ \mathcal{D}_-}. \quad (7.18)$$

We can write the self energy in (7.9) as

$$\begin{aligned} \Sigma(P) &= -\mathcal{A}(\omega, p)\not{P} - \mathcal{B}(\omega, p)\gamma_0 \\ &= -(\mathcal{A}\omega + \mathcal{B})\gamma_0 + \mathcal{A}p \vec{\gamma} \cdot \hat{\mathbf{p}} \\ &= \frac{1}{2} [-(\mathcal{A}\omega + \mathcal{B})\gamma_0 - (\mathcal{A}\omega + \mathcal{B})\gamma_0 - \mathcal{A}p\gamma_0 + \mathcal{A}p\gamma_0 + \mathcal{A}p \vec{\gamma} \cdot \hat{\mathbf{p}} + \mathcal{A}p \vec{\gamma} \cdot \hat{\mathbf{p}} \\ &\quad - (\mathcal{A}\omega + \mathcal{B})\vec{\gamma} \cdot \hat{\mathbf{p}} + (\mathcal{A}\omega + \mathcal{B})\vec{\gamma} \cdot \hat{\mathbf{p}}] \\ &= \frac{1}{2} [-(\mathcal{A}\omega + \mathcal{B})(\gamma_0 - \vec{\gamma} \cdot \hat{\mathbf{p}}) - (\mathcal{A}\omega + \mathcal{B})(\gamma_0 + \vec{\gamma} \cdot \hat{\mathbf{p}}) - \mathcal{A}p(\gamma_0 - \vec{\gamma} \cdot \hat{\mathbf{p}}) + \mathcal{A}p(\gamma_0 + \vec{\gamma} \cdot \hat{\mathbf{p}})] \\ &= -\frac{1}{2} [(\mathcal{A}(\omega + p) + \mathcal{B})(\gamma_0 - \vec{\gamma} \cdot \hat{\mathbf{p}}) + (\mathcal{A}(\omega - p) + \mathcal{B})(\gamma_0 + \vec{\gamma} \cdot \hat{\mathbf{p}})]. \end{aligned} \quad (7.19)$$

Now we can write

$$\begin{aligned} \not{P} &= \gamma_0\omega - p\vec{\gamma} \cdot \hat{\mathbf{p}} = \frac{1}{2} [\gamma_0\omega + \gamma_0\omega - \gamma_0p + \gamma_0p - p\vec{\gamma} \cdot \hat{\mathbf{p}} - p\vec{\gamma} \cdot \hat{\mathbf{p}} + \omega\vec{\gamma} \cdot \hat{\mathbf{p}} - \omega\vec{\gamma} \cdot \hat{\mathbf{p}}] \\ &= \frac{1}{2} [(\omega - p)(\gamma_0 + \vec{\gamma} \cdot \hat{\mathbf{p}}) + (\omega + p)(\gamma_0 - \vec{\gamma} \cdot \hat{\mathbf{p}})]. \end{aligned} \quad (7.20)$$

In the rest frame of heat bath the inverse of the effective propagator in (7.11) can now be written as

$$\begin{aligned}
S^{\star-1}(P) &= \not{P} - \Sigma(P) \\
&= \frac{1}{2} [\{(\omega - p) + \mathcal{A}(\omega - p) + \mathcal{B}\} (\gamma_0 + \vec{\gamma} \cdot \hat{\mathbf{p}}) + \{(\omega + p) + \mathcal{A}(\omega + p) + \mathcal{B}\} (\gamma_0 - \vec{\gamma} \cdot \hat{\mathbf{p}})] \\
&= \frac{1}{2} [(1 + \mathcal{A})(\omega - p) + \mathcal{B}] (\gamma_0 + \vec{\gamma} \cdot \hat{\mathbf{p}}) + \frac{1}{2} [(1 + \mathcal{A})(\omega + p) + \mathcal{B}] (\gamma_0 - \vec{\gamma} \cdot \hat{\mathbf{p}}) \\
&= \frac{1}{2} (\gamma_0 + \vec{\gamma} \cdot \hat{\mathbf{p}}) \mathcal{D}_+ + \frac{1}{2} (\gamma_0 - \vec{\gamma} \cdot \hat{\mathbf{p}}) \mathcal{D}_-
\end{aligned} \tag{7.21}$$

Using (7.21) in (7.18), one finally obtains the effective fermion propagator as

$$S^{\star}(P) = \frac{1}{2} \frac{(\gamma_0 - \vec{\gamma} \cdot \hat{\mathbf{p}})}{\mathcal{D}_+(\omega, p)} + \frac{1}{2} \frac{(\gamma_0 + \vec{\gamma} \cdot \hat{\mathbf{p}})}{\mathcal{D}_-(\omega, p)}, \tag{7.22}$$

which is decomposed in helicity eigenstates.

In free fermion case, the propagator becomes

$$S(P) = \frac{1}{2} \frac{(\gamma_0 - \vec{\gamma} \cdot \hat{\mathbf{p}})}{d_+(\omega, p)} + \frac{1}{2} \frac{(\gamma_0 + \vec{\gamma} \cdot \hat{\mathbf{p}})}{d_-(\omega, p)}, \tag{7.23}$$

where $d_{\pm}(\omega, p)$ are given in (7.17) and has already been used in Sec.6.3.3 in (6.89).

8 General structure of Gauge Boson Two-point Functions at $T \neq 0$

8.1 Covariant Description

. The general structure of the gauge boson self-energy in vacuum [73] is given as

$$\Pi^{\mu\nu}(P^2) = V^{\mu\nu} \Pi(P^2), \tag{8.1}$$

where the form factor $\Pi(P^2)$ is Lorentz invariant and depends only on the four scalar P^2 . The vacuum projection operator is given by

$$V^{\mu\nu} = \eta^{\mu\nu} - \frac{P^{\mu} P^{\nu}}{P^2}, \tag{8.2}$$

which satisfies the gauge invariance through the transversality condition

$$P_{\mu} \Pi^{\mu\nu} = 0, \tag{8.3}$$

with $\eta^{\mu\nu} \equiv (1, -1, -1, -1)$ and $P \equiv (\omega, \vec{p})$. It is also symmetric under the exchange of $\mu \leftrightarrow \nu$ as

$$\Pi_{\mu\nu}(P^2) = \Pi_{\nu\mu}(P^2). \tag{8.4}$$

The presence of the heat bath or the finite temperature ($\beta = 1/T$) breaks the Lorentz invariance of the system. One collects all the four vectors and tensors in order to construct a general covariant structure of the gauge boson self-energy at finite temperature. These are

P^μ and $\eta^{\mu\nu}$ from vacuum, and the four-velocity u^μ of the heat bath. With these one can form four types of tensors, namely $P^\mu P^\nu$, $P^\mu u^\nu + u^\mu P^\nu$, $u^\mu u^\nu$ and $\eta^{\mu\nu}$ [12, 77]. These four tensors can form two independent tensors by virtue of two constraints provided by the transversality condition in (8.3). One can form two mutually orthogonal projection tensors from these two independent tensors in order to construct Lorentz-invariant structure of the gauge boson two point functions at finite temperature.

Now, we define the Lorentz scalars, vectors and tensors that characterise the heat bath:

$$\begin{aligned} u^\mu &= (1, 0, 0, 0), \\ P^\mu u_\mu &= P \cdot u = \omega, \end{aligned} \quad (8.5)$$

8.2 Tensor Decomposition

Similar to vacuum, we can define $\tilde{\eta}^{\mu\nu}$ transverse to u^μ as

$$\tilde{\eta}^{\mu\nu} = \eta^{\mu\nu} - u^\mu u^\nu \quad (8.6a)$$

$$u_\mu \tilde{\eta}^{\mu\nu} = u_\mu \eta^{\mu\nu} - u_\mu u^\mu u^\nu = u^\nu - u^\nu = 0. \quad (8.6b)$$

So u^μ and $\tilde{\eta}^{\mu\nu}$ are transverse.

Any four vector can be decomposed parallel and orthogonal component with respect to u^μ :

$$P_\parallel^\mu = (P \cdot u) u^\mu = \omega u^\mu, \quad (8.7a)$$

$$P_\perp^\mu = \tilde{P}^\mu = P^\mu - P_\parallel^\mu = P^\mu - \omega u^\mu. \quad (8.7b)$$

Now,

$$\tilde{P}^2 = (P^\mu - \omega u^\mu)(P_\mu - \omega u_\mu) = P^2 - \omega^2 - \omega^2 + \omega^2 = P^2 - \omega^2 = -p^2. \quad (8.8)$$

We can also define any four vector parallel and perpendicular to P^μ

$$u_\parallel^\mu = \frac{(P \cdot u) P^\mu}{P^2} = \frac{\omega P^\mu}{P^2}, \quad (8.9a)$$

$$\bar{u}^\mu \equiv u_\perp^\mu = u^\mu - u_\parallel^\mu = u^\mu - \frac{\omega P^\mu}{P^2}. \quad (8.9b)$$

So, $P^\mu \bar{u}_\mu = 0$.

Again,

$$V^{\mu\nu} = \eta^{\mu\nu} - \frac{P^\mu P^\nu}{P^2}, \quad (8.10a)$$

$$P_\mu V^{\mu\nu} = 0. \quad (8.10b)$$

Given these, it is possible to construct only two independent second rank symmetric tensors at finite temperature from $\eta^{\mu\nu}$, $P^\mu P^\nu$, $u^\mu u^\nu$, $P^\mu u^\nu + u^\mu P^\nu$ which are orthogonal to P^μ . These two tensors are [12]

$$A^{\mu\nu} = \tilde{\eta}^{\mu\nu} - \frac{\tilde{P}^\mu \tilde{P}^\nu}{\tilde{P}^2}, \quad (8.11)$$

and

$$B^{\mu\nu} = \frac{P^2}{\tilde{P}^2} \bar{u}^\mu \bar{u}^\nu = \frac{\bar{u}^\mu \bar{u}^\nu}{\bar{u}^2}, \quad (8.12)$$

where

$$A^{\mu\nu} + B^{\mu\nu} = V^{\mu\nu} = \eta^{\mu\nu} - \frac{P^\mu P^\nu}{P^2}. \quad (8.13)$$

We show that $A^{\mu\nu}$ and $B^{\mu\nu}$ are orthogonal to P^μ :

$$\begin{aligned} P_\mu A^{\mu\nu} &= P_\mu \tilde{\eta}^{\mu\nu} - P_\mu \frac{\tilde{P}^\mu \tilde{P}^\nu}{\tilde{P}^2} \\ &= P_\mu (\eta^{\mu\nu} - u^\mu u^\nu) - \frac{P_\mu (P^\mu - \omega u^\mu) \tilde{P}^\nu}{\tilde{P}^2} \\ &= (P^\nu - \omega u^\nu) - (P^2 - \omega^2) \frac{\tilde{P}^\nu}{\tilde{P}^2} \\ &= \tilde{P}^\nu - \frac{\tilde{P}^2 \tilde{P}^\nu}{\tilde{P}^2} \\ &= 0. \end{aligned} \quad (8.14)$$

$$\begin{aligned} P_\mu B^{\mu\nu} &= \frac{P^2}{\tilde{P}^2} P_\mu \left(u^\mu - \frac{\omega P^\mu}{P^2} \right) \left(u^\nu - \frac{\omega P^\nu}{P^2} \right) \\ &= \frac{P^2}{\tilde{P}^2} \left[\left(\omega - \frac{\omega P^2}{P^2} \right) \left(u^\nu - \frac{\omega P^\nu}{P^2} \right) \right] \\ &= 0. \end{aligned} \quad (8.15)$$

$A^{\mu\nu}$ and $B^{\mu\nu}$ also satisfy following relations:

$$A^{\mu\nu} B_{\mu\nu} = \left(\tilde{\eta}_{\mu\nu} - \frac{\tilde{P}_\mu \tilde{P}_\nu}{\tilde{P}^2} \right) \frac{P^2}{\tilde{P}^2} \bar{u}^\mu \bar{u}^\nu = 0 \quad (8.16a)$$

$$A_{\mu\nu} A^{\nu\rho} = \left(\tilde{\eta}_{\mu\rho} - \frac{\tilde{P}_\mu \tilde{P}_\rho}{\tilde{P}^2} \right) \left(\tilde{\eta}^{\rho\nu} - \frac{\tilde{P}^\rho \tilde{P}^\nu}{\tilde{P}^2} \right) = A_\mu^\rho, \quad (8.16b)$$

$$\begin{aligned} B_{\mu\nu} B^{\nu\rho} &= (V_{\mu\rho} - A_{\mu\rho}) (V^{\rho\nu} - A^{\rho\nu}) \\ &= V_{\mu\rho} V^{\rho\nu} - 2A_{\mu\rho} V^{\rho\nu} + A_{\mu\rho} A^{\rho\nu} \\ &= V_\mu^\nu - 2A_\mu^\nu + A_\mu^\nu = B_\mu^\nu, \end{aligned} \quad (8.16c)$$

$$A^{\mu\nu} A_{\mu\nu} = 2, \quad (8.16d)$$

$$B^{\mu\nu} B_{\mu\nu} = 1, \quad (8.16e)$$

$$A_{\mu\nu}(P) = A_{\nu\mu}(P) = A_{\mu\nu}(-P), \quad (8.16f)$$

$$B_{\mu\nu}(P) = B_{\nu\mu}(P) = B_{\mu\nu}(-P). \quad (8.16g)$$

Finally, one can obtain

$$\begin{aligned} A^{\mu\nu} &= \eta^{\mu\nu} - u^\mu u^\nu - \frac{(P^\mu - \omega u^\mu)(P^\nu - \omega u^\nu)}{P^2 - \omega^2} \\ &= \frac{1}{P^2 - \omega^2} [(P^2 - \omega^2)(\eta^{\mu\nu} - u^\mu u^\nu) - P^\mu P^\nu - \omega^2 u^\mu u^\nu + \omega(P^\mu u^\nu + u^\mu P^\nu)] , \end{aligned} \quad (8.17a)$$

$$\begin{aligned} B^{\mu\nu} &= \frac{P^2}{\tilde{P}^2} \bar{u}^\mu \bar{u}^\nu = \frac{P^2}{P^2 - \omega^2} \left[\left(u^\mu - \frac{\omega P^\mu}{P^2} \right) \left(u^\nu - \frac{\omega P^\nu}{P^2} \right) \right] \\ &= \frac{P^2}{P^2 - \omega^2} \left[u^\mu u^\nu - \frac{\omega P^\mu u^\nu}{P^2} - \frac{\omega u^\mu P^\nu}{P^2} + \frac{\omega^2 P^\mu P^\nu}{P^4} \right] \\ &= \frac{1}{P^2(P^2 - \omega^2)} [P^4 u^\mu u^\nu + \omega^2 P^\mu P^\nu - \omega P^2(P^\mu u^\nu + u^\mu P^\nu)] . \end{aligned} \quad (8.17b)$$

8.3 General Structure of Self-energy of a Vector Particle in a Thermal Medium

The self-energy of a vector particle in a medium (finite temperature/density) can be written as

$$\Pi_{\mu\nu} = \Pi_T(\omega, p) A_{\mu\nu} + \Pi_L(\omega, p) B_{\mu\nu}, \quad (8.18)$$

It obeys the current conservation or transversality condition as

$$\begin{aligned} P^\mu \Pi_{\mu\nu} &= \Pi_T P^\mu A_{\mu\nu} + \Pi_L P^\mu B_{\mu\nu} \\ &= 0 . \end{aligned} \quad (8.19)$$

Also note that at zero temperature

$$\Pi_{\mu\nu}^{(0)}(\omega, p) = \Pi^{(0)}(P^2) \left(\eta_{\mu\nu} - \frac{P_\mu P_\nu}{P^2} \right) , \quad (8.20)$$

where

$$\Pi_L^{(0)}(\omega, p) = \Pi_T^{(0)}(\omega, p) = \Pi^{(0)}(P^2) . \quad (8.21)$$

Using (8.18) we can write

$$\Pi_{00}(\omega, p) = \Pi_T(\omega, p) A_{00} + \Pi_L(\omega, p) B_{00} . \quad (8.22)$$

We obtain from (8.17a) and (8.17b), respectively, as

$$A_{00} = 0 , \quad (8.23a)$$

$$B_{00} = -\frac{p^2}{P^2} . \quad (8.23b)$$

Using (8.23a) and (8.23b) in (8.22), one obtains [12]

$$\Pi_L(\omega, p) = \left(-\frac{P^2}{p^2} \right) \Pi_{00}(\omega, p) . \quad (8.24)$$

Again, we can write

$$\eta^{\mu\nu} \Pi_{\mu\nu} = \Pi_T \eta^{\mu\nu} A_{\mu\nu} + \Pi_L \eta^{\mu\nu} B_{\mu\nu} . \quad (8.25)$$

One obtains

$$\begin{aligned}\eta^{\mu\nu} A_{\mu\nu} &= \eta^{\mu\nu} A_{\mu\nu} - u^\mu u_\mu - \frac{\tilde{P}^\mu \tilde{P}_\mu}{\tilde{P}^2} \\ &= D - 1 - 1 = D - 2,\end{aligned}\tag{8.26}$$

where $D = 4$ is the dimension of the system. Also, one can obtain

$$\begin{aligned}\eta^{\mu\nu} B_{\mu\nu} &= \eta^{\mu\nu} \frac{P^2}{\tilde{P}^2} \bar{u}_\mu \bar{u}_\nu = \frac{P^2}{\tilde{P}^2} \bar{u}_\mu \bar{u}^\mu = \frac{P^2}{\tilde{P}^2} \left(u_\mu - \frac{\omega P_\mu}{P^2} \right) \left(u^\mu - \frac{\omega P^\mu}{P^2} \right) \\ &= \frac{P^2}{\tilde{P}^2} \left[u_\mu u^\mu - \frac{\omega}{P^2} (P_\mu u^\mu + P^\mu u_\mu) + \frac{\omega^2}{P^4} P_\mu P^\mu \right] \\ &= \frac{P^2}{\tilde{P}^2} \left(1 - \frac{2\omega^2}{P^2} + \frac{\omega^2}{P^2} \right) = \frac{P^2}{P^2 - \omega^2} \left(\frac{P^2 - \omega^2}{P^2} \right) = 1.\end{aligned}\tag{8.27}$$

Equation (8.26) denotes the presence of two transverse modes whereas (8.27) corresponds to a longitudinal mode of the gauge boson.

Using (8.26) and (8.27) in (8.25) we obtain [12]

$$\Pi_T(\omega, p) = \frac{1}{D-2} [\Pi_\mu^\mu(\omega, p) - \Pi_L(\omega, p)] = \frac{1}{2} [\Pi_\mu^\mu(\omega, p) - \Pi_L(\omega, p)].\tag{8.28}$$

8.4 Massless Vector Gauge Boson Propagator in Covariant Gauge

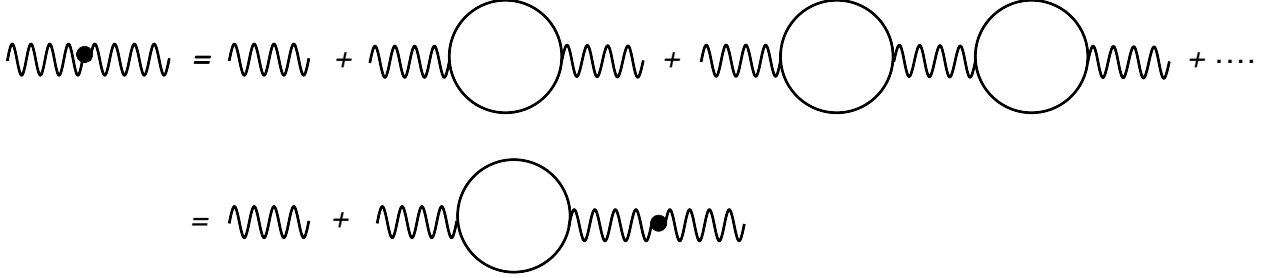


Figure 24: Effective gauge boson propagator.

We represent the full propagator by D_{mn} and the bare propagator by $D_{\mu\nu}^0$ and each blob that appears in the summation as $\Pi_{\mu\nu}$. One can work out this summation in Fig. 24 in tensorial form for the effective gauge boson propagator in Fig. 24 as

$$\begin{aligned}D^{\mu\rho} &= D^{0\mu\rho} + D^{0\mu\alpha} \Pi_{\alpha\beta} D^{\beta\rho} \\ D^{\mu\rho} D_{\rho\nu}^{-1} &= D^{0\mu\rho} D_{\rho\nu}^{-1} + D^{0\mu\alpha} \Pi_{\alpha\beta} D^{\beta\rho} D_{\rho\nu}^{-1} \\ \delta_\nu^\mu &= D^{0\mu\rho} D_{\rho\nu}^{-1} + D^{0\mu\alpha} \Pi_{\alpha\beta} \delta_\nu^\beta \\ \delta_\nu^\mu &= D^{0\mu\rho} D_{\rho\nu}^{-1} + D^{0\mu\alpha} \Pi_{\alpha\nu} \\ \delta_\nu^\mu (D_{\mu\gamma}^0)^{-1} &= D^{0\mu\rho} (D_{\mu\gamma}^0)^{-1} D_{\rho\nu}^{-1} + D^{0\mu\alpha} (D_{\mu\gamma}^0)^{-1} \Pi_{\alpha\nu} \\ (D_{\nu\gamma}^0)^{-1} &= \delta_\gamma^\rho D_{\rho\nu}^{-1} + \delta_\gamma^\alpha \Pi_{\alpha\nu} \\ D_{\nu\gamma}^{-1} &= (D_{\nu\gamma}^0)^{-1} - \Pi_{\nu\gamma}.\end{aligned}\tag{8.29}$$

Effective photon propagator is given by

$$D_{\mu\nu}^{-1} = (D_{\mu\nu}^0)^{-1} - \Pi_{\mu\nu}, \quad (8.30)$$

which is known as Dyson-Schwinger equation.

For massless gauge boson propagator is given in (9.29) as

$$D_{\mu\nu}^0 = -\frac{\eta_{\mu\nu}}{P^2} + (1 - \xi) \frac{P_\mu P_\nu}{P^4} \quad (8.31)$$

where ξ is the gauge fixing parameter with $\xi = 1$ in Feynman gauge and $\xi = 0$ in Landau gauge. We will discuss the gauge fixing and gauge boson propagator in subsec 9.4.

Dyson-Schwinger equation is given in (8.30) as

$$D_{\mu\nu}^{-1} = (D_{\mu\nu}^0)^{-1} - \Pi_{\mu\nu}. \quad (8.32)$$

So we have to calculate the inverse of $D_{\mu\nu}^0$.

Lets define

$$(D_{\mu\rho}^0)^{-1} = a\eta_{\mu\rho} + bP_\mu P_\rho. \quad (8.33)$$

We know

$$\begin{aligned} D_{\mu\rho}^0 (D^{0\rho\nu})^{-1} &= \delta_\mu^\nu \\ \frac{1}{P^2} \left(-\eta_{\mu\rho} + (1 - \xi) \frac{P_\mu P_\rho}{P^2} \right) (a\eta^{\rho\nu} + bP^\rho P^\nu) &= \delta_\mu^\nu \\ \frac{1}{P^2} \left(-a\delta_\mu^\nu + \frac{a(1 - \xi)}{P^2} P_\mu P^\nu - bP_\mu P^\nu + b(1 - \xi) P_\mu P^\nu \right) &= \delta_\mu^\nu. \end{aligned} \quad (8.34)$$

Equating coefficients of both side, we get

$$a = -P^2, \quad b = -\frac{1 - \xi}{\xi}. \quad (8.35)$$

Using (8.35) in (8.33), one obtains

$$(D_{\mu\nu}^0)^{-1} = -P^2 \eta_{\mu\nu} - \frac{1 - \xi}{\xi} P_\mu P_\nu. \quad (8.36)$$

We know from (8.13)

$$P_\mu P_\nu = P^2 (\eta_{\mu\nu} - A_{\mu\nu} - B_{\mu\nu}). \quad (8.37)$$

Substituting this in $(D_{\mu\nu}^0)^{-1}$, one can have

$$\begin{aligned} (D_{\mu\nu}^0)^{-1} &= -P^2 \eta_{\mu\nu} - \frac{1 - \xi}{\xi} P^2 (\eta_{\mu\nu} - A_{\mu\nu} - B_{\mu\nu}) \\ &= -\frac{P^2}{\xi} \eta_{\mu\nu} + \frac{1 - \xi}{\xi} P^2 (A_{\mu\nu} + B_{\mu\nu}), \end{aligned} \quad (8.38)$$

which is the inverse of $D_{\mu\nu}^0$.

Using (8.38) and (8.18) in (8.30) one can find

$$\begin{aligned} D_{\mu\nu}^{-1} &= -\frac{P^2}{\xi}\eta_{\mu\nu} + \frac{1-\xi}{\xi}P^2(A_{\mu\nu} + B_{\mu\nu}) - \Pi_T A_{\mu\nu} - \Pi_L B_{\mu\nu} \\ &= -\frac{P^2}{\xi}\eta_{\mu\nu} + (P_m^2 - \Pi_T)A_{\mu\nu} + (P_m^2 - \Pi_L)B_{\mu\nu}, \end{aligned} \quad (8.39)$$

where $P_m^2 = \frac{(1-\xi)}{\xi}P^2$. Eq.(8.39) is inverse of $D_{\mu\nu}$. Now we have to find out $D_{\mu\nu}$ from $D_{\mu\nu}^{-1}$.

Lets define

$$D_{\mu\rho} = cP_\mu P_\rho + dA_{\mu\rho} + eB_{\mu\rho}. \quad (8.40)$$

We know

$$\begin{aligned} D_{\mu\rho}(D^{\rho\nu})^{-1} &= \delta_\mu^\nu \\ \frac{cP^2}{\xi}P_\mu P^\nu + d(P^2 + \Pi_T)A_\mu^\nu + e(P^2 + \Pi_L)B_\mu^\nu &= -\delta_\mu^\nu. \end{aligned} \quad (8.41)$$

Substituting A_μ^ν and B_μ^ν from (8.17a) and (8.17b), the above equation becomes

$$\begin{aligned} \frac{cP^2}{\xi}P_\mu P^\nu + d(P^2 + \Pi_T) \left[\delta_\mu^\nu - \frac{P^2}{P^2 - \omega^2}u_\mu u^\nu - \frac{P_\mu P^\nu}{P^2 - \omega^2} + \frac{\omega}{P^2 - \omega^2}(u_\mu P^\nu + P_\mu u^\nu) \right] \\ + e(P^2 + \Pi_L) \frac{P^2}{P^2 - \omega^2} \left[u_\mu u^\nu - \frac{\omega}{P^2}(u_\mu P^\nu + P_\mu u^\nu) + \frac{\omega^2}{P^4}P_\mu P^\nu \right] &= -\delta_\mu^\nu. \end{aligned} \quad (8.42)$$

Now equating coefficients on both side, we get

$$\text{Coefficients of } \delta_\mu^\nu : \quad d = -\frac{1}{P^2 + \Pi_T}, \quad (8.43a)$$

$$\text{Coefficients of } u_\mu P^\nu + P_\mu u^\nu : \quad e = -\frac{1}{P^2 + \Pi_L}, \quad (8.43b)$$

$$\text{Coefficients of } P_\mu P^\nu : \quad c = -\frac{\xi}{P^4}. \quad (8.43c)$$

Using (8.43a), (8.43b) and (8.43c) in (8.40), one obtains the effective propagator of interacting photon [12] in presence of thermal medium as

$$D_{\mu\nu} = -\frac{\xi}{P^4}P_\mu P_\nu - \frac{1}{P^2 + \Pi_T}A_{\mu\nu} - \frac{1}{P^2 + \Pi_L}B_{\mu\nu}. \quad (8.44)$$

8.5 Massive Vector Boson Propagator

The free propagator for massive vector boson is given as

$$\begin{aligned} D_{\mu\nu}^0 &= \frac{-\eta_{\mu\nu} + \frac{P_\mu P_\nu}{m_v^2}}{P^2 - m_v^2} \\ &\equiv \frac{-\eta_{\mu\nu} + \frac{P_\mu P_\nu}{m_v^2}}{X}, \end{aligned} \quad (8.45)$$

where $X = P^2 - m_v^2$ and m_v is the mass of the vector boson.

The inverse of $D_{\mu\nu}^0$ can be written as

$$(D_{\rho\nu}^0)^{-1} = a\eta_{\rho\nu} + bP_\rho P_\nu. \quad (8.46)$$

We have

$$\begin{aligned} D_{\mu\rho}^0 (D^{0\rho\nu})^{-1} &= \delta_\mu^\nu \\ \left(\frac{-\eta_{\mu\rho} + \frac{P_\mu P_\rho}{m_v^2}}{X} \right) (a\eta^{\rho\nu} + bP^\rho P^\nu) &= \delta_\mu^\nu \\ -a\delta_\mu^\nu - bP_\mu P^\nu + a\frac{P_\mu P^\nu}{m_v^2} + b\frac{P^2 P_\mu P^\nu}{m_v^2} &= X\delta_\mu^\nu. \end{aligned} \quad (8.47)$$

Equating coefficients of δ_μ^ν , and $P_\mu P^\nu$ yields,

$$a = -X = -(P^2 - m_v^2), \quad (8.48)$$

and

$$\begin{aligned} \frac{a}{m_v^2} - b + \frac{bP^2}{m_v^2} &= 0 \\ b &= 1. \end{aligned} \quad (8.49)$$

Now the inverse of the free propagator in (8.46) becomes

$$(D_{\mu\nu}^0)^{-1} = -(P^2 - m_v^2)\eta_{\mu\nu} + P_\mu P_\nu. \quad (8.50)$$

Using (8.13) we get

$$P_\mu P_\nu = P^2 (\eta_{\mu\nu} - A_{\mu\nu} - B_{\mu\nu}), \quad (8.51)$$

one gets

$$\begin{aligned} (D_{\mu\nu}^0)^{-1} &= -(P^2 - m_v^2)\eta_{\mu\nu} + P^2 (\eta_{\mu\nu} - A_{\mu\nu} - B_{\mu\nu}) \\ &= m_v^2 \eta_{\mu\nu} - P^2 (A_{\mu\nu} + B_{\mu\nu}). \end{aligned} \quad (8.52)$$

Putting back this value in Dyson equation in (8.30)

$$D_{\mu\nu}^{-1} = m_v^2 \eta_{\mu\nu} - P^2 (A_{\mu\nu} + B_{\mu\nu}) - \Pi_{\mu\nu}. \quad (8.53)$$

Using Eq.(8.18) we get

$$\begin{aligned} D_{\mu\nu}^{-1} &= m_v^2 \eta_{\mu\nu} - P^2 (A_{\mu\nu} + B_{\mu\nu}) - \Pi_T A_{\mu\nu} - \Pi_L B_{\mu\nu} \\ &= m_v^2 \eta_{\mu\nu} - (P^2 + \Pi_T) A_{\mu\nu} - (P^2 + \Pi_L) B_{\mu\nu} \end{aligned} \quad (8.54)$$

Now we have to find $D_{\mu\nu}$. Lets define

$$D^{\rho\nu} = \alpha P^\rho P^\nu + \beta A^{\rho\nu} + \gamma B^{\rho\nu}. \quad (8.55)$$

We can write

$$\begin{aligned}
D_{\mu\rho}(D^{\rho\nu})^{-1} &= \delta_\mu^\nu \\
(\alpha P_\mu P_\rho + \beta A_{\mu\rho} + \gamma B_{\mu\rho}) (m_v^2 \eta^{\rho\nu} - P^2 (A^{\rho\nu} + B^{\rho\nu}) - \Pi_T A^{\rho\nu} - \Pi_L B^{\rho\nu}) &= \delta_\mu^\nu \\
\alpha m_v^2 P_\mu P^\nu + \beta m_v^2 A_\mu^\nu - \beta (P^2 + \Pi_T) A_\mu^\nu + \gamma m_v^2 B_\mu^\nu - \gamma (P^2 + \Pi_L) B_\mu^\nu &= \delta_\mu^\nu \\
\alpha m_v^2 P_\mu P^\nu + \beta (m_v^2 - P^2 - \Pi_T) A_\mu^\nu + \gamma (m_v^2 - P^2 - \Pi_L) B_\mu^\nu &= \delta_\mu^\nu. \quad (8.56)
\end{aligned}$$

Substituting A_μ^ν, B_μ^ν from Eq.(8.17a),Eq.(8.17b) and equating coefficients we get,

$$\text{Coefficients of } \delta_\mu^\nu : \quad \beta = \frac{1}{m_v^2 - P^2 - \Pi_T}, \quad (8.57a)$$

$$\text{Coefficients of } u_\mu u^\nu : \quad \gamma = \frac{1}{m_v^2 - P^2 - \Pi_L}, \quad (8.57b)$$

$$\text{Coefficients of } P_\mu P^\nu : \quad \alpha = \frac{1}{P^2 m_v^2}. \quad (8.57c)$$

Using (8.57a) to (8.57c) in (8.55) one gets the propagator for massive vector boson in a thermal medium

$$D_{\mu\nu} = \frac{P_\mu P_\nu}{P^2 m_v^2} - \frac{A_{\mu\nu}}{P^2 - m_v^2 + \Pi_T} - \frac{B_{\mu\nu}}{P^2 - m_v^2 + \Pi_L}. \quad (8.58)$$

9 Quantum Electrodynamics (QED)

Quantum electrodynamics (QED) is an abelian gauge theory. The symmetry group is $U(1)$ abelian group which are also commutative group. In QED, the interaction between two spin 1/2 fermionic fields is mediated by electromagnetic field photon, A_μ , which is a gauge field. Before doing anything else it is essential to introduce gauge and gauge fixing first.

9.1 Dirac Field

The Dirac Lagrangian density in (6.54) describes the free fermion and given as

$$\mathcal{L}_D = \bar{\psi} (i\partial - m) \psi. \quad (9.1)$$

As we have seen in subsec. 6.3.1 that it is invariant under a global phase transformation, $e^{-ie\alpha} \psi(X)$, with a fixed phase parameter which does not depend upon space and time. This is a global transformation. If the phase factor α is any differentiable function of space-time, $\alpha(X)$, i.e., at each space-time point it is different, then the transformation,

$$\psi(X) \rightarrow e^{-ie\alpha(X)} \psi(X), \quad (9.2)$$

is called local transformation. The Lagrangian density in (9.1) is no longer invariant under such local transformation as seen in (6.62):

$$\begin{aligned}
\mathcal{L}_D &\rightarrow \mathcal{L}'_D = \bar{\psi} e^{ie\alpha(X)} (i\partial - m) \psi e^{-ie\alpha(X)} \\
&= \bar{\psi} (i\partial - m) \psi + e\bar{\psi} \partial \alpha(X) \psi \\
&= \mathcal{L}_D + e\bar{\psi} \partial \alpha(X) \psi. \quad (9.3)
\end{aligned}$$

One needs to include a gauge potential (field) A_μ in the theory. As we will see below that this gauge field A_μ together with the original fermionic fields make the Lagrangian invariant under such local phase transformation. This is also called local gauge transformation.

Under the local gauge transformation, the modified Dirac invariant Lagrangian in (9.1) now reads as

$$\mathcal{L}_D = \bar{\psi} (i\partial\!\!\!/ - m) \psi - e\bar{\psi}\gamma^\mu A_\mu \psi = \bar{\psi} (i\mathcal{D} - m) \psi, \quad (9.4)$$

where the original partial differential operator is replaced by the covariant differential operator

$$\partial_\mu \rightarrow D_\mu = \partial_\mu + ieA_\mu, \quad (9.5)$$

along with the transformation of the gauge field as

$$A_\mu \rightarrow A_\mu + \partial_\mu \alpha(X). \quad (9.6)$$

[Now lets check the invariance of (9.4) under local gauge transformation: $\psi(X) \rightarrow \psi' = e^{-ie\alpha(X)}\psi$

$$\begin{aligned} \bar{\psi}' D_\mu \psi' &= \bar{\psi}' [\partial_\mu + ieA_\mu] e^{-ie\alpha(X)} \psi \\ &= \bar{\psi}' e^{-ie\alpha(X)} \partial_\mu \psi - ie\bar{\psi}' (\partial_\mu \alpha(X)) e^{-ie\alpha(X)} \psi + ie\bar{\psi}' A_\mu \psi e^{-ie\alpha(X)}. \end{aligned} \quad (9.7)$$

If (9.7) vis-a-vis (9.4) is to be invariant under local transformation of the fermionic field $\psi(X) \rightarrow \psi' = e^{-ie\alpha(X)}\psi$, the gauge field has also to be transformed as $A_\mu \rightarrow A_\mu + \partial_\mu \alpha(X)$ as given in (9.6). So

$$\begin{aligned} \bar{\psi}' D_\mu \psi' &= \bar{\psi}' e^{-ie\alpha(X)} \partial_\mu \psi - ie\bar{\psi}' (\partial_\mu \alpha(X)) e^{-ie\alpha(X)} \psi + ie\bar{\psi}' (A_\mu + \partial_\mu \alpha(X)) e^{-ie\alpha(X)} \psi \\ &= \bar{\psi}' (\partial_\mu + ieA_\mu) \psi = \bar{\psi}' D_\mu \psi. \end{aligned} \quad (9.8)$$

This suggests that (9.4) is invariant under local gauge transformation.]

9.2 Pure Gauge Field

Following Maxwell's equations both electric field \mathbf{E} and the magnetic field \mathbf{B} can be written from pure gauge field A_μ in a manifestly covariant form as

$$F_{\mu\nu} = \partial_\mu A_\nu - \partial_\nu A_\mu, \quad (9.9)$$

which is known as electromagnetic field tensor. This is a gauge invariant quantity and also antisymmetric, $F_{\mu\nu} = -F_{\nu\mu}$, under the exchange of the Lorentz indices $\mu \leftrightarrow \nu$. One can now construct a Lorentz scalar out of $F_{\mu\nu}$, which can be included in the Lagrangian density for pure gauge field as

$$\mathcal{L}_\gamma = -\frac{1}{4} F_{\mu\nu} F^{\mu\nu}, \quad (9.10)$$

where the normalisation factor $1/4$ is chosen in such a way that it gives the correct equation of motion for electromagnetic field.

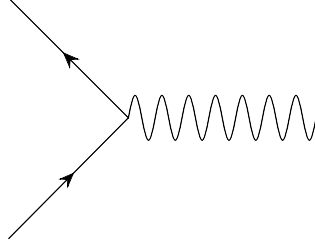


Figure 25: Electron-photon interaction vertex.

9.3 Electromagnetic Lagrangian

Now one can write the total electromagnetic Lagrangian density [72, 73] describing fermions, electromagnetic field and interaction between them as

$$\begin{aligned}
 \mathcal{L}_{em} &= \mathcal{L}_\gamma + \mathcal{L}_D \\
 &= -\frac{1}{4}F_{\mu\nu}F^{\mu\nu} + \bar{\psi}(i\not{D} - m)\psi \\
 &= -\frac{1}{4}F_{\mu\nu}F^{\mu\nu} + \bar{\psi}(i\gamma^\mu\partial_\mu - m)\psi - e\bar{\psi}\gamma^\mu\psi A_\mu.
 \end{aligned} \tag{9.11}$$

We note the following:

- The first term corresponds to the free Lagrangian density of a gauge field (photon)
- The second term is the Lagrangian density that describes the free fermions with mass m . Now if one wants to include chemical potential μ , one should follow as done in (6.67) in Subsec. 6.3.1 . The presence of the chemical potential is like shifting the temporal component of the gauge field by $\partial_0 - i\mu$.
- The third term originates from the local $U(1)$ gauge symmetry and corresponds to the interaction Lagrangian density of fermionic and gauge field in which gauge field interact with fermionic field through the dimensionless coupling parameter e . This interaction is represented in Fig. 25. Using this interaction in perturbative techniques, one can compute Feynman diagrams for the theory.
- The second and third term together will lead to the equation of motion for gauge field $\partial_\mu F^{\mu\nu} = -j^\nu$.
- If one checks the gauge invariance of second and third term together, then it will lead to a conserved current density and the Lagrangian density will then differ by a total derivative, but leaves the equation of motion unchanged .

9.4 Gauge Fixing

One of the problem of (9.11) is that it can not be quantised. One way to see this is that the propagator for photon does not exist. As we have already experienced from scalar and

fermionic fields that the propagator is obtained from free theory, we start with the free Lagrangian density for gauge field (photon)

$$\begin{aligned}
\mathcal{L}_\gamma &= -\frac{1}{4}F_{\mu\nu}F^{\mu\nu} = -\frac{1}{4}[\partial_\mu A_\nu - \partial_\nu A_\mu][\partial^\mu A^\nu - \partial^\nu A^\mu] \\
&= -\frac{1}{2}\partial_\mu A_\nu[\partial^\mu A^\nu - \partial^\nu A^\mu] + \partial_\mu(\cdots) \\
&= \frac{1}{2}A_\nu[\eta^{\mu\nu}\square - \partial^\mu\partial^\nu]A_\mu,
\end{aligned} \tag{9.12}$$

where we have interchanged $\mu \rightarrow \nu$ in the second term inside the first square braces in the second line. We have done the integration by parts to arrive at third line. Now using the Fourier decomposition of the gauge field one can get

$$\mathcal{L}_\gamma = -\frac{1}{2}A_\nu[-\eta^{\mu\nu}P^2 + P^\mu P^\nu]A^\mu, \tag{9.13}$$

where the quantity inside the square braces should in principle be the inverse of photon propagator say $(D_0^{\mu\nu})^{-1}$ as

$$(D_0^{\mu\nu})^{-1} = -\eta^{\mu\nu}P^2 + P^\mu P^\nu. \tag{9.14}$$

The inverse of $(D_0^{\mu\nu})^{-1}$ should give the photon propagator as

$$D_0^{\mu\nu} = a\eta^{\mu\nu} + bP^\mu P^\nu. \tag{9.15}$$

Now

$$\begin{aligned}
D_0^{\mu\lambda}(D_0)_{\lambda\nu}^{-1} &= \delta_\nu^\mu \\
(a\eta^{\mu\lambda} + bP^\mu P^\lambda)(-\eta_{\lambda\nu}P^2 + P_\lambda P_\nu) &= \delta_\nu^\mu \\
-aP^2\delta_\nu^\mu + aP^\mu P_\nu - bP^2P^\mu P_\nu + bP^2P^\mu P^\nu &= \delta_\nu^\mu \\
-aP^2\delta_\nu^\mu + aP^\mu P_\nu &= \delta_\nu^\mu.
\end{aligned} \tag{9.16}$$

Comparing the coefficients in both sides, one gets $a = -1/P^2$ and $a = 0$ but b remains undetermined. The matrix $(D_0^{\mu\nu})^{-1}$ is not invertible, so the propagator $D_0^{\mu\nu}$ does not exist.

[Another way: In general any second rank tensor can be written as

$$\mathcal{M}^{\mu\nu} = c\mathcal{P}_L^{\mu\nu} + d\mathcal{P}_T^{\mu\nu}, \tag{9.17}$$

where the longitudinal and transverse projection operator in orthogonal subspace are

$$\begin{aligned}
\mathcal{P}_L^{\mu\nu} &= P^\mu P^\nu / P^2, \\
\mathcal{P}_T^{\mu\nu} &= (\eta^{\mu\nu} - P^\mu P^\nu / P^2),
\end{aligned} \tag{9.18}$$

which satisfy the properties of the projection operator as

$$\mathcal{P}_L^{\mu\nu} + \mathcal{P}_T^{\mu\nu} = \eta^{\mu\nu}, \quad \mathcal{P}_L^2 = \mathcal{P}_L, \quad \mathcal{P}_T^2 = \mathcal{P}_T, \quad \mathcal{P}_L\mathcal{P}_T = 0 \tag{9.19}$$

The inverse of (9.17) can be written as

$$(\mathcal{M}^{\mu\nu})^{-1} = c^{-1}\mathcal{P}_L^{\mu\nu} + d^{-1}\mathcal{P}_T^{\mu\nu}. \quad (9.20)$$

Now (9.14) can be written in terms of projection operator as

$$(D^{\mu\nu})^{-1} = -\eta^{\mu\nu}P^2 + P^\mu P^\nu = (0)\mathcal{P}_L^{\mu\nu} + (-P^2)\mathcal{P}_T^{\mu\nu}. \quad (9.21)$$

Now comparing (9.21) with (9.17) one gets $c = 0$ and $d = -P^2$. Therefore, (9.20) suggests that $d^{-1} = -1/P^2$ and c^{-1} does not exist as $c^{-1} = 1/0$. Thus the inverse of (9.21) also does not exist.]

Some of the reasons are noted below:

- The momenta conjugate to the A^μ are given by

$$\pi^\mu = \frac{\delta\mathcal{L}_{em}}{\delta\dot{A}_\mu} = \frac{\delta\mathcal{L}_{em}}{\delta(\partial_0 A_\mu)} = F^{\mu 0} \quad (9.22)$$

which give $\pi^0 = 0$, as the diagonal components of $F^{\mu\nu}$ are zero. This clearly indicates that one of the canonical momenta does not exist. The equations defining canonical momenta cannot therefore be inverted to express quantities \dot{A}_μ in terms of the momenta. So, the Hamiltonian formalism also does not exist.

- In Maxwell's equations there are six field variables from both \mathbf{E} and \mathbf{B} but the two homogeneous equations imply four constraints on the electromagnetic field components so that there only are two independent component of electromagnetic fields. Therefore, all components of the gauge field A^μ are not independent but they are connected by gauge transformation, even though only two components are independent.
- The matrix in the transverse projection operator in (9.14) has zero eigenvalue as can be seen

$$\begin{aligned} (-\eta^{\mu\nu}P^2 + P^\mu P^\nu) P_\nu &= 0 \\ \left(\eta^{\mu\nu} - \frac{P^\mu P^\nu}{P^2} \right) P_\nu &= 0 \\ \mathcal{P}_T^{\mu\nu} P_\nu &= 0. \end{aligned} \quad (9.23)$$

The (9.23) is the transversality condition that projects on to orthogonal subspace. This also indicates that the presence of zero eigenvalues of the $\mathcal{P}_T^{\mu\nu}$ is a direct consequence of the gauge invariance of the theory. Gauge invariance implies that the theory contains fewer degrees of freedom (only transverse degrees of freedom), which reflects itself the presence of zero eigenvalues in the quadratic part of the Lagrangian density in (9.10) vis-a-vis (9.12). However, gauge field A^μ is represented by four components A^μ , all of which are not independent but connected by gauge transformation. There are only two

independent components and one needs to eliminate or restrict the additional degrees of gauge freedom. It is also to be noted that the degrees of gauge freedom absent in (9.10) should not reappear through the interaction. That is ensured through the interaction of the gauge field with a conserved fermionic current as noted in the last item after (9.11) in previous page.

Before quantisation this redundancy is dealt by fixing the gauge that restrict the gauge degrees of freedom in the theory. The Lagrangian density for the gauge field (photon) in $U(1)$ gauge theory can be rewritten along with an addition term (referred as gauge fixing term with a gauge parameter ξ) as

$$\begin{aligned}
\mathcal{L}_\gamma &= -\frac{1}{4}F_{\mu\nu}F^{\mu\nu} - \frac{1}{2\xi}(\partial_\nu A^\nu)(\partial_\mu A^\mu) \\
&= -\frac{1}{4}[\partial_\mu A_\nu - \partial_\nu A_\mu][\partial^\mu A^\nu - \partial^\nu A^\mu] - \frac{1}{2\xi}(\partial_\nu A^\nu)(\partial_\mu A^\mu) \\
&= -\frac{1}{2}\partial_\mu A_\nu[\partial^\mu A^\nu - \partial^\nu A^\mu] - \frac{1}{2\xi}(\partial_\nu A^\nu)(\partial_\mu A^\mu) + \partial_\mu(\cdots) \\
&= \frac{1}{2}A_\nu \left[\eta^{\mu\nu} \square - \left(1 - \frac{1}{\xi}\right) \partial^\mu \partial^\nu \right] A_\mu,
\end{aligned} \tag{9.24}$$

where the inverse of the propagator can be written as

$$(D_0^{\mu\nu})^{-1} = \left[-\eta^{\mu\nu} P^2 + \left(1 - \frac{1}{\xi}\right) P^\mu P^\nu \right], \tag{9.25}$$

and the inverse of which should give us the correct form the propagator as

$$D_0^{\mu\nu} = \left[a\eta^{\mu\nu} + b \left(1 - \frac{1}{\xi}\right) P^\mu P^\nu \right]. \tag{9.26}$$

As before solving for coefficients a and b :

$$\begin{aligned}
D_0^{\mu\lambda}(D_0)_{\lambda\nu}^{-1} &= \delta_\nu^\mu \\
\left[a\eta^{\mu\lambda} + b \left(1 - \frac{1}{\xi}\right) P^\mu P^\lambda \right] \left[-\eta_{\lambda\nu} P^2 + \left(1 - \frac{1}{\xi}\right) P_\lambda P_\nu \right] &= \delta_\nu^\mu \\
-aP^2\delta_\nu^\mu + \left(1 - \frac{1}{\xi}\right) \left[a - bP^2 + b \left(1 - \frac{1}{\xi}\right) P^2 \right] P^\mu P_\nu &= \delta_\nu^\mu,
\end{aligned} \tag{9.27}$$

where comparing the coefficients, one gets

$$\begin{aligned}
a &= -\frac{1}{P^2}, \\
\left[a - bP^2 + b \left(1 - \frac{1}{\xi}\right) P^2 \right] &= 0 \\
\Rightarrow b &= -\frac{\xi}{P^4}.
\end{aligned} \tag{9.28}$$

With these the photon propagator from (9.26) reads as

$$D_0^{\mu\nu} = -\frac{1}{P^2} \left[\eta^{\mu\nu} - (1 - \xi) \frac{P^\mu P^\nu}{P^2} \right]. \quad (9.29)$$

The Feynman propagator will read as

$$\mathcal{D}_0^{\mu\nu} = iD_0^{\mu\nu} = -\frac{i}{P^2} \left[\eta^{\mu\nu} - (1 - \xi) \frac{P^\mu P^\nu}{P^2} \right]. \quad (9.30)$$

It is worth noting at this point if a gauge field has mass then the gauge fixing is not required, as we will see later when the massive vector boson discussed in subsec 8.5. In different gauges ξ takes different values as $\xi = 1$ (Feynman gauge) and $\xi = 0$ (Landau gauge). However, the final result is independent of gauge choice, so one can choose it conveniently for the purpose.

After gauge fixing the QED Lagrangian reads as

$$\mathcal{L}_{em} = -\frac{1}{4}F_{\mu\nu}F^{\mu\nu} - \frac{1}{2\xi}(\partial_\mu A^\mu)^2 + \bar{\psi}(i\gamma^\mu\partial_\mu - m)\psi - e\bar{\psi}\gamma^\mu\psi A_\mu. \quad (9.31)$$

Now one can show that this gauge fixing term does not change the Lagrangian or the Maxwell's equations as long as the current is conserved: The new equation of motion becomes

$$\square A^\nu - \left(1 - \frac{1}{\xi}\right) \partial^\nu (\partial_\mu A^\mu) = -j^\nu. \quad (9.32)$$

Operating 4-divergence and using the current conservation $\partial_\mu j^\mu = 0$ one gets

$$\begin{aligned} \square (\partial_\mu A^\mu) &= -\partial_\mu j^\mu = 0 \\ \rightarrow \partial_\mu A^\mu &= 0, \end{aligned} \quad (9.33)$$

with appropriate boundary condition on A^μ so that (9.33) is satisfied. This implies that one can always transform A^μ according to (9.6) so that it satisfies (9.33). This is called gauge fixing condition in covariant gauge. Now one can compute canonical momenta and do the Hamiltonian formulation.

9.5 Free Photon Partition Function

The free photon Lagrangian density can be written from (9.31) as

$$\mathcal{L}_\gamma = -\frac{1}{4}F_{\mu\nu}F^{\mu\nu}. \quad (9.34)$$

In vacuum, photon partition function can be written as,

$$\begin{aligned} \mathcal{Z} &= \int \mathcal{D}A_\mu \exp[iS] \\ &= \int \mathcal{D}A_\mu \exp \left[i \int d^4X \left(-\frac{1}{4}F_{\mu\nu}F^{\mu\nu} \right) \right], \end{aligned} \quad (9.35)$$

where $\mathcal{D}A_\mu = \mathcal{D}A_0\mathcal{D}A_1\mathcal{D}A_2\mathcal{D}A_3$. Gauge transformations should not change anything physically.

We now choose a covariant gauge condition as

$$G(A) = \partial_\mu A^\mu = w(X), \quad (9.36)$$

which can be imposed to (9.35) by inserting a identity [64] given as

$$\int \mathcal{D}\alpha(x) \delta(G(A, \alpha) - w(X)) \left| \frac{\delta(G(A, \alpha) - w(X))}{\delta\alpha} \right| = 1. \quad (9.37)$$

Lorentz gauge condition can be recovered by taking $w = 0$. There is still a residual gauge freedom as one shifts the gauge field

$$A_\mu \rightarrow A_\mu + \partial_\mu \alpha(X), \quad (9.38)$$

where the phase factor, $\alpha(X)$ is differentiable function of space-time. Now we can write the gauge condition in (9.36) as

$$G(A, \alpha) = \partial_\mu A^\mu + \partial_\mu \partial^\mu \alpha. \quad (9.39)$$

The determinant term can be obtained as

$$\frac{\delta(G(A, \alpha(X)) - w(X))}{\delta\alpha(Y)} = \partial_\mu \partial^\mu \delta^{(4)}(X - Y). \quad (9.40)$$

So (9.35) becomes,

$$\mathcal{Z} = \int \mathcal{D}A_\mu \mathcal{D}\alpha(X) \delta(G(A, \alpha) - w(X)) \left| \frac{\delta(G(A, \alpha) - w(X))}{\delta\alpha} \right| \exp \left[i \int d^4X \left(-\frac{1}{4} F_{\mu\nu} F^{\mu\nu} \right) \right]. \quad (9.41)$$

Since there is a residual gauge freedom, we shift the gauge field as (9.38) and write (9.41) as

$$\mathcal{Z} = \int \mathcal{D}A_\mu \mathcal{D}\alpha(X) \delta(G(A) - w(X)) \det \partial^2 \exp \left[i \int d^4X \left(-\frac{1}{4} F_{\mu\nu} F^{\mu\nu} \right) \right]. \quad (9.42)$$

Now the integrand does not contain α and the α integration gives diverging result. This is due to the redundancy of the residual gauge transformation. Now, $w(X)$ is an arbitrary function of X and the behaviour of $w(X)$ is not known, so the integral involved in the partition function can not be solved. One can avoid this problem by averaging over $w(X)$ around zero with a Gaussian width ξ

$$\int \mathcal{D}w \frac{1}{\sqrt{2\pi\xi}} \exp \frac{w^2(X)}{2\xi}, \quad (9.43)$$

where ξ is a gauge fixing parameter that one chooses for the convenience of calculations and $\frac{1}{\sqrt{2\pi\xi}}$ is normalisation factor. Now the integration over w is performed in (9.42) and one gets

$$\mathcal{Z} = \int \mathcal{D}A_\mu \det \partial^2 \exp \left[i \int d^4X \left(-\frac{1}{4} F_{\mu\nu} F^{\mu\nu} - \frac{(\partial_\mu A^\mu)^2}{2\xi} \right) \right]. \quad (9.44)$$

Now we can write $\det \partial^2$ term using Grassmann property given in (2.78) as

$$\det \partial^2 = \int \mathcal{D}\bar{C} \mathcal{D}C \exp(-\bar{C} \partial^2 C), \quad (9.45)$$

where C is Grassmann field which is also known as ghost field. This plays a crucial role to cancel the redundant gauge degrees of freedom. Now,

$$\begin{aligned} \mathcal{Z} &= \int \mathcal{D}A \mathcal{D}\bar{C} \mathcal{D}C \exp \left[i \int d^4 X (\mathcal{L}_\gamma + \mathcal{L}_{\text{gf}} + \mathcal{L}_{\text{gh}}) \right] \\ &= \mathcal{Z}_{\gamma+\text{gf}} \mathcal{Z}_{\text{gh}}, \end{aligned} \quad (9.46)$$

where gauge fixing and ghost terms, respectively, are

$$\begin{aligned} \mathcal{L}_{\text{gf}} &= -\frac{(\partial_\mu A^\mu)^2}{2\xi}, \\ \mathcal{L}_{\text{gh}} &= -\bar{C} \partial^2 C. \end{aligned}$$

Let us calculate the contributions of gauge and gauge fixing part of (9.46) to the partition function as

$$\begin{aligned} \mathcal{Z}_{\gamma+\text{gf}} &\stackrel{=}{=} \int \mathcal{D}A \exp \left(\frac{i}{2} \int d^4 X A_\nu \left[\eta^{\mu\nu} \square - (1 - \frac{1}{\xi}) \partial^\mu \partial^\nu \right] A_\mu \right) \\ &= \int \mathcal{D}A \exp \left(-\frac{1}{2} \int_0^\beta d\tau d^3 \vec{x} A_i \left[\delta^{ij} \square_\tau + (1 - \frac{1}{\xi}) \partial^i \partial^j \right] A_j \right), \end{aligned} \quad (9.47)$$

where we have used $\eta^{\mu\nu} \leftrightarrow -\delta^{ij}$.

The Fourier transform of the gauge field is given as

$$\begin{aligned} A_i(X) &= A_i(\vec{x}, \tau) \stackrel{=}{=} \int_{p_0 \rightarrow i\omega_n} \frac{1}{\sqrt{V\beta}} \sum_P e^{-iP \cdot X} A_i(P) \\ &= \frac{1}{\sqrt{V\beta}} \sum_{n, \vec{p}} e^{i\vec{p} \cdot \vec{x}} e^{-i\omega_n \tau} A_i(\omega_n, \vec{p}). \end{aligned} \quad (9.48)$$

One can write the partition function in (9.47) in frequency momentum space as

$$\begin{aligned} \mathcal{Z}_{\gamma+\text{gf}} &= \int \mathcal{D}A(\omega_n, \vec{p}) \exp \left(- \sum_{n, \vec{p}} \frac{1}{2} A_i^*(\omega_n, \vec{p}) \left[\delta^{ij} (\omega_n^2 + p^2) - (1 - \frac{1}{\xi}) p^i p^j \right] A_j(\omega_n, \vec{p}) \right) \\ &= \int \mathcal{D}A(\omega_n, \vec{p}) \exp \left(- \sum_{n, \vec{p}} \frac{1}{2} A_i^*(\omega_n, \vec{p}) D_{ij}^{-1} A_j(\omega_n, \vec{p}) \right) \\ &= \prod_{n, \vec{p}} \sqrt{\frac{\pi^D}{\det D_{ij}^{-1}(\xi)}} \end{aligned} \quad (9.49)$$

where D_{ij}^{-1} is a 4×4 matrix and inverse of the gauge boson propagator. Let us set $p = (0, 0, p)$ as three space part of p are in equal footing now [64]. In Feynman gauge we have $\xi = 1$.

$$D_{ij}^{-1} = \begin{pmatrix} p^2 + \omega_n^2 & 0 & 0 & 0 \\ 0 & p^2 + \omega_n^2 & 0 & 0 \\ 0 & 0 & p^2 + \omega_n^2 & 0 \\ 0 & 0 & 0 & p^2 + \omega_n^2 \end{pmatrix}$$

$$\therefore \det D_{ij}^{-1} = (p^2 + \omega_n^2)^4. \quad (9.50)$$

$$\begin{aligned} \text{So, } \ln \mathcal{Z}_{\gamma+\text{gf}} &= -\frac{1}{2} \sum_{n, \vec{p}} \ln \det [D_{ij}^{-1}] \\ &= -4 \times \frac{1}{2} \sum_{P_E} \ln [P_E^2], \end{aligned} \quad (9.51)$$

where P_E is Euclidean momentum and \sum_{P_E} is a bosonic sum-integral.

Now we have to calculate ghost contribution to the partition function from (9.46) as

$$\mathcal{Z}_{\text{gh}} = \int \mathcal{D}\bar{C} \mathcal{D}C \exp \left(-i \int d^4 X \bar{C} \partial^2 C \right) = \int \mathcal{D}\bar{C} \mathcal{D}C \exp \left(\int_0^\beta d\tau \int d^3 x \bar{C} \square_\tau C \right). \quad (9.52)$$

The Fourier transform of the ghost field is given as

$$C(\tau, \vec{x}) = \frac{1}{\sqrt{V\beta}} \sum_{n, \vec{p}} e^{i\vec{p}\cdot\vec{x}} e^{-i\omega_n\tau} C(\omega_n, \vec{p}). \quad (9.53)$$

Combining (9.52) and (9.53), one can get the ghost partition function in frequency momentum space as

$$\begin{aligned} \mathcal{Z}_{\text{gh}} &= \int \mathcal{D}\bar{C}(\omega_n, \vec{p}) \mathcal{D}C(\omega_n, \vec{p}) \exp \left(- \sum_{n, \vec{p}} \bar{C}(\omega_n, \vec{p}) (\omega_n^2 + p^2) C(\omega_n, \vec{p}) \right) \\ &= \prod_{n, \vec{p}} (\omega_n^2 + p^2). \end{aligned} \quad (9.54)$$

$$\text{So, } \ln \mathcal{Z}_{\text{gh}} = 2 \times \frac{1}{2} \sum_{P_E} \ln [P_E^2]. \quad (9.55)$$

The logarithm of the photon partition function can be written as

$$\begin{aligned} \ln \mathcal{Z} &= \ln \mathcal{Z}_{\gamma+\text{gf}} + \ln \mathcal{Z}_{\text{gh}} \\ &= -4 \times \frac{1}{2} \sum_{P_E} \ln [P_E^2] + 2 \times \frac{1}{2} \sum_{P_E} \ln [P_E^2] \\ &= - \sum_{P_E} \ln [P_E^2]. \end{aligned} \quad (9.56)$$

So, ghost contribution cancels two unphysical degrees of freedom of photon. Now there are two physical transverse degrees of freedom of photon.

By calculating the frequency sum one gets,

$$\ln \mathcal{Z} = -2V \int \frac{d^3 p}{(2\pi)^3} \left[\frac{\beta \omega_p}{2} + \ln(1 - \exp(-\beta \omega_p)) \right]. \quad (9.57)$$

which agrees with one bosonic degree of freedom in (2.13).

So free energy density of non-interacting photon at finite temperature is given by (ignoring vacuum part)

$$\begin{aligned} F_0 &= -\frac{T}{V} \ln \mathcal{Z} = 2 \int \frac{d^3 p}{(2\pi)^3} \ln(1 - \exp(-\beta \omega_p)) \\ &= -\frac{\pi^2 T^4}{45}. \end{aligned} \quad (9.58)$$

The pressure for non-interacting photon

$$\mathcal{P}_0 = -F_0 = \frac{\pi^2 T^4}{45}. \quad (9.59)$$

9.6 One-loop Fermion Self-energy Σ and Structure Functions \mathcal{A} and \mathcal{B} in HTL approximation

We have electron-photon interaction Lagrangian from (9.31) as

$$\mathcal{L}_{int} = -e \bar{\psi} \gamma_\mu \psi A^\mu. \quad (9.60)$$

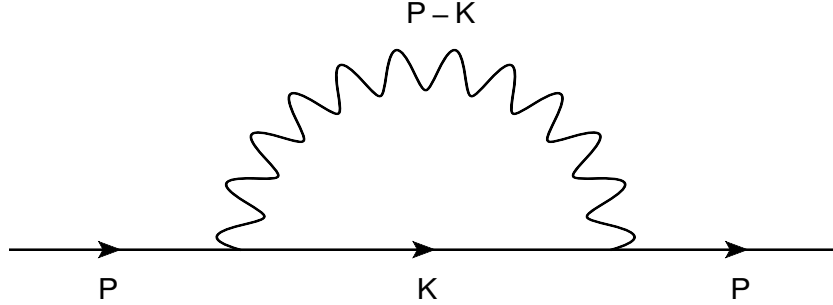


Figure 26: One loop fermion self-energy diagram.

The one loop fermion self-energy in Fig. 26 can be written in Feynman gauge as

$$\begin{aligned} \Sigma(P) &= x^2 C_F T \sum_{\{K\}} \gamma_\mu \frac{K}{K^2} \gamma^\mu \frac{1}{(P-K)^2} \\ &= -2x^2 C_F T \sum_{\{K\}} \frac{K}{K^2 Q^2}, \end{aligned} \quad (9.61)$$

where $Q = (P - K)$ and $\sum_{\{K\}}$ is a fermionic sum-integral. Also x and C_F are, respectively, coupling and Casimir invariant for a given group. For $U(1)$ group $x = e$ and $C_F = 1$ and Eq.(9.61) corresponds to electron self-energy. For $SU(3)$ group $x = g$ and $C_F = 4/3$ and Eq.(9.61) corresponds to quark self-energy with internal photon line should be replaced by gluon line.

We now would like to compute the structure functions as given in the rest frame of the heat bath, respectively, in (7.6) and (7.8) as

$$\mathcal{A}(\omega, p) = \frac{1}{4p^2} (\text{Tr} [\Sigma \not{P}] - \omega \text{Tr} [\Sigma \not{\psi}]), \quad (9.62a)$$

$$\mathcal{B}(\omega, p) = \frac{1}{4p^2} (P^2 \text{Tr} [\Sigma \not{\psi}] - (P \cdot u) \text{Tr} [\Sigma \not{P}]). \quad (9.62b)$$

Now, we can write

$$\text{Tr} [\Sigma \not{P}] = -8x^2 C_F T \sum_{\{K\}} \frac{k_0 \omega - \vec{k} \cdot \vec{p}}{K^2 Q^2}, \quad (9.63a)$$

$$\text{Tr} [\Sigma \not{\psi}] = -8x^2 C_F T \sum_{\{K\}} \frac{k_0}{K^2 Q^2}. \quad (9.63b)$$

Using (9.63a) and (9.63b) in (9.62a), we get

$$\mathcal{A}(\omega, p) = \frac{2x^2 C_F}{p^2} T \sum_{\{K\}} \frac{\vec{k} \cdot \vec{p}}{K^2 Q^2}. \quad (9.64)$$

We use the following frequency sum in mixed representation

$$\begin{aligned} T \sum_{k_0} \frac{1}{K^2 Q^2} &= \frac{1}{4kq} \left[(1 - n_F(k) + n_B(q)) \left(\frac{1}{\omega + k + q} - \frac{1}{\omega - k - q} \right) \right. \\ &\quad \left. + (n_B(q) + n_F(k)) \left(\frac{1}{\omega + k - q} - \frac{1}{\omega - k + q} \right) \right], \end{aligned} \quad (9.65)$$

where $n_B(y) = (e^{y/T} \pm 1)^{-1}$. When loop momentum is hard, $K \sim T$, compare to the external momentum P is called hard thermal loop (HTL) approximation [78]. Under this HTL approximation⁶ one can make following simplifications as

$$q = |\vec{p} - \vec{k}| = \sqrt{p^2 + k^2 - 2pk \cos \theta} = \sqrt{p^2 + k^2 - 2pkc} \approx k - pc = k - \vec{p} \cdot \hat{k}, \quad (9.66a)$$

$$n_B(q) = n_B(k - \vec{p} \cdot \hat{k}) \approx n_B(k) - \vec{p} \cdot \hat{k} \frac{dn_B(k)}{dk}, \quad (9.66b)$$

$$\omega \pm k \pm q = \omega \pm k \pm k \mp \vec{p} \cdot \hat{k} \approx \pm 2k, \quad (9.66c)$$

$$\omega \pm k \mp q = \omega \pm k \mp k \pm \vec{p} \cdot \hat{k} \approx \omega \pm \vec{p} \cdot \hat{k}. \quad (9.66d)$$

⁶The details of HTL approximation will be discussed in section 12.

Using (9.66a) to (9.66d) in (9.65), one can write

$$T \sum_{k_0} \frac{1}{K^2 Q^2} = \frac{1}{4k^2} \left[\left(1 - n_F(k) + n_B(k) - \vec{p} \cdot \hat{k} \frac{dn_B(k)}{dk} \right) \left(\frac{1}{k} \right) + \left(n_B(k) + n_F(k) - \vec{p} \cdot \hat{k} \frac{dn_B(k)}{dk} \right) \left(\frac{1}{\omega + \vec{p} \cdot \hat{k}} - \frac{1}{\omega - \vec{p} \cdot \hat{k}} \right) \right], \quad (9.67)$$

Combining (9.67) and (9.64), we get

$$\mathcal{A}(\omega, p) = \frac{2x^2 C_F}{p^2} \int \frac{d^3 k}{(2\pi)^3} \frac{\vec{p} \cdot \vec{k}}{4k^2} \left[\left(1 - n_F(k) + n_B(k) - \vec{p} \cdot \hat{k} \frac{dn_B(k)}{dk} \right) \left(\frac{1}{k} \right) + \left(n_B(k) + n_F(k) - \vec{p} \cdot \hat{k} \frac{dn_B(k)}{dk} \right) \left(\frac{1}{\omega + \vec{p} \cdot \hat{k}} - \frac{1}{\omega - \vec{p} \cdot \hat{k}} \right) \right]. \quad (9.68)$$

We note that the term $1/k$ inside the square bracket contributes as proportional to T , which is sub-leading in T . This term can be neglected. We now evaluate the second term only that contributes as T^2 , which is leading order in T . We further note that the term $\vec{p} \cdot \hat{k} \frac{dn_B(k)}{dk}$ has soft momentum and is neglected. With this the (9.68) reduces as

$$\mathcal{A}(\omega, p) = \frac{2x^2 C_F}{4p^2} \int \frac{k dk d\Omega}{(2\pi)^3} (n_B(k) + n_F(k)) \left[\frac{\vec{p} \cdot \hat{k}}{\omega + \vec{p} \cdot \hat{k}} - \frac{\vec{p} \cdot \hat{k}}{\omega - \vec{p} \cdot \hat{k}} \right]. \quad (9.69)$$

Now putting $\cos \theta \rightarrow -\cos \theta$ in the first term inside the square bracket, the above equation then becomes

$$\mathcal{A}(\omega, p) = -\frac{x^2 C_F}{p^2} \int_0^\infty k dk (n_B(k) + n_F(k)) \int \frac{d\Omega}{(2\pi)^3} \frac{\vec{p} \cdot \hat{k}}{\omega - \vec{p} \cdot \hat{k}}. \quad (9.70)$$

We can perform the k -integration as

$$\int_0^\infty k dk (n_B(k) + n_F(k)) = \frac{\pi^2 T^2}{4}. \quad (9.71)$$

Using (9.71) we can obtain

$$\begin{aligned} \mathcal{A}(\omega, p) &= -\frac{m_{\text{th}}^2}{p^2} \int \frac{d\Omega}{4\pi} \frac{\vec{p} \cdot \hat{k}}{\omega - \vec{p} \cdot \hat{k}} \\ &= -\frac{m_{\text{th}}^2}{p^2} \int \frac{d\Omega}{4\pi} \frac{\vec{p} \cdot \hat{k}}{P \cdot \hat{K}}, \end{aligned} \quad (9.72)$$

where $\hat{K} = (1, \hat{k})$ is a light like vector and the thermal mass of the fermion is given as

$$m_{\text{th}}^2 = \frac{x^2 C_F T^2}{8}. \quad (9.73)$$

For electron the thermal mass becomes $m_{\text{th}}^2 = \frac{e^2 T^2}{8}$ whereas for quark $m_{\text{th}}^2 = \frac{g^2 T^2}{6}$.

The angular integration can be performed using the following integrals

$$\int_{-1}^1 \frac{dy}{a-by} = \frac{1}{b} \ln \frac{a+b}{a-b}, \quad (9.74a)$$

$$\int_{-1}^1 \frac{y dy}{a-by} = -\frac{2}{b} + \frac{a}{b^2} \ln \frac{a+b}{a-b}. \quad (9.74b)$$

After performing the angular integration in (9.72) we finally get [76, 79]

$$\mathcal{A}(\omega, p) = \frac{m_{\text{th}}^2}{p^2} \left[1 - \frac{\omega}{2p} \ln \left(\frac{\omega+p}{\omega-p} \right) \right], \quad (9.75)$$

Using (9.63a) and (9.63b) in (9.62b) we write the structure function $\mathcal{B}(\omega, p)$ as

$$\mathcal{B}(\omega, p) = \frac{2x^2 C_F}{p^2} \left[p^2 T \sum_{\{K\}} \frac{k_0}{K^2 Q^2} - (P \cdot u) T \sum_{\{K\}} \frac{\vec{p} \cdot \vec{k}}{K^2 Q^2} \right]. \quad (9.76)$$

The frequency sum in the second term inside square bracket is already done in (9.65). The frequency sum needed for the first term is given in mixed representation as

$$\begin{aligned} T \sum_{k_0} \frac{k_0}{K^2 Q^2} &= -\frac{1}{4q} \left[(1 - n_F(k) + n_B(q)) \left(\frac{1}{\omega + k + q} + \frac{1}{\omega - k - q} \right) \right. \\ &\quad \left. + (n_B(q) + n_F(k)) \left(\frac{1}{\omega + k - q} + \frac{1}{\omega - k + q} \right) \right], \end{aligned} \quad (9.77)$$

Using HTL approximations in (9.66a) to (9.66d), the frequency sum becomes

$$T \sum_{k_0} \frac{k_0}{K^2 Q^2} = -\frac{1}{4k} \left[\left(n_B(k) + n_F(k) - \vec{p} \cdot \hat{k} \frac{dn_B(k)}{dk} \right) \left(\frac{1}{\omega + \vec{p} \cdot \hat{k}} + \frac{1}{\omega - \vec{p} \cdot \hat{k}} \right) \right] \quad (9.78)$$

Substituting (9.67) and (9.78) in (9.76), we get

$$\begin{aligned} \mathcal{B}(\omega, p) &= \frac{2x^2 C_F}{p^2} \left[-p^2 \int \frac{d^3 k}{(2\pi)^3} \frac{1}{4k} \left(n_B(k) + n_F(k) - \vec{p} \cdot \hat{k} \frac{dn_B(k)}{dk} \right) \left(\frac{1}{\omega + \vec{p} \cdot \hat{k}} + \frac{1}{\omega - \vec{p} \cdot \hat{k}} \right) \right. \\ &\quad - (P \cdot u) \int \frac{d^3 k}{(2\pi)^3} \frac{1}{4k^2} \left(1 - n_F(k) + n_B(k) - \vec{p} \cdot \hat{k} \frac{dn_B(k)}{dk} \right) \frac{1}{k} \\ &\quad \left. - (P \cdot u) \int \frac{d^3 k}{(2\pi)^3} \frac{1}{4k^2} \left(n_B(k) + n_F(k) - \vec{p} \cdot \hat{k} \frac{dn_B(k)}{dk} \right) \left(\frac{\vec{p} \cdot \vec{k}}{\omega + \vec{p} \cdot \hat{k}} - \frac{\vec{p} \cdot \vec{k}}{\omega - \vec{p} \cdot \hat{k}} \right) \right] \quad (9.79) \end{aligned}$$

As before we neglect the second term inside the square bracket that gives a contribution proportional to T , which is sub-leading in T . Also $\vec{p} \cdot \hat{k} \frac{dn_B(k)}{dk}$ term is neglected as the soft momentum is associated with it. Then, the above equation can be written as

$$\mathcal{B}(\omega, p) = \frac{x^2 C_F}{p^2} \left[\int_0^\infty k dk (n_B(k) + n_F(k)) \int \frac{d\Omega}{(2\pi)^3} \frac{(P \cdot u)(\vec{p} \cdot \hat{k}) - p^2}{\omega - \vec{p} \cdot \hat{k}} \right]. \quad (9.80)$$

After performing the k -integration using (9.71), we get

$$\mathcal{B}(\omega, p) = \frac{m_{\text{th}}^2}{p^2} \int \frac{d\Omega}{4\pi} \frac{(P \cdot u)(\vec{p} \cdot \hat{\mathbf{k}}) - p^2}{P \cdot \hat{K}}, \quad (9.81)$$

Now performing the angular integrations using (9.74a) and (9.74b), we finally get [76, 79]

$$\mathcal{B}(\omega, p) = \frac{m_{\text{th}}^2}{p} \left[-\frac{\omega}{p} + \left(\frac{\omega^2}{p^2} - 1 \right) \frac{1}{2} \ln \left(\frac{\omega + p}{\omega - p} \right) \right]. \quad (9.82)$$

The fermion self-energy can be written from (9.61) as

$$\Sigma(P) = -2x^2 C_F T \sum_K \left[\frac{k_0 \gamma_0}{K^2 Q^2} - \frac{\vec{\gamma} \cdot \vec{\mathbf{k}}}{K^2 Q^2} \right]. \quad (9.83)$$

Following the same procedures as those structure functions, the fermion self-energy contribution within HTL approximation can be written as

$$\Sigma(P) = x^2 C_F \int_0^\infty k dk (n_B(k) + n_F(k)) \int \frac{d\Omega}{(2\pi)^3} \left[\frac{\gamma_0}{\omega - \vec{p} \cdot \hat{\mathbf{k}}} - \frac{\vec{\gamma} \cdot \hat{\mathbf{k}}}{\omega - \vec{p} \cdot \hat{\mathbf{k}}} \right], \quad (9.84)$$

which after k -integration becomes

$$\Sigma(P) = m_{\text{th}}^2 \int \frac{d\Omega}{4\pi} \frac{\hat{K}}{P \cdot \hat{K}}. \quad (9.85)$$

After explicit calculations, we obtain

$$\Sigma(P) = \frac{m_{\text{th}}^2}{2p} \ln \left(\frac{\omega + p}{\omega - p} \right) \gamma_0 + \frac{m_{\text{th}}^2}{p} \left[1 - \frac{\omega}{2p} \ln \left(\frac{\omega + p}{\omega - p} \right) \right] (\vec{\gamma} \cdot \hat{\mathbf{p}}). \quad (9.86)$$

This expression can also be obtained directly by combining (7.9), (9.75) and (9.82).

9.7 Dispersion of Fermionic Quasiparticles and Collective Excitations in HTL Approximation

We can obtain $\mathcal{D}_\pm(\omega, p)$ by combining (7.16), (9.75) and (9.82) as

$$\begin{aligned} \mathcal{D}_\pm(\omega, p) &= \left[1 + \frac{m_{\text{th}}^2}{p^2} \left(1 - \frac{\omega}{2p} \ln \left(\frac{\omega + p}{\omega - p} \right) \right) \right] (\omega \mp p) + \frac{m_{\text{th}}^2}{p} \left[-\frac{\omega}{p} + \left(\frac{\omega^2}{p^2} - 1 \right) \frac{1}{2} \ln \left(\frac{\omega + p}{\omega - p} \right) \right] \\ &= (\omega \mp p) - \frac{m_{\text{th}}^2}{p} \left[\frac{1}{2} \left(1 \mp \frac{\omega}{p} \right) \ln \left(\frac{\omega + p}{\omega - p} \right) \pm 1 \right]. \end{aligned} \quad (9.87)$$

One can obtain the in-medium fermion propagator reads from (7.22)

$$S^*(P) = \frac{1}{2} \frac{(\gamma_0 - \vec{\gamma} \cdot \hat{\mathbf{p}})}{\mathcal{D}_+(\omega, p)} + \frac{1}{2} \frac{(\gamma_0 + \vec{\gamma} \cdot \hat{\mathbf{p}})}{\mathcal{D}_-(\omega, p)}, \quad (9.88)$$

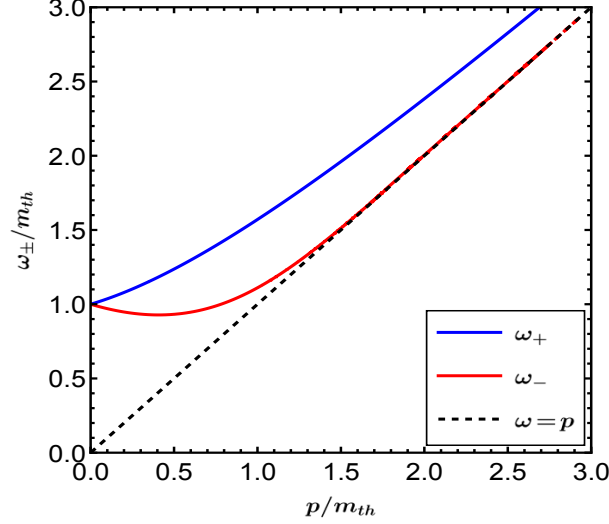


Figure 27: Plot of quasiparticles dispersion in HTL approximation.

The charge invariance demands that $\mathcal{D}_{\pm}(-\omega, p) = -\mathcal{D}_{\mp}(\omega, p)$ which implies that $\mathcal{A}(-\omega, p) = \mathcal{A}(\omega, p)$ and $\mathcal{B}(-\omega, p) = -\mathcal{B}(\omega, p)$. $\mathcal{D}(\omega, p)$ has imaginary part for space like momenta P ($p_0^2 < p^2$), it is also useful to define the parity properties for both real and imaginary parts of $\mathcal{D}(\omega, p)$ as $\text{Re}\mathcal{D}_+(-\omega, p) = -\text{Re}\mathcal{D}_-(\omega, p)$ and $\text{Im}\mathcal{D}_+(-\omega, p) = \text{Im}\mathcal{D}_-(\omega, p)$.

Although the effective propagator in (9.88) manifests the chiral symmetry, the poles of $\mathcal{D}_{\pm}(\omega, p)$ do not occur at light cone, $\omega = \pm p$. This means that the poles of the effective fermion propagator will be away from the light cone in the time like domain. This is because the extra term $\mathcal{B}\gamma_0$ appears in self-energy in (7.9) due to the breaking of Lorentz invariance at finite temperature [76]. The zeros of $\mathcal{D}_{\pm}(\omega, p)$ define dispersion property of a quark in the thermal bath. $\mathcal{D}_+(\omega, p) = 0$ has two poles at $\omega = \omega_+(p)$ and $\omega = -\omega_-(p)$ whereas $\mathcal{D}_-(\omega, p) = 0$ has two poles at $\omega = \omega_-(p)$ and $\omega = -\omega_+(p)$. Only the positive energy solutions are displayed in Fig. 27. A mode with energy ω_+ represents the in-medium propagation of a particle excitation This is a Dirac spinors and eigenstate of $(\gamma_0 - \vec{\gamma} \cdot \hat{\mathbf{p}})$ with chirality to helicity ratio +1. On the other hand there is a new long wavelength mode known as *plasmino* with energy ω_- and eigenstate of $(\gamma_0 + \vec{\gamma} \cdot \hat{\mathbf{p}})$ with chirality to helicity ratio -1. The ω_- branch has a minimum at low momentum and then approaches free dispersion curve at large momentum. It is important to note that the minimum leads to Van Hove singularities in soft dilepton rate [80] and meson spectral function [81].

Below we present the approximate analytic solutions of $\omega_{\pm}(p)$ for small and large values of momentum p . For small values of momentum ($p \ll m_{\text{th}}$), the dispersion relations are

$$\omega_+(p) \approx m_{\text{th}} + \frac{1}{3}p + \frac{1}{3}\frac{p^2}{m_{\text{th}}} - \frac{16}{135}\frac{p^3}{m_{\text{th}}^2}, \quad (9.89a)$$

$$\omega_-(p) \approx m_{\text{th}} - \frac{1}{3}p + \frac{1}{3}\frac{p^2}{m_{\text{th}}} + \frac{16}{135}\frac{p^3}{m_{\text{th}}^2}, \quad (9.89b)$$

whereas for large values of momentum ($m_{\text{th}} \ll p \ll T$), one obtains

$$\omega_+(p) \approx p + \frac{m_{\text{th}}^2}{p} - \frac{m_{\text{th}}^4}{2p^3} \ln \frac{m_{\text{th}}^2}{2p^2} + \frac{m_{\text{th}}^6}{4p^5} \left[\ln^2 \frac{m_{\text{th}}^2}{2p^2} + \ln \frac{m_{\text{th}}^2}{2p^2} - 1 \right], \quad (9.90a)$$

$$\omega_-(p) \approx p + 2p \exp \left(-\frac{2p^2 + m_{\text{th}}^2}{m_{\text{th}}^2} \right). \quad (9.90b)$$

We note that at large (hard) momentum the collective mode with chirality to helicity ratio +1 resembles the free particle in vacuum whereas the long wave length mode, plasmino with chirality to helicity ratio -1 decouples from the plasma. These are clearly evident from (9.90a) and (9.90b). At small momenta both collective modes are equally important which could be seen from (9.89a) and (9.89b). In addition to the pole contributions coming from time like domain ($\omega^2 > p^2$), $\mathcal{D}_\pm(\omega, p)$ contains a discontinuous part corresponding to *Landau damping* coming from space like domain ($\omega^2 < p^2$) due to the presence of logarithmic term in (9.87).

9.8 Spectral Representation of Fermion Propagator

From (7.22) the in-medium fermion propagator reads as

$$S^*(P) = \frac{1}{2} \frac{(\gamma_0 - \vec{\gamma} \cdot \hat{p})}{\mathcal{D}_+(\omega, p)} + \frac{1}{2} \frac{(\gamma_0 + \vec{\gamma} \cdot \hat{p})}{\mathcal{D}_-(\omega, p)}, \quad (9.91)$$

where $\mathcal{D}_\pm(\omega, p)$ are given in (9.87) as

$$\mathcal{D}_\pm(\omega, p) = p \left(\frac{\omega}{p} \mp 1 \right) - \frac{m_{\text{th}}^2}{p} \left[\frac{1}{2} \left(1 \mp \frac{\omega}{p} \right) \ln \left(\frac{\frac{\omega}{p} + 1}{\frac{\omega}{p} - 1} \right) \pm 1 \right]. \quad (9.92)$$

According to (7.17), $\mathcal{D}_\pm(\omega, p) = d_\pm(\omega, p) = \omega \pm p$, for free massless case. The corresponding free spectral function can be obtained following (A.11) as

$$\begin{aligned} \rho_\pm^f(\omega, k) &= \lim_{\epsilon \rightarrow 0} \frac{1}{\pi} \text{Im} \frac{1}{d_\pm(\omega, p)} \Big|_{\omega \rightarrow \omega + i\epsilon} \\ &= \lim_{\epsilon \rightarrow 0} \frac{1}{\pi} \text{Im} \frac{1}{\omega \mp p + i\epsilon} = \frac{\delta(\omega \mp p)}{\left| \frac{d(\omega \mp p)}{d\omega} \right|} = \delta(\omega \mp p). \end{aligned} \quad (9.93)$$

As discussed in subsec 9.7 that $\mathcal{D}_\pm(\omega, p)$ has solutions at $\omega_\pm(k)$ and $-\omega_\mp(p)$ and a cut part due to space like momentum, $\omega^2 < p^2$. In-medium spectral function corresponding to the effective fermion propagator in (9.91) will have both pole and cut contribution as

$$\rho_\pm(\omega, p) = \rho_\pm^{\text{pole}}(\omega, p) + \rho_\pm^{\text{cut}}(\omega, p). \quad (9.94)$$

The pole part of the spectral function can be obtained following (A.11) as

$$\begin{aligned} \rho_\pm^{\text{pole}}(\omega, p) &= \lim_{\epsilon \rightarrow 0} \frac{1}{\pi} \text{Im} \frac{1}{\mathcal{D}_\pm(\omega, p)} \Big|_{\omega \rightarrow \omega + i\epsilon} = \frac{\delta(\omega - \omega_\pm)}{\left| \frac{d\mathcal{D}_\pm}{d\omega} \right|_{\omega=\omega_\pm}} + \frac{\delta(\omega + \omega_\mp)}{\left| \frac{d\mathcal{D}_\mp}{d\omega} \right|_{\omega=-\omega_\mp}} \\ &= \frac{(\omega^2 - p^2)}{2m_{\text{th}}^2} \delta(\omega - \omega_\pm) + \frac{(\omega^2 - p^2)}{2m_{\text{th}}^2} \delta(\omega + \omega_\mp). \end{aligned} \quad (9.95)$$

For $\omega^2 < p^2$, there is a discontinuity in $\ln \frac{\omega+p}{\omega-p}$ as $\ln y = \ln |y| - i\pi$, which leads to the spectral function, $\rho_{\pm}^{\text{cut}}(\omega, p)$, corresponding to the discontinuity in $\mathcal{D}_{\pm}(\omega, p)$ can be obtained from (A.9) as

$$\begin{aligned} \rho_{\pm}^{\text{cut}}(\omega, p) &= \frac{1}{2\pi i} \text{Disc} \frac{1}{\mathcal{D}_{\pm}(\omega, p)} = \frac{1}{\pi} \lim_{\epsilon \rightarrow 0} \text{Im} \frac{1}{\mathcal{D}_{\pm}(\omega, p)} \Big|_{\substack{\omega \rightarrow \omega + i\epsilon \\ \omega < p}} \\ &= \frac{\frac{m_{\text{th}}^2}{2p} \left(\pm \frac{\omega}{p} - 1 \right) \Theta(p^2 - \omega^2)}{\left[\omega \mp p - \frac{m_{\text{th}}^2}{p} \left(\pm 1 - \frac{p \mp \omega}{2p} \ln \frac{p+\omega}{p-\omega} \right) \right]^2 + \left[\pi \frac{m_{\text{th}}^2}{2p} \left(1 \mp \frac{\omega}{p} \right) \right]^2} \\ &= \beta_{\pm}(\omega, p) \Theta(p^2 - \omega^2). \end{aligned} \quad (9.96)$$

9.9 Calculation of Π_L and Π_T from One-loop Photon Self-energy in HTL Approximation

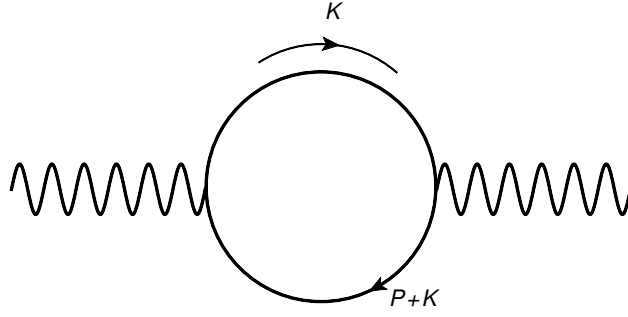


Figure 28: One loop photon self-energy diagram.

We have QED interaction Lagrangian from (9.31)

$$\mathcal{L}_{\text{int}} = -e \bar{\psi} \gamma_{\mu} \psi A^{\mu}. \quad (9.97)$$

So using Fig. 28 photon self energy can be written as

$$\begin{aligned} \Pi_{\mu\nu} &= - \int \frac{d^4 K}{(2\pi)^4} \text{Tr} \left[(-ie\gamma_{\mu}) \frac{i\mathcal{K}}{K^2} (-ie\gamma_{\nu}) \frac{i(\mathcal{P} + \mathcal{K})}{(K+P)^2} \right] \\ &= -e^2 \int \frac{d^4 K}{(2\pi)^4} \text{Tr} \left[\frac{\gamma_{\mu} \mathcal{K} \gamma_{\nu} (\mathcal{P} + \mathcal{K})}{K^2 (P+K)^2} \right] \\ &= -4e^2 \int \frac{d^4 K}{(2\pi)^4} \left[\frac{2K_{\mu} K_{\nu} - \eta_{\mu\nu} K^2 - \eta_{\mu\nu} K \cdot P + (K_{\mu} P_{\nu} + P_{\mu} K_{\nu})}{K^2 (P+K)^2} \right]. \end{aligned} \quad (9.98)$$

Now in HTL approximation one can neglect external soft momentum [77, 78, 82, 83], i.e., one or higher power of P . So we get,

$$\begin{aligned} \Pi_{\mu\nu} &\approx -8e^2 \int \frac{d^4 K}{(2\pi)^4} \left[\frac{K_{\mu} K_{\nu}}{K^2 (P+K)^2} \right] + 4\eta_{\mu\nu} \int \frac{d^4 K}{(2\pi)^4} \frac{1}{(P+K)^2} \\ &\approx -8e^2 \int \frac{d^4 K}{(2\pi)^4} [K_{\mu} K_{\nu} \Delta_F(K) \Delta_F(Q)] + 4\eta_{\mu\nu} \int \frac{d^4 K}{(2\pi)^4} \Delta_F(Q), \end{aligned} \quad (9.99)$$

where $\Delta_F(K) = \frac{1}{K^2}$ and $\Delta_F(Q) = \frac{1}{(P+K)^2} = \frac{1}{Q^2}$ with $Q = P + K$. We also note that F stands for fermionic part of the propagator.

We take the time-time part of $\Pi_{\mu\nu}$ as [84, 85]

$$\begin{aligned}
\Pi_{00} &= -8e^2T \sum_{\{K\}}^f k_0^2 \Delta_F(K) \Delta_F(Q) + 4e^2T \sum_{\{K\}}^f \Delta_F(Q) \\
&= -8e^2T \sum_{\{K\}}^f (K^2 + k^2) \Delta_F(K) \Delta_F(Q) + 4e^2T \sum_{\{K\}}^f \Delta_F(Q) \\
&= -4e^2T \sum_{\{K\}}^f \Delta_F(K) - 8e^2T \sum_{\{K\}}^f k^2 \Delta_F(K) \Delta_F(Q), \tag{9.100}
\end{aligned}$$

where $\sum_{\{K\}}^f$ is a fermionic sum-integral and we have used $\Delta_F(Q) = 1/(P+K)^2 \approx 1/K^2 = \Delta_F(K)$ in the first term.

Also we obtain [84, 85]

$$\begin{aligned}
\Pi_\mu^\mu &= -8e^2T \sum_{\{K\}}^f K^2 \Delta_F(K) \Delta_F(Q) + 4e^2\delta_\mu^\mu T \sum_{\{K\}}^f \Delta_F(Q) \\
&= 8e^2T \sum_{\{K\}}^f \Delta_F(Q) \approx 8e^2T \sum_{\{K\}}^f \Delta_F(K). \tag{9.101}
\end{aligned}$$

We know the results of frequency sums:

$$T \sum_{k_0} \Delta_F(K) = T \sum_{k_0} \frac{1}{K^2} = \frac{1}{2k} (1 - 2n_F(k)), \tag{9.102a}$$

$$\begin{aligned}
T \sum_{k_0} \Delta_F(K) \Delta_F(Q) &= \frac{1}{4kq} \left[(1 - n_F(k) - n_F(q)) \left(\frac{1}{\omega - k - q} - \frac{1}{\omega + k + q} \right) \right. \\
&\quad \left. - (n_F(k) - n_F(q)) \left(\frac{1}{\omega + k - q} - \frac{1}{\omega - k + q} \right) \right], \tag{9.102b}
\end{aligned}$$

where $k = |\vec{k}|$, $q = |\vec{k} + \vec{p}|$ and the Fermi distribution is given as $n_F(x) = 1/(\exp(\beta x) + 1)$.

Now using (9.102a) in (9.101), one gets

$$\Pi_\mu^\mu = 8e^2 \int \frac{d^3k}{(2\pi)^3} \frac{1}{2k} (1 - 2n_F(k)). \tag{9.103}$$

Neglecting vacuum part, one can have

$$\begin{aligned}
\Pi_\mu^\mu &= -\frac{4e^2}{\pi^2} \int_0^\infty k n_F(k) dk \\
&= -\frac{4e^2}{\pi^2} \times \frac{\pi^2 T^2}{12} \\
&= -\frac{e^2 T^2}{3} = -m_D^2, \tag{9.104}
\end{aligned}$$

where the Debye mass in QED is given as $m_D^2 = e^2 T^2/3$.

Now using (9.102a) and (9.102b) in (9.100), one can write the time-time component as

$$\begin{aligned} \Pi_{00} = & -4e^2 \int \frac{d^3k}{(2\pi)^3} \frac{1}{2k} (1 - 2n_F(k)) - 8e^2 \int \frac{d^3k}{(2\pi)^3} \frac{k^2}{4kq} \\ & \times \left[(1 - n_F(k) - n_F(q)) \left(\frac{1}{\omega - k - q} - \frac{1}{\omega + k + q} \right) \right. \\ & \left. - (n_F(k) - n_F(q)) \left(\frac{1}{\omega + k - q} - \frac{1}{\omega - k + q} \right) \right]. \end{aligned} \quad (9.105)$$

Under the HTL approximation [78] one can make following simplifications as

$$q = |\vec{p} + \vec{k}| = \sqrt{p^2 + k^2 + 2pk \cos \theta} = \sqrt{p^2 + k^2 + 2pkc} \approx k + pc = k + \vec{p} \cdot \hat{k}, \quad (9.106a)$$

$$n_F(q) = n_B(k + \vec{p} \cdot \hat{k}) \approx n_F(k) + \vec{p} \cdot \hat{k} \frac{dn_F(k)}{dk}, \quad (9.106b)$$

$$\omega \pm k \pm q = \omega \pm k \pm k \pm \vec{p} \cdot \hat{k} \approx \pm 2k, \quad (9.106c)$$

$$\omega \pm k \mp q = \omega \pm k \mp k \mp \vec{p} \cdot \hat{k} \approx \omega \mp \vec{p} \cdot \hat{k}. \quad (9.106d)$$

Now using (9.106a) to (9.106d) in (9.102b), one can write the time-time component as

$$\begin{aligned} \Pi_{00} = & -4e^2 \int \frac{d^3k}{(2\pi)^3} \frac{1}{2k} (1 - 2n_F(k)) - 2e^2 \int \frac{d^3k}{(2\pi)^3} \left[\left(1 - 2n_F(k) - \vec{p} \cdot \hat{k} \frac{dn_F(k)}{dk} \right) \left(-\frac{1}{k} \right) \right. \\ & \left. + \vec{p} \cdot \hat{k} \frac{dn_F(k)}{dk} \left(\frac{1}{\omega - \vec{p} \cdot \hat{k}} - \frac{1}{\omega + \vec{p} \cdot \hat{k}} \right) \right] \\ = & -4e^2 \int \frac{d^3k}{(2\pi)^3} \frac{1}{2k} (1 - 2n_F(k)) + 4e^2 \int \frac{d^3k}{(2\pi)^3} \frac{1}{2k} (1 - 2n_F(k)) \\ & - 2e^2 \int \frac{d^3k}{(2\pi)^3} \frac{\vec{p} \cdot \hat{k}}{k} \frac{dn_F(k)}{dk} - 2e^2 \int \frac{d^3k}{(2\pi)^3} \frac{dn_F(k)}{dk} \left(\frac{\vec{p} \cdot \hat{k}}{\omega - \vec{p} \cdot \hat{k}} - \frac{\vec{p} \cdot \hat{k}}{\omega + \vec{p} \cdot \hat{k}} \right) \\ \approx & -2e^2 \int \frac{d^3k}{(2\pi)^3} \frac{dn_F(k)}{dk} \left(\frac{\vec{p} \cdot \hat{k}}{\omega - \vec{p} \cdot \hat{k}} - \frac{\vec{p} \cdot \hat{k}}{\omega + \vec{p} \cdot \hat{k}} \right), \end{aligned} \quad (9.107)$$

where we have neglected the third term in second line for soft momentum. Now considering $\cos \theta = -\cos \theta$ in the second term of the last line we get

$$\begin{aligned} \Pi_{00}(\omega, p) = & -2e^2 \int_0^\infty \frac{k^2}{2\pi^2} \frac{dk}{dk} \frac{dn_F(k)}{dk} \int \frac{d\Omega}{4\pi} \frac{2\vec{p} \cdot \hat{k}}{\omega - \vec{p} \cdot \hat{k}} \\ = & \frac{4e^2}{T} \int_0^\infty \frac{k^2}{2\pi^2} \frac{n_F(k)(1 - n_F(k))}{2\pi^2} dk \int \frac{d\Omega}{4\pi} \frac{\omega - P \cdot \hat{K}}{P \cdot \hat{K}} \\ = & \frac{4e^2}{2\pi^2 T} \int_0^\infty k^2 n_F(k)(1 - n_F(k)) dk \int_{-1}^1 \frac{dc}{2} \left(\frac{\omega}{\omega - pc} - 1 \right) \\ = & \frac{4e^2}{2\pi^2 T} \times \frac{\pi^2 T^3}{6} \times \left[\frac{\omega}{2p} \ln \frac{\omega + p}{\omega - p} - 1 \right] = \frac{e^2 T^2}{3} \left[\frac{\omega}{2p} \ln \frac{\omega + p}{\omega - p} - 1 \right] \\ = & m_D^2 \left[\frac{\omega}{2p} \ln \frac{\omega + p}{\omega - p} - 1 \right]. \end{aligned} \quad (9.108)$$

Using (9.108) in (8.24) one obtains the longitudinal component of the photon self-energy [84, 85] as

$$\begin{aligned}\Pi_L(\omega, p) &= -\frac{P^2}{p^2}\Pi_{00}(\omega, p) \\ &= \frac{m_D^2 P^2}{p^2} \left[1 - \frac{\omega}{2p} \ln \frac{\omega + p}{\omega - p} \right].\end{aligned}\quad (9.109)$$

Now using (9.104) and (9.109) in (8.28), one obtains the transverse component of the photon self-energy [84, 85] as

$$\begin{aligned}\Pi_T(\omega, p) &= \frac{1}{2} [\Pi_\mu^\mu - \Pi_L] \\ &= \frac{1}{2} \left[-m_D^2 - \frac{m_D^2 P^2}{p^2} \left(1 - \frac{\omega}{2p} \ln \frac{\omega + p}{\omega - p} \right) \right] \\ &= -\frac{m_D^2 \omega^2}{2p^2} \left[1 + \frac{p^2 - \omega^2}{2\omega p} \ln \frac{\omega + p}{\omega - p} \right].\end{aligned}\quad (9.110)$$

The photon self-energies in (9.109) and (9.110) in HTL approximation can also be derived from the Vlasov equation, i.e., a transport equation without collision term considering a mean field. The only non-classical quantity, entering thereby, is Fermi-Dirac distribution for the electrons and positrons. The photon self-energy is obtained via the dielectric constants [86–88] which follow from the solution of the Vlasov equation for the distribution function assuming a small derivation from equilibrium [89]. The coincidence of the self-energy, found in the HTL approximation with the one in Vlasov equation is caused by the equivalence of high temperature limit, $T \rightarrow \infty$, and the classical limit, $\hbar \rightarrow 0$. As a matter of fact Silin [90] had found in 1960 the results given in (9.109) and (9.110) for studying the properties of a relativistic but classical electromagnetic plasma.

We now note that in the IR limit ($\omega \rightarrow 0$), one gets can also be derived from

$$\lim_{\omega \rightarrow 0} \Pi_L(\omega, p) = \lim_{\omega \rightarrow 0} -\frac{P^2}{p^2} \Pi_{00}(\omega, p) = -m_D^2, \quad (9.111a)$$

$$\lim_{\omega \rightarrow 0} \Pi_T(\omega, p) = 0. \quad (9.111b)$$

In QED the (9.111a) is the Debye electric screening mass of photon acts as a IR regulator at the static electric scale ($\sim eT$). On the other hand (9.111b) indicates that there is no screening for magnetic fields in QED as the 1-loop photon transverse self-energy in leading order HTL approximation vanishes in the IR limit and provides no magnetic screening mass for photon as it is a nonperturbative effect which can not be calculated perturbatively [91, 92].

9.10 Dispersion Relation and Collective Excitations of Photon in HTL Approximation

Now we can find the dispersion relations of photon using the thermal propagator given in (8.44). The poles of the propagator give the dispersion relations of photon in thermal medium

and one needs to solve the following equations:

$$P^2 + \Pi_L = 0 \implies \omega^2 - p^2 + \frac{P^2 m_D^2}{p^2} \left[1 - \frac{\omega}{2p} \ln \frac{\omega + p}{\omega - p} \right] = 0, \quad (9.112a)$$

$$P^2 + \Pi_T = 0 \implies \omega^2 - p^2 - \frac{m_D^2 \omega^2}{2} \frac{1}{p^2} \left[1 + \frac{p^2 - \omega^2}{2\omega p} \ln \frac{\omega + p}{\omega - p} \right] = 0. \quad (9.112b)$$

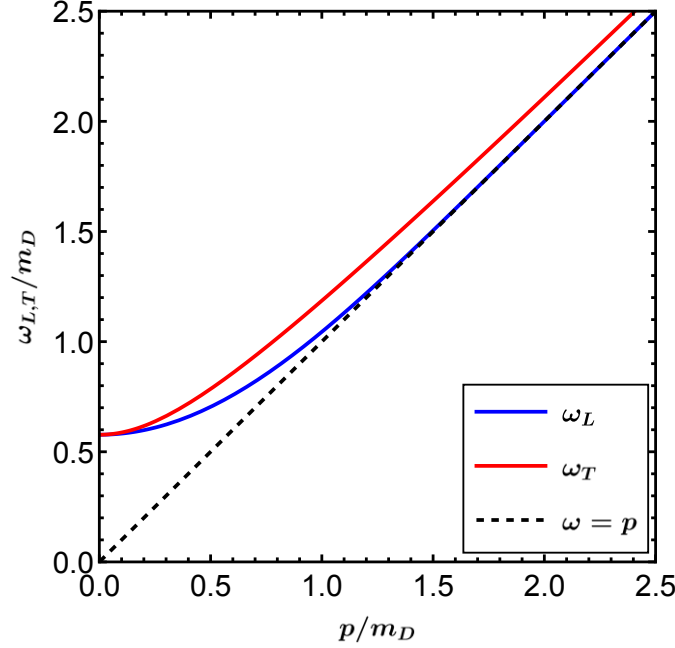


Figure 29: Dispersion of photon in heat bath.

The first condition in (9.112a) gives the longitudinal mode of propagation with energy ω_L known as plasmon and the second condition in (9.112b) gives the transverse mode with energy ω_T , which is doubly degenerate as evident from (8.16d). The plasmon mode with energy ω_L is a long wavelength mode that arises solely due to the presence of the thermal medium. The dispersion relations for photon at one loop are plotted in Fig 29. Energy of photon splits in two modes due to the presence of a thermal medium. The longitudinal one with energy ω_L is a long wavelength mode which reduces to free dispersion very fast than the transverse one with energy ω_T . The same behaviour was also found by Silin [90] for a relativistic but classical electromagnetic plasma using Vlasov equation. We further note that at large (hard) momentum the collective mode with energy ω_T resembles the transverse photon in vacuum whereas the long wave length mode, the plasmon with energy ω_L , decouples from the plasma. This is clearly evident from (9.114a) and (9.114b). At small momenta both collective modes are equally important which can be seen from (9.113a) and (9.113b).

Below we obtain approximate analytic solutions of $\omega_{L,T}$ for small and large values of

momentum. For small value of momentum ($p \ll m_D$),

$$\omega_L \approx \frac{m_D}{\sqrt{3}} \left[1 + \frac{9}{10} \frac{p^2}{m_D^2} - \frac{27}{280} \frac{p^4}{m_D^4} + \frac{9}{2000} \frac{p^6}{m_D^6} \right], \quad (9.113a)$$

$$\omega_T \approx \frac{m_D}{\sqrt{3}} \left[1 + \frac{9}{5} \frac{p^2}{m_D^2} - \frac{81}{35} \frac{p^4}{m_D^4} + \frac{792}{125} \frac{p^6}{m_D^6} \right]. \quad (9.113b)$$

For large value of momentum ($p \gg m_D$),

$$\omega_L \approx p + 2p \exp\left(-\frac{2(p^2 + m_D^2)}{m_D^2}\right), \quad (9.114a)$$

$$\omega_T \approx p + \frac{m_D^2}{P} + \frac{m_D^4}{32p^3} \left[3 - 2 \ln \frac{8p^2}{m_D^2} \right] + \frac{m_D^6}{128p^5} \left[2 \ln^2 \frac{8p^2}{m_D^2} - 10 \ln \frac{8p^2}{m_D^2} + 7 \right]. \quad (9.114b)$$

In addition to the pole contributions coming from time like domain $\omega^2 > p^2$ above the light cone, there is also a discontinuous part corresponding to Landau damping coming from space like domain $\omega^2 < p^2$ due to the presence of logarithmic terms in (9.109) and (9.110).

9.11 Spectral Representation of Gauge Boson Propagator

The effective propagator of a gauge boson in presence of thermal medium can be written from (8.44) as

$$D_{\mu\nu} = -\frac{\xi}{P^4} P_\mu P_\nu - \frac{1}{P^2 + \Pi_T} A_{\mu\nu} - \frac{1}{P^2 + \Pi_L} B_{\mu\nu}, \quad (9.115)$$

where

$$P^2 + \Pi_L = \omega^2 - p^2 + \frac{(\omega^2 - p^2)}{p^2} m_D^2 \left[1 - \frac{\omega}{2p} \ln \frac{\omega + p}{\omega - p} \right], \quad (9.116a)$$

$$P^2 + \Pi_T = \omega^2 - p^2 - \frac{m_D^2 \omega^2}{2} \left[1 + \frac{p^2 - \omega^2}{2\omega p} \ln \frac{\omega + p}{\omega - p} \right]. \quad (9.116b)$$

As discussed in subsec. 9.10 that $P^2 + \Pi_L = 0$ has solutions at $\omega = \pm\omega_L$ and $P^2 + \Pi_T = 0$ has solutions at $\omega = \pm\omega_T$. Both also have a cut part due to space like momentum $\omega^2 < p^2$. In-medium spectral function corresponding to the effective photon propagator in (9.115) will have both pole and cut contribution as

$$\rho_L(\omega, p) = \rho_L^{\text{pole}}(\omega, p) + \rho_L^{\text{cut}}(\omega, p), \quad (9.117a)$$

$$\rho_T(\omega, p) = \rho_T^{\text{pole}}(\omega, p) + \rho_T^{\text{cut}}(\omega, p). \quad (9.117b)$$

The pole part of the longitudinal spectral function can be obtained using (A.11) as

$$\begin{aligned} \rho_L^{\text{pole}}(\omega, p) &= \lim_{\epsilon \rightarrow 0} \frac{1}{\pi} \text{Im} \frac{1}{P^2 + \Pi_L} \Big|_{\omega \rightarrow \omega + i\epsilon} \\ &= \frac{\delta(\omega - \omega_L)}{\left| \frac{d}{d\omega}(P^2 + \Pi_L) \right|_{\omega=\omega_L}} + \frac{\delta(\omega + \omega_L)}{\left| \frac{d}{d\omega}(P^2 + \Pi_L) \right|_{\omega=-\omega_L}} \\ &= \frac{\omega}{p^2 + m_D^2 - \omega^2} [\delta(\omega - \omega_L) + \delta(\omega + \omega_L)]. \end{aligned} \quad (9.118)$$

Similarly, the pole part corresponding to the transverse spectral function can be obtained using (A.11) as

$$\begin{aligned}
\rho_T^{\text{pole}}(\omega, p) &= \lim_{\epsilon \rightarrow 0} \frac{1}{\pi} \text{Im} \frac{1}{P^2 + \Pi_T} \Big|_{\omega \rightarrow \omega + i\epsilon} \\
&= \frac{\delta(\omega - \omega_T)}{\left| \frac{d}{d\omega}(P^2 + \Pi_T) \right|_{\omega=\omega_T}} + \frac{\delta(\omega + \omega_T)}{\left| \frac{d}{d\omega}(P^2 + \Pi_T) \right|_{\omega=-\omega_T}} \\
&= \frac{\omega(\omega^2 - p^2)}{m_D^2 \omega^2 + p^2(\omega^2 - p^2)} [\delta(\omega - \omega_T) + \delta(\omega + \omega_T)]. \tag{9.119}
\end{aligned}$$

For $\omega^2 < p^2$, there is a discontinuity in $\ln \frac{\omega+p}{\omega-p}$ as $\ln y = \ln |y| - i\pi$, which leads to the spectral function, $\rho_{L,T}^{\text{cut}}(\omega, p)$, corresponding to the discontinuity in $P^2 + \Pi_{L,T}$. The cut contribution to the longitudinal spectral function can be obtained using (A.9) as

$$\begin{aligned}
\rho_L^{\text{cut}}(\omega, p) &= \frac{1}{2\pi i} \text{Disc} \frac{1}{P^2 + \Pi_L} \\
&= \frac{1}{\pi} \lim_{\epsilon \rightarrow 0} \text{Im} \frac{1}{P^2 + \Pi_L} \Big|_{\substack{\omega \rightarrow \omega + i\epsilon \\ \omega < p}} \\
&= \frac{(1-x^2)x m_D^2 \Theta(1-x^2)/2}{\left[p^2(x^2-1) + (x^2-1)m_D^2 - (x^2-1)x \frac{m_D^2}{2} \ln \left| \frac{x+1}{x-1} \right| \right]^2 + \left[\pi(x^2-1)x \frac{m_D^2}{2} \right]^2} \\
&= \beta_L(x) \Theta(1-x^2), \tag{9.120}
\end{aligned}$$

where $x = \omega/p$. Similarly, the cut part of the transverse spectral function can be obtained using (A.9) as

$$\begin{aligned}
\rho_T^{\text{cut}}(\omega, p) &= \frac{1}{2\pi i} \text{Disc} \frac{1}{P^2 + \Pi_T} \\
&= \frac{1}{\pi} \lim_{\epsilon \rightarrow 0} \text{Im} \frac{1}{P^2 + \Pi_T} \Big|_{\substack{\omega \rightarrow \omega + i\epsilon \\ \omega < p}} \\
&= \frac{(x^2-1)x m_D^2 \Theta(1-x^2)/4}{\left[p^2(x^2-1) - \frac{m_D^2}{2} \left(x^2 - \frac{(x^2-1)x}{2} \ln \left| \frac{x+1}{x-1} \right| \right) \right]^2 + \left[\pi(x^2-1)x \frac{m_D^2}{4} \right]^2} \\
&= \beta_T(x) \Theta(1-x^2). \tag{9.121}
\end{aligned}$$

10 Quantum Chromodynamics (QCD)

QCD is the theory of strong interaction which is a non-abelian $SU(3)$ gauge theory. It describes the quarks and gluons in the similar way as QED does for electrons and photons. The major difference between the two theories is that QCD contains three colour charges in fundamental representation. So, a quark can be represented by a vector with three colour states. The gauge field known as gluon mediates the interaction of colour charges. The special unitary group $SU(3)$ has $3^2 - 1 = 8$ generators, the number of charge mediating particles, corresponding to eight gluons in QCD.

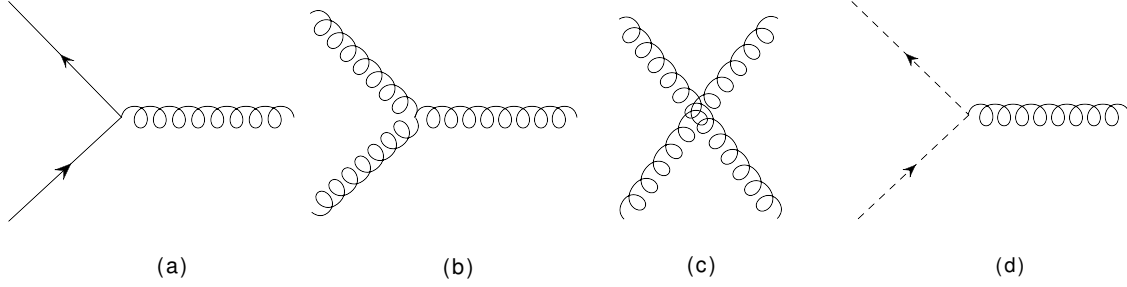


Figure 30: The QCD vertices. (a) quark-gluon interaction, (b) three gluon interaction, (c) four gluon interaction and (d) ghost-gluon interaction.

10.1 QCD Lagrangian

The QCD Lagrangian [72, 73] is written as

$$\mathcal{L}_{\text{QCD}} = \bar{\psi}_{ab}(i\not{D} - m_q)\psi_{ab} - g(\bar{\psi}_{ab}\lambda_i\psi_{ab})A^i - \frac{1}{4}G_{\mu\nu}^i G_i^{\mu\nu} + \mathcal{L}_{\text{gf}} + \mathcal{L}_{\text{gh}}. \quad (10.1)$$

We note that ψ_{ab} is quark spinor with colour indices $a = (r, g, b)$ and b indicates the flavour index. The Lagrangian in (10.1) is quite similar to QED Lagrangian in (9.31), with the differences that the electromagnetic field strength tensor $F^{\mu\nu}$, is replaced by the gluonic field strength tensor $G_{\mu\nu}^i$ and an another set of indices has crept in. The first term represents the non-interacting quarks with current mass m_q . The second term represents quark-gluon interaction with QCD coupling g and shown in Fig. 30(a). The Gell-Mann matrices λ_i were not there in QED. λ_i matrices change the colour of the interacting particles. These matrices are traceless and obey the commutation relation $[\lambda_i, \lambda_j] = i\varepsilon^{ijk}\lambda_k$ with normalisation relation $\text{Tr}\lambda_i\lambda_j = 2\delta_{ij}$, ε^{ijk} is the structure constant of the group which is number. It is also totally antisymmetric and vanishes if two of the indices become same. Now, $G_{\mu\nu}^i$ indicates the gluon fields which is invariant under gauge transformation and can be defined as

$$G_i^{\mu\nu} = F_i^{\mu\nu} + g\varepsilon_{ijk}A_j^\mu A_k^\nu, \quad (10.2)$$

where first term is the QED field tensor and the second term represents the self interaction of gluons. In contrast to QED, the mediator gluons have colour charge which enable them to interact among themselves. Now the gluonic part of the Lagrangian can be written as

$$\mathcal{L}_G = -\frac{1}{4}G_{i\mu\nu}G_i^{\mu\nu} = -\frac{1}{4}F_{i\mu\nu}F_i^{\mu\nu} + g\varepsilon_{ijk}A_{i\mu}A_{j\nu}\partial^\mu A_k^\nu - \frac{1}{4}g^2\varepsilon_{ijk}\varepsilon_{ilm}A_j^\mu A_k^\nu A_{l\mu}A_{m\nu}. \quad (10.3)$$

The first term in (10.3) describes the Lagrangian for eight non-interacting, massless spin 1 gluon fields. The second and third term, respectively, in (10.3) describe the self interactions of gluon fields. This produces three- and four-point vertices in perturbation theory, displayed in Fig. 30(b) and Fig. 30(c), respectively. The last two features have no analogue in QED, as photons do not self interact.

Finally, the gauge fixing and ghost terms [73] are, respectively, given as

$$\mathcal{L}_{\text{gf}} = -\frac{1}{2\xi}(\partial_\mu A_a^\mu)^2, \quad (10.4a)$$

$$\mathcal{L}_{\text{gh}} = -\bar{C}_i \partial^2 C_i - g \varepsilon_{ijk} \bar{C}_i \partial_\mu (A_j^\mu C_k), \quad (10.4b)$$

where C is the ghost field which are Grassmann variable. The gauge fixing Lagrangian in (10.4a) is required to eliminate the unphysical degrees of freedom present in the system. The ghost Lagrangian in covariant gauge is given in (10.4b) which depends on the choice of the gauge fixing term. The first term in (10.4b) represents free ghost fields whereas the second term indicates interaction between ghost and gluon as shown in Fig. 30(d)

We note that the previous discussion on QED in sec. 9.9 in HTL approximation would provide a good starting point for QCD, since these two theories follow the similar formalism. We know that QCD is a non-Abelian $SU(3)$ gauge theory whereas QED is a $U(1)$ gauge theory. Thus, the generalization of QED results to QCD would mostly involve group-theoretical factors as we will see below.

10.2 One-loop Gluon Self-energy in HTL Approximation

We calculate the one-loop gluon self-energy [14, 77, 79, 83] and the relevant diagrams are given in Fig. 31. The contribution of the first diagram (tadpole) in HTL approximation can be written as

$$\Pi_{\mu\nu}^{(a)}(P) = -3C_A g^2 \delta_{\mu\nu} \int \frac{d^4 K}{(2\pi)^4} \Delta_B(K), \quad (10.5)$$

where g is the strong or QCD coupling constant, $C_A (= 3)$ is the group factor and Δ_B is the bosonic part of the propagator.

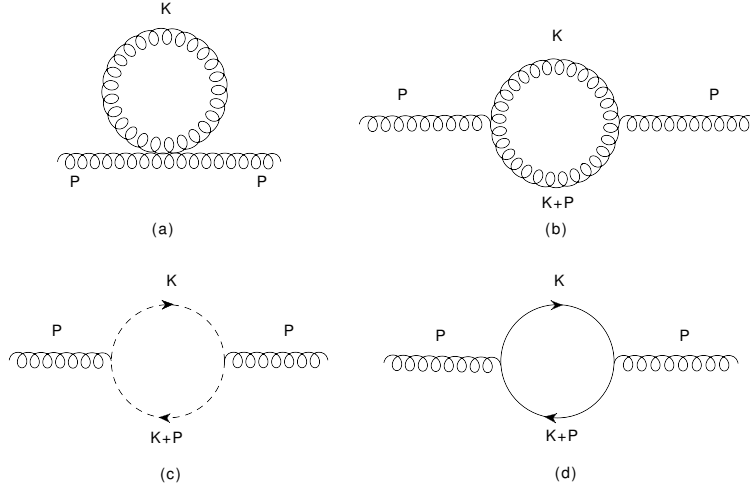


Figure 31: One-loop gluon self-energy diagrams.

The contribution of the second diagram (gluon loop) in HTL approximation is obtained as

$$\Pi_{\mu\nu}^{(b)}(P) = g^2 C_A \int \frac{d^4 K}{(2\pi)^4} 5K_\mu K_\nu \Delta_B(K) \Delta_B(K+P) + g^2 C_A \delta_{\mu\nu} \int \frac{d^4 K}{(2\pi)^4} \Delta_B(K). \quad (10.6)$$

The contribution of the third diagram (ghost loop) can be obtained as

$$\Pi_{\mu\nu}^{(c)}(P) = -g^2 C_A \int \frac{d^4 K}{(2\pi)^4} K_\mu K_\nu \Delta_B(K) \Delta_B(K+P). \quad (10.7)$$

Combining these three diagrams, one can write

$$\begin{aligned} \Pi_{\mu\nu}^{(a+b+c)}(P) &= 4g^2 C_A \int \frac{d^4 K}{(2\pi)^4} K_\mu K_\nu \Delta_B(K) \Delta_B(K+P) - 2g^2 C_A \delta_{\mu\nu} \int \frac{d^4 K}{(2\pi)^4} \Delta_B(K) \\ &\approx g^2 C_A \int \frac{d^4 K}{(2\pi)^4} [4K_\mu K_\nu - 2K^2 \delta_{\mu\nu}] \Delta_B(K) \Delta_B(K+P), \end{aligned} \quad (10.8)$$

where we have used in the last step as $\Delta_B(K+P) = 1/(K+P)^2 \approx 1/K^2$.

Now the contribution of the fourth diagram (quark loop) can be obtained similar to QED in (9.99) as

$$\Pi_{\mu\nu}^{(d)}(P) = -g^2 \frac{N_f}{2} \int \frac{d^4 K}{(2\pi)^4} [8K_\mu K_\nu - 4K^2 \delta_{\mu\nu}] \Delta_F(K) \Delta_F(K+P), \quad (10.9)$$

where N_f is the number of quark flavour. We note that one can go from fermionic loop to bosonic loop by the following transformations:

$$\int \frac{d^4 K}{(2\pi)^4} \Delta_F(K) = -\frac{1}{2} \int \frac{d^4 K}{(2\pi)^4} \Delta_B(K), \quad (10.10a)$$

$$\int \frac{d^4 K}{(2\pi)^4} \Delta_F(K) \Delta_F(K+P) = -\frac{1}{2} \int \frac{d^4 K}{(2\pi)^4} \Delta_B(K) \Delta_B(K+P). \quad (10.10b)$$

Using (10.10b), one can write (10.9) as

$$\Pi_{\mu\nu}^{(d)}(P) = g^2 \frac{N_f}{2} \int \frac{d^4 K}{(2\pi)^4} [4K_\mu K_\nu - 2K^2 \delta_{\mu\nu}] \Delta_B(K) \Delta_B(K+P), \quad (10.11)$$

Now the contributions of all four diagrams in gluon self energy can be written by combining (10.8) and (10.11) as

$$\Pi_{\mu\nu}^{(a+b+c+d)}(P) = g^2 \left(C_A + \frac{N_f}{2} \right) \int \frac{d^4 K}{(2\pi)^4} [4K_\mu K_\nu - 2K^2 \delta_{\mu\nu}] \Delta_B(K) \Delta_B(K+P). \quad (10.12)$$

The photon self-energy can be written from (9.99) as

$$\Pi_{\mu\nu}(P) = -e^2 \int \frac{d^4 K}{(2\pi)^4} [8K_\mu K_\nu - 4K^2 \delta_{\mu\nu}] \Delta_F(K) \Delta_F(K+P), \quad (10.13)$$

Using (10.10b), one gets

$$\Pi_{\mu\nu}(P) = e^2 \int \frac{d^4 K}{(2\pi)^4} [4K_\mu K_\nu - 2K^2 \delta_{\mu\nu}] \Delta_B(K) \Delta_B(K+P), \quad (10.14)$$

Now the only difference between (10.12) and (10.14) is the overall factor. From QED to QCD or photon to gluon, one changes

$$e^2 \Rightarrow g^2 \left(C_A + \frac{N_f}{2} \right). \quad (10.15)$$

With this one can transform QED Debye mass in (9.104) to QCD Debye mass as

$$\frac{e^2 T^2}{3} \Rightarrow \frac{g^2 T^2}{3} \left(C_A + \frac{N_f}{2} \right) = m_D^2 : \quad \text{QCD Debye mass.} \quad (10.16)$$

Therefore, we note that the HTL self-energies of photon given in (9.108), (9.109) and (9.110) will be same for gluons with the replacement of Debye mass m_D^2 for QCD as given in (10.16). We further note that in the IR limit the gluon transverse self-energy in leading order in HTL vanishes implying there is no magnetic screening in QCD and provides no magnetic screening mass for gluons. This is a nonperturbative effect which can not be calculated perturbatively [91, 92]. However, the longitudinal component of gluon self-energy in the IR limit becomes m_D^2 which acts as a IR regulator in the static electric scale.

We also note that the collective excitations of gluons is same as photons which are displayed in Fig. 29.

10.3 One-loop Quark Self-energy in HTL Approximation

The evaluation of quark self-energy at one-loop order is even simpler. This is because there is only one diagram which is similar to Fig. 26 where the internal photon line is to be replaced by gluon line. The one loop quark self-energy can be written as

$$\begin{aligned} \Sigma(P)\delta_{ij} &= T \sum_{\{K\}} (-ig\gamma_\mu(\lambda^a)_{ik}) \frac{i\hat{K}}{K^2} (-ig\gamma^\mu(\lambda^a)_{kj}) \frac{i}{(P-K)^2} \\ &= g^2 C_F \delta_{ij} T \sum_{\{K\}} \gamma_\mu \frac{\hat{K}}{K^2} \gamma^\mu \frac{1}{(P-K)^2}, \end{aligned} \quad (10.17)$$

where we have used the identity $(\lambda^a \lambda^a)_{ij} = \frac{N_c^2-1}{2N_c} \delta_{ij} = C_F \delta_{ij}$ with $N_c = 3$. After performing the frequency sum and k -integration as done in subsec. 9.6, the quark self-energy becomes

$$\Sigma(P) = \frac{g^2 T^2}{8} C_F \int \frac{d\Omega}{4\pi} \frac{\hat{K}}{P \cdot \hat{K}}. \quad (10.18)$$

The electron self-energy is obtained in (9.85)

$$\Sigma(P) = \frac{e^2 T^2}{8} \int \frac{d\Omega}{4\pi} \frac{\hat{K}}{P \cdot \hat{K}}. \quad (10.19)$$

The only difference between (10.19) and (10.18) is overall group factor as $C_F = 1$ for $U(1)$ gauge theory whereas $C_F = 4/3$ for $SU(3)$ gauge theory. So one obtains QCD results for quark by generalizing the QED results of electron by replacing

$$e^2 \Rightarrow g^2 C_F. \quad (10.20)$$

With this one can transform electron thermal mass in (9.73) to quark thermal mass as

$$\frac{e^2 T^2}{8} \Rightarrow \frac{g^2 T^2}{8} C_F = \frac{g^2 T^2}{8} \times \frac{4}{3} = \frac{g^2 T^2}{6} = m_{\text{th}}^2 : \quad \text{quark thermal mass in QCD.} \quad (10.21)$$

Now the expression for electron self-energy given in (9.85) and (9.86) will be same for quark self-energy with the replacement of electron thermal mass ($e^2 T^2/8$) by quark thermal mass ($g^2 T^2/6$) as given in (10.21). Also the structure constants appearing in the general structure of fermion self-energy and propagator need to be replaced by quark thermal mass to study the collective excitations of quark in thermal medium, which are same as electrons displayed in Fig. 27.

Therefore, we learn about the collective excitations in a QCD plasma from the acquired knowledge of QED plasma excitations by replacing the QED Debye mass and electron thermal mass by QCD Debye mass in (10.16) and quark thermal mass in (10.21), respectively, in photon self-energy, effective photon propagator, electron self-energy and effective electron propagator.

11 Subtleties in Finite Temperature Field Theory

Let us start by introducing the parametric scales appearing in finite temperature field theory. The periodicity or anti-periodicity over Euclidean time introduces a scale present in the non-interacting theory where momentum, $p \sim 2\pi T$, known as hard scale and the bosonic zero modes do not acquire any scale in the non-interacting theory. As we have seen in previous sections that interaction introduces softer scales corresponding to collective excitations in the thermal medium. In particular, scalar fields and the electric component of gauge fields are screened in Debye scale where momentum, $p \sim gT$. On the other hand, the magnetic component of gauge field is screened only non-perturbatively [91, 92] at the scale where momentum, $p \sim g^2 T$, known as the ultra-soft scale or non-perturbative magnetic scale.

There is an expansion parameter related to bosonic fluctuations with momentum (or mass) scale p of the form

$$\epsilon_b \sim \frac{1}{\pi} g^2 (2\pi T) n_B(p) = \frac{g^2 (2\pi T)}{\pi (e^{p/T} - 1)} \stackrel{p \ll T}{\sim} \frac{g^2 (2\pi T) T}{\pi p}. \quad (11.1)$$

Thus, for the hard scale: $p \sim 2\pi T$, the expansion parameter becomes a series in $\sim g^2/\pi^2$, the even power of g like $T = 0$ case. For soft (electric) scale, $p \sim gT$, the series becomes $\sim g/\pi$. For ultra-soft (magnetic) scale $\sim g^2 T$, there is no perturbative series at all [91, 92] and it has to be determined non-perturbatively. Therefore, at very high temperature compared to any

intrinsic mass scale of a given theory and the coupling g is less than unity, there appears a hierarchy of momentum (mass) scales in the system and there are three distinct scales: hard, soft (electric) and ultra-soft (magnetic).

In naive perturbation theory, both static and dynamic quantities can be computed by expanding in coupling constant around the free theory. This works in hard scale regime that uses free propagators and vertices, and the contribution appears in even power of coupling (g^{2n}) as discussed above. However, the naive application of perturbation theory would in most cases result in infrared⁷ and/or collinear singularities, and some cases gauge dependent results. It is to be noted that the infrared problems are associated with bosonic excitations but not with fermionic excitations as the fermionic expansion parameter remains finite for $p < T$. These in turn signal sensitivity to soft region ($p \sim gT$) of the phase space, where naive perturbation theory breaks down. This breakdown corresponds to the emergence of collective effects, arising from the dynamics of the thermal medium as discussed in previous sections. In the soft (electric) scale $\sim gT$, for which perturbation theory in principle works, does not exist in non-interacting theory but needs to be generated. This means that the perturbation theory needs to be resummed or re-organised. This is done through the effective field theory like the hard thermal loop (HTL) resummation [78, 93–97] techniques and thereby HTL perturbation theory (HTLpt) [98–104].

12 Hard Thermal Loop (HTL) Resummation and HTL Perturbation Theory

12.1 HTL Resummation

As discussed in sec. 11 that the naive perturbation theory suffers from infrared and/or collinear singularities and gauge dependence results of some quantities. This is because certain classes of diagrams were not considered in naive perturbation theory which are higher order in the loop expansion that contribute to the same order in the coupling constant as the one loop diagram [78]. These diagrams can be identified through the scale separation as discussed below.

Considering the loop momenta to be hard ($\sim 2\pi T$), the amplitude for higher-order loop diagrams [78] can be written through power counting as

$$\sim \frac{g^2 T^2}{P^2} \times \text{Tree level amplitude}, \quad (12.1)$$

where P is the external momentum. If the external momentum is hard, $P \sim 2\pi T$, then the amplitude is suppressed by g^2 of its tree level amplitude. If the external momentum is soft, $P \sim gT$ then the amplitude becomes equivalent to tree level amplitude. This indicates that diagrams of higher order in loop expansion contribute to same order in coupling as the one-loop by distinguishing the hard ($\sim 2\pi T$) arising from loop momenta and soft scale ($\sim gT$)

⁷singularities from both electric and magnetic sectors.

from external momenta. Therefore, one needs to take into account those diagrams if the external momentum is sensitive to the soft(electric) scale. The effective theory built around hard thermal loops resums those diagrams. This is as illustrated below:

1. One can resum those HTL diagrams in geometrical series through the effective propagators and vertices in one loop as done in subsections 7.2 and 8.4. They are related by the Ward-Takahashi identity in QED and by the Slanov-Taylor identity in QCD.
2. At the same time medium effects: *viz.*, the electric screening mass, the thermal mass, the collective behaviour of quasiparticles and the Landau damping, are taken into account due to resummations. The effective N -point functions can be used in perturbation theory leading to an effective perturbation theory known as HTL perturbation theory (HTLpt) which will be discussed in subsec 12.2. This effective perturbation theory leads to gauge independent results and also complete in certain order of the coupling.
3. In scalar field theory the infrared problems are cured due to appropriate resummations which take into account the presence of the electric screening (Debye) mass of order gT . In gauge theories like QED and QCD, the IR singularities are improved due to electric scale. But there exists also another sort of infrared problems associated with static magnetic fields. Static magnetic fields are not screened at leading order in HTL because the 1-loop transverse photon/gluon self-energy vanishes in all gauges in the infrared limit. Up to order g^5 , the quantities can be calculated using HTLpt that takes into account the screening of the chromoelectric scale but breaks down at g^6 order due to the absence of magnetic screening [91, 92].

Now we write down the HTL improved Lagrangian in non-Abelian gauge theory (QCD) [93–96] as

$$\mathcal{L}_{\text{HTL}} = im_{\text{th}}^2 \bar{\psi} \gamma^\mu \left\langle \frac{y_\mu}{y \cdot D} \right\rangle_y \psi - \frac{1}{2} m_D^2 \text{Tr} \left(G_{\mu\alpha} \left\langle \frac{y^\alpha y_\beta}{(y \cdot D)^2} \right\rangle_y G^{\mu\beta} \right), \quad (12.2)$$

where G is the gluon field strength, D is the covariant derivative, $y^\mu = (1, \hat{\mathbf{y}})$ is a light-like four-vector with $\hat{\mathbf{y}}$ = three-dimensional unit vector, and angular braces represent the average over the directions specified by $\hat{\mathbf{y}}$. The overall trace in the second term in (12.2) is for group indices. The two parameters m_D and m_{th} are, respectively, the Debye screening mass and the thermal quark mass which take into account the screening effects. The Lagrangian is non-local and gauge symmetric, which forces the presence of the covariant derivative in the denominator of (12.2), which makes it also non-linear. When expanded in powers of gauge field, (12.2) generates an infinite series of non-local self-energy and vertex corrections (*viz.*, HTL N -point functions). These N -point functions are related by Slanov-Taylor identity. Note that since diagrams with external ghost legs do not produce hard thermal loops, the ordinary ghost-gluon vertex remains the same. For details we refer to the review article in Ref. [57].

12.2 HTL perturbation Theory (HTLpt)

QCD Lagrangian density in Minkowski space can be written from (10.1) as

$$\mathcal{L}_{\text{QCD}} = \bar{\psi}_{ab} i \not{D} \psi_{ab} - g(\bar{\psi}_{ab} \lambda_i \psi_{ab}) A^i - \frac{1}{4} G_{\mu\nu}^i G_i^{\mu\nu} + \mathcal{L}_{\text{gf}} + \mathcal{L}_{\text{gh}} + \Delta\mathcal{L}_{\text{QCD}}, \quad (12.3)$$

where the counterterm $\Delta\mathcal{L}_{\text{QCD}}$ is necessary to cancel the ultraviolet (UV) divergences in perturbative calculations. HTLpt is a reorganization of thermal QCD perturbation theory. The HTLpt Lagrangian density [98–104] can be written as

$$\mathcal{L}_{\text{HTLpt}} = (\mathcal{L}_{\text{QCD}} + (1 - \delta)\mathcal{L}_{\text{HTL}})|_{g \rightarrow \sqrt{\delta}g} + \Delta\mathcal{L}_{\text{HTL}} \quad (12.4)$$

where $\Delta\mathcal{L}_{\text{HTL}}$ is additional counterterm needed to cancel the UV divergences generated in HTLpt. The HTL improved Lagrangian, \mathcal{L}_{HTL} is given in (12.2). HTLpt is defined by considering δ as a formal expansion parameter. By adding the HTL improvement term in (12.4) to the QCD Lagrangian in (12.3), HTLpt consistently shifts the perturbative expansion from an ideal gas of massless particles, to a gas of massive quasiparticles which are the more apt physical degrees of freedom at high temperature and chemical potential. It is worth here to mention that the HTLpt Lagrangian (12.4) becomes the QCD Lagrangian in (12.3) if one puts $\delta = 1$.

Physical quantities are computed in HTLpt through expansion in powers of δ , terminating at some specified order, and then putting $\delta = 1$. As mentioned before, this signifies a rearrangement of the perturbation series in which the screening effects through m_D^2 and m_{th}^2 terms in (12.4) have been considered to all orders but then systematically subtracted out at higher orders in perturbation theory by the δm_D^2 and δm_{th}^2 terms in (12.4). One usually expands to orders δ^0 , δ^1 , δ^2 , respectively, for computing leading order (LO), next-to-leading order (NLO), and next-to-next-leading order (NNLO) results. Note that HTLpt is gauge invariant order-by-order in the δ -expansion and, consequently, the results obtained would be gauge independent.

If the δ -expansion could be computed to all orders the results would not depend on m_D and m_{th} when one puts $\delta = 1$. However, any termination of the δ -expansion generates m_D and m_{th} dependent results. Therefore, a prescription is needed to determine m_D and m_{th} as a function of T , μ and α_s . There are several prescriptions and some of them had been discussed in [105] at zero chemical potential. The HTL perturbation expansion produces UV divergences. In QCD perturbation theory, renormalizability restricts the UV divergences in such a way that they can be eliminated by the counterterm Lagrangian $\Delta\mathcal{L}_{\text{QCD}}$. Usually the renormalization of HTLpt can be considered by adding a counterterm Lagrangian $\Delta\mathcal{L}_{\text{HTL}}$ in (12.4). However, there is no such proof yet that the HTLpt is renormalizable, so the general structure of the UV divergences remain unknown. The most optimistic scenario is that HTLpt would be renormalizable, such that the UV divergences in the physical observables can all be eliminated using proper counterterms.

The HTLpt has been used to study the various physical quantities relevant for understanding the properties of QGP, viz., the thermodynamic properties [74, 75, 98–114],

dilepton production rate [80, 115–120], photon production rate [121–127], single quark and quark-antiquark potentials [128–135], fermion damping rate [136, 137], photon damping rate [138, 139], gluon damping rate [140, 141] and parton energy-loss [88, 142–145].

12.3 One-loop Quark Free Energy in HTLpt

In thermal field theory the partition function is defined by a functional determinant of the inverse propagator and by which the quark part of the free energy density in one-loop order at the leading order in the δ -expansion can be written from Fig. 32 as

$$F_q^{1\text{-loop}} = -N_c N_f \int \frac{d^4 P}{(2\pi)^4} \ln (\det [S^{*-1}(P)]), \quad (12.5)$$

where $P \equiv (p_0, \vec{p})$ is the four momentum with $p = |\vec{p}|$, N_c is number of colour and N_f is

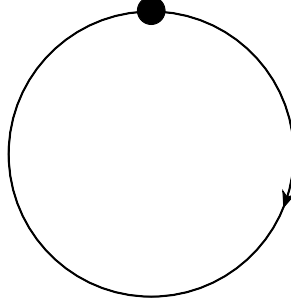


Figure 32: one-loop quark contribution to free energy density.

number of flavour. For ideal gas of quarks the $\det [S^{*-1}(P)] = P^4$ as obtained in (6.74) and the free energy density reads as

$$\begin{aligned} F_q^{\text{ideal}} &= -2N_c N_f \int \frac{d^4 P}{(2\pi)^4} \ln (P^2) \\ &= -2N_c N_f \sum_{\{P\}}^f \ln(P^2) \\ &= -\frac{7\pi^2 T^4}{180} N_c N_f \left(1 + \frac{120}{7} \hat{\mu}^2 + \frac{240}{7} \hat{\mu}^4 \right), \end{aligned} \quad (12.6)$$

where $\hat{\mu} = \mu/2\pi T$.

Now, the effective quark propagator is given in (7.21) as

$$\begin{aligned} S^{*-1}(P) &= \not{P} - \Sigma(P) \\ &= \frac{1}{2}(\gamma_0 + \vec{\gamma} \cdot \hat{\mathbf{p}}) \mathcal{D}_+ + \frac{1}{2}(\gamma_0 - \vec{\gamma} \cdot \hat{\mathbf{p}}) \mathcal{D}_- \\ &= \gamma_0 p_0 \mathcal{C} - \vec{\gamma} \cdot \vec{p} \mathcal{D}, \end{aligned} \quad (12.7)$$

where

$$\mathcal{C} = \frac{1}{2p_0} (\mathcal{D}_+ + \mathcal{D}_-) , \quad (12.8a)$$

$$\mathcal{D} = \frac{1}{2p} (\mathcal{D}_- - \mathcal{D}_+) . \quad (12.8b)$$

Using (7.16) one can have

$$\mathcal{C} = 1 + \mathcal{A} + \frac{\mathcal{B}}{p_0} = 1 - \mathcal{A}' , \quad (12.9a)$$

$$\mathcal{D} = 1 + \mathcal{A} . \quad (12.9b)$$

where

$$\mathcal{A}' = -\mathcal{A} - \frac{\mathcal{B}}{p_0} . \quad (12.10)$$

From (9.72) we get structure constant \mathcal{A} as

$$\mathcal{A}(p_0, p) = -\frac{m_{\text{th}}^2}{p^2} \int \frac{d\Omega}{4\pi} \frac{\vec{p} \cdot \hat{\mathbf{k}}}{P \cdot \hat{K}} = \frac{m_{\text{th}}^2}{p^2} [1 - \mathcal{T}_P] , \quad (12.11)$$

where

$$\mathcal{T}_P = \int \frac{d\Omega}{4\pi} \frac{p_0}{p_0 - \vec{p} \cdot \hat{\mathbf{k}}} , \quad (12.12)$$

and in presence of chemical potential μ the quark thermal mass of (9.73) can be written as

$$m_{\text{th}}^2 = \frac{g^2 T^2 C_F}{8} (1 + 4\hat{\mu}^2) . \quad (12.13)$$

Using (12.11) and (9.81) one can write (12.10) as

$$\mathcal{A}' = \frac{m_{\text{th}}^2}{p_0^2} \int \frac{d\Omega}{4\pi} \frac{p_0}{p_0 - \vec{p} \cdot \hat{\mathbf{k}}} = \frac{m_{\text{th}}^2}{p_0^2} \mathcal{T}_P . \quad (12.14)$$

Similarly, one obtains

$$\mathcal{C} = 1 - \frac{m_{\text{th}}^2}{p_0^2} \mathcal{T}_P , \quad (12.15a)$$

$$\mathcal{D} = 1 + \frac{m_{\text{th}}^2}{p^2} [1 - \mathcal{T}_P] . \quad (12.15b)$$

Now we calculate the $\det(S^{*-1})$:

$$\begin{aligned} \det(S^{*-1}) &= \det(\gamma_0 p_0 \mathcal{C} - \vec{\gamma} \cdot \vec{p} \mathcal{D}) \\ &= \det \left\{ \begin{bmatrix} p_0 \mathcal{C} & 0 \\ 0 & -p_0 \mathcal{C} \end{bmatrix} + \mathcal{D} \begin{bmatrix} 0 & \vec{\sigma} \cdot \vec{p} \\ -\vec{\sigma} \cdot \vec{p} & 0 \end{bmatrix} \right\} \\ &= \det \begin{bmatrix} p_0 \mathcal{C} & \mathcal{D} (\vec{\sigma} \cdot \vec{p}) \\ -\mathcal{D} (\vec{\sigma} \cdot \vec{p}) & -p_0 \mathcal{C} \end{bmatrix} . \end{aligned} \quad (12.16)$$

We know

$$\begin{aligned}
\vec{\sigma} \cdot \vec{p} &= \sigma_x p_x + \sigma_y p_y + \sigma_z p_z \\
&= \begin{bmatrix} 0 & p_x \\ p_x & 0 \end{bmatrix} + \begin{bmatrix} 0 & ip_y \\ -ip_y & 0 \end{bmatrix} + \begin{bmatrix} p_z & 0 \\ 0 & -p_z \end{bmatrix} \\
&= \begin{bmatrix} p_z & p_x + ip_y \\ p_x - ip_y & -p_z \end{bmatrix}.
\end{aligned} \tag{12.17}$$

Using (12.17) in (12.16) one can write

$$\begin{aligned}
\det(S^{*-1}) &= \det \begin{bmatrix} p_0 \mathcal{C} & 0 & -\mathcal{D}p_z & -\mathcal{D}(p_x + ip_y) \\ 0 & p_0 \mathcal{C} & -\mathcal{D}(p_x - ip_y) & \mathcal{D}p_z \\ \mathcal{D}p_z & \mathcal{D}(p_x + ip_y) & -p_0 \mathcal{C} & 0 \\ \mathcal{D}(p_x - ip_y) & -\mathcal{D}p_z & 0 & -p_0 \mathcal{C} \end{bmatrix} \\
&= \left\{ p_0 \mathcal{C} \begin{vmatrix} p_0 \mathcal{C} & -\mathcal{D}(p_x - ip_y) & \mathcal{D}p_z \\ \mathcal{D}(p_x + ip_y) & -p_0 \mathcal{C} & 0 \\ -\mathcal{D}p_z & 0 & -p_0 \mathcal{C} \end{vmatrix} - \mathcal{D}p_z \begin{vmatrix} 0 & p_0 \mathcal{C} & \mathcal{D}p_z \\ \mathcal{D}p_z & \mathcal{D}(p_x + ip_y) & 0 \\ \mathcal{D}(p_x - ip_y) & -\mathcal{D}p_z & -p_0 \mathcal{C} \end{vmatrix} \right. \\
&\quad \left. + \mathcal{D}(p_x + ip_y) \begin{vmatrix} 0 & p_0 \mathcal{C} & -\mathcal{D}(p_x - ip_y) \\ \mathcal{D}p_z & \mathcal{D}(p_x + ip_y) & -p_0 \mathcal{C} \\ \mathcal{D}(p_x - ip_y) & -\mathcal{D}p_z & 0 \end{vmatrix} \right\} \\
&= p_0^2 \mathcal{C}^4 - p_0^2 p^2 \mathcal{C}^2 \mathcal{D}^2 - p_0^2 p_z^2 \mathcal{C}^2 \mathcal{D}^2 + p_z^2 p^2 \mathcal{D}^4 - p_0^2 (p_x^2 + p_y^2) \mathcal{C}^2 \mathcal{D}^2 + (p_x^2 + p_y^2) p^2 \mathcal{D}^2 \\
&= (p_0^2 \mathcal{C}^2 - p^2 \mathcal{D}^2)^2.
\end{aligned} \tag{12.18}$$

Using (12.15a) and (12.15b), we get

$$\begin{aligned}
\det(S^{*-1}) &= \left[\left\{ p_0 - \frac{m_{\text{th}}^2}{p_0} \mathcal{T}_P \right\}^2 - \left\{ p + \frac{m_{\text{th}}^2}{p} (1 - \mathcal{T}_P) \right\}^2 \right]^2 \\
&= [A_0^2 - A_S^2]^2,
\end{aligned} \tag{12.19}$$

where

$$A_0 = p_0 - \frac{m_{\text{th}}^2}{p_0} \mathcal{T}_P, \tag{12.20a}$$

$$A_S = p + \frac{m_{\text{th}}^2}{p} (1 - \mathcal{T}_P). \tag{12.20b}$$

Combining (12.5) and (12.19), the one-loop quark free energy density in HTL approximation can be written as

$$\begin{aligned}
F_q^{1\text{-loop}} &= -N_c N_f \int \frac{d^4 P}{(2\pi)^4} \ln (A_0^2 - A_S^2)^2 = -2N_c N_f \int \frac{d^4 P}{(2\pi)^4} \ln (A_0^2 - A_S^2) \\
&= -2N_c N_f \int \frac{d^4 P}{(2\pi)^4} \ln (P^2) - 2N_c N_f \int \frac{d^4 P}{(2\pi)^4} \ln \left(\frac{A_0^2 - A_S^2}{P^2} \right).
\end{aligned} \tag{12.21}$$

Now the argument of the logarithm in the second term in (12.21) can be simplified using (12.20a) and (12.20b) as

$$\begin{aligned}
\frac{(A_0^2 - A_S^2)}{P^2} &= \frac{1}{P^2} \left[p_0^2 - 2m_{\text{th}}^2 \mathcal{T}_P + \frac{m_{\text{th}}^4}{p_0^2} \mathcal{T}_P^2 - p^2 - 2m_{\text{th}}^2(1 - \mathcal{T}_P) - \frac{m_{\text{th}}^4}{p^2} (1 - \mathcal{T}_P)^2 \right] \\
&= \frac{1}{P^2} \left[P^2 - 2p_0^2 \mathcal{A}' + p_0^2 \mathcal{A}'^2 - 2p^2 \mathcal{A} - p^2 \mathcal{A}^2 \right] \\
&= 1 + \left(\frac{\mathcal{A}'(\mathcal{A}' - 2)p_0^2 - \mathcal{A}(\mathcal{A} + 2)p^2}{P^2} \right), \tag{12.22}
\end{aligned}$$

where in the second line we have used (12.11) and (12.14). In the high temperature approximation, the logarithmic term in (12.21) can be expanded in a series of coupling constants g and then keeping terms up to $\mathcal{O}(g^4)$ one obtains

$$\begin{aligned}
\ln \left[\frac{(A_0^2 - A_S^2)}{P^2} \right] &= \frac{\mathcal{A}'^2 p_0^2 - \mathcal{A}^2 p^2 - 2\mathcal{A}' p_0^2 - 2\mathcal{A} p^2}{P^2} - 2 \frac{(\mathcal{A}' p_0^2 + \mathcal{A} p^2)^2}{P^4} + \mathcal{O}(g^6) \\
&= \frac{\mathcal{A}'^2 p_0^2 - \mathcal{A}^2 p^2}{P^2} - 2 \frac{\mathcal{A}' p_0^2 + \mathcal{A} p^2}{P^2} - 2 \frac{(\mathcal{A}' p_0^2 + \mathcal{A} p^2)^2}{P^4} + \mathcal{O}(g^6). \tag{12.23}
\end{aligned}$$

Using (12.11) and (12.14), we can obtain

$$(\mathcal{A}' p_0^2 + \mathcal{A} p^2) = m_{\text{th}}^2, \tag{12.24a}$$

$$(\mathcal{A}'^2 p_0^2 - \mathcal{A}^2 p^2) = m_{\text{th}}^4 \left[\frac{\mathcal{T}_P^2}{p_0^2} - \frac{(1 - \mathcal{T}_P)^2}{p^2} \right]. \tag{12.24b}$$

Now (12.23) becomes

$$\ln \left[\frac{(A_0^2 - A_S^2)}{P^2} \right] = -\frac{2m_{\text{th}}^2}{P^2} + m_{\text{th}}^4 \left[\frac{\mathcal{T}_P^2}{p_0^2 P^2} - \frac{2}{P^4} - \frac{1}{p^2 P^2} + \frac{2\mathcal{T}_P}{p^2 P^2} - \frac{\mathcal{T}_P^2}{p^2 P^2} \right]. \tag{12.25}$$

Using (12.25) in (12.21), the one-loop free energy density up to $\mathcal{O}(g^4)$ can be written as

$$\begin{aligned}
F_q^{\text{1-loop}} &= N_c N_f \left[-2 \int \frac{d^4 P}{(2\pi)^4} \ln(P^2) + 4m_{\text{th}}^2 \int \frac{d^4 P}{(2\pi)^4} \frac{1}{P^2} \right. \\
&\quad \left. - m_{\text{th}}^4 \int \frac{d^4 P}{(2\pi)^4} \left(\frac{2\mathcal{T}_P^2}{p_0^2 P^2} - \frac{4}{P^4} - \frac{2}{p^2 P^2} - \frac{2\mathcal{T}_P^2}{p^2 P^2} + \frac{4\mathcal{T}_P}{p^2 P^2} \right) \right] \\
&= N_c N_f \left[-2 \sum_{\{P\}} \ln(P^2) + 4m_{\text{th}}^2 \sum_{\{P\}} \frac{1}{P^2} \right. \\
&\quad \left. - m_{\text{th}}^4 \left(\sum_{\{P\}} \frac{2\mathcal{T}_P^2}{p_0^2 P^2} - \sum_{\{P\}} \frac{4}{P^4} - \sum_{\{P\}} \frac{2}{p^2 P^2} - \sum_{\{P\}} \frac{2\mathcal{T}_P^2}{p^2 P^2} + \sum_{\{P\}} \frac{4\mathcal{T}_P}{p^2 P^2} \right) \right]. \tag{12.26}
\end{aligned}$$

Using the sum-integrals of (A.2a) to (A.2g) given in appendix A.1, the one-loop quark free energy density becomes

$$\begin{aligned}
F_q^{1\text{-loop}} = & N_c N_f \left[-\frac{7\pi^2 T^4}{180} \left(1 + \frac{120}{7} \hat{\mu}^2 + \frac{240}{7} \hat{\mu}^4 \right) \right. \\
& + \frac{m_{\text{th}}^2 T^2}{6} \left(\frac{\Lambda}{4\pi T} \right)^{2\epsilon} (1 + 12\hat{\mu}^2 + 2\epsilon[1 + 12\hat{\mu}^2 + 12\aleph(1, z)]) \\
& \left. + 4m_{\text{th}}^4 \left(1 + \frac{1 - 2\Delta_3 + \Delta_4'' - \Delta_3''}{2-d} \right) \sum_{\{P\}}^f \frac{1}{P^4} \right]. \quad (12.27)
\end{aligned}$$

Substituting (A.3a) to (A.3c) and (A.2c), we get leading order quark free energy density [111] in thermal medium as

$$\begin{aligned}
F_q^{1\text{-loop}} = & N_c N_f \left[-\frac{7\pi^2 T^4}{180} \left(1 + \frac{120}{7} \hat{\mu}^2 + \frac{240}{7} \hat{\mu}^4 \right) \right. \\
& + \frac{m_{\text{th}}^2 T^2}{6} \left(\frac{\Lambda}{4\pi T} \right)^{2\epsilon} (1 + 12\hat{\mu}^2 + 2\epsilon[1 + 12\hat{\mu}^2 + 12\aleph(1, z)]) \\
& \left. + 4m_{\text{th}}^4 \left[\left(\frac{\pi^2}{3} - 2 \right) \epsilon \right] \frac{1}{(4\pi)^2} \left(\frac{\Lambda}{4\pi T} \right)^{2\epsilon} \left[\frac{1}{\epsilon} - \aleph(z) \right] \right] \\
\stackrel{\epsilon \rightarrow 0}{=} & N_c N_f \left[-\frac{7\pi^2 T^4}{180} \left(1 + \frac{120}{7} \hat{\mu}^2 + \frac{240}{7} \hat{\mu}^4 \right) + \frac{m_{\text{th}}^2 T^2}{6} (1 + 12\hat{\mu}^2) + \frac{m_{\text{th}}^4}{12\pi^2} (\pi^2 - 6) \right] \\
= & N_c N_f \left[-\frac{7\pi^2 T^4}{180} \left(1 + \frac{120\hat{\mu}^2}{7} + \frac{240\hat{\mu}^4}{7} \right) + \frac{g^2 C_F T^4}{48} (1 + 4\hat{\mu}^2) (1 + 12\hat{\mu}^2) \right. \\
& \left. + \frac{g^4 C_F^2 T^4}{768\pi^2} (1 + 4\hat{\mu}^2)^2 (\pi^2 - 6) \right]. \quad (12.28)
\end{aligned}$$

12.4 One-loop Gluon Free Energy in HTLpt

Similar to photon partition function in QED in subsec 9.5, the QCD partition function for a gluon can be written in Euclidean space-time as

$$\mathcal{Z}_g = \mathcal{Z} \mathcal{Z}^{\text{gh}}, \quad \mathcal{Z} = N_\xi \prod_{n, \mathbf{p}} \sqrt{\frac{\pi^D}{\det D_{\mu\nu, E}^{-1}}}, \quad \mathcal{Z}^{\text{gh}} = \prod_{n, \mathbf{p}} P_E^2, \quad (12.29)$$

where the product over n is for the discrete bosonic Matsubara frequencies ($\omega_n = 2\pi n\beta$; $n = 0, 1, 2, \dots$) due to Euclidean time whereas that of \mathbf{p} is for the spatial momentum. $D_{\mu\nu, E}^{-1}$ is the inverse gauge boson propagator in Euclidean space, $P_E^2 = \omega_n^2 + p^2$ is the square of the Euclidean four-momentum and D is the space-time dimension of the theory. As discussed in subsec. 9.5 the normalization $N_\xi = 1/(\pi^D \xi)^{1/2}$ arises due to the introduction of the Gaussian integral at every location of position while averaging over the gauge condition function with

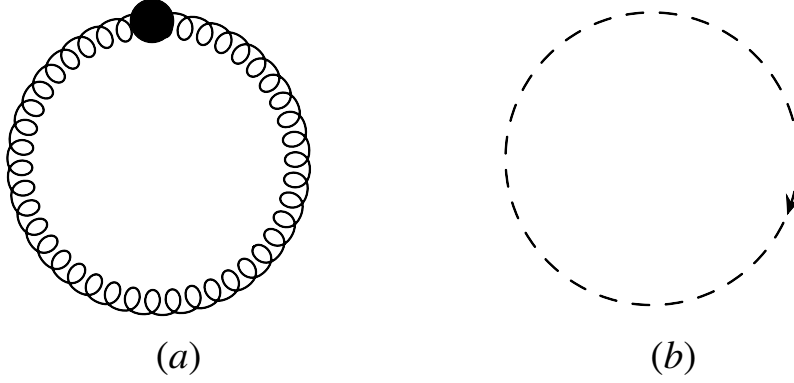


Figure 33: One-loop gluon and ghost contribution to free energy density.

a width ξ , the gauge fixing parameter. Gluon free energy can now be written from Fig. 33 as

$$F_g = -(N_c^2 - 1) \frac{T}{V} \ln \mathcal{Z}_g = (N_c^2 - 1) \left[\frac{1}{2} \oint_{P_E} \ln \left[\det \left(D_{\mu\nu,E}^{-1}(P_E) \right) \right] - \oint_{P_E} \ln P_E^2 + \frac{1}{2} \ln \xi \right]. \quad (12.30)$$

where \oint_{P_E} is a bosonic sum-integral and the gauge dependence will explicitly cancel as can be seen later. For an ideal case $\det \left(D_{\mu\nu,E}^{-1}(P) \right) = (P_E^2)^4 / \xi$ as obtained in (9.50) and hence the free energy for $(N_c^2 - 1)$ massless spin one gluons yields as

$$F_g^{\text{ideal}} = (N_c^2 - 1) \oint_{P_E} \ln P_E^2 = -(N_c^2 - 1) \frac{\pi^2 T^4}{45}, \quad (12.31)$$

where P_E is the four-momentum in Euclidean space and can be written as $P^2 = p_0^2 + p^2$.

In presence of thermal background medium one can have

$$\det \left(D_{\mu\nu,E}^{-1}(P_E) \right) = \frac{P_E^2}{\xi} (-P_E^2 + \Pi_T)^2 (-P_E^2 + \Pi_L), \quad (12.32)$$

with four eigenvalues; respectively P_E^2 , $(-P_E^2 + \Pi_L)$ and two fold degenerate $(-P_E^2 + \Pi_T)$. Here Π_T and Π_L are the transverse and longitudinal part of the gluon self-energy in thermal medium. Using (12.32) in (12.30), one gets 1-loop gluon free energy at the leading order in δ -expansion as

$$F_g = (N_c^2 - 1) \left[\frac{1}{2} \oint_{P_E} \ln \left(1 - \frac{\Pi_L}{P_E^2} \right) + \oint_{P_E} \ln (P_E^2 - \Pi_T) \right], \quad (12.33)$$

where a term $i\pi$ has been neglected as that would make the free energy complex. Now transforming into Minkowski space ($P_E^2 \rightarrow -P^2$) we have

$$F_g = (N_c^2 - 1) \left[\frac{1}{2} \sum_P \ln \left(1 + \frac{\Pi_L}{P^2} \right) + \sum_P \ln (P^2 + \Pi_T) \right] = (N_c^2 - 1) [F_g^L + F_g^T] \quad (12.34)$$

where F_g^L and F_g^T are, respectively, the longitudinal and transverse part of the gluon free energy and are given as

$$F_g^L = \frac{1}{2} \sum_P \ln \left(1 + \frac{\Pi_L}{P^2} \right) , \quad (12.35a)$$

$$F_g^T = \sum_P \ln (P^2 + \Pi_T) . \quad (12.35b)$$

The longitudinal and transverse part of the gluon self-energy can, respectively, be written from (9.108) and (9.110) as

$$\Pi_L = \frac{m_D^2 P^2}{p^2} (1 - \mathcal{T}_P) , \quad (12.36a)$$

$$\Pi_T = -\frac{m_D^2}{2p^2} (p_0^2 - P^2 \mathcal{T}_P) , \quad (12.36b)$$

where \mathcal{T}_P is given in (12.12) and the QCD Debye mass in presence of quark chemical potential is given as

$$m_D^2 = \frac{g^2 T^2}{3} \left[C_A + \frac{N_f}{2} (1 + 12\hat{\mu}^2) \right] . \quad (12.37)$$

Now expanding the logarithm in high temperature approximation as

$$\begin{aligned} F_g^L &= \frac{1}{2} \sum_P \ln \left(1 + \frac{\Pi_L}{P^2} \right) = \frac{1}{2} \sum_P \left(\frac{\Pi_L}{P^2} - \frac{\Pi_L^2}{2P^4} \right) \\ &= \frac{m_D^2}{2} \sum_P \frac{1}{p^2} - \frac{m_D^2}{2} \sum_P \frac{\mathcal{T}_P}{p^2} - m_D^4 \sum_P \left[\frac{1}{4p^4} - \frac{\mathcal{T}_P}{2p^4} + \frac{\mathcal{T}_P^2}{4p^4} \right] \end{aligned} \quad (12.38)$$

and

$$\begin{aligned} F_g^T &= \sum_P \ln (P^2 + \Pi_T) = \sum_P \ln(P^2) + \sum_P \ln \left(1 + \frac{\Pi_T}{P^2} \right) = \sum_P \ln(P^2) + \sum_P \left(\frac{\Pi_T}{P^2} - \frac{\Pi_T^2}{2P^4} \right) \\ &= \sum_P \ln(P^2) - m_D^2 \sum_P \frac{p_0^2}{2p^2 P^2} + m_D^2 \sum_P \frac{\mathcal{T}_P}{2p^2} - m_D^4 \sum_P \left[\frac{p_0^4}{8p^4 P^4} - \frac{p_0^2 \mathcal{T}_P}{4p^4 P^2} + \frac{\mathcal{T}_P^2}{8p^4} \right] , \end{aligned} \quad (12.39)$$

where we have kept terms up to $\mathcal{O}[m_D^4]$. The hard contribution to gluon free energy can be obtained combining (12.38) and (12.39) with (12.34) as

$$F_g^{\text{hard}} = (N_c^2 - 1) (F_g^L + F_g^T) = (N_c^2 - 1) \left[\sum_P \ln(P^2) - \frac{m_D^2}{2} \sum_P \frac{1}{P^2} - \frac{m_D^4}{8} \sum_P \left[\frac{1}{P^4} + \frac{2}{p^2 P^2} - \frac{2\mathcal{T}_P}{p^2 P^2} - \frac{6\mathcal{T}_P}{p^4} + \frac{3\mathcal{T}_P^2}{p^4} \right] \right]. \quad (12.40)$$

The bosonic sum integrals have been obtained in (A.6a) to (A.6f) in appendix A.2. Using them in (12.40) one gets the hard contribution to gluon free energy as

$$F_g^{\text{hard}} = (N_c^2 - 1) \left[-\frac{\pi^2 T^4}{45} + \frac{m_D^2 T^2}{24} \left(\frac{\Lambda}{4\pi T} \right)^{2\epsilon} (1 + \mathcal{O}[\epsilon]) - \frac{m_D^4}{128\pi^2} \left(\frac{\Lambda}{4\pi T} \right)^{2\epsilon} \left(\frac{1}{\epsilon} + 2\gamma_E + \frac{2\pi^2}{3} - 7 \right) \right]. \quad (12.41)$$

For the soft contribution the only important term in the integral is $p_0 = 0$. Putting $p_0 = 0$, we get from (12.36a) and (12.36b), respectively, as

$$\Pi_L = -m_D^2, \quad (12.42a)$$

$$\Pi_T = 0, \quad (12.42b)$$

where the longitudinal mode provides the electric screening through the Debye mass m_D but the transverse mode does not contribute in the soft scale which provides no magnetic screening in HTL.

The soft contribution from longitudinal part can be written from (12.34) as

$$F_g^{\text{soft}} = \frac{(N_c^2 - 1)}{2} \sum_P \ln(p^2 + m_D^2) = -(N_c^2 - 1) \frac{m_D^3 T}{12\pi} \left(\frac{\Lambda}{2m_D} \right)^{2\epsilon} \left[1 + \frac{8}{3}\epsilon \right]. \quad (12.43)$$

Now total gluon free energy in 1-loop can be written as

$$F_g^{\text{1-loop}} = F_g^{\text{hard}} + F_g^{\text{soft}} + \Delta_0 \mathcal{E}_0, \quad (12.44)$$

where the HTL leading order vacuum counter term [101] is given as

$$\Delta_0 \mathcal{E}_0 = \frac{(N_c^2 - 1)m_D^4}{128\pi^2 \epsilon}. \quad (12.45)$$

Substituting (12.41), (12.43) and (12.45) in (12.44), one gets leading order gluon free energy [101] as

$$\begin{aligned}
F_g^{1\text{-loop}} &= (N_c^2 - 1) \left[-\frac{\pi^2 T^4}{45} + \frac{m_D^2 T^2}{24} \left(\frac{\Lambda}{4\pi T} \right)^{2\epsilon} (1 + \mathcal{O}[\epsilon]) - \frac{m_D^3 T}{12\pi} \left(\frac{\Lambda}{2m_D} \right)^{2\epsilon} (1 + \mathcal{O}[\epsilon]) \right. \\
&\quad \left. - \frac{m_D^4}{128\pi^2} \left(\frac{\Lambda}{4\pi T} \right)^{2\epsilon} \left(\frac{1}{\epsilon} + 2\gamma_E + \frac{2\pi^2}{3} - 7 \right) \right] + \frac{(N_c^2 - 1)m_D^4}{128\pi^2\epsilon} \\
&\stackrel{\epsilon \rightarrow 0}{=} (N_c^2 - 1) \left[-\frac{\pi^2 T^4}{45} + \frac{m_D^2 T^2}{24} - \frac{m_D^3 T}{12\pi} - \frac{m_D^4}{128\pi^2} \left(2 \ln \left(\frac{\Lambda}{4\pi T} \right) + 2\gamma_E + \frac{2\pi^2}{3} - 7 \right) \right. \\
&\quad \left. - \frac{m_D^4}{128\pi^2\epsilon} \right] + \frac{(N_c^2 - 1)m_D^4}{128\pi^2\epsilon} \\
&= -(N_c^2 - 1) \frac{\pi^2 T^4}{45} \left[1 - \frac{15}{2} \hat{m}_D^2 + 30 \hat{m}_D^3 + \frac{45}{8} \hat{m}_D^4 \left(2 \ln \left(\frac{\hat{\Lambda}}{2} \right) + 2\gamma_E + \frac{2\pi^2}{3} - 7 \right) \right] \\
&= F_g^{\text{ideal}} \left[1 - \frac{15}{2} \hat{m}_D^2 + 30 \hat{m}_D^3 + \frac{45}{8} \hat{m}_D^4 \left(2 \ln \left(\frac{\hat{\Lambda}}{2} \right) + 2\gamma_E + \frac{2\pi^2}{3} - 7 \right) \right], \quad (12.46)
\end{aligned}$$

where

$$\hat{m}_D = \frac{m_D}{2\pi T}, \quad (12.47a)$$

$$\hat{\Lambda} = \frac{\Lambda}{2\pi T}. \quad (12.47b)$$

12.5 Leading Order (LO) Thermodynamics of QGP in HTLpt

The leading order free energy density of quarks and gluons above the deconfinement temperature is defined as

$$F^{\text{LO}} = F_q^{1\text{-loop}} + F_g^{1\text{-loop}}, \quad (12.48)$$

where one-loop quark and gluon free energy density are, respectively, given in (12.28) and (12.46). Using them the free energy at leading order in the δ -expansion becomes

$$\begin{aligned}
F^{\text{LO}} &= -d_A \frac{\pi^2 T^4}{45} \left[1 + \frac{7}{4} \frac{d_F}{d_A} \left(1 + \frac{120}{7} \hat{\mu}^2 + \frac{240}{7} \hat{\mu}^4 \right) - 30 \frac{d_F}{d_A} (1 + 12 \hat{\mu}^2) \hat{m}_{\text{th}}^2 \right. \\
&\quad \left. - \frac{15}{2} \hat{m}_D^2 + 30 \hat{m}_D^3 - 60 \frac{d_F}{d_A} (\pi^2 - 6) \hat{m}_{\text{th}}^4 + \frac{45}{8} \hat{m}_D^4 \left(2 \ln \left(\frac{\hat{\Lambda}}{2} \right) + 2\gamma_E + \frac{2\pi^2}{3} - 7 \right) \right], \quad (12.49)
\end{aligned}$$

where $d_F = N_c N_f$, $d_A = N_c^2 - 1$ and $\hat{m}_{\text{th}}^2 = m_{\text{th}}^2 / 2\pi T$. The leading order pressure is given by

$$\mathcal{P}^{\text{LO}} = -F^{\text{LO}}. \quad (12.50)$$

12.6 Next-to-leading Order (NLO) Thermodynamics of QGP in HTLpt

The NLO free energy density from two-loop HTLpt has been obtained complete analytically in Ref. [111, 112] as

$$\begin{aligned}
F^{\text{NLO}} = F^{2\text{-loop}} = & -d_A \frac{\pi^2 T^4}{45} \left\{ 1 + \frac{7}{4} \frac{d_F}{d_A} \left(1 + \frac{120}{7} \hat{\mu}^2 + \frac{240}{7} \hat{\mu}^4 \right) - 15 \hat{m}_D^3 - \frac{45}{4} \left(\log \frac{\hat{\Lambda}}{2} - \frac{7}{2} + \gamma_E + \frac{\pi^2}{3} \right) \hat{m}_D^4 \right. \\
& + 60 \frac{d_F}{d_A} (\pi^2 - 6) \hat{m}_{\text{th}}^4 + \frac{\alpha_s}{\pi} \left[-\frac{5}{4} \left(c_A + \frac{5}{2} s_F \left(1 + \frac{72}{5} \hat{\mu}^2 + \frac{144}{5} \hat{\mu}^4 \right) \right) \right. \\
& + 15 (c_A + s_F (1 + 12 \hat{\mu}^2)) \hat{m}_D - \frac{55}{4} \left\{ c_A \left(\log \frac{\hat{\Lambda}}{2} - \frac{36}{11} \log \hat{m}_D - 2.001 \right) \right. \\
& + \frac{4}{11} s_F \left[\left(\log \frac{\hat{\Lambda}}{2} - 2.337 \right) + (24 - 18\zeta(3)) \left(\log \frac{\hat{\Lambda}}{2} - 15.662 \right) \hat{\mu}^2 + 120 (\zeta(5) - \zeta(3)) \right. \\
& \times \left. \left(\log \frac{\hat{\Lambda}}{2} - 1.0811 \right) \hat{\mu}^4 + \mathcal{O}(\hat{\mu}^6) \right] \left. \right\} \hat{m}_D^2 - 45 s_F \left\{ \log \frac{\hat{\Lambda}}{2} + 2.198 - 44.953 \hat{\mu}^2 \right. \\
& - \left. \left(288 \ln \frac{\hat{\Lambda}}{2} + 19.836 \right) \hat{\mu}^4 + \mathcal{O}(\hat{\mu}^6) \right\} \hat{m}_{\text{th}}^2 + \frac{165}{2} \left\{ c_A \left(\log \frac{\hat{\Lambda}}{2} + \frac{5}{22} + \gamma_E \right) \right. \\
& - \frac{4}{11} s_F \left(\log \frac{\hat{\Lambda}}{2} - \frac{1}{2} + \gamma_E + 2 \ln 2 - 7\zeta(3) \hat{\mu}^2 + 31\zeta(5) \hat{\mu}^4 + \mathcal{O}(\hat{\mu}^6) \right) \left. \right\} \hat{m}_D^3 \\
& + 15 s_F \left(2 \frac{\zeta'(-1)}{\zeta(-1)} + 2 \ln \hat{m}_D \right) [(24 - 18\zeta(3)) \hat{\mu}^2 + 120(\zeta(5) - \zeta(3)) \hat{\mu}^4 + \mathcal{O}(\hat{\mu}^6)] \hat{m}_D^3 \\
& \left. + 180 s_F \hat{m}_D \hat{m}_{\text{th}}^2 \right\}, \tag{12.51}
\end{aligned}$$

where $c_A = N_c$ and $s_F = N_f/2$. The NLO pressure is given by

$$\mathcal{P}^{\text{NLO}} = -F^{\text{NLO}}. \tag{12.52}$$

12.7 Next-to-next-leading Order (NNLO) Thermodynamics of QGP in HTLpt

The NNLO free energy density from three-loop HTLpt has been obtained complete analytically in Ref. [103, 104] as

$$F^{\text{NNLO}} = F_q^{3\text{-loop}} + F_g^{3\text{-loop}}, \tag{12.53}$$

where the 3-loop quark contribution is given. [103, 104] as

$$\begin{aligned}
F_q^{3\text{-loop}} = & -\frac{d_A \pi^2 T^4}{45} \left[\frac{7}{4} \frac{d_F}{d_A} \left(1 + \frac{120}{7} \hat{\mu}^2 + \frac{240}{7} \hat{\mu}^4 \right) - \frac{s_F \alpha_s}{\pi} \left[\frac{5}{8} (1 + 12\hat{\mu}^2) (5 + 12\hat{\mu}^2) \right. \right. \\
& - \frac{15}{2} (1 + 12\hat{\mu}^2) \hat{m}_D - \frac{15}{2} \left(2 \ln \frac{\hat{\Lambda}}{2} - 1 - \aleph(z) \right) \hat{m}_D^3 + 90 \hat{m}_{\text{th}}^2 \hat{m}_D \left. \right] \\
& + s_{2F} \left(\frac{\alpha_s}{\pi} \right)^2 \left[\frac{15}{64} \left\{ 35 - 32 (1 - 12\hat{\mu}^2) \frac{\zeta'(-1)}{\zeta(-1)} + 472 \hat{\mu}^2 + 1328 \hat{\mu}^4 \right. \right. \\
& + 64 \left(-36 i \hat{\mu} \aleph(2, z) + 6(1 + 8\hat{\mu}^2) \aleph(1, z) + 3i \hat{\mu} (1 + 4\hat{\mu}^2) \aleph(0, z) \right) \left. \right\} \\
& - \frac{45}{2} \hat{m}_D (1 + 12\hat{\mu}^2) \left. \right] + \left(\frac{s_F \alpha_s}{\pi} \right)^2 \left[\frac{5}{4 \hat{m}_D} (1 + 12\hat{\mu}^2)^2 + 30 (1 + 12\hat{\mu}^2) \frac{\hat{m}_{\text{th}}^2}{\hat{m}_D} \right. \\
& + \frac{25}{12} \left\{ \left(1 + \frac{72}{5} \hat{\mu}^2 + \frac{144}{5} \hat{\mu}^4 \right) \ln \frac{\hat{\Lambda}}{2} + \frac{1}{20} (1 + 168 \hat{\mu}^2 + 2064 \hat{\mu}^4) + \frac{3}{5} (1 + 12\hat{\mu}^2)^2 \gamma_E \right. \\
& - \frac{8}{5} (1 + 12\hat{\mu}^2) \frac{\zeta'(-1)}{\zeta(-1)} - \frac{34}{25} \frac{\zeta'(-3)}{\zeta(-3)} - \frac{72}{5} \left[8 \aleph(3, z) + 3 \aleph(3, 2z) - 12 \hat{\mu}^2 \aleph(1, 2z) \right. \\
& + 12 i \hat{\mu} (\aleph(2, z) + \aleph(2, 2z)) - i \hat{\mu} (1 + 12\hat{\mu}^2) \aleph(0, z) - 2(1 + 8\hat{\mu}^2) \aleph(1, z) \left. \right] \left. \right\} \\
& - \frac{15}{2} \left\{ (1 + 12\hat{\mu}^2) \left(2 \ln \frac{\hat{\Lambda}}{2} - 1 - \aleph(z) \right) \right\} \hat{m}_D \left. \right] \\
& + \left(\frac{c_A \alpha_s}{3\pi} \right) \left(\frac{s_F \alpha_s}{\pi} \right) \left[\frac{15}{2 \hat{m}_D} (1 + 12\hat{\mu}^2) - \frac{235}{16} \left\{ \left(1 + \frac{792}{47} \hat{\mu}^2 + \frac{1584}{47} \hat{\mu}^4 \right) \ln \frac{\hat{\Lambda}}{2} \right. \right. \\
& - \frac{144}{47} (1 + 12\hat{\mu}^2) \ln \hat{m}_D + \frac{319}{940} \left(1 + \frac{2040}{319} \hat{\mu}^2 + \frac{38640}{319} \hat{\mu}^4 \right) - \frac{24 \gamma_E}{47} (1 + 12\hat{\mu}^2) \\
& - \frac{44}{47} \left(1 + \frac{156}{11} \hat{\mu}^2 \right) \frac{\zeta'(-1)}{\zeta(-1)} - \frac{268}{235} \frac{\zeta'(-3)}{\zeta(-3)} - \frac{72}{47} \left[4 i \hat{\mu} \aleph(0, z) \right. \\
& + (5 - 92 \hat{\mu}^2) \aleph(1, z) + 144 i \hat{\mu} \aleph(2, z) + 52 \aleph(3, z) \left. \right] \left. \right\} + 90 \frac{\hat{m}_{\text{th}}^2}{\hat{m}_D} \\
& + \frac{315}{4} \left\{ \left(1 + \frac{132}{7} \hat{\mu}^2 \right) \ln \frac{\hat{\Lambda}}{2} + \frac{11}{7} (1 + 12\hat{\mu}^2) \gamma_E + \frac{9}{14} \left(1 + \frac{132}{9} \hat{\mu}^2 \right) \right. \\
& + \frac{2}{7} \aleph(z) \left. \right\} \hat{m}_D \left. \right] \Bigg] \Bigg] , \tag{12.54}
\end{aligned}$$

whereas the free energy density up to three-loop pure glue case has been calculated in [100, 101] and read as

$$\begin{aligned}
F_g^{3\text{-loop}} = & -\frac{d_A \pi^2 T^4}{45} \left[1 - \frac{15}{4} \hat{m}_D^3 + \frac{c_A \alpha_s}{3\pi} \left[-\frac{15}{4} + \frac{45}{2} \hat{m}_D - \frac{135}{2} \hat{m}_D^2 - \frac{495}{4} \left(\ln \frac{\hat{\Lambda}_g}{2} + \frac{5}{22} + \gamma_E \right) \hat{m}_D^3 \right] \right. \\
& + \left(\frac{c_A \alpha_s}{3\pi} \right)^2 \left[\frac{45}{4 \hat{m}_D} - \frac{165}{8} \left(\ln \frac{\hat{\Lambda}_g}{2} - \frac{72}{11} \ln \hat{m}_D - \frac{84}{55} - \frac{6}{11} \gamma_E - \frac{74}{11} \frac{\zeta'(-1)}{\zeta(-1)} + \frac{19}{11} \frac{\zeta'(-3)}{\zeta(-3)} \right) \right. \\
& \left. \left. + \frac{1485}{4} \left(\ln \frac{\hat{\Lambda}_g}{2} - \frac{79}{44} + \gamma_E + \ln 2 - \frac{\pi^2}{11} \right) \hat{m}_D \right] \right]. \quad (12.55)
\end{aligned}$$

It is important to note that chemical potential dependence also appears in pure glue diagrams from the internal quark loop in effective gluon propagators and effective vertices. This chemical potential(μ) dependence are present within Debye mass(m_D). Besides the choice of the renormalization scales, the analytic result does not contain any free fit parameters and the result is also gauge-invariant. The NNLO pressure is given by

$$\mathcal{P}^{\text{NNLO}} = -F^{\text{NNLO}}. \quad (12.56)$$

The higher orders thermodynamical quantities [103, 104] of hot and dense matter, such as, the entropy density, the equation of state, the speed of sound, the interaction measure or the trace anomaly and various susceptibilities associated with conserved density fluctuations can be computed using NNLO free energy density and pressure. The equation of state is a generic quantity of a hot and dense many particle system and is required to investigate the expansion dynamics of hot and dense matter by using hydrodynamics. The obtained results on thermodynamic quantities [103, 104] are very good agreement with lattice results within error down to 200 MeV temperature. These calculations certainly have huge impact on the thermodynamics of QCD matter at finite temperature and chemical potential that agree quite well with data from lattice QCD, a first principle calculation. On the other hand the higher order thermodynamic quantities and various order quark number susceptibilities (QNS) are of huge interest to both theorists and experimentalists, for understanding the phase diagram of QCD.

Apart from QCD thermodynamics [74, 75, 98–114], if readers are interested in application to other physical quantities related to QGP created in heavy-ion collisions can go through the following extensive list of references: for dilepton production rate [80, 115–120], photon production rate [121–127], single quark and quark-antiquark potentials [128–135], fermion damping rate [136, 137], photon damping rate [138, 139], gluon damping rate [140, 141] and parton energy-loss [88, 142–145].

13 Thermal Medium with Non-perturbative Effects

Finite temperature QCD has been applied to study the properties of a QGP, which is believed to have existed in the early Universe, just a few microsecond after the big bang and in

the fireball created in high energy relativistic heavy-ion collisions at RHIC in BNL and at LHC in CERN. Lattice QCD (lQCD) provides a first-principles-based method that can take into account the non-perturbative effects of QCD. lQCD has been applied to investigate the behaviour of QCD near the critical temperature T_c , where hadronic matter undergoes a phase transition to the deconfined QGP phase. Beside lQCD also perturbation theory has been used to investigate the phenomenologically relevant properties of QGP. In contrast to lQCD computations the perturbative method is able to deal with dynamical quantities, a finite baryon density and non-equilibrium situations. To perturbatively understand the properties of QGP one needs to have very good understanding of the different collective excitations appear due to the presence of a thermal bath. There are three types of collective excitations which are associated with different thermal scales, They are (i) the energy (or hard) scale T , (ii) the electric scale gT , and (iii) the magnetic scale g^2T . In the literature the hard and electric scales are well studied, but not the magnetic scale since it is related to the difficult non-perturbative physics of confinement.

Based on the HTL resummations [78, 93, 95, 96, 140], a reorganization of finite-temperature and chemical potential perturbation theory known as HTL perturbation theory (HTLpt) has been discussed in sec. 12.2. HTLpt deals with the hard scale T and the electric scale gT as the soft scale. This has been widely applied to compute various physical quantities associated with QGP by using HTL resummed propagators and vertices. HTLpt works well at a temperature of approximately $2T_c$ and above, where $T_c \sim 160$ MeV is the critical temperature for the QGP phase transition. Near T_c , the running coupling g is moderately high and the QGP could therefore be completely non-perturbative in the vicinity of T_c .

Given the uncertainty involved in the lattice computation of dynamical quantities and also HTLpt near T_c , it is always desirable to formulate an alternative approach to consider non-perturbative effects which can be dealt in a similar way as done in HTLpt. There are some approaches available in the literature: one such approach is a semi-empirical way to include non-perturbative effects by considering a gluon condensate within the Green functions in momentum space [146–148]. The gluon condensate has a substantial effect on the equation of state of QCD matter, in contrast to the quark condensate. In subsec. 13.1 the quark propagation in QGP with gluon condensate will be discussed. Another approach [149, 150] would be to consider the non-perturbative physics involved in the QCD magnetic scale. This is taken into account through the non-perturbative magnetic screening scale within the Gribov-Zwanziger (GZ) action [151, 152]. The inclusion of magnetic scale regulates the magnetic infrared (IR) behaviour of QCD, the physics associated with it is completely non-perturbative. The gluon propagator with the GZ action is IR regulated which mimics confinement. This also makes the calculations more compatible with the results of lQCD. In subsec. 13.2 the quark propagation in QGP with GZ action will be discussed.

13.1 Quark Propagation in QGP with Gluon Condensate

13.1.1 Quark self-energy

Now in the rest frame of the heat bath, $u^\mu = (1, 0, 0, 0)$, the most general ansatz for fermionic self-energy reads from (7.9) as

$$\Sigma(L) = -\mathcal{A}(\omega, l)\not{L} - \mathcal{B}(\omega, l)\gamma_0, \quad (13.1)$$

with structure functions

$$\mathcal{A}(\omega, l) = \frac{1}{4l^2} (\text{Tr} [\Sigma \not{L}] - \omega \text{Tr} [\Sigma \gamma_0]), \quad (13.2a)$$

$$\mathcal{B}(\omega, l) = \frac{1}{4l^2} (L^2 \text{Tr} [\Sigma \gamma_0] - \omega \text{Tr} [\Sigma \not{L}]), \quad (13.2b)$$

where the four momentum of fermion is $L \equiv (\omega, \vec{l})$ with $l = |\vec{l}|$.

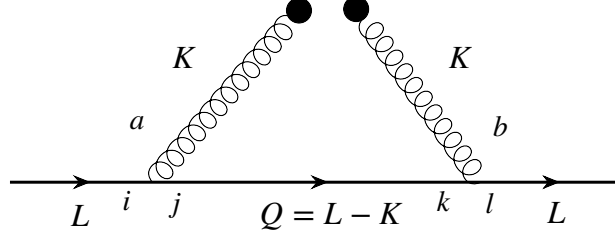


Figure 34: Quark self-energy containing gluon condensate.

The lowest order interaction of a quark with gluon condensate is given by self-energy diagram in Fig. 34. One can write the quark self-energy following Fig. 34 as

$$\begin{aligned} \Sigma(L)\delta_{il} &= T \sum_K (-ig\gamma^\mu \lambda_{ij}^a) \left(\frac{i\not{Q}\delta_{jk}}{Q^2} \right) (-ig\gamma^\nu \lambda_{kl}^b) i\tilde{D}_{\mu\nu}^{ab}(K)\delta_{ab} \\ \Sigma(L) &= \frac{4}{3}g^2T \sum_K \tilde{D}_{\mu\nu}(K)\gamma^\mu \frac{\not{Q}}{Q^2}\gamma^\nu \end{aligned} \quad (13.3)$$

where $Q = L - K$, \sum_K is a bosonic sum-integral, $\lambda_{ij}^a \lambda_{jl}^a = \frac{(N_c^2-1)}{2N_c} \delta_{il} = \frac{4}{3} \delta_{il}$ with $N_c = 3$ and $\tilde{D}_{\mu\nu}$ is the non-perturbative gluon propagator containing gluon condensate. We will consider purely non-perturbative input from lQCD as parametrized by temperature dependent gluon condensates. The most general ansatz for the non-perturbative gluon propagator at finite temperature can be written as

$$\tilde{D}_{\mu\nu}(K) = \tilde{D}_L(k_0, k)P_{\mu\nu}^L + \tilde{D}_T(k_0, k)P_{\mu\nu}^T, \quad (13.4)$$

where the longitudinal and transverse projectors are given by

$$P_{\mu\nu}^L = \frac{K_\mu K_\nu}{K^2} - \eta^{\mu\nu} - P_{\mu\nu}^T, \quad (13.5a)$$

$$P_{\mu 0}^T = 0, \quad (13.5b)$$

$$P_{ij}^T = \delta_{ij} - \frac{k_i k_j}{k^2}. \quad (13.5c)$$

In order to relate the propagator in (13.4) to the gluon condensate one can follow the zero temperature calculation [146] and expand the quark propagator in (13.3) for small loop momenta. Then considering terms which are only bilinear in K , one can relate the gluon condensates with the moments of the gluon propagator. Following this one can obtain [147] the structure functions in (13.2a) and (13.2b) as

$$\begin{aligned} \mathcal{A} = & -\frac{4}{3}g^2 \frac{1}{L^6} T \sum_K \left[\frac{1}{K^2} \left\{ -\omega^2 k_0^4 + \frac{22}{3}\omega^2 k_0^2 k^2 - \frac{1}{3}l^2 k_0^4 + \frac{34}{15}l^2 k_0^2 k^2 + \frac{5}{3}\omega^2 k^4 - \frac{1}{3}l^2 k^4 \right\} \tilde{D}_L(k_0, k) \right. \\ & \left. + \left\{ -2\omega^2 k_0^2 - \frac{2}{3}l^2 k_0^2 - 2\omega^2 k^2 + \frac{2}{5}l^2 k^2 \right\} \tilde{D}_T(k_0, k) \right], \end{aligned} \quad (13.6a)$$

$$\begin{aligned} \mathcal{B} = & -\frac{4}{3}g^2 \frac{l_0}{L^6} T \sum_K \left[\frac{1}{K^2} \left\{ -\frac{8}{3}l^2 k_0^4 - \left(\frac{40}{3}\omega^2 + \frac{104}{15}l^2 \right) k_0^2 k^2 - \frac{8}{3}\omega^2 k^4 \right\} \tilde{D}_L(k_0, k) \right. \\ & \left. - \left\{ \frac{16}{3}l^2 k_0^2 + \frac{16}{15}l^2 k^2 \right\} \tilde{D}_T(k_0, k) \right]. \end{aligned} \quad (13.6b)$$

Assuming the temperature scale to be large, $T \gg l$ and one can set $k_0 = 2\pi i n T = 0$ under the plane wave approximation. The above two equations become

$$\mathcal{A}(\omega, l) = -\frac{4}{3}g^2 \frac{1}{L^6} T \int \frac{d^3 k}{(2\pi)^3} \left[\left(\frac{1}{3}\omega^2 - \frac{5}{3}l^2 \right) k^2 \tilde{D}_L(0, k) + \left(-2\omega^2 + \frac{2}{5}l^2 \right) k^2 \tilde{D}_T(0, k) \right], \quad (13.7a)$$

$$\mathcal{B}(\omega, l) = -\frac{4}{3}g^2 \frac{\omega}{L^6} T \int \frac{d^3 k}{(2\pi)^3} \left[\frac{8}{3}\omega^2 k^2 \tilde{D}_L(0, k) - \frac{16}{15}l^2 k^2 \tilde{D}_T(0, k) \right]. \quad (13.7b)$$

The moments of the longitudinal and the transverse gluon propagators, respectively, in (13.7a) and (13.7b) can be related to the chromoelectric and the chromomagnetic condensates as

$$\langle E^2 \rangle_T = 8T \int \frac{d^3 k}{(2\pi)^3} k^2 \tilde{D}_L(0, k) + \mathcal{O}(g), \quad (13.8a)$$

$$\langle B^2 \rangle_T = -16T \int \frac{d^3 k}{(2\pi)^3} k^2 \tilde{D}_T(0, k) + \mathcal{O}(g). \quad (13.8b)$$

Using (13.8a) and (13.8b) in (13.7a) and (13.7b), one can write the structure functions as

$$\mathcal{A}(\omega, l) = -\frac{1}{6}g^2 \frac{1}{L^6} \left[\left(\frac{1}{3}\omega^2 - \frac{5}{3}l^2 \right) \langle E^2 \rangle_T + \left(\frac{1}{5}l^2 - \omega^2 \right) \langle B^2 \rangle_T \right], \quad (13.9a)$$

$$\mathcal{B}(\omega, l) = -\frac{4}{9}g^2 \frac{\omega}{L^6} \left[\omega^2 \langle E^2 \rangle_T + \frac{1}{5}l^2 \langle B^2 \rangle_T \right], \quad (13.9b)$$

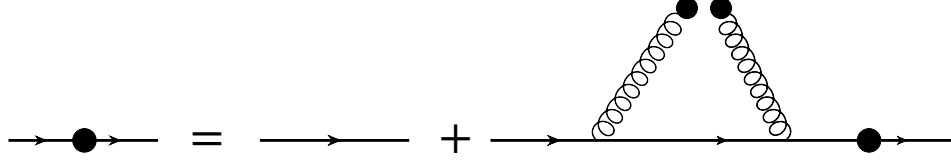


Figure 35: Effective quark propagator containing gluon condensate.

where $g^2 = 4\pi\alpha_s$. These condensates can be obtained in terms of the spacelike (Δ_σ) and timelike (Δ_τ) plaquette expectation values computed on a lattice [153] in Minkowski space as [147]

$$\frac{\alpha_s}{\pi}\langle E^2 \rangle_T = \frac{4}{11}T^4\Delta_\tau - \frac{2}{11}\langle G^2 \rangle_{T=0} , \quad (13.10a)$$

$$\frac{\alpha_s}{\pi}\langle B^2 \rangle_T = -\frac{4}{11}T^4\Delta_\sigma + \frac{2}{11}\langle G^2 \rangle_{T=0} . \quad (13.10b)$$

The plaquette expectation values are related to the gluon condensate above T_c as [153, 154]

$$\langle G^2 \rangle_T = \langle G^2 \rangle_{T=0} - \Delta T^4 , \quad (13.11)$$

where $\Delta = \Delta_\sigma + \Delta_\tau$ and $\langle G^2 \rangle_{T=0} = (2.5 \pm 1.0)T_c^4$.

13.1.2 Quark propagator and dispersion

The effective quark propagator containing gluon condensate follows from diagram in Fig. 35. In helicity representation, the effective quark propagator is given in (7.22) as

$$S^*(L) = \frac{1}{\not{L} - \Sigma(L)} = \frac{\gamma_0 - \vec{\gamma} \cdot \hat{\boldsymbol{l}}}{2\mathcal{D}_+(\omega, l)} + \frac{\gamma_0 + \vec{\gamma} \cdot \hat{\boldsymbol{l}}}{2\mathcal{D}_-(\omega, l)} , \quad (13.12)$$

where

$$\mathcal{D}_\pm(\omega, l) = (\omega \mp l)(1 + \mathcal{A}) + \mathcal{B}, \quad (13.13)$$

and the expressions for \mathcal{A} and \mathcal{B} are obtained in terms of the chromoelectric and the chromomagnetic condensates in (13.9a) and (13.9b).

The dispersion relation of a quark interacting with the thermal gluon condensate is obtained by the poles of $\mathcal{D}_\pm(\omega, l) = 0$ in (13.13). The functions \mathcal{A} and \mathcal{B} have been determined by using (13.10a) and (13.10b), where the plaquette expectation values are taken from the lattice calculations of Ref. [153]. $\mathcal{D}_+(\omega, l) = 0$ has two poles at $\omega = \omega^+(l)$ and $\omega = -\omega^-(l)$ whereas $\mathcal{D}_-(\omega, l) = 0$ has two poles at $\omega = \omega^-(l)$ and $\omega = -\omega^+(l)$. In Fig. 36 we have displayed the dispersion relation of a quark having momentum l for $T = 1.1T_c$ (left panel) and $2T_c$ (right panel), respectively. Only positive solutions of $\mathcal{D}_\pm(L) = 0$ have been displayed in Fig. 36. The mode with energy ω^+ describes the in-medium propagation of a particle

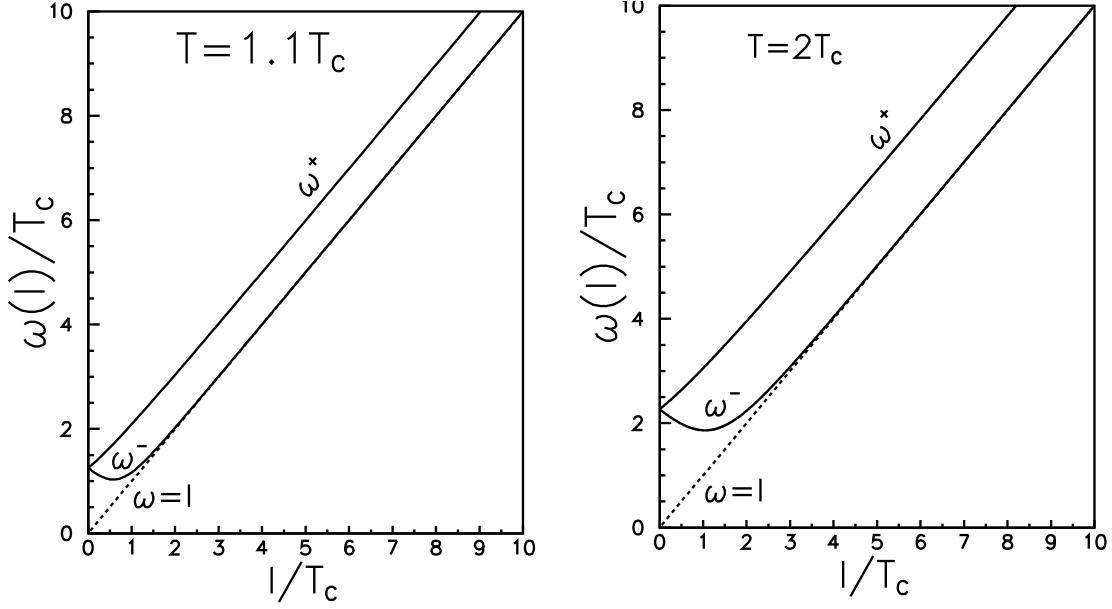


Figure 36: Quark dispersion in presence of gluon condensate. These figures are taken from Ref. [148].

excitation. It is a Dirac spinors which is a eigenstate of $(\gamma_0 - \vec{\gamma} \cdot \hat{l})$ with chirality to helicity ratio +1. Also there is a new long wavelength mode known as *plasmino* with energy ω^- . It is also a Dirac spinor and is a eigenstate of $(\gamma_0 + \vec{\gamma} \cdot \hat{l})$ with chirality to helicity ratio -1. Both branches are situated in the time like domain (i.e., above the free dispersion relation $\omega = l$), and they begin from a common effective mass which is obtained in the $l \rightarrow 0$ limit as [147]

$$\omega^+(0) = \omega^-(0) = m_{\text{eff}} = \left[\frac{2\pi\alpha_s}{3} (\langle E^2 \rangle_T + \langle B^2 \rangle_T) \right]^{1/4}, \quad (13.14)$$

which is given by $m_{\text{eff}} \approx 1.15 T$ and found to be independent of g . For small momenta $l \rightarrow 0$, the dispersion relation behaves [147] like

$$\omega^\pm = m_{\text{eff}} \pm c_2 l, \quad (13.15)$$

where

$$c_2 = \frac{3}{4} \frac{\langle E^2 \rangle_T}{\langle E^2 \rangle_T + \langle B^2 \rangle_T}. \quad (13.16)$$

It is to be noted that because of the opposite slopes of two branches, ω^- branch has a minimum at low momenta then it rapidly approaches the free dispersion for large momenta, indicating a purely long wavelength mode. This minimum leads to Van Hove singularities in soft dilepton rate [148] akin to HTL case [80, 81] and will be discussed in subsec 13.3.2. On the other hand, the ω^+ mode at large momenta is given by [147]

$$\omega^+ = l + c_1, \quad (13.17)$$

where

$$c_1 = \left[\frac{2\pi}{9} \alpha_s (\langle E^2 \rangle_T + \langle B^2 \rangle_T) \right]^{1/4}. \quad (13.18)$$

The dispersion relation of a quark interacting with the in-medium gluon condensate is similar to that obtained from the HTL resummed quark propagator displayed in Fig. 27. It is important to note that the dispersion relations with the HTL approximation and gluon condensate, respectively, exhibit similar features which is the general consequence of the presence of the heat bath.

13.1.3 Spectral representation of the quark propagator

The spectral functions, $\rho^\pm(\omega, l)$, corresponding to the effective propagator in (13.12) can be obtained following subsec. 9.8 or (A.11) in appendix A.3 as [148]

$$\rho^\pm(\omega, l) = R^\pm(\omega, l) \delta(\omega - \omega^\pm) + R^\mp(-\omega, l) \delta(\omega + \omega^\mp), \quad (13.19)$$

where

$$R^\pm = \left| \frac{(\omega^2 - l^2)^3}{C^\pm} \right| \quad (13.20)$$

with

$$C^\pm = - \left[(1 + \mathcal{A}) (\omega^2 - l^2)^3 + \frac{\mathcal{B} (\omega^2 - l^2)^3}{\omega} + 6 \omega (\omega \mp l) (\omega^2 - l^2)^2 + \frac{g^2}{3} \omega (\omega \mp l) \left(\frac{5}{3} \langle E^2 \rangle_T - \langle B^2 \rangle_T \right) - \frac{8}{9} g^2 \omega^2 \langle E^2 \rangle_T \right]. \quad (13.21)$$

The spectral functions in (13.19) has only contribution from the poles of the effective propagator. The solutions are collective quark modes with energy ω^\pm . Since the effective quark propagator (13.12) does not have an imaginary part coming from the quark self-energy, the spectral functions do not have a contribution from discontinuities or Landau cut.

13.2 Quark Propagation in QGP with Gribov-Zwanziger Action

13.2.1 Gribov-Zwanziger action and its consequences

Gribov showed in 1978 [151] that in a non-Abelian gauge theory, fixing the divergence of the potential does not commute with the gauge fixing. Unfortunately, the solutions of the differential equations, which specify the gauge fixing with vanishing divergence, can have several copies (Gribov copies) or none at all. This is known as Gribov ambiguity. To resolve this ambiguity, the domain of functional integral has to be restricted within a fundamental modular region, bounded by Gribov horizon. Following this in 1989 Zwanziger [152] derived a local, renormalizable action for non-Abelian gauge theories which fulfills the idea of restriction. He also showed that by introducing this GZ action the divergences may be absorbed by suitable field and coupling constant renormalization.

The GZ action is given by [155]

$$S_{\text{GZ}} = S_0 + S_{\gamma\text{G}}; \quad (13.22)$$

$$S_0 = S_{\text{YM}} + S_{\text{gf}} + \int d^D x \left(\bar{\phi}_\mu^{ac} \partial_\nu D_\nu^{ab} \phi_\mu^{bc} - \bar{\omega}_\mu^{ac} \partial_\nu D_\nu^{ab} \omega_\mu^{bc} \right) + \Delta S_0; \quad (13.23)$$

$$S_{\gamma\text{G}} = \gamma_G^2 \int d^D x g f^{abc} A_\mu^a \left(\phi_\mu^{bc} + \bar{\phi}_\mu^{bc} \right) + \Delta S_\gamma; \quad (13.24)$$

where $(\phi_\mu^{bc} + \bar{\phi}_\mu^{bc})$ and $(\omega_\mu^{bc} + \bar{\omega}_\mu^{bc})$ are a pair of complex conjugate bosonic and Grassmann fields respectively, introduced due to localization of the GZ action. S_{YM} and S_{gf} are the normal Yang-Mills and the gauge fixing term of the action and D is the dimension of the theory. ΔS_0 and ΔS_γ are the corresponding counterterms of the γ_G independent and dependent parts of GZ action. γ_G is called the Gribov parameter. In reality, γ_G is computed self-consistently using a one-loop⁸ gap equation and at asymptotically high temperatures it becomes [149, 156, 157]

$$\gamma_G = \frac{D-1}{D} \frac{N_c}{4\sqrt{2}\pi} g^2 T, \quad (13.25)$$

where N_c is the number of colors. The one-loop running strong coupling, $g^2 = 4\pi\alpha_s$, is

$$g^2(T) = \frac{48\pi^2}{(33 - 2N_f) \ln \left(\frac{Q_0^2}{\Lambda_0^2} \right)}, \quad (13.26)$$

where Q_0 is the renormalization scale, which is usually chosen to be $2\pi T$ unless specified and N_f is the number of quark flavors. The scale Λ_0 is fixed by requiring that $\alpha_s(1.5 \text{ GeV}) = 0.326$, which is obtained from lattice calculations [159]. For one-loop running, this procedure gives $\Lambda_0 = 176 \text{ MeV}$.

We know that gluons have an important role in confinement. In the GZ action [151, 152] the confinement is expected to be governed kinematically with the gluon propagator in covariant gauge [151, 152]

$$D^{\mu\nu}(P) = - \left[\eta^{\mu\nu} - (1 - \xi) \frac{P^\mu P^\nu}{P^2} \right] \frac{P^2}{P^4 + \gamma_G^4}, \quad (13.27)$$

where the four-momentum $P = (p_0, \vec{p})$ and ξ is the gauge parameter. The term γ_G in the denominator in (13.27) shifts the poles of the gluon propagator off the energy axis and there are no asymptotic gluon modes exist. For maintaining the consistency of the theory, obviously these unphysical poles should not appear in gauge-invariant quantities. This indicates that the gluons are unphysical excitations. In reality, this means that the addition of the Gribov parameter yields the effective confinement of gluons.

⁸Equation (13.25) is a one-loop result. In the vacuum, the two-loop result has been computed [158] and the form of Gribov propagator in (13.27) remains unaffected. Only γ_G itself is changed to take into account the two-loop correction. It is expected that this would be valid also at finite temperature.

13.2.2 Quark self-energy

In the high-temperature limit one can calculate the quark self-energy Σ using the modified gluon propagator given in (13.27) as [149, 150]

$$\begin{aligned} \Sigma(P) &= C_F T \sum_{\{K\}} (-ig\gamma_\mu) \left(\frac{iK}{K^2} \right) (-ig\gamma_\nu) (iD^{\mu\nu}(P-K)) \approx g^2 C_F \sum_{\pm} \int_0^\infty \frac{dk}{2\pi^2} k^2 \int \frac{d\Omega}{4\pi} \\ &\times \frac{\tilde{n}_\pm(k, \gamma_G)}{4E_\pm^0} \left[\frac{\gamma_0 + \hat{\mathbf{k}} \cdot \vec{\gamma}}{\omega + k - E_\pm^0 + \frac{\vec{p} \cdot \vec{k}}{E_\pm^0}} + \frac{\gamma_0 - \hat{\mathbf{k}} \cdot \vec{\gamma}}{\omega - k + E_\pm^0 - \frac{\vec{p} \cdot \vec{k}}{E_\pm^0}} \right], \end{aligned} \quad (13.28)$$

where Casimir factor $C_F = 4/3$, $\sum_{\{K\}}$ is a fermionic sum-integral and

$$\begin{aligned} \tilde{n}_\pm(k, \gamma_G) &\equiv n_B \left(\sqrt{k^2 \pm i\gamma_G^2} \right) + n_F(k), \\ E_\pm^0 &= \sqrt{k^2 \pm i\gamma_G^2}, \end{aligned} \quad (13.29)$$

with n_B and n_F are Bose-Einstein and Fermi-Dirac distribution functions, respectively. In presence of the Gribov term the modified thermal quark mass can also be obtained as [149]

$$m_q^2(\gamma_G) = \frac{g^2 C_F}{4\pi^2} \sum_{\pm} \int_0^\infty dk \frac{k^2}{E_\pm^0} \tilde{n}_\pm(k, \gamma_G). \quad (13.30)$$

13.2.3 Quark propagator and dispersion

The effective quark propagator is an important ingredient for computing various properties of a hot and dense QGP using (semi-)perturbative methods. Using the modified quark self-energy given in (13.28), it would now be convenient to obtain the effective quark propagator with the Gribov term. The resummed quark propagator in (7.21) can now be rearranged as

$$\begin{aligned} S^{\star-1}(P) &= \not{P} - \Sigma(P) \\ &= \frac{1}{2}(\gamma_0 + \vec{\gamma} \cdot \hat{\mathbf{p}}) \mathcal{D}_+ + \frac{1}{2}(\gamma_0 - \vec{\gamma} \cdot \hat{\mathbf{p}}) \mathcal{D}_- \\ &= \gamma_0 \mathcal{A}_0 - \vec{\gamma} \cdot \vec{p} \mathcal{A}_s, \end{aligned} \quad (13.31)$$

where

$$\mathcal{A}_0 = \frac{1}{2} (\mathcal{D}_+ + \mathcal{D}_-), \quad (13.32a)$$

$$\mathcal{A}_s = \frac{1}{2} (\mathcal{D}_- - \mathcal{D}_+). \quad (13.32b)$$

\mathcal{A}_0 and \mathcal{A}_s are obtained within the HTL approximation as [149, 150]

$$\mathcal{A}_0(\omega, p) = \omega - \frac{2g^2 C_F}{(2\pi)^2} \sum_{\pm} \int dk k \tilde{n}_\pm(k, \gamma_G) [Q_0(\tilde{\omega}_1^\pm, p) + Q_0(\tilde{\omega}_2^\pm, p)], \quad (13.33a)$$

$$\mathcal{A}_s(\omega, p) = p + \frac{2g^2 C_F}{(2\pi)^2} \sum_{\pm} \int dk k \tilde{n}_\pm(k, \gamma_G) [Q_1(\tilde{\omega}_1^\pm, p) + Q_1(\tilde{\omega}_2^\pm, p)]. \quad (13.33b)$$

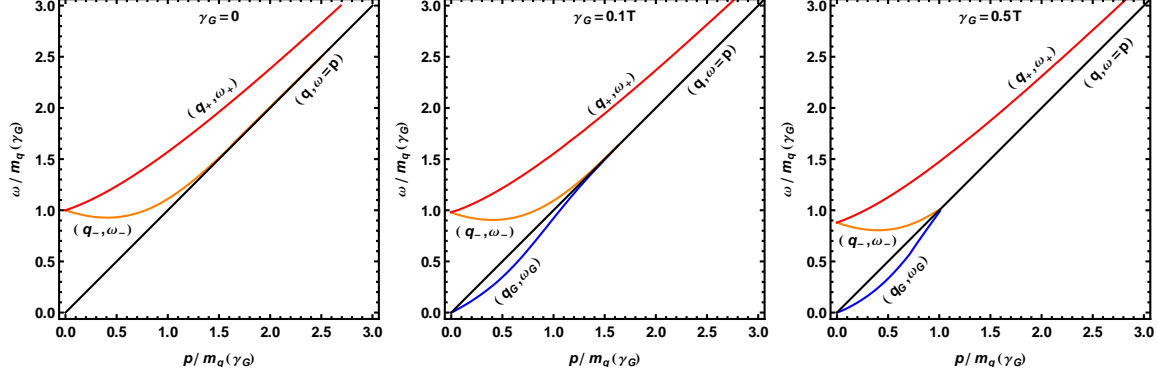


Figure 37: Plot of the dispersion relations for different values of γ_G . In the parenthesis, the first one represents a collective excitation mode whereas the second one is the corresponding energy of that mode. These figures are taken from Ref. [150].

The shifted frequencies are defined here as $\tilde{\omega}_1^\pm \equiv E_\pm^0(\omega + k - E_\pm^0)/k$ and $\tilde{\omega}_2^\pm \equiv E_\pm^0(\omega - k + E_\pm^0)/k$. The Legendre functions of the second kind, Q_0 and Q_1 , are given as

$$Q_0(\omega, p) = Q_0\left(\frac{\omega}{p}\right) \equiv \frac{1}{2p} \ln \frac{\frac{\omega}{p} + 1}{\frac{\omega}{p} - 1}, \quad (13.34a)$$

$$Q_1(\omega, p) = Q_1\left(\frac{\omega}{p}\right) \equiv \frac{1}{p} \left[1 - \omega Q_0\left(\frac{\omega}{p}\right) \right]. \quad (13.34b)$$

Following (7.22) the effective quark propagator in helicity representation can also be written as

$$S^*(P) = \frac{1}{2} \frac{(\gamma_0 - \vec{\gamma} \cdot \hat{\mathbf{p}})}{\mathcal{D}_+} + \frac{1}{2} \frac{(\gamma_0 + \vec{\gamma} \cdot \hat{\mathbf{p}})}{\mathcal{D}_-}, \quad (13.35)$$

where \mathcal{D}_\pm are obtained as

$$\begin{aligned} \mathcal{D}_+(\omega, p, \gamma_G) &= \mathcal{A}_0(\omega, p) - \mathcal{A}_s(\omega, p) = \omega - p - \frac{2g^2 C_F}{(2\pi)^2} \sum_{\pm} \int dk k \tilde{n}_{\pm}(k, \gamma_G) \\ &\quad \times [Q_0(\tilde{\omega}_1^\pm, p) + Q_1(\tilde{\omega}_1^\pm, p) + Q_0(\tilde{\omega}_2^\pm, p) + Q_1(\tilde{\omega}_2^\pm, p)], \end{aligned} \quad (13.36a)$$

$$\begin{aligned} \mathcal{D}_-(\omega, p, \gamma_G) &= \mathcal{A}_0(\omega, p) + \mathcal{A}_s(\omega, p) = \omega + p - \frac{2g^2 C_F}{(2\pi)^2} \sum_{\pm} \int dk k \tilde{n}_{\pm}(k, \gamma_G) \\ &\quad \times [Q_0(\tilde{\omega}_1^\pm, p) - Q_1(\tilde{\omega}_1^\pm, p) + Q_0(\tilde{\omega}_2^\pm, p) - Q_1(\tilde{\omega}_2^\pm, p)]. \end{aligned} \quad (13.36b)$$

The zeros of $\mathcal{D}_\pm(\omega, p, \gamma_G)$ correspond to the dispersion relations for the collective excitations in the non-perturbative medium. In Fig. 37 the dispersion relations are displayed for three values of γ_G . For HTL case when $\gamma_G = 0$, one gets two massive quasiparticle modes. One is a normal quark mode q_+ with energy ω_+ and another one is a long wavelength plasmino mode

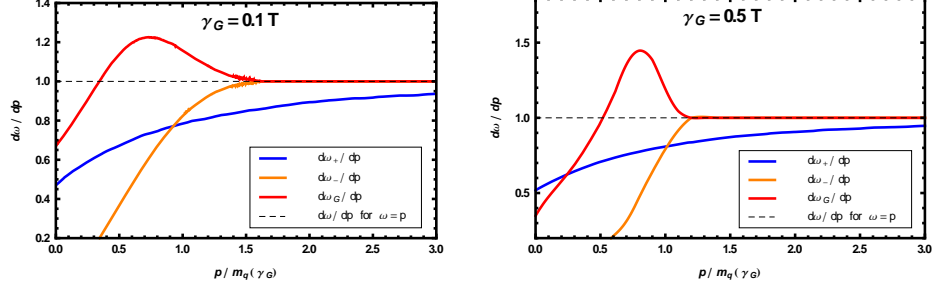


Figure 38: Plot of the group velocity for different values of γ_G . The group velocity for the space like Gribov mode $d\omega_G/dp$ becomes superluminal, as can be seen from both plots.

q_- with energy ω_- . They are displayed in Fig. 27 also in the left panel of Fig. 37. The q_- mode has a minimum and then it quickly approaches to the non-interacting massless mode in the high-momentum limit. The minimum in q_- mode (plasmino mode) leads to Van Hove singularities in soft dilepton production rate [150] which will be discussed in subsec 13.3.3. In presence of the γ_G , there appears a new massless spacelike mode q_G with energy ω_G , in addition to the two massive modes, q_+ and q_- [149] as shown in the middle and in the right panel of Fig. 37. This new spacelike massless mode q_G in spacelike domain is due to the inclusion of the magnetic scale through the GZ action. It becomes lightlike at large momentum as can also be seen from the middle and the right panel of Fig. 37. The existence of this extra spacelike mode could affect lattice calculations of the dilepton rate because the recent lQCD results [160, 161] considered that there were only two poles of the in-medium propagator leading to a quark mode and a plasmino mode motivated by the HTL approximation.

It is also to be noted that the slope of the dispersion curve for the new massless spacelike mode q_G exceeds unity in some domain of momentum. This indicates that the group velocity, $d\omega_G/dp$, of the new mode is superluminal, and then it approaches to the light cone ($d\omega/dp = 1$) from above as shown in Fig. 38. Since the mode is spacelike, there is no causality problem but could be termed as anomalous dispersion because the presence γ_G converts the Landau damping in the spacelike domain into amplification of a massless spacelike dispersive mode.

13.2.4 Spectral representation of the quark propagator

In absence of Gribov parameter ($\gamma_G = 0$), i.e., in the HTL approximation apart from poles the propagator contains a discontinuity in complex plane originating from the logarithmic terms in (13.36a) and (13.36b) due to spacelike momentum $\omega^2 < p^2$. The HTL spectral function contains contributions from two collective excitations and the Landau cut as discussed in subsec. 9.8. On the other hand, for $\gamma_G \neq 0$ there are three collective excitations q_+ , q_- and q_G , and no Landau cut contributions in the complex plane due to the fact that the poles come in complex-conjugate pairs and ultimately cancel out. It seems that the Landau cut contribution in spacelike domain for $\gamma_G = 0$ is converted into a new massless spacelike

dispersive mode in presence of magnetic scale ($\gamma_G \neq 0$). Since there is no Landau cut contribution, the spectral representation of the quark propagator \mathcal{D}_\pm^{-1} for $\gamma_G \neq 0$ has only pole contributions and obtained following subsec. 9.8 or (A.11) in appendix A.3 as [150]

$$\rho_\pm^G(\omega, p) = \frac{\omega^2 - p^2}{2m_q^2(\gamma_G)} [\delta(\omega \mp \omega_+) + \delta(\omega \pm \omega_-) + \delta(\omega \pm \omega_G)], \quad (13.37)$$

where \mathcal{D}_+ has poles at ω_+ , $-\omega_-$, and $-\omega_G$ and \mathcal{D}_- has poles at ω_- , $-\omega_+$, and ω_G with a prefactor, $(\omega^2 - p^2)/2m_q^2(\gamma_G)$, as the residue.

13.2.5 Quark-Photon vertex

The quark-photon three-point vertex can be obtained [150] by using the Ward-Takahashi identity⁹ as

$$(P_1 - P_2)_\mu \Gamma^\mu(P_1, P_2) = S^{-1}(P_1) - S^{-1}(P_2). \quad (13.38)$$

The temporal and spatial parts of the modified effective vertex can be written as

$$\Gamma^0 = a_G \gamma^0 + b_G \boldsymbol{\gamma} \cdot \hat{\mathbf{p}}, \quad (13.39a)$$

$$\Gamma^i = c_G \gamma^i + b_G \hat{p}^i \gamma_0 + d_G \hat{p}^i (\boldsymbol{\gamma} \cdot \hat{\mathbf{p}}), \quad (13.39b)$$

where the coefficients are given by

$$a_G = 1 - \frac{2g^2 C_F}{(2\pi)^2} \sum_{\pm} \int dk k \tilde{n}_{\pm}(k, \gamma_G) \frac{1}{\omega_1 - \omega_2} [\delta Q_{01}^{\pm} + \delta Q_{02}^{\pm}], \quad (13.40a)$$

$$b_G = -\frac{2g^2 C_F}{(2\pi)^2} \sum_{\pm} \int dk k \tilde{n}_{\pm}(k, \gamma_G) \frac{1}{\omega_1 - \omega_2} [\delta Q_{11}^{\pm} + \delta Q_{12}^{\pm}], \quad (13.40b)$$

$$c_G = 1 + \frac{2g^2 C_F}{(2\pi)^2} \sum_{\pm} \int dk k \tilde{n}_{\pm}(k, \gamma_G) \frac{1}{3(\omega_1 - \omega_2)} [\delta Q_{01}^{\pm} + \delta Q_{02}^{\pm} - \delta Q_{21}^{\pm} - \delta Q_{22}^{\pm}], \quad (13.40c)$$

$$d_G = \frac{2g^2 C_F}{(2\pi)^2} \sum_{\pm} \int dk k \tilde{n}_{\pm}(k, \gamma_G) \frac{1}{\omega_1 - \omega_2} [\delta Q_{21}^{\pm} + \delta Q_{22}^{\pm}], \quad (13.40d)$$

with

$$\delta Q_{n1}^{\pm} = Q_n(\tilde{\omega}_{11}^{\pm}, p) - Q_n(\tilde{\omega}_{21}^{\pm}, p) \text{ for } n = 0, 1, 2, \quad (13.41a)$$

$$\omega_{m1}^{\pm} = E_{\pm}^0(\omega_m + k - E_{\pm}^0)/k \text{ for } m = 1, 2, \quad (13.41b)$$

$$\omega_{m2}^{\pm} = E_{\pm}^0(\omega_m - k + E_{\pm}^0)/k \text{ for } m = 1, 2 \quad (13.41c)$$

Similarly, the quark-photon four-point function can be obtained from the following generalized Ward-Takahashi identity

$$P_\mu \Gamma^{\mu\nu}(-P_1, P_1; -P_2, P_2) = \Gamma^\nu(P_1 - P_2, -P_1; P_2) - \Gamma^\nu(-P_1 - P_2, P_1; P_2). \quad (13.42)$$

⁹This procedure only constrains the longitudinal part of the vertex function.

13.3 Dilepton Production Rate from QGP

Thermal dileptons ($q\bar{q} \rightarrow \gamma^* \rightarrow l^+l^-$, where q and \bar{q} are (anti)quark, γ^* is virtual photon and l^+l^- are lepton pair) emitted from the fireball in ultrarelativistic heavy ion collisions might serve as a promising signature [162] for the QGP formation in such collisions. In contrast to hadronic signals dileptons and photons carry direct information about the early phase of the fireball, since they do not interact with the surrounding medium after their production. Therefore, they can be used as a direct probe for the QGP. Unfortunately there is a huge background coming from hadronic decays. Hence it would be desirable to have some specific features in the dilepton spectrum which could signal the presence of deconfined matter. Indeed perturbative calculations [80, 81] have shown distinct structures (van Hove peaks [163, 164], gaps) in the production rate of low mass dileptons caused by non-trivial in-medium quark dispersion relations. In the following subsec 13.3.1 we briefly discuss the dilepton production rate from a thermal medium.

13.3.1 Dilepton rate in presence of thermal medium

The dilepton multiplicity per unit space-time volume is given [165] as

$$\frac{dN}{d^4X} = 2\pi e^2 e^{-\beta p_0} L_{\mu\nu} \rho^{\mu\nu} \frac{d^3\vec{q}_1}{(2\pi)^3 E_1} \frac{d^3\vec{q}_2}{(2\pi)^3 E_2}, \quad (13.43)$$

where e is the electromagnetic coupling, \vec{q}_i and E_i with $i = 1, 2$ are three momentum and energy of the lepton pairs. The photonic tensor or the electromagnetic spectral function in thermal medium can be written as

$$\rho^{\mu\nu}(p_0, \vec{p}) = -\frac{1}{\pi} \frac{e^{\beta p_0}}{e^{\beta p_0} - 1} \text{Im} [D^{\mu\nu}(p_0, \vec{p})] \equiv -\frac{1}{\pi} \frac{e^{\beta p_0}}{e^{\beta p_0} - 1} \frac{1}{P^4} \text{Im} [\Pi^{\mu\nu}(p_0, \vec{p})], \quad (13.44)$$

where ‘Im’ stands for imaginary part, $\Pi^{\mu\nu}$ is the two point current-current correlation function or the self-energy of photon and $D^{\mu\nu}$ represents the photon propagator. Here we have used the relation [165]

$$D^{\mu\nu}(p_0, \vec{p}) = \frac{1}{P^4} \Pi^{\mu\nu}(p_0, \vec{p}), \quad (13.45)$$

where $P \equiv (p_0, \vec{p})$ is the four momenta of the photon.

Also the leptonic tensor in terms of Dirac spinors is given by

$$\begin{aligned} L_{\mu\nu} &= \frac{1}{4} \sum_{\text{spins}} \text{Tr} [\bar{u}(Q_2) \gamma_\mu v(Q_1) \bar{v}(Q_1) \gamma_\nu u(Q_2)] \\ &= Q_{1\mu} Q_{2\nu} + Q_{1\nu} Q_{2\mu} - (Q_1 \cdot Q_2 + m_l^2) g_{\mu\nu}, \end{aligned} \quad (13.46)$$

where $Q_i \equiv (q_0, \vec{q}_i)$ is the four momentum of the i -th lepton and m_l is the mass of the lepton.

Now inserting $\int d^4P \delta^4(Q_1 + Q_2 - P) = 1$, one can write the dilepton multiplicity from (13.43) as

$$\frac{dN}{d^4X} = 2\pi e^2 e^{-\beta p_0} \int d^4P \delta^4(Q_1 + Q_2 - P) L_{\mu\nu} \rho^{\mu\nu} \frac{d^3\vec{q}_1}{(2\pi)^3 E_1} \frac{d^3\vec{q}_2}{(2\pi)^3 E_2}. \quad (13.47)$$

Using the identity

$$\begin{aligned} \int \frac{d^3 \vec{q}_1}{E_1} \frac{d^3 \vec{q}_2}{E_2} \delta^4(Q_1 + Q_2 - P) L_{\mu\nu} &= \frac{2\pi}{3} \left(1 + \frac{2m_l^2}{P^2}\right) \sqrt{\left(1 - \frac{4m_l^2}{P^2}\right)} (P_\mu P_\nu - P^2 g_{\mu\nu}) \\ &= \frac{2\pi}{3} F_1(m_l, P^2) (P_\mu P_\nu - P^2 g_{\mu\nu}), \end{aligned} \quad (13.48)$$

the dilepton production rate in (13.47) comes out to be

$$\begin{aligned} \frac{dN}{d^4 X d^4 P} &= \frac{dR}{d^4 P} = \frac{\alpha}{12\pi^4} \frac{n_B(p_0)}{P^2} F_1(m_l, P^2) \text{Im} [\Pi_\mu^\mu(p_0, \vec{p})] \\ \frac{dR}{d^4 P} &= \frac{\alpha}{12\pi^4} \frac{n_B(p_0)}{P^2} F_1(m_l, P^2) \frac{1}{2i} \text{Disc} [\Pi_\mu^\mu(p_0, \vec{p})], \end{aligned} \quad (13.49)$$

where $n_B(p_0) = (e^{p_0/T} - 1)^{-1}$ and $e^2 = 4\pi\alpha$, α is the electromagnetic coupling constant. We have also used the transversality condition $P_\mu \Pi^{\mu\nu} = 0$. The invariant mass of the lepton pair is defined as $M^2 \equiv P^2 (= p_0^2 - |\vec{p}|^2 = \omega^2 - |\vec{p}|^2)$. We note that for massless lepton ($m_l = 0$) $F_1(m_l, P^2) = 1$.

The (13.49) is the familiar result most widely used for the dilepton emission rate from a thermal medium. It must be emphasized that this relation is valid only to $\mathcal{O}(e^2)$ since it does not account for the possible reinteractions of the virtual photon on its way out of the thermal bath. The possibility of emission of more than one photon has also been neglected here. However, the expression is true to all orders in strong interaction.

13.3.2 Dilepton production rate from QGP with gluon condensate

In this subsection we calculate the effect of an in-medium gluon condensates, as discussed in subsec 13.1, on the production rate of lepton pairs from QGP [148]. This effect can be included by using effective propagators, S^* , as given in (13.12) containing the gluon condensate for the exchanged quarks in photon self-energy in Fig. 39. The photon self energy in Fig. 39 can now be written as

$$\Pi^{\mu\nu}(P) = -3 \times 2 \times \frac{5}{9} e^2 T \sum_{\{k_0\}} \int \frac{d^3 k}{(2\pi)^3} \text{Tr} [S^*(K) \gamma^\mu S^*(Q) \gamma^\nu], \quad (13.50)$$

where $\sum_{\{k_0\}}$ is the frequency sum over fermionic Matsubara frequency, K and $Q = P - K$ are the fermionic loop four-momenta. We have considered only massless u and d quarks and the total electric charge of two flavours is $(\frac{2}{3})^2 e^2 + (\frac{1}{3})^2 e^2 = \frac{5}{9} e^2$, the factor 2 is for antiquarks and the color factor of quark is 3.

Substitution of (13.12) in (13.50) and performing the traces one gets

$$\begin{aligned} \Pi_\mu^\mu(P) &= -\frac{10}{3} e^2 T \sum_{\{k_0\}} \int \frac{d^3 k}{(2\pi)^3} \left[\frac{1}{D_+(K)} \left(\frac{1 - \hat{k} \cdot \hat{q}}{D_+(Q)} + \frac{1 + \hat{k} \cdot \hat{q}}{D_-(Q)} \right) \right. \\ &\quad \left. + \frac{1}{D_-(K)} \left(\frac{1 + \hat{k} \cdot \hat{q}}{D_+(Q)} + \frac{1 - \hat{k} \cdot \hat{q}}{D_-(Q)} \right) \right]. \end{aligned} \quad (13.51)$$

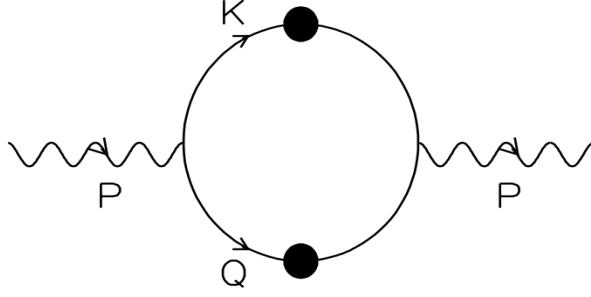


Figure 39: One-loop photon self-energy with effective quark propagators containing gluon condensate. This figure is taken from Ref. [148].

Now according to (13.49) one needs to compute the imaginary or discontinuity part of $\Pi_\mu^\mu(P)$. The discontinuity can be obtained by using the Braaten-Pisarski-Yuan (BPY) prescription [80] obtained in (A.23) in appendix A.3 as

$$\begin{aligned} \text{Im } T \sum_{k_0} F_1(k_0) F_2(q_0) &= \frac{1}{2i} \text{Disc } T \sum_{k_0} F_1(k_0) F_2(q_0) \\ &= \pi(1 - e^{\beta\omega}) \int d\omega_1 \int d\omega_2 n_F(\omega_1) n_F(\omega_2) \\ &\quad \times \delta(\omega - \omega_1 - \omega_2) \rho_1(\omega_1) \rho_2(\omega_2), \end{aligned} \quad (13.52)$$

where $\delta(\omega - \omega_1 - \omega_2)$ is the energy conserving δ -function, n_F is the Fermi-Dirac distribution function and ρ_1 and ρ_2 are the spectral functions corresponding to the functions F_1 and F_2 .

Now using (13.52) one can write the imaginary part of Π_μ^μ as

$$\begin{aligned} \text{Im } \Pi_\mu^\mu(P) &= \frac{10\pi}{3} e^2 \left(e^{E/T} - 1 \right) \int \frac{d^3 k}{(2\pi)^3} \int_{-\infty}^{\infty} d\omega \int_{-\infty}^{\infty} d\omega' \\ &\quad \times \delta(E - \omega - \omega') n_F(\omega) n_F(\omega') \\ &\quad \times \left[\left(1 + \hat{\mathbf{q}} \cdot \hat{\mathbf{k}} \right) \left\{ \rho^+(\omega, k) \rho^-(\omega', q) + \rho^-(\omega, k) \rho^+(\omega', q) \right\} \right. \\ &\quad \left. + \left(1 - \hat{\mathbf{q}} \cdot \hat{\mathbf{k}} \right) \left\{ \rho^+(\omega, k) \rho^+(\omega', q) + \rho^-(\omega, k) \rho^-(\omega', q) \right\} \right], \end{aligned} \quad (13.53)$$

where ρ^\pm are the spectral functions corresponding to $1/\mathcal{D}_\pm(L)$ and obtained in (13.19). Inserting (13.19) into (13.53) and performing the ω -integrations by exploiting the delta functions of the spectral functions, one finds ($x = \hat{\mathbf{p}} \cdot \hat{\mathbf{k}}$)

$$\begin{aligned} \text{Im } \Pi_\mu^\mu(P) &= \frac{5}{6\pi} e^2 \left(e^{E/T} - 1 \right) \int_0^\infty dk k^2 \int_{-1}^{+1} dx \\ &\quad \times \left[\left(1 + \hat{\mathbf{q}} \cdot \hat{\mathbf{k}} \right) A + \left(1 - \hat{\mathbf{q}} \cdot \hat{\mathbf{k}} \right) B \right], \end{aligned} \quad (13.54)$$

where

$$\begin{aligned}
A = & n_F(\omega^+(k)) n_F(\omega^-(q)) R_+(\omega^+(k), k) R_-(\omega^-(q), q) \delta(E - \omega^+(k) - \omega^-(q)) \\
& + n_F(-\omega^-(k)) n_F(\omega^-(q)) R_-(\omega^-(k), k) R_-(\omega^-(q), q) \delta(E + \omega^-(k) - \omega^-(q)) \\
& + n_F(\omega^+(k)) n_F(-\omega^+(q)) R_+(\omega^+(k), k) R_+(\omega^+(q), q) \delta(E - \omega^+(k) + \omega^+(q)) \\
& + n_F(-\omega^-(k)) n_F(-\omega^+(q)) R_-(\omega^-(k), k) R_+(\omega^+(q), q) \delta(E + \omega^-(k) + \omega^+(q)) \\
& + n_F(\omega^-(k)) n_F(\omega^+(q)) R_-(\omega^-(k), k) R_+(\omega^+(q), q) \delta(E - \omega^-(k) - \omega^+(q)) \\
& + n_F(-\omega^+(k)) n_F(\omega^+(q)) R_+(\omega^+(k), k) R_+(\omega^+(q), q) \delta(E + \omega^+(k) - \omega^+(q)) \\
& + n_F(\omega^-(k)) n_F(-\omega^-(q)) R_-(\omega^-(k), k) R_-(\omega^-(q), q) \delta(E - \omega^-(k) + \omega^-(q)) \\
& + n_F(-\omega^+(k)) n_F(-\omega^-(q)) R_+(\omega^+(k), k) R_-(\omega^-(q), q) \delta(E + \omega^+(k) + \omega^-(q)) ,
\end{aligned} \tag{13.55}$$

and

$$\begin{aligned}
B = & n_F(\omega^+(k)) n_F(\omega^+(q)) R_+(\omega^+(k), k) R_+(\omega^+(q), q) \delta(E - \omega^+(k) - \omega^+(q)) \\
& + n_F(-\omega^-(k)) n_F(\omega^+(q)) R_-(\omega^-(k), k) R_+(\omega^+(q), q) \delta(E + \omega^-(k) - \omega^+(q)) \\
& + n_F(\omega^+(k)) n_F(-\omega^-(q)) R_+(\omega^+(k), k) R_-(\omega^-(q), q) \delta(E - \omega^+(k) + \omega^-(q)) \\
& + n_F(-\omega^-(k)) n_F(-\omega^-(q)) R_-(\omega^-(k), k) R_-(\omega^-(q), q) \delta(E + \omega^-(k) + \omega^-(q)) \\
& + n_F(\omega^-(k)) n_F(\omega^-(q)) R_-(\omega^-(k), k) R_-(\omega^-(q), q) \delta(E - \omega^-(k) - \omega^-(q)) \\
& + n_F(-\omega^+(k)) n_F(\omega^-(q)) R_+(\omega^+(k), k) R_-(\omega^-(q), q) \delta(E + \omega^+(k) - \omega^-(q)) \\
& + n_F(\omega^-(k)) n_F(-\omega^+(q)) R_-(\omega^-(k), k) R_+(\omega^+(q), q) \delta(E - \omega^-(k) + \omega^+(q)) \\
& + n_F(-\omega^+(k)) n_F(-\omega^+(q)) R_+(\omega^+(k), k) R_+(\omega^+(q), q) \delta(E + \omega^+(k) + \omega^+(q)) .
\end{aligned} \tag{13.56}$$

Changing the integration variable from x to $q = |\vec{p} - \vec{k}| = \sqrt{p^2 + k^2 - 2pkx}$ the dilepton production rate in (13.49) with massless leptons can be written as

$$\begin{aligned}
\frac{dN}{d^4X d^4P} = & \frac{5}{18\pi^4} \frac{\alpha^2}{M^2} \frac{1}{p} \left[\int_0^p dk \int_{p-k}^{p+k} dq + \int_p^\infty dk \int_{k-p}^{p+k} dq \right] \\
& \times [(p^2 - (k - q)^2) A + ((k + q)^2 - p^2) B] .
\end{aligned} \tag{13.57}$$

where the invariant mass of the dilepton is $M^2 \equiv P^2 (= p_0^2 - |\vec{p}|^2 = E^2 - |\vec{p}|^2)$, where E is the photon energy.

Now one can perform the q -integration by means of the remaining δ -functions in A and B leading to

$$\begin{aligned}
\frac{dN}{d^4X d^4P} = & \frac{5}{18\pi^4} \frac{\alpha^2}{M^2} \frac{1}{p} \int_0^\infty dk [(p^2 - (k - q_s)^2) (A_1 + A_2 + A_3 + A_5 + A_6 + A_7) \\
& + ((k + q_s)^2 - p^2) (B_1 + B_2 + B_3 + B_5 + B_6 + B_7)]_{|p-k| \leq q_s \leq p+k} , \tag{13.58}
\end{aligned}$$

where the q_s determined by the various δ -functions in (13.55) and (13.56) can assume two different values in the case of the plasmino branch due to the presence of the minimum and

$$\begin{aligned}
A_1 &= n_F(\omega^+(k)) n_F(\omega^-(q_s)) R_+(\omega^+(k), k) \frac{R_-(\omega^-(q_s), q_s)}{|d\omega^-(q)/dq|_{q_s}}, \\
A_2 &= n_F(-\omega^-(k)) n_F(\omega^-(q_s)) R_-(\omega^-(k), k) \frac{R_-(\omega^-(q_s), q_s)}{|d\omega^-(q)/dq|_{q_s}}, \\
A_3 &= n_F(\omega^+(k)) n_F(-\omega^+(q_s)) R_+(\omega^+(k), k) \frac{R_+(\omega^+(q_s), q_s)}{|d\omega^+(q)/dq|_{q_s}}, \\
A_5 &= n_F(\omega^-(k)) n_F(\omega^+(q_s)) R_-(\omega^-(k), k) \frac{R_+(\omega^+(q_s), q_s)}{|d\omega^+(q)/dq|_{q_s}}, \\
A_6 &= n_F(-\omega^+(k)) n_F(\omega^+(q_s)) R_+(\omega^+(k), k) \frac{R_+(\omega^+(q_s), q_s)}{|d\omega^+(q)/dq|_{q_s}}, \\
A_7 &= n_F(\omega^-(k)) n_F(-\omega^-(q_s)) R_-(\omega^-(k), k) \frac{R_-(\omega^-(q_s), q_s)}{|d\omega^-(q)/dq|_{q_s}}, \\
B_1 &= n_F(\omega^+(k)) n_F(\omega^+(q_s)) R_+(\omega^+(k), k) \frac{R_+(\omega^+(q_s), q_s)}{|d\omega^+(q)/dq|_{q_s}}, \\
B_2 &= n_F(-\omega^-(k)) n_F(\omega^+(q_s)) R_-(\omega^-(k), k) \frac{R_+(\omega^+(q_s), q_s)}{|d\omega^+(q)/dq|_{q_s}}, \\
B_3 &= n_F(\omega^+(k)) n_F(-\omega^-(q_s)) R_+(\omega^+(k), k) \frac{R_-(\omega^-(q_s), q_s)}{|d\omega^-(q)/dq|_{q_s}}, \\
B_5 &= n_F(\omega^-(k)) n_F(\omega^-(q_s)) R_-(\omega^-(k), k) \frac{R_-(\omega^-(q_s), q_s)}{|d\omega^-(q)/dq|_{q_s}}, \\
B_6 &= n_F(-\omega^+(k)) n_F(\omega^-(q_s)) R_+(\omega^+(k), k) \frac{R_-(\omega^-(q_s), q_s)}{|d\omega^-(q)/dq|_{q_s}}, \\
B_7 &= n_F(\omega^-(k)) n_F(-\omega^+(q_s)) R_-(\omega^-(k), k) \frac{R_+(\omega^+(q_s), q_s)}{|d\omega^+(q)/dq|_{q_s}},
\end{aligned} \tag{13.59}$$

The group velocity factors in (13.59) follow from the dispersion relation, $\mathcal{D}_\pm(L) = 0$, of (13.13) as

$$\frac{d\omega^\pm(l)}{dl} = \pm \frac{F^\pm(\omega^\pm(l), \mathcal{A}, \mathcal{B}, l)}{G^\pm(\omega^\pm(l), \mathcal{A}, \mathcal{B}, l)}, \tag{13.60}$$

where

$$\begin{aligned}
F^\pm &= (1 + \mathcal{A})^2 (\omega^{\pm 2}(l) - l^2)^3 \mp 6\mathcal{B} (\omega^{\pm 2}(l) - l^2)^2 l \mp \frac{g^2}{6} \mathcal{B} \left(\frac{2}{3} \langle E^2 \rangle_T - \frac{2}{5} \langle B^2 \rangle_T \right) l \\
&\quad \pm \frac{8}{45} g^2 (1 + \mathcal{A}) l \omega^\pm(l) \langle B^2 \rangle_T, \\
G^\pm &= -(1 + \mathcal{A}) C_\pm,
\end{aligned} \tag{13.61}$$

and \mathcal{A} , \mathcal{B} , and C_\pm are given in (13.9a), (13.9b) and (13.21), respectively. As we will see that the group velocity leads to a characteristic feature of the dilepton rate. In (13.58)

we have dropped terms A_4 , A_8 , B_4 and B_8 as the corresponding δ -functions in (13.56) can never be satisfied by virtue of energy conservation since ω^\pm is always positive. Now, one can perform the k -integration in (13.58) numerically, and we find that the terms, which satisfy the energy conservation, correspond to various physical processes involving two quasiparticles with different momentum k and q .

The dilepton production rate for $\vec{p} = 0$ is obtained by setting $\vec{q} = -\vec{k}$ in (13.54) as

$$\begin{aligned} \frac{dN}{d^4X d^4P}(\vec{p} = 0) = & \frac{20}{9\pi^4} \frac{\alpha^2}{M^2} \int_0^\infty dk k^2 \left[n_F^2(\omega^+(k)) R_+^2(\omega^+(k)) \delta(E - 2\omega^+(k)) \right. \\ & + 2n_F(\omega^+(k)) n_F(-\omega^-(k)) R_+(\omega^+(k)) R_-(\omega^-(k)) \delta(E - \omega^+(k) + \omega^-(k)) \\ & + 2n_F(\omega^-(k)) n_F(-\omega^+(k)) R_+(\omega^+(k)) R_-(\omega^-(k)) \delta(E + \omega^+(k) - \omega^-(k)) \\ & \left. + n_F^2(\omega^-(k)) R_-^2(\omega^-(k)) \delta(E - 2\omega^-(k)) \right] . \end{aligned} \quad (13.62)$$

First we would like to discuss the dilepton production from a QGP at momentum $\vec{p} = \mathbf{0}$ of the virtual photon. The different terms in (13.62) correspond to various physical processes involving two quasiparticles q^+ and q^- with same momentum k . The first term represents the annihilation process $q^+ \bar{q}^+ \rightarrow \gamma^*$. The second term corresponds to $q^+ \rightarrow q^- \gamma^*$, a decay process from a q^+ mode to a plasmino plus a virtual photon. Energy conservation does not allow the process given by the third term ($q^- \rightarrow \bar{q}^+ \gamma^*$). Finally, the fourth term corresponds to a process, $q^- \bar{q}^- \rightarrow \gamma^*$, i.e. annihilation of plasmino modes.

The k -integration in (13.62) can be performed using the standard delta function identity

$$\delta(f(x)) = \sum_i \frac{\delta(x - x_i)}{|f'(x)|_{x=x_i}}, \quad (13.63)$$

where x_i are the solutions of $f(x_i) = 0$. After performing the k -integration in (13.62) the expression for the dilepton rate at $\vec{p} = 0$ becomes

$$\begin{aligned} \frac{dN}{d^4X d^4P}(\vec{p} = 0) = & \frac{20}{9\pi^4} \frac{\alpha^2}{M^2} \sum_{k_s} k_s^2 \left[n_F^2(\omega^+(k_s)) R_+^2(\omega^+(k_s)) \frac{1}{2} \left| \frac{d\omega^+(k)}{dk} \right|_{k_s}^{-1} \right. \\ & + 2n_F(\omega^+(k_s)) n_F(-\omega^-(k_s)) R_+(\omega^+(k_s)) R_-(\omega^-(k_s)) \left| \frac{d(\omega^+(k) - \omega^-(k))}{dk} \right|_{k_s}^{-1} \\ & + 2n_F(\omega^-(k_s)) n_F(-\omega^+(k_s)) R_+(\omega^+(k_s)) R_-(\omega^-(k_s)) \left| \frac{d(\omega^-(k) - \omega^+(k))}{dk} \right|_{k_s}^{-1} \\ & \left. + n_F^2(\omega^-(k_s)) R_-^2(\omega^-(k_s)) \frac{1}{2} \left| \frac{d\omega^-(k)}{dk} \right|_{k_s}^{-1} \right] . \end{aligned} \quad (13.64)$$

The static differential rate of the aforementioned processes are displayed in Fig. 40 for $T = 1.1T_c$ (solid line), $2T_c$ (dashed curve) and $4T_c$ (dotted curve). Similar to the hard thermal loop case [80] the differential rate in the presence of a gluon condensate also shows peaks (van Hove singularities¹⁰) at different invariant masses of the virtual photon. Now we discuss the

¹⁰A van Hove peak [163, 164] appears where the density of states diverges due to the vanishing group velocity.

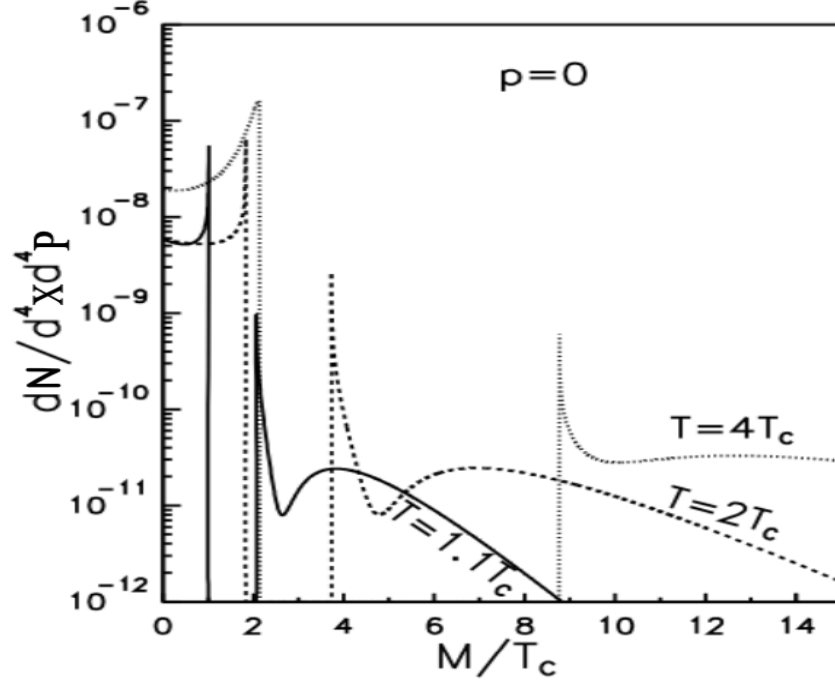


Figure 40: The dilepton rate from QGP with gluon condensate at virtual photon momentum $\vec{p} = 0$. This figure is taken from Ref. [148].

contributions to the rate from each process in detail. The channel, $q^+ \rightarrow q^- \gamma^*$, opens up at $M = 0$. This process continues up to the first peak appears due to the vanishing group velocity $dE/dk = 0$ at the maximum $E = M = \omega^+(k) - \omega^-(k)$, since the density of states is inversely proportional to the group velocity. The $q^+ \rightarrow q^- \gamma^*$ channel terminates at the peak, after which there is a gap because neither of the other processes is possible in this invariant mass regime. The size of the gap depends on the temperature. For $T = 1.1T_c$ it ranges from $M = 1.01T_c$ to $2.07T_c$, for $T = 2T_c$ from $M = 1.83T_c$ to $3.73T_c$, and for $T = 4T_c$ from $M = 2.14T_c$ to $8.76T_c$.

The process, $q^- \bar{q}^- \rightarrow \gamma^*$, starts at an energy which is twice the energy of the minimum of the plasmino branch, $E = M = 2\omega_-(k_{min})$. The diverging density of states at that point again causes a van Hove singularity [80, 163, 164]. This process continues with increasing M but falls off very fast due to two reasons: i) as M increases the high energy plasmino modes come into the game and the corresponding square of the residue $R_-^2(\omega^-(k), k)$, to which the rate is proportional, becomes very small since it is proportional to $(\omega^-(k) - k^2)^6$, and ii) with increasing M the density of states decreases gradually.

At $M = E = 2\omega_+(k) \geq 2m_{eff}$, the process, $q^+ \bar{q}^+ \rightarrow \gamma^*$, shows up. As M increases, the contribution from this process grows and dominates over the plasmino annihilation process, resulting in a dip in the dilepton rate. For large M this annihilation process is solely re-

sponsible for the dilepton rate, which approaches the Born contribution ($q\bar{q}$ annihilation of massless quarks) there [80, 166]:

$$\frac{dN^{\text{Born}}}{d^4X d^4P}(\vec{p}=0) = \frac{5}{18\pi^4} \alpha^2 e^{-E/T} . \quad (13.65)$$

The reason for this is that for high energy quarks the effective propagator reduces to the bare one and the contribution to the dilepton rate comes from hard loop momenta in Fig. 40.

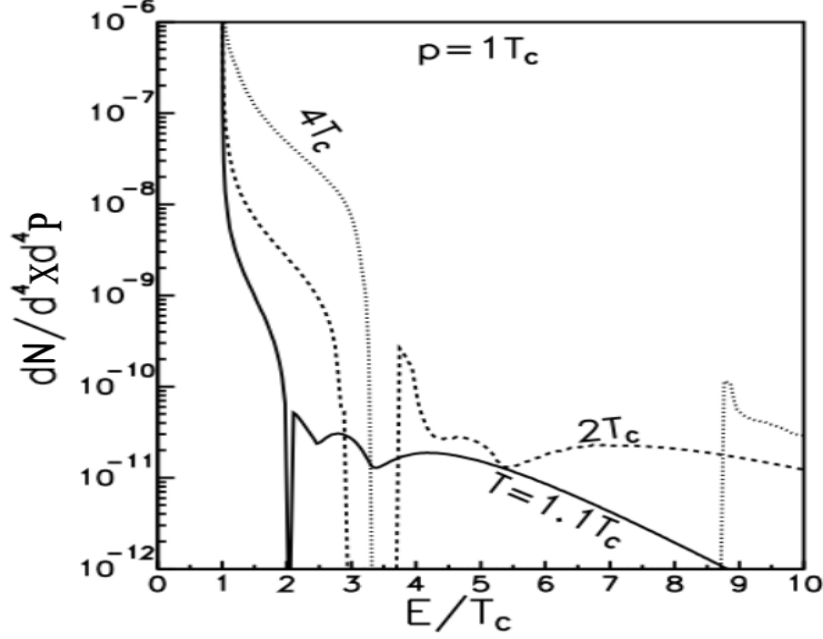


Figure 41: The dilepton rate from QGP with gluon condensate at virtual photon momentum $\vec{p} = T_c$. This figure is taken from Ref. [148].

Next, we turn our attention to the dilepton rate at non-zero virtual photon momentum. The corresponding rate is given in (13.58). The processes corresponding to terms A_2 , A_3 , A_6 , A_7 , B_6 and B_7 , namely transitions within a branch and transitions from the lower to the upper branch, do not contribute to the rate, because they are forbidden for timelike photons decaying into dileptons due to energy conservation [167]. The processes corresponding to A_1 and A_5 indicate annihilation between a quark (q^+) and a plasmino mode (q^-) with different momentum to a virtual photon with energy E , which were absent at $\vec{p} = 0$. The process given by B_1 is the annihilation between a quark and antiquark ($q^+(k)\bar{q}^-(q) \rightarrow \gamma^*$), whereas B_5 corresponds to the annihilation ($q^-(k)\bar{q}^-(q) \rightarrow \gamma^*$) between two plasmino modes. The term B_2 corresponds to the decay process, $q^+(q) \rightarrow q^-(k)\gamma^*$, whereas B_3 corresponds to $q_+(k) \rightarrow q^-(q)\gamma^*$. The differential rate involving these processes are displayed in Fig. 41 for virtual photon momentum $p = T_c$ at different temperatures, namely $T = 1.1T_c$ (solid line), $2T_c$ (dashed line), and $4T_c$ (dotted line).

13.3.3 Dilepton production rate from QGP with Gribov-Zwanziger action

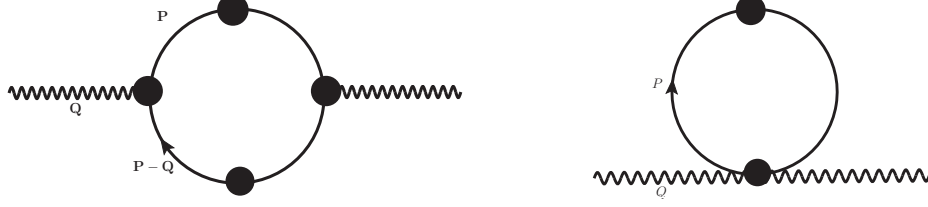


Figure 42: One-loop photon self-energy diagram (left) and tadpole diagram (right) with the effective propagators and vertices with GZ action. These diagrams are taken from Ref. [150].

The general features of non-perturbative GZ action have been discussed in subsec 13.2. Now, in this subsec we want to compute the dilepton production rate [150] with the GZ action from QGP. At one-loop order, the dilepton production rate is associated with photon self-energy and tadpole diagrams as shown in Fig. 42. The contributions to the one-loop photon self-energy can be written from the two diagrams in Fig. 42 as

$$\begin{aligned} \Pi_\mu^\mu(Q) = & -\frac{10}{3}e^2T \sum_{\{p_0\}} \int \frac{d^3p}{(2\pi)^3} \left\{ \text{Tr} \left[S^*(P) \Gamma_\mu(K, Q, -P) S^*(K) \Gamma^\mu(-K, -Q, P) \right] \right. \\ & \left. + \text{Tr} \left[S^*(P) \Gamma_\mu^\mu(-P, P; -Q, Q) \right] \right\}, \end{aligned} \quad (13.66)$$

where $K = P - Q$, S^* is the effective quark propagator as given in (13.35), Γ^μ is the quark-photon vertex as given in (13.38) and Γ_μ^μ are four-point quark-photon vertex as given in (13.42). The second term in (13.66) is due to the tadpole diagram shown in Fig. 42 which eventually does not contribute as $\Gamma_\mu^\mu = 0$. However, the tadpole diagram is essential to satisfy the Ward-Takahashi identity $Q_\mu \Pi^{\mu\nu}(Q) = 0$ and thus the gauge invariance and charge conservation in the system.

Using the N -point functions and performing traces, one obtains the photon self-energy with photon three momentum, $\vec{q} = 0$ as

$$\begin{aligned} \Pi_\mu^\mu(\vec{q} = 0) = & -\frac{10}{3}e^2T \sum_{p_0} \int \frac{d^3p}{(2\pi)^3} \\ & \times \left[\left\{ \frac{(a_G + b_G)^2}{\mathcal{D}_+(\omega_1, p, \gamma_G) \mathcal{D}_-(\omega_2, p, \gamma_G)} + \frac{(a_G - b_G)^2}{\mathcal{D}_-(\omega_1, p, \gamma_G) \mathcal{D}_+(\omega_2, p, \gamma_G)} \right\} \right. \\ & - \left\{ \frac{(c_G + b_G + d_G)^2}{\mathcal{D}_+(\omega_1, p, \gamma_G) \mathcal{D}_-(\omega_2, p, \gamma_G)} + \frac{(c_G - b_G + d_G)^2}{\mathcal{D}_-(\omega_1, p, \gamma_G) \mathcal{D}_+(\omega_2, p, \gamma_G)} \right\} \\ & \left. - 2c_G^2 \left\{ \frac{1}{\mathcal{D}_+(\omega_1, p, \gamma_G) \mathcal{D}_+(\omega_2, p, \gamma_G)} + \frac{1}{\mathcal{D}_-(\omega_1, p, \gamma_G) \mathcal{D}_-(\omega_2, p, \gamma_G)} \right\} \right] \end{aligned} \quad (13.67)$$

where \mathcal{D}_\pm are given, respectively, in (13.36a) and (13.36b) whereas a_G , b_G , c_G and d_G are given, respectively, in (13.40a), (13.40b), (13.40c) and (13.40d).

Now using the BPY prescription [80] given in (13.52) or in (A.23) in appendix A.3 we first find out the imaginary or discontinuous part of the (13.67) and then performing some more algebra, we write down the dilepton production rate with massless leptons following (13.49) as

$$\begin{aligned} \frac{dR}{d\omega d^3q}(\vec{q}=0) &= \frac{20\alpha^2}{9\pi^4} \frac{1}{\omega^2} \int_0^\infty p^2 dp \int_{-\infty}^\infty d\omega_1 \int_{-\infty}^\infty d\omega_2 n_F(\omega_1) n_F(\omega_2) \delta(\omega - \omega_1 - \omega_2) \\ &\quad \left[4 \left(1 - \frac{\omega_1^2 - \omega_2^2}{2p\omega} \right)^2 \rho_+^G(\omega_1, p) \rho_-^G(\omega_2, p) \right. \\ &\quad + \left(1 + \frac{\omega_1^2 + \omega_2^2 - 2p^2 - 2m_q^2(\gamma_G)}{2p\omega} \right)^2 \rho_+^G(\omega_1, p) \rho_+^G(\omega_2, p) \\ &\quad \left. + \left(1 - \frac{\omega_1^2 + \omega_2^2 - 2p^2 - 2m_q^2(\gamma_G)}{2p\omega} \right)^2 \rho_-^G(\omega_1, p) \rho_-^G(\omega_2, p) \right], \quad (13.68) \end{aligned}$$

where ω is the photon energy and ρ_\pm^G are the spectral functions in presence of Gribov term given in (13.37). Using (13.37) one can obtain the dilepton production rate as

$$\begin{aligned} \left. \frac{dR}{d\omega d^3q} \right|^{pp}(\vec{q}=0) &= \frac{20\alpha^2}{9\pi^4} \frac{1}{\omega^2} \int_0^\infty p^2 dp \times \\ &\quad \left[\delta(\omega - 2\omega_+) n_F^2(\omega_+) \left(\frac{\omega_+^2 - p^2}{2m_q^2(\gamma_G)} \right)^2 \left\{ 1 + \frac{\omega_+^2 - p^2 - m_q^2(\gamma_G)}{p\omega} \right\}^2 \right. \\ &\quad + \delta(\omega - 2\omega_-) n_F^2(\omega_-) \left(\frac{\omega_-^2 - p^2}{2m_q^2(\gamma_G)} \right)^2 \left\{ 1 - \frac{\omega_-^2 - p^2 - m_q^2(\gamma_G)}{p\omega} \right\}^2 \\ &\quad + \delta(\omega - 2\omega_G) n_F^2(\omega_G) \left(\frac{\omega_G^2 - p^2}{2m_q^2(\gamma_G)} \right)^2 \left\{ 1 - \frac{\omega_G^2 - p^2 - m_q^2(\gamma_G)}{p\omega} \right\}^2 \\ &\quad + 4 \delta(\omega - \omega_+ - \omega_-) n_F(\omega_+) n_F(\omega_-) \left(\frac{\omega_+^2 - p^2}{2m_q^2(\gamma_G)} \right) \left(\frac{\omega_-^2 - p^2}{2m_q^2(\gamma_G)} \right) \\ &\quad \times \left\{ 1 - \frac{\omega_+^2 - \omega_-^2}{2p\omega} \right\}^2 \\ &\quad + \delta(\omega - \omega_+ + \omega_-) n_F(\omega_+) n_F(-\omega_-) \left(\frac{\omega_+^2 - p^2}{2m_q^2(\gamma_G)} \right) \left(\frac{\omega_-^2 - p^2}{2m_q^2(\gamma_G)} \right) \\ &\quad \left. \times \left\{ 1 + \frac{\omega_+^2 + \omega_-^2 - 2p^2 - 2m_q^2(\gamma_G)}{2p\omega} \right\}^2 \right]. \quad (13.69) \end{aligned}$$

The momentum integration in (13.69) can be performed using the standard delta function identity given in (13.63). Now, inspecting the arguments of the various energy conserving δ -functions in (13.69) one can understand the physical processes originating from the poles

of the propagator. The first three terms in (13.69) correspond to the annihilation processes of $q_+\bar{q}_+ \rightarrow \gamma^*$, $q_-\bar{q}_- \rightarrow \gamma^*$, and $q_G\bar{q}_G \rightarrow \gamma^*$, respectively. The fourth term corresponds to the annihilation of $q_+\bar{q}_- \rightarrow \gamma^*$. On the other hand, the fifth term corresponds to a process, $q_+ \rightarrow q_-\gamma^*$, where a q_+ mode makes a transition to a q_- mode along with a virtual photon. These processes involve soft quark modes (q_+ , q_- , and q_G and their antiparticles) which originate by cutting the self-energy diagram in Fig. 42 through the internal lines without a “blob”. The virtual photon, γ^* , in all these five processes decays to lepton pair and can be visualized from the dispersion plot as displayed in the Fig. 43.

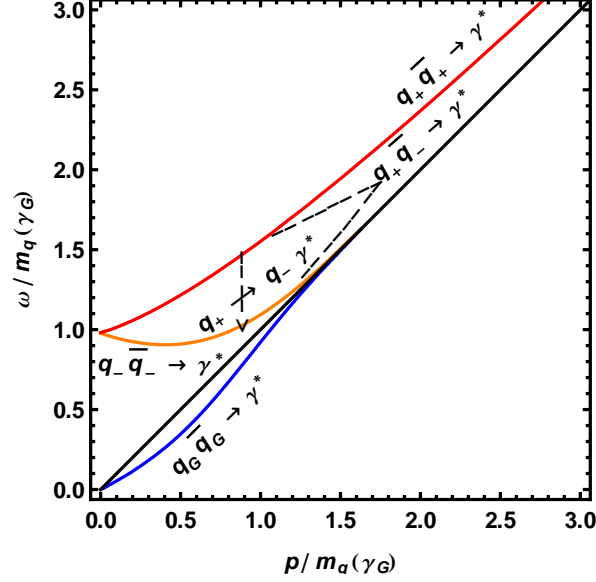


Figure 43: Various dilepton processes originate from the in-medium dispersion of quasiparticles with Gribov term are displayed. This figure is taken from Ref. [150].

The contribution of various individual processes to the dilepton production rate in presence of the Gribov term are displayed in the Fig. 44. The transition process, $q_+ \rightarrow q_-\gamma^*$, begins at the energy $\omega = 0$ and ends up with a van-Hove peak where all of the transitions from q_+ branch are directed towards the minimum of the q_- branch. The annihilation process involving the massless spacelike Gribov modes, $q_G\bar{q}_G \rightarrow \gamma^*$, also starts at $\omega = 0$ and falls-off very quickly. The annihilation of the two plasmino modes, $q_-\bar{q}_- \rightarrow \gamma^*$, opens up with again a van-Hove peak at $\omega = 2 \times$ the minimum energy of the plasmino mode. The contribution of this process decreases exponentially. At $\omega = 2m_q(\gamma_G)$, the annihilation processes involving usual quark modes, $q_+\bar{q}_+ \rightarrow \gamma^*$, and that of a quark and a plasmino mode, $q_+\bar{q}_- \rightarrow \gamma^*$, begin. However, the former one ($q_+\bar{q}_+ \rightarrow \gamma^*$) grows with the energy and would converge to the usual Born rate (leading order perturbative rate) [166] at high mass whereas the later one ($q_+\bar{q}_- \rightarrow \gamma^*$) initially grows at a very fast rate, but then decreases slowly and finally drops very quickly. The behavior of the latter process can easily be understood from the dispersion

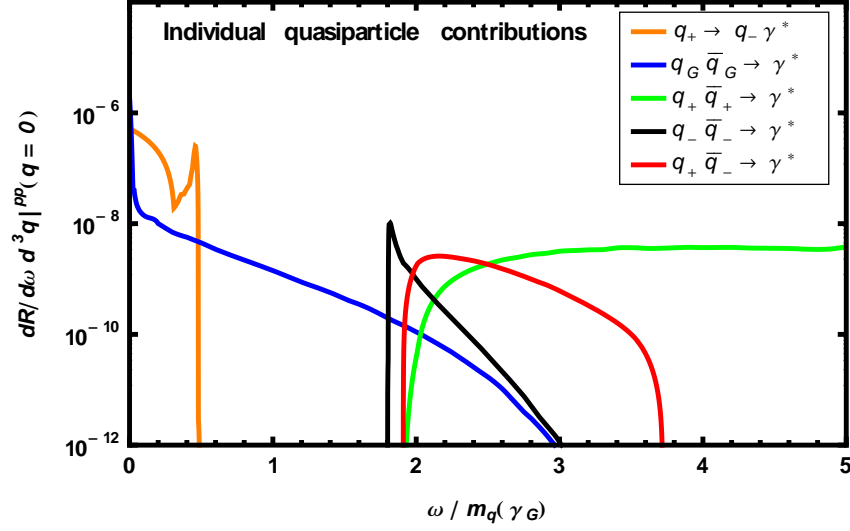


Figure 44: The dilepton production rates corresponding to quasiparticle processes in Fig. 43. This figure is taken from Ref. [150].

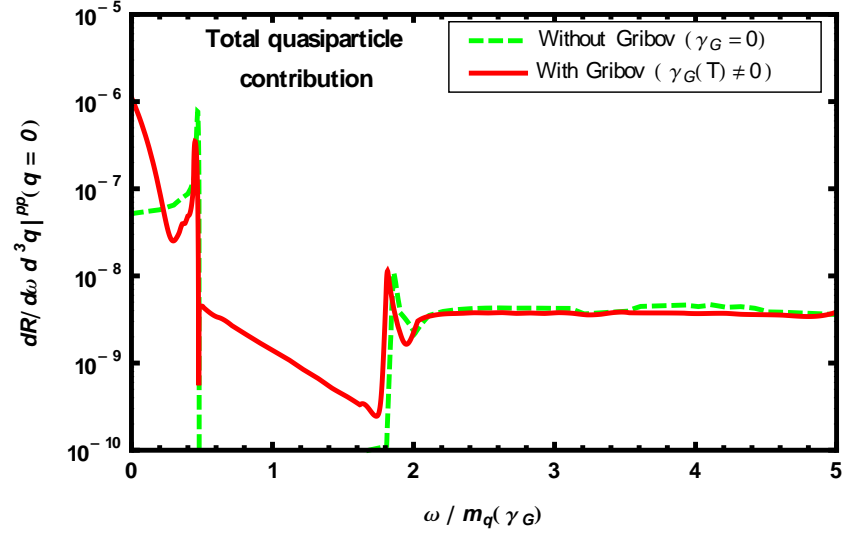


Figure 45: Comparison of dilepton production rates involving various quasiparticle modes with and without inclusion of γ_G . This figure is taken from Ref. [150].

properties of quark and plasmino mode. Summing up, the total contribution of all these five processes is displayed in Fig. 45. This is compared with the similar dispersive contribution when $\gamma_G = 0$ [80], comprising processes $q_+ \rightarrow q_- \gamma^*$, $q_+ \bar{q}_+ \rightarrow \gamma^*$, $q_- \bar{q}_- \rightarrow \gamma^*$ and $q_+ \bar{q}_- \rightarrow \gamma^*$. We note that when $\gamma_G = 0$, the dilepton rate contains both van-Hove peaks and an energy

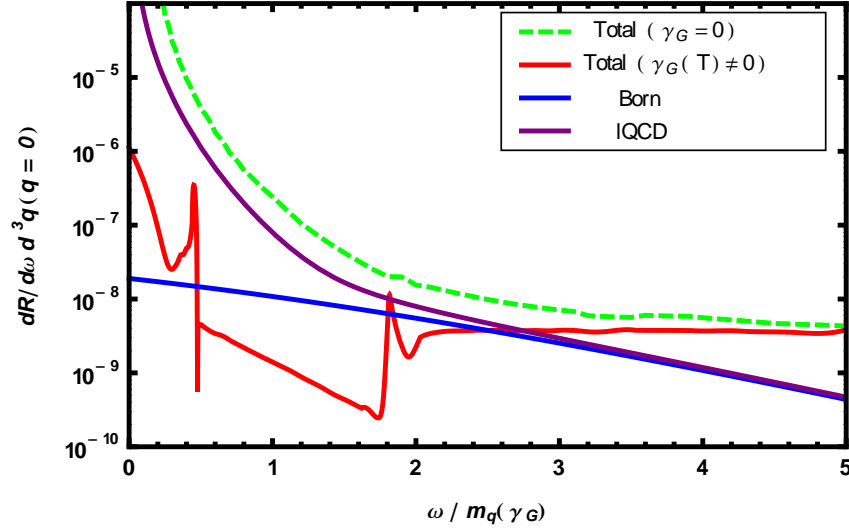


Figure 46: Comparison of various dilepton production rates from the deconfined matter. This figure is taken from Ref. [150].

gap [80]. In presence of the Gribov term ($\gamma_G \neq 0$), the van-Hove peaks remain, but the energy gap disappears due to the annihilation of new massless Gribov modes, $q_G \bar{q}_G \rightarrow \gamma^*$. This new contribution could be important for low mass dilepton spectra.

In Fig. 46 we compare the rates obtained using various approximations: leading-order perturbative (Born) rate [166], quenched lattice QCD (lQCD) rate [168, 169], and with and without the Gribov term. The non-perturbative rate with the Gribov term shows important structures compared to the Born rate at low energies. But when compared to the total HTLpt rate¹¹ it is suppressed in the low mass region due to the absence of Landau cut contribution for $\gamma_G \neq 0$. It seems as if the higher order Landau cut contribution due to spacelike momenta for $\gamma_G = 0$ is replaced by the soft process involving spacelike Gribov modes in the collective excitations for $\gamma_G \neq 0$. We also note that the dilepton rate [170] using the spectral function constructed with two pole ansatz by analyzing lQCD propagator in quenched approximation [160, 161] shows similar structure as found here for $\gamma_G \neq 0$. On the other hand, such structure at low mass is also expected in the direct computation of dilepton rate from lQCD in quenched approximation [168, 169].

¹¹The HTL spectral function (i.e., $\gamma_G = 0$) has both pole and Landau cut contribution as obtained in 9.94. Therefore, the HTLpt dilepton rate [80] contains an additional *higher order* contribution due to the Landau cut stemming from spacelike momenta.

14 Conclusion

In this review article some basics of the thermal field theory within the imaginary time formalism have been discussed in details. The imaginary time formalism has been introduced through two methods: the operatorial and the path integral methods. The prescriptions to calculate the discrete frequency have been discussed. The Green's function has been obtained both in real and imaginary time. The self-energy in ϕ^3 theory and the tadpole diagram in $\lambda\phi^4$ theory have been calculated and their implications have been discussed. The partition function for non-interacting scalar, fermion, photon field and interacting scalar field have been computed using the functional integration approach. The general characteristics of a material medium in presence of a thermal bath have been outlined in details. We have computed the two-point functions for fermions and gauge bosons in HTL approximation for both QED and QCD. The collective excitations in both QED and QCD plasma have also been discussed. We have discussed some subtleties in finite temperature field theory and shortcomings of naive perturbation theory. Then we introduced the HTL resummation and HTL perturbation theory. The HTLpt has been applied to calculate the LO, NLO and NNLO free energy and pressure of deconfined QCD medium produced in high energy heavy-ion collisions. For interested readers, I have also provided an extensive list of literatures for the application of HTLpt to the various properties of deconfined QCD matter. Then we have discussed the general properties of hot QCD medium in presence of non-perturbative effects like gluon condensate and Gribov-Zwanziger term. The collective excitations of deconfined QCD medium have also been discussed in the presence of non-perturbative effects. Finally, we computed the dilepton production rate from deconfined QCD medium with those non-perturbative effects. Also some useful literatures have been provided for the application of thermal field theory beyond QCD, viz., the phase transitions involving symmetry restoration in theories with spontaneously broken symmetry, the evolution of the universe at early times and cosmology, thermal neutrino production, neutrino oscillations, leptogenesis, $\mathcal{N} = 4$ supersymmetric Yang-Mills theory, string theory and Anti de-sitter space/Conformal Field Theory (Ads/CFT) correspondence, blackhole physics, thermal axion production and condensed matter physics.

A Appendix

A.1 One-loop Fermionic Sum Integrals

The dimensionally regularized fermionic sum-integrals are defined as,

$$\not{\sum}_{\{P\}} = \left(\frac{e^{\gamma_E} \Lambda^2}{4\pi} \right)^\epsilon T \sum_{\substack{\{p_0=i\omega_n\} \\ \omega_n=(2n+1)\pi T-i\mu}} \int \frac{d^{d-2\epsilon}p}{(2\pi)^{d-2\epsilon}}, \quad (\text{A.1})$$

where $d - 2\epsilon$ is the spatial dimension, P is the fermion loop momentum, Λ is the $\overline{\text{MS}}$ renormalization scale that introduces the factor $(\frac{e^{\gamma_E}}{4\pi})^\epsilon$ along with it, where γ_E being the Euler-Mascheroni constant.

The result of various fermionic sum-integrals are listed below:

$$2 \oint_{\{P\}} \ln(P^2) = \frac{7\pi^2 T^4}{180} + \frac{\mu^2 T^2}{6} + \frac{\mu^4}{12\pi^2} = \frac{7\pi^2 T^4}{180} \left(1 + \frac{120}{7} \hat{\mu}^2 + \frac{240}{7} \hat{\mu}^4 \right), \quad (\text{A.2a})$$

$$\oint_{\{P\}} \frac{1}{P^2} = \frac{T^2}{24} \left(\frac{\Lambda}{4\pi T} \right)^{2\epsilon} [1 + 12\hat{\mu}^2 + 2\epsilon(1 + 12\hat{\mu}^2 + 12\aleph(1, z))], \quad (\text{A.2b})$$

$$\oint_{\{P\}} \frac{1}{P^4} = \frac{1}{(4\pi)^2} \left(\frac{\Lambda}{4\pi T} \right)^{2\epsilon} \left[\frac{1}{\epsilon} - \aleph(z) \right], \quad (\text{A.2c})$$

$$\oint_{\{P\}} \frac{1}{p^2 P^2} = -\frac{2}{d-2} \oint_{\{P\}} \frac{1}{P^4}, \quad (\text{A.2d})$$

$$\oint_{\{P\}} \frac{1}{p^2 P^2} \mathcal{T}_P = -\frac{2\Delta_3}{d-2} \oint_{\{P\}} \frac{1}{P^4}, \quad (\text{A.2e})$$

$$\oint_{\{P\}} \frac{1}{p^2 P^2} \mathcal{T}_P^2 = -\frac{2\Delta_4''}{d-2} \oint_{\{P\}} \frac{1}{P^4}, \quad (\text{A.2f})$$

$$\oint_{\{P\}} \frac{1}{p_0^2 P^2} \mathcal{T}_P^2 = -\frac{2\Delta_3''}{d-2} \oint_{\{P\}} \frac{1}{P^4}, \quad (\text{A.2g})$$

where the angular integrations are given as

$$\begin{aligned} \Delta_3 &= \left\langle \frac{1 - c^{4-d}}{1 - c^2} \right\rangle_c = \ln 2 + \left(\frac{\pi^2}{6} - (2 - \ln 2) \ln 2 \right) \epsilon \\ &\quad + \left\{ \frac{2}{3} (\ln 2)^2 (\ln 2 - 3) + \frac{\pi^2}{3} (\ln 2 - 1) + \zeta(3) \right\} \epsilon^2 + \mathcal{O}[\epsilon]^3, \end{aligned} \quad (\text{A.3a})$$

$$\Delta_3'' = \left\langle \frac{1 - c_1^{4-d}}{(1 - c_1^2)(c_1^2 - c_2^2)} + c_1 \leftrightarrow c_2 \right\rangle_{c_1, c_2} = -\frac{\pi^2}{12} + \left(\frac{\pi^2}{3} - \frac{\zeta(3)}{2} \right) \epsilon + \mathcal{O}(\epsilon^2), \quad (\text{A.3b})$$

$$\begin{aligned} \Delta_4'' &= \left\langle \frac{1 - c_1^{6-d}}{(1 - c_1^2)(c_1^2 - c_2^2)} + c_1 \leftrightarrow c_2 \right\rangle_{c_1, c_2} \\ &= -\frac{\pi^2}{12} + \ln 4 + \left(\frac{\pi^2}{3} - \ln 4 (2 - \ln 2) - \frac{\zeta(3)}{2} \right) \epsilon + \mathcal{O}(\epsilon^2), \end{aligned} \quad (\text{A.3c})$$

with

$$\aleph(z) = -2\gamma_E - 4\ln 2 + 14\zeta(3)\hat{\mu}^2 - 62\zeta(5)\hat{\mu}^4 + 254\zeta(7)\hat{\mu}^6 + \mathcal{O}(\hat{\mu}^8), \quad (\text{A.4a})$$

$$\begin{aligned} \aleph(1, z) = & -\frac{1}{12} \left(\ln 2 - \frac{\zeta'(-1)}{\zeta(-1)} \right) - (1 - 2\ln 2 - \gamma_E) \hat{\mu}^2 - \frac{7}{6} \zeta(3) \hat{\mu}^4 \\ & + \frac{31}{15} \zeta(5) \hat{\mu}^6 + \mathcal{O}(\hat{\mu}^8). \end{aligned} \quad (\text{A.4b})$$

A.2 One-loop Bosonic Sum Integrals

The dimensionally regularized bosonic sum-integrals are defined as,

$$\oint_P = \left(\frac{e^{\gamma_E} \Lambda^2}{4\pi} \right)^\epsilon T \sum_{\substack{p_0=i\omega_n \\ \omega_n=2n\pi T}} \int \frac{d^{d-2\epsilon} p}{(2\pi)^{d-2\epsilon}}, \quad (\text{A.5})$$

where $d-2\epsilon$ is the spatial dimension, P is the boson loop momentum, Λ is the $\overline{\text{MS}}$ renormalization scale that introduces the factor $\left(\frac{e^{\gamma_E}}{4\pi} \right)^\epsilon$ along with it, where γ_E being the Euler-Mascheroni constant.

Below we list various bosonic sum-integrals:

$$\oint_P \frac{1}{P^2} = -\frac{T^2}{12} \left(\frac{\Lambda}{4\pi T} \right)^{2\epsilon} \left[1 + 2\epsilon \left(1 + \frac{\zeta'(-1)}{\zeta(-1)} \right) + \mathcal{O}[\epsilon]^2 \right], \quad (\text{A.6a})$$

$$\oint_P \frac{1}{p^2 P^2} = -\frac{2}{(4\pi)^2} \left(\frac{\Lambda}{4\pi T} \right)^{2\epsilon} \left[\frac{1}{\epsilon} + 2\gamma_E + 2 + \epsilon \left(4 + 4\gamma_E + \frac{\pi^2}{4} - 4\gamma_1 \right) + \mathcal{O}[\epsilon]^2 \right], \quad (\text{A.6b})$$

$$\oint_P \frac{1}{P^4} = \frac{1}{(4\pi)^2} \left(\frac{\Lambda}{4\pi T} \right)^{2\epsilon} \left[\frac{1}{\epsilon} + 2\gamma_E + \epsilon \left(\frac{\pi^2}{4} - 4\gamma_1 \right) + \mathcal{O}[\epsilon]^2 \right], \quad (\text{A.6c})$$

$$\oint_P \frac{\mathcal{T}_P}{p^4} = -\frac{1}{(4\pi)^2} \left(\frac{\Lambda}{4\pi T} \right)^{2\epsilon} \left[\frac{1}{\epsilon} + 2\gamma_E + 2\ln 2 + \mathcal{O}[\epsilon] \right], \quad (\text{A.6d})$$

$$\oint_P \frac{\mathcal{T}_P}{p^2 P^2} = -\frac{1}{(4\pi)^2} \left(\frac{\Lambda}{4\pi T} \right)^{2\epsilon} \left[2\ln 2 \left(\frac{1}{\epsilon} + 2\gamma_E \right) + 2\ln^2 2 + \frac{\pi^2}{3} + \mathcal{O}[\epsilon] \right], \quad (\text{A.6e})$$

$$\oint_P \frac{\mathcal{T}_P^2}{p^4} = -\frac{2}{3} \frac{1}{(4\pi)^2} \left(\frac{\Lambda}{4\pi T} \right)^{2\epsilon} \left[(1 + 2\ln 2) \left(\frac{1}{\epsilon} + 2\gamma_E \right) - \frac{4}{3} + \frac{22}{3} \ln 2 + 2\ln^2 2 + \mathcal{O}[\epsilon] \right]. \quad (\text{A.6f})$$

A.3 Braaten-Pisarski-Yuan (BPY) Prescription

Lets consider a complex function $f(z)$ having branch cut

$$f(z) = \frac{1}{2\pi i} \oint \frac{f(\xi) d\xi}{\xi - z}. \quad (\text{A.7})$$

considering $\xi = x + i\epsilon$, one can write

$$f(z) = \frac{1}{2\pi i} \int_{-\infty}^{+\infty} \frac{f(x+i\epsilon) - f(x-i\epsilon)}{x-z} dx = \frac{1}{2\pi i} \int_{-\infty}^{+\infty} \frac{\text{Disc}f(x+i\epsilon)}{x-z} dx. \quad (\text{A.8})$$

where the discontinuity is related to the imaginary part of a complex function as

$$\text{Disc}f(x+i\epsilon) = f(x+i\epsilon) - f(x-i\epsilon) = 2i \text{Im}f(x+i\epsilon). \quad (\text{A.9})$$

Combining (A.8) and (A.9) one can write

$$f(z) = \frac{1}{\pi} \int_{-\infty}^{+\infty} \frac{\text{Im}f(x+i\epsilon)}{x-z} dx = \int_{-\infty}^{+\infty} \frac{\rho(x)}{x-z} dx \quad (\text{A.10})$$

where the spectral density ρ is defined as

$$\rho(x) = \frac{1}{\pi} \text{Im}f(x+i\epsilon). \quad (\text{A.11})$$

The spectral density $\rho_1(\omega_1)$ is related to the any complex function $F_1(k_0)$ as given in (A.10)

$$F_1(k_0) = \int_{-\infty}^{+\infty} \frac{\rho_1(\omega_1) d\omega_1}{\omega_1 - k_0 - i\epsilon_1}. \quad (\text{A.12})$$

We note that $K \equiv (k_0, \vec{k})$ is the fermionic momentum with $k_0 = (2m+1)i\pi T$.

Lets have,

$$\int_0^{1/T} d\tau_1 e^{x\tau_1} = \frac{e^{x/T} - 1}{x} \Rightarrow \frac{1}{x} = \frac{1}{e^{x/T} - 1} \int_0^{1/T} d\tau_1 e^{x\tau_1}, \quad (\text{A.13})$$

where T is the temperature. Now, considering $x = (\omega_1 - k_0 - i\epsilon_1)$ one can write (A.13) as

$$\frac{1}{\omega_1 - k_0 - i\epsilon_1} = \frac{1}{e^{\frac{(\omega_1 - k_0)}{T}} - 1} \int_0^{1/T} d\tau_1 e^{(\omega_1 - k_0 - i\epsilon_1)\tau_1}. \quad (\text{A.14})$$

Combining (A.14) with (A.12), one gets

$$F_1(k_0) = \int_{-\infty}^{+\infty} \frac{\rho_1(\omega_1) d\omega_1}{e^{\frac{(\omega_1 - k_0)}{T}} - 1} \int_0^{1/T} d\tau_1 e^{(\omega_1 - k_0 - i\epsilon_1)\tau_1}. \quad (\text{A.15})$$

Now, using $e^{k_0/T} = e^{(2m+1)i\pi} = -1$, one can write as

$$\begin{aligned} F_1(k_0) &= - \int_{-\infty}^{+\infty} \frac{\rho_1(\omega_1) d\omega_1}{e^{\frac{\omega_1}{T}} - 1} \int_0^{1/T} d\tau_1 e^{(\omega_1 - k_0 - i\epsilon_1)\tau_1} \\ &= - \int_{-\infty}^{+\infty} n_F(\omega_1) \rho_1(\omega_1) d\omega_1 \int_0^{1/T} d\tau_1 e^{(\omega_1 - k_0 - i\epsilon_1)\tau_1}. \end{aligned} \quad (\text{A.16})$$

Similarly, one can write another complex function $F_2(q_0)$ as

$$F_2(q_0) = - \int_{-\infty}^{+\infty} n_F(\omega_2) \rho_2(\omega_2) d\omega_2 \int_0^{1/T} d\tau_2 e^{(\omega_2 - q_0 - i\epsilon_2)\tau_2}, \quad (\text{A.17})$$

where $q_0 = (p_0 - k_0)$ and P is the bosonic momentum with $p_0 = 2mi\pi T$.

We would like to compute the imaginary part of the product of two complex functions $T \sum_{k_0} F_1(k_0) F_2(q_0)$:

$$\begin{aligned} \text{Im } T \sum_{k_0} F_1(k_0) F_2(q_0) &= \text{Im } T \sum_{k_0} \int_{-\infty}^{+\infty} d\omega_1 \int_{-\infty}^{+\infty} d\omega_2 n_F(\omega_1) n_F(\omega_2) \rho_1(\omega_1) \rho_2(\omega_2) \\ &\quad \times \int_0^{1/T} d\tau_1 \int_0^{1/T} d\tau_2 e^{(\omega_1 - k_0 - i\epsilon_1)\tau_1} e^{(\omega_2 - q_0 - i\epsilon_2)\tau_2} \\ &= \text{Im} \int_{-\infty}^{+\infty} d\omega_1 \int_{-\infty}^{+\infty} d\omega_2 n_F(\omega_1) n_F(\omega_2) \rho_1(\omega_1) \rho_2(\omega_2) \\ &\quad \times \int_0^{1/T} d\tau_1 \int_0^{1/T} d\tau_2 e^{(\omega_1 - i\epsilon_1)\tau_1} e^{(\omega_2 - p_0 - i\epsilon_2)\tau_2} \underbrace{T \sum_{k_0} e^{-k_0(\tau_1 - \tau_2)}}_{\delta(\tau_1 - \tau_2)} \end{aligned} \quad (\text{A.18})$$

Performing τ_2 -integration using δ -function, one can write

$$\begin{aligned} \text{Im } T \sum_{k_0} F_1(k_0) F_2(q_0) &= \text{Im} \int_{-\infty}^{+\infty} d\omega_1 \int_{-\infty}^{+\infty} d\omega_2 n_F(\omega_1) n_F(\omega_2) \rho_1(\omega_1) \rho_2(\omega_2) \\ &\quad \times \int_0^{1/T} d\tau_1 e^{(\omega_1 + \omega_2 - p_0 - i\epsilon)\tau_1}, \end{aligned} \quad (\text{A.19})$$

where $\epsilon = \epsilon_1 + \epsilon_2$. Now performing the τ_1 -integration, one gets

$$\begin{aligned} \text{Im } T \sum_{k_0} F_1(k_0) F_2(q_0) &= \text{Im} \int_{-\infty}^{+\infty} d\omega_1 \int_{-\infty}^{+\infty} d\omega_2 n_F(\omega_1) n_F(\omega_2) \rho_1(\omega_1) \rho_2(\omega_2) \\ &\quad \times \frac{e^{(\omega_1 + \omega_2 - p_0)/T} - 1}{\omega_1 + \omega_2 - p_0 - i\epsilon} \\ &= \int_{-\infty}^{+\infty} d\omega_1 \int_{-\infty}^{+\infty} d\omega_2 n_F(\omega_1) n_F(\omega_2) \rho_1(\omega_1) \rho_2(\omega_2) \\ &\quad \times \left(e^{(\omega_1 + \omega_2 - p_0)/T} - 1 \right) \text{Im} \left(\frac{1}{\omega_1 + \omega_2 - p_0 - i\epsilon} \right). \end{aligned} \quad (\text{A.20})$$

Now using

$$e^{-p_0/T} = e^{-2m\pi i} = 1, \quad (\text{A.21a})$$

$$p_0 = \omega + i\epsilon', \quad (\text{A.21b})$$

$$\frac{1}{\omega_1 + \omega_2 - p_0 - i\epsilon} = \frac{1}{\omega_1 + \omega_2 - \omega - i\epsilon' - i\epsilon} = \frac{1}{\omega_1 + \omega_2 - \omega - i\epsilon''}, \quad (\text{A.21c})$$

$$\text{Im} \left(\frac{1}{\omega_1 + \omega_2 - \omega - i\epsilon''} \right) = -\pi \delta(\omega_1 + \omega_2 - \omega), \quad (\text{A.21d})$$

one gets

$$\begin{aligned} \text{Im} \ T \sum_{k_0} F_1(k_0) F_2(q_0) &= -\pi \int_{-\infty}^{+\infty} d\omega_1 \int_{-\infty}^{+\infty} d\omega_2 \ n_F(\omega_1) n_F(\omega_2) \rho_1(\omega_1) \rho_2(\omega_2) \\ &\quad \times \left(e^{(\omega_1 + \omega_2)/T} - 1 \right) \delta(\omega_1 + \omega_2 - \omega) \\ &= \pi \left(1 - e^{\beta\omega} \right) \int_{-\infty}^{+\infty} d\omega_1 \int_{-\infty}^{+\infty} d\omega_2 \ n_F(\omega_1) n_F(\omega_2) \\ &\quad \times \rho_1(\omega_1) \rho_2(\omega_2) \delta(\omega_1 + \omega_2 - \omega), \end{aligned} \quad (\text{A.22})$$

where $\beta = 1/T$.

We finally obtain following (A.9) and (A.22), the discontinuity or the imaginary part of a product of two complex functions [80] as

$$\begin{aligned} \text{Disc} \ T \sum_{k_0} F_1(k_0) F_2(q_0) &= 2i \ \text{Im} \ T \sum_{k_0} F_1(k_0) F_2(q_0) \\ &= 2\pi i \left(1 - e^{\beta\omega} \right) \int_{-\infty}^{+\infty} d\omega_1 \int_{-\infty}^{+\infty} d\omega_2 \ n_F(\omega_1) n_F(\omega_2) \\ &\quad \times \rho_1(\omega_1) \rho_2(\omega_2) \delta(\omega_1 + \omega_2 - \omega). \end{aligned} \quad (\text{A.23})$$

Acknowledgement: I would like to thank Aritra Bandyopadhyay, Aritra Das, Bithika Kar-makar, Chowdhury Aminul Islam, Najmul Haque and Ritesh Ghosh for various discussions and help received during the preparation of this article. It is also a great pleasure to acknowledge the support received from Sanjay Ghosh and Rajarshi Ray who were tutors of my lectures given at SERC Advanced School on Theoretical High Energy Physics, November 16-December 5, 2015 at Birla institute of Technology, Pilani, India. Finally, I would like to thank Department of Atomic Energy, Government of India for the project TPAES in Theory division of Saha Institute of Nuclear Physics.

Data Availability Statement: No Data associated in the manuscript.

References

- [1] T. Matsubara, *A new approach to quantum statistical mechanics*, Prog. Theor. Phys. **14** (1955) 351.
- [2] J. Schwinger, *Brownian motion of a quantum oscillator*, J. Math. Phys. **2** (1961) 407; J. Schwinger, *Lecture Notes Of Brandeis University Summer Institute* (1960).
- [3] L. V. Keldysh, *Diagram technique for non-equilibrium processes*, Zh. Eksp. Teor. Fiz. **47** (1964) 1515.
- [4] H. Umezawa, H. Matsumoto and M. Tachiki, *Thermo Field Dynamics and Condensed States*, North-Holland, Amsterdam, 1982.
- [5] R. Kubo, *Statistical mechanical theory of irreversible processes; 1. General theory and simple applications in magnetic and conduction problems*, J. Phys. Soc. Jap. **12** (1957) 570.
- [6] A. L. Fetter and J. D. Walecka, *Quantum Theory of Many Particle Systems*, McGraw-Hill (1971).
- [7] A. A. Abrikosov, L. P. Gorkov and I. E. Dzyaloshinski, *Methods of Quantum Field Theory in Statistical Physics*, Dover (1975).
- [8] L. Dolan and R. Jackiw, *Symmetry Behavior at Finite Temperature*, Phys. Rev. D **9** (1974) 3320.
- [9] S. Weinberg, *Gauge and Global Symmetries at High Temperature*, Phys. Rev. D **9** (1974) 3357.
- [10] D. J. Gross, R. D. Pisarski and L. G. Yaffe, *QCD and Instantons at Finite Temperature*, Rev. Mod. Phys. **53** (1981) 43.
- [11] N. P. Landsman and C. G. van Weert, *Real and Imaginary Time Field Theory at Finite Temperature and Density*, Phys. Rep. **145** (1987) 141.
- [12] Ashok Das, *Finite Temperature Field Theory*, World Scientific, 1997.
- [13] J. I. Kapusta and C. Gale, *Finite-Temperature Field Theory: Principles and Applications*, Second Edition, Cambridge Monographs on Mathematical Physics, (2006).
- [14] M. Le-Bellac *Thermal Field Theory*, Cambridge Monographs on Mathematical Physics (2011) .
- [15] D. A. Kirzhnits and A. D. Linde, *Macroscopic Consequences of the Weinberg Model*, Phys. Lett. B **42** (1979) 471.
- [16] M. Laine, *Finite temperature field theory- with application to cosmology*, ICTP Lect. Notes Ser. **14** (2003) 189.
- [17] M. S. Turner, *The Case for $\Omega(M) = 0.33 \pm 0.035$* , Astrophys. J. Lett. **576** (2002) L101.
- [18] V. A. Kuzmin, V. A. Rubakov and M. E. Shaposhnikov, *On the Anomalous Electroweak Baryon Number Nonconservation in the Early Universe*, Phys. Lett. B **155** (1985) 36.
- [19] M. E. Shaposhnikov, *Baryon Asymmetry of the Universe in Standard Electroweak Theory* Nucl. Phys. B **287** (1987) 757.
- [20] S. Weinberg, *Gravitation and Cosmology*, Wiley, New-York, 1972.
- [21] R. Baier, E. Pilon, B. Pire and D. Schiff, *Finite temperature radiative corrections to early universe Neutron-Proton Ratio: Cancellation of Infrared and Mass Singularities*, Nucl. Phys. B **336** (1990) 157.

- [22] J. Ghiglieri and M. Laine, *Neutrino dynamics below the electroweak crossover*, JCAP **1607** (07) (2016) 015.
- [23] G. Jackson and M. Laine, *A thermal neutrino interaction rate at NLO*, Nucl. Phys. B **950** (2020) 114870.
- [24] I. Ghisoiu and M. Laine, *Right-handed neutrino production rate at $T = 160$ GeV*, JCAP **1412** (12) (2014) 032.
- [25] A. Salvio, P. Lodone and A. Strumia, *Towards leptogenesis at NLO: the righthanded neutrino interaction rate*, JHEP **08** (2011) 116.
- [26] M. Laine and Y. Schröder, *Thermal right-handed neutrino production rate in the non-relativistic regime*, JHEP **02** (2012) 068.
- [27] S. Biondini, N. Brambilla, M. A. Escobedo and A. Vairo, *An effective field theory for non-relativistic Majorana neutrinos*, JHEP **12** (2013) 028.
- [28] J. Ghiglieri and M. Laine, *GeV-scale hot sterile neutrino oscillations: a derivation of evolution equations*, JHEP **05** (2017) 132.
- [29] S. Biondini, et al., *Status of rates and rate equations for thermal leptogenesis*, Int. J. Mod. Phys. A **33** (05n06) (2018) 1842004.
- [30] M. Drewes, B. Garbrecht, P. Hernandez, M. Kekic, J. Lopez-Pavon, J. Racker, N. Rius, J. Salvado and D. Teresi, *ARS Leptogenesis*, Int. J. Mod. Phys. A **33** (05n06) (2018) 1842002.
- [31] J. Ghiglieri and M. Laine, *Precision study of GeV-scale resonant leptogenesis*, JHEP **02** (2019) 014.
- [32] J. Pradler and F. D. Steffen, *Thermal gravitino production and collider tests of leptogenesis*, Phys. Rev. D **75** (2007) 023509.
- [33] J. Casalderrey-Solana, H. Liu, D. Mateos, K. Rajagopal and U. A. Wiedemann, *Gauge/String Duality, Hot QCD and Heavy Ion Collisions*, arXiv: 1101.0618.
- [34] S. Caron-Huot, P. Kovtun, G. D. Moore, A. Starinets and L. G. Yaffe, *Photon and dilepton production in supersymmetric Yang-Mills plasma*, JHEP **0612** (2006) 015.
- [35] S. C. Huot, S. Jeon and G. D. Moore, *Shear viscosity in weakly coupled $N = 4$ super Yang-Mills theory compared to QCD*, Phys. Rev. Lett. **98** (2007) 172303.
- [36] P. M. Chesler and A. Vuorinen, *Heavy flavor diffusion in weakly coupled $N=4$ super Yang-Mills theory*, JHEP **11** (2006) 037.
- [37] G. Policastro, D. T. Son and A. O. Starinets, *The Shear viscosity of strongly coupled $N=4$ supersymmetric Yang-Mills plasma*, Phys. Rev. Lett. **87** (2001) 081601.
- [38] J. M. Maldacena, *The Large N limit of superconformal field theories and supergravity*, Adv. Theor. Math. Phys. **2** (1998) 231.
- [39] E. Witten, *Anti-de Sitter space and holography*, Adv. Theor. Math. Phys. **2** (1998) 253.
- [40] S. Gubser, I. R. Klebanov and A. M. Polyakov, *Gauge theory correlators from noncritical string theory*, Phys. Lett. B **428** (1998) 105.
- [41] A. Buchel, *Shear viscosity of CFT plasma at finite coupling*, Phys. Lett. B **665** (2008) 298.

- [42] P. Kovtun, D. T. Son, A. O. Starinets, *Viscosity in strongly interacting quantum field theories from black hole physics*, Phys. Rev. Lett. **94** (2005) 111601.
- [43] P. Graf and F. D. Steffen, *Thermal axion production in the primordial quark-gluon plasma*, Phys. Rev. **D83** (2011) 075011.
- [44] P. Graf and F. D. Steffen, *Axions and saxions from the primordial supersymmetric plasma and extra radiation signatures*, JCAP **1302** (2013) 018.
- [45] A. Salvio, A. Strumia and W. Xue, *Thermal axion production*, JCAP **1401** (2014) 011.
- [46] J. Pradler and F. D. Steffen, *Constraints on the Reheating Temperature in Gravitino Dark Matter Scenarios*, Phys. Lett. **B648** (2007) 224.
- [47] V. S. Rychkov and A. Strumia, *Thermal production of gravitinos*, Phys. Rev. **D75** (2007) 075011.
- [48] J. Ghiglieri and M. Laine, *Gravitational wave background from Standard Model physics: Qualitative features*, JCAP **1507** (07) (2015) 022.
- [49] D. Forster, *Hydrodynamic fluctuation, broken symmetry and correlation functions*, (Benjamin/Cummings, Melno Park, CA, 1975).
- [50] J. W. Negele and H. Orland, *Quantum many-particle systems*, Addison-Wesley, Redwood City, 1988.
- [51] H. B. Callen and T. A. Welton, Phys. Rev. **122** (1961) 34.
- [52] G. D. Mahan, *Many-Particle Physics - Physics of Solids and Liquids*, Springer Science & Business Media, 1990
- [53] B. Müller, *The Physics of the Quark-Gluon Plasma*, Lecture Notes in Physics **225** (Springer, Berlin, 1985);
- [54] J. W. Harris and B. Müller, *The Search for the quark-gluon plasma*, Annu. Rev. Nucl. Part. Sci. **46** (1996) 71.
- [55] R. C. Hwa (Ed.), *Quark-Gluon Plasma 1 and 2* (World Scientific, Singapore, 1990 and 1995).
- [56] C. Y. Wong, *Introduction to High Energy Heavy Ion Collisions* (World Scientific, Singapore, 1994).
- [57] J. Ghiglieri, A. Kurkela, M. Strickland, and A. Vuorinen, *Perturbative Thermal QCD: Formalism and Applications*, Phys. Rept. **880** (2020) 1.
- [58] M. Laine and A. Vuorinen, *Basics of Thermal Field Theory*, Lect. Notes Phys. **925** (2016) 1.
- [59] J.-P. Blaizot and E. Iancu, *The Quark gluon plasma: Collective dynamics and hard thermal loops*, Phys. Rept. **359** (2002) 355.
- [60] U. Kraemmer, A. Rebhan, *Advances in perturbative thermal field theory*, Rept. Prog. Phys. **67** (2004) 351.
- [61] M. H. Thoma, *New developments and applications of thermal field theory*, arXiv:hep-ph/0010164.
- [62] M. H. Thoma, *Application of high-temperature field theory to heavy-ion collisions*, arXiv:hep-ph/9503400.
- [63] A. Schmitt, *Thermal field theory*, Master Thesis, 2013.

- [64] Y Yang, *An Introduction to Thermal Field Theory*, Master Thesis, 2011.
- [65] I. Strumke, *Field Theory at finite Temperature and Density - Applications to Quark Stars*.
- [66] F. Reif, *Fundamentals of Statistical and Thermal Physics*, McGraw-Hill, New York, 1965.
- [67] J. J. Sakurai, *Advanced Quantum Mechanics*, Addison-Wesley, 1999.
- [68] R. P. Feynman, *Space-Time Approach to Non-Relativistic Quantum Mechanics*, Rev. Mod. Phys. **20** (1948) 367.
- [69] R. P. Feynman and A. R. Hibbs, *Quantum Mechanics and Path Integrals*, McGraw-Hill (1965).
- [70] D. J. Chandlin, Nuovo Cim., **4** (1956) 426.
- [71] F. A. Berezin, *Method of Second Quantization*, Academic Press, New York, 1966.
- [72] A. Lahiri and P. B. Pal, *A First Book of Quantum Field Theory*, Second Edition, Narosa Publishing House Pvt. Ltd., New Delhi, 2005.
- [73] M. E. Peskin and D. V. Schroeder, *An Introduction to Quantum Field Theory*, CRC press.
- [74] N. Haque and M. G. Mustafa, *A Modified Hard Thermal Loop Perturbation Theory*, e-Print: 1007.2076 [hep-ph].
- [75] N. Haque, M. G. Mustafa and M. H. Thoma, *Conserved Density Fluctuation and Temporal Correlation Function in HTL Perturbation Theory*, Phys. Rev. D **84** (2011) 054009 .
- [76] H. A. Weldon, *Effective fermion masses of order gT in high-temperature gauge theories with exact chiral invariance*, Phys. Rev. D **26** (1982) 2789.
- [77] H. A. Weldon, *Covariant Calculations at Finite Temperature: The Relativistic Plasma*, Phys. Rev. D **26** (1982) 1394.
- [78] E. Braaten, R. D. Pisarski, *Soft Amplitudes in Hot Gauge Theories: A General Analysis*, Nucl. Phys. B **337** (1990) 569.
- [79] V. V. Klimov, *Collective excitations in a hot quark gluon plasma*, Sov. Phys. JETP **55** (1982) 199.
- [80] E. Braaten, R. D. Pisarski, and T.-C. Yuan, *Production of Soft Dileptons in the Quark-Gluon Plasma*, Phys. Rev. Lett. **64** (1990) 2242.
- [81] F. Karsch, M.G. Mustafa and M.H. Thoma, *Finite temperature meson correlation functions in HTL approximation*, Phys. Lett. B **497** (2001) 249.
- [82] E. S. Fradkin, *Proc. Lebedev Inst.*, Vol. 29, 1965, p. 6.
- [83] O. K. Kalashnikov and V. V. Klimov, *Infrared Behavior of the Polarization Operator in Scalar Electrodynamics at Finite Temperature*, Phys. Lett. B **95** (1980) 423.
- [84] A. Bandyopadhyay, Post M.Sc project report on *Application of Hard Thermal/Dense Loop to hot and dense matter*, 2013.
- [85] B. Karmakar, Post M.Sc project report on *Finite temperature Field Theory; an imaginary time formalism and its application*, December 2016-July, 2017.
- [86] H.T. Elze and U. Heinz, *Quark-Gluon Transport Theory*, Phys. Rep. **183** (1989), 81.
- [87] S. Mrówczyński, *Quark-Gluon Plasma*, ed. R. Hwa (World Scientific, Singapore), p. 185.

- [88] M. H. Thoma and M. Gyulassy, *Quark Damping and Energy Loss in the High Temperature QCD*, Nucl. Phys. **B351** (1991) 491.
- [89] E. M. Landau and L. P. Pitaevskii, *Physical Kinematics* (pergamon, New York).
- [90] V. P. Silin, *On the electromagnetic properties of a relativistic plasma*, Sov. Phys. JETP **11** (1960) 1136.
- [91] A. D. Linde, *Phase Transitions in Gauge Theories and Cosmology*, Rept. Prog. Phys. **42** (1979) 389.
- [92] A. D. Linde, *Infrared Problem in Thermodynamics of the Yang-Mills Gas*, Phys. Lett. **B96** (1980) 289.
- [93] E. Braaten and R. D. Pisarski, *Simple effective Lagrangian for hard thermal loops*, Phys. Rev. D. **45** (1992) 1827.
- [94] E. Braaten and R. D. Pisarski, *Deducing Hard Thermal Loops From Ward Identities*, Nucl. Phys. **B339** (1990) 310.
- [95] J. Taylor and S. Wong, *The Effective Action of Hard Thermal Loops in QCD*, Nucl. Phys. **B346** (1990) 115.
- [96] J. Frenkel and J. C. Taylor, *Hard thermal QCD, forward scattering and effective actions*, Nucl. Phys. **B374** (1992)
- [97] G. Barton, *On the Finite Temperature Quantum Electrodynamics of Free Electrons and Photons*, Annals Phys. **200** (1990) 271.
- [98] J.O. Andersen, E. Braaten and M. Strickland, *Hard thermal loop resummation of the free energy of a hot gluon plasma*, Phys. Rev. Lett. **83** (1999) 2139.
- [99] J. O. Andersen, E. Petitgirard, and M. Strickland, *HTL perturbation theory to two loops*, Phys. Rev. **D66** (2002) 085016; *Two loop HTL thermodynamics with quarks*, Phys. Rev. **D70** (2004) 045001.
- [100] N. Su., J. O. Andersen, and M. Strickland, *Gluon Thermodynamics at Intermediate Coupling*, Phys. Rev. Lett. **104** (2010) 122003.
- [101] J. O. Andersen, M. Strickland, and N. Su, *Three-loop HTL gluon thermodynamics at intermediate coupling*, JHEP **1008** (2010) 113.
- [102] J. O. Andersen, L. E. Leganger, M. Strickland and N. Su, *NNLO hard- thermal-loop thermodynamics for QCD*, Phys. Lett. **B696** (2011) 468.
- [103] N. Haque, A. Bandyopadhyay, J. O. Andersen, M. G. Mustafa, Michael Strickland and N. Su, *Three-loop HTLpt thermodynamics at finite temperature and chemical potential*, JHEP **05** (2014) 027.
- [104] N. Haque, J. O. Andersen, M. G. Mustafa, M. Strickland and N. Su, *Three-loop pressure and susceptibility at finite temperature and density from hard-thermal-loop perturbation theory*, Phys. Rev. D **89**, No. 6 (2014) 061701.
- [105] J.O. Andersen, L.E. Leganger, M. Strickland and N. Su, *Three-loop HTL QCD thermodynamics*, JHEP **08** (2011) 053.

- [106] J. O. Andersen, E. Braaten and M. Strickland, *Hard thermal loop resummation of the thermodynamics of a hot gluon plasma*, Phys. Rev. D **61** (2000) 014017.
- [107] P. Chakraborty, M. G. Mustafa, and M. H. Thoma, *Quark number susceptibility in hard thermal loop approximation*, Eur. Phys. J. C. **23** (2002) 591.
- [108] P. Chakraborty, M. G. Mustafa, and M. H. Thoma, *Chiral susceptibility in hard thermal loop approximation*, Phys. Rev. D **67** (2003) 114004 (2003).
- [109] P. Chakraborty, M. G. Mustafa, and M. H. Thoma, *Quark number susceptibility, thermodynamic sum rule, and hard thermal loop approximation*, Phys. Rev. D **68** (2003) 085012 (2003).
- [110] J. O. Andersen, E. Braaten and M. Strickland, *Hard thermal loop resummation of the free energy of a hot quark-gluon plasma*, Phys. Rev. D **61** (2000) 074016.
- [111] N. Haque, M. G. Mustafa and M. Strickland, *Two-loop hard thermal loop pressure at finite temperature and chemical potential*, Phys. Rev. D **87**, No. 10 (2013) 105007.
- [112] N. Haque, M. G. Mustafa and M. Strickland, *Quark Number Susceptibilities from Two-Loop Hard Thermal Loop Perturbation Theory*, JHEP **1307** (2013) 184.
- [113] J. O. Andersen, L. E. Leganger, M. Strickland and N. Su, *The QCD trace anomaly*, Phys. Rev. D **84** (2011) 087703.
- [114] J. O. Andersen, N. Haque, M. G. Mustafa and Michael Strickland, *Three-loop hard-thermal-loop perturbation theory thermodynamics at finite temperature and finite baryonic and isospin chemical potential*, Phys. Rev. D **93** (2016) 5, 054045.
- [115] L. D. McLerran and T. Toimela, *Photon and dilepton emission from the quark-gluon plasma: some general considerations*, Phys. Rev. D **31** (1985) 545.
- [116] R. Baier, B. Pire and D. Schiff, *Dilepton production at finite temperature: Perturbative treatment at order α_s* , Phys. Rev. D **38** (1988) 2814.
- [117] C. Greiner, N. Haque, M. G. Mustafa and M. H. Thoma, *Low Mass Dilepton Rate from the Deconfined Phase*, Phys. Rev. C **83** (2011) 014908.
- [118] I. Ghisoiu and M. Laine, *Interpolation of hard and soft dilepton rates*, JHEP **10** (2014) 083.
- [119] J. Ghiglieri and G. D. Moore, *Low mass thermal dilepton production at NLO in a weakly coupled quark-gluon plasma*, JHEP **12** (2014) 029.
- [120] J. Ghiglieri, *The thermal dilepton rate at NLO at small and large invariant mass*, Nucl. Part. Phys. Proc. **276-278** (2016) 305.
- [121] J. I. Kapusta, P. Lichard and D. Seibert, *High-energy photons from quark -gluon plasma versus hot hadronic gas*, Phys. Rev. D **44** (1991) 2774.
- [122] R. Baier, H. Nakkagawa, A. Niegawa and K. Redlich, *Production rate of hard thermal photons and screening of quark mass singularity*, Z. Phys. C **53** (1992) 433.
- [123] P. Aurenche, F. Gelis, R. Kobes and H. Zaraket, *Bremsstrahlung and photon production in thermal QCD*, Phys. Rev. D **58** (1998) 085003.
- [124] P. B. Arnold, G. D. Moore and L. G. Yaffe, *Photon emission from ultrarelativistic plasmas*, JHEP **0111** (2001) 057.

- [125] P. B. Arnold, G. D. Moore and L. G. Yaffe, *Photon emission from quark gluon plasma: Complete leading order results*, JHEP **0112** (2001) 009.
- [126] T. Peitzmann and M. H. Thoma, *Direct photons from relativistic heavy ion collisions*, Phys. Rept. **364** (2002) 175.
- [127] J. Ghiglieri, J. Hong, A. Kurkela, E. Lu, G. D. Moore and D. Teaney, *Next-to-leading order thermal photon production in a weakly coupled quark-gluon plasma*, JHEP **1305** (2013) 010.
- [128] M. G. Mustafa, M. H. Thoma and P. Chakraborty, *Screening of moving parton in the quark-gluon plasma*, Phys. Rev. C **71**, 017901 (2005).
- [129] M. G. Mustafa, P. Chakraborty and M. H. Thoma, *Dynamical screening in a quark gluon plasma*, J. Phys. Conf. Ser. **50** (2006) 438.
- [130] P. Chakraborty, M. G. Mustafa and M. H. Thoma, *Wakes in the quark-gluon plasma*, Phys. Rev. D **74** (2006) 094002.
- [131] P. Chakraborty, M. G. Mustafa, R. Ray and M. H. Thoma, *Wakes in a collisional quark-gluon plasma*, J. Phys. G **34** (2007) 2141.
- [132] M. Laine, O. Philipsen, P. Romatschke and M. Tassler, *Real-time static potential in hot QCD*, JHEP **0703** (2007) 054.
- [133] A. Dumitru, Y. Guo and M. Strickland, *The heavy-quark potential in an anisotropic plasma*, Phys. Lett. B **662** (2008) 37.
- [134] A. Dumitru, Y. Guo, A. Mocsy and M. Strickland, *Quarkonium states in an anisotropic QCD plasma*, Phys. Rev. D **79** (2009) 054019.
- [135] L. Thakur, N. Haque, U. Kakade and B. K. Patra, *Dissociation of quarkonium in an anisotropic hot QCD medium*, Phys. Rev. D **88** (2013) 054022.
- [136] R. D. Pisarski, *Damping rates for moving particles in hot QCD*, Phys. Rev. D **47** (1993) 5589.
- [137] S. Peigne, E. Pilon and D. Schiff, *The Heavy fermion damping rate puzzle*, Z. Phys. C **60** (1993) 455.
- [138] M.H. Thoma, *Damping rate of a hard photon in a relativistic plasma*, Phys. Rev. D **51** (1995) 862.
- [139] A. Abada and N. Daira-Aifa, *Photon damping in one-loop HTL perturbation theory*, JHEP **1204** (2012) 071.
- [140] E. Braaten and R. D. Pisarski, *Resummation and gauge Invariance of the gluon damping rate in hot QCD*, Phys. Rev. Lett. **64** (1990) 1338.
- [141] E. Braaten and R. D. Pisarski, *Calculation of the gluon damping rate in hot QCD*, Phys. Rev. D **42** (1990) 2156.
- [142] E. Braaten and M. H. Thoma, *Energy loss of a heavy fermion in a hot plasma*, Phys. Rev. D **44** (1991) 1298.
- [143] E. Braaten and M. H. Thoma, *Energy loss of a heavy quark in the quark-gluon plasma*, Phys. Rev. D **44** (1991) 2625.
- [144] P. Chakraborty, M. G. Mustafa and M. H. Thoma, *Energy gain of heavy quarks by fluctuations in the QGP*, Phys. Rev. C **75** (2007) 064908.

- [145] J. Ghiglieri, G. D. Moore and D. Teaney, *Jet-medium interactions at NLO in a weakly-coupled quark-gluon plasma*, JHEP **03** (2016) 095.
- [146] M. J. Lavelle and M. Schaden, *Propagators and condensates in QCD*, Phys. Lett. B **208** (1988) 419.
- [147] A. Schäfer and M. H. Thoma, *Quark propagation in a quark-gluon plasma with gluon condensate*, Phys. Lett. B **451** (1999) 195.
- [148] M. G. Mustafa, A. Schafer, and M. H. Thoma, *Non-perturbative dilepton production from a quark-gluon plasma*, Phys. Rev. C **61** (2000) 024902 .
- [149] N. Su and K. Tywoniuk, *Massless Mode and Positivity Violation in Hot QCD*, Phys. Rev. Lett. **114** (2015) 161601.
- [150] A. Bandyopadhyay, N. Haque, M. G. Mustafa, M. Strickland, *Dilepton rate and quark number susceptibility with the Gribov action*, Phys. Rev. D **93**, no. 6 (2016) 065004.
- [151] V. N. Gribov, *Quantization of non-abelian gauge theories*, Nucl. Phys. B. **139** (1978) 1.
- [152] D. Zwanziger, *Local and renormalizable action from the Gribov horizon*, Nucl. Phys. B. **323** (1989) 513.
- [153] G. Boyd et al., *Thermodynamics of SU(3) lattice gauge theory*, Nucl. Phys. **B469** (1996) 419.
- [154] H. Leutwyler, in Proc. Conf. QCD - 20 years later, Eds. P. M. Zerwas and H. A. Kastrup (World Scientific, Singapore,1993) p. 693.
- [155] N. Vandersickel, *A study of Gribov-Zwanziger action: from propagators to glueballs*, PhD Thesis, Gent U., 1104.1315.
- [156] D. Zwanziger, *Equation of State of Gluon Plasma from Local Action*, Phys. Rev. D. **76** (2007) 125014.
- [157] K. Fukushima and N. Su, *Stabilizing perturbative Yang-Mills thermodynamics with Gribov quantization*, Phys. Rev. D. **88** (2013) 076008.
- [158] J. A. Gracey, *Two loop correction to the Gribov mass gap equation in Landau gauge QCD*, Phys. Lett. B **632** (2006) 282.
- [159] A. Bazavov, N. Brambilla, X. Garcia i Tormo, P. Petreczky, J. Soto and A. Vairo, *Determination of α_s from the QCD static energy*, Phys. Rev. D **86** (2012) 114031.
- [160] M. Kitazawa and F. Karsch, *Spectral Properties of Quarks at Finite Temperature in Lattice QCD*, Nucl. Phys. A **830** (2009) 223c.
- [161] O. Kaczmarek, F. Karsch, M. Kitazawa, and W. Soldner, *Thermal mass and dispersion relations of quarks in the deconfined phase of quenched QCD*, Phys. Rev. D. **86** (2012) 036006.
- [162] P. V. Ruuskanen, *Electromagnetic probes of quark-gluon plasma in relativistic heavy ion collisions*, Nucl. Phys. **A544** (1992) 169c.
- [163] L. Van Hove, *The Occurrence of Singularities in the Elastic Frequency Distribution of a Crystal*, Phys. Rev. **89** (1953) 1189.
- [164] N.W. Ashcroft and N.D.Mermin, *Solid State Physics* (Saunders College, Philadelphia, 1976).
- [165] H. A. Weldon, *Reformulation of finite temperature dilepton production*, Phys. Rev. D **42** (1990) 2384.

- [166] J. Cleymans, J. Fingberg, and K. Redlich, *Transverse Momentum Distribution of Dileptons in Different Scenarios for the QCD Phase Transition*, Phys. Rev. D **35** (1987) 2153.
- [167] S.M.H. Wong, *The Production of soft dileptons in the quark-gluon plasma in resummed perturbation theory* Z. Phys. C **53** (1992) 465.
- [168] H.-T. Ding, A. Francis, O. Kaczmarek, F. Karsch, E. Laermann and W. Soeldner, *Thermal dilepton rate and electrical conductivity: An analysis of vector current correlation functions in quenched lattice QCD*, Phys. Rev. D **83**, 034504 (2011).
- [169] F. Karsch, E. Laermann, P. Petreczky, S. Stickan and I. Wetzorke, *A Lattice calculation of thermal dilepton rates*, Phys. Lett. B **530**, 147 (2002) [hep-lat/0110208].
- [170] T. Kim, M. Asakawa and M Kitazawa, *Dilepton production spectrum above T_c with a lattice propagator*, [arXiv:1505.07195v1\[nucl-th\]](#).